Genetic and Biochemical Insights into the Mycobacterial PrrAB System as a Regulator of Respiration and Central Metabolism

by

Jason Dean Maarsingh

A Dissertation Presented in Partial Fulfillment
of the Requirements for the Degree
Doctor of Philosophy

Approved April 2019 by the
Graduate Supervisory Committee:

Shelley E. Haydel, Chair
Heather Bean
Todd Sandrin
Kenneth Roland

ARIZONA STATE UNIVERSITY

May 2019

ABSTRACT

Mycobacterium tuberculosis (*Mtb*), the causative agent of tuberculosis, is the 10th leading cause of death, worldwide. The prevalence of drug-resistant clinical isolates and the paucity of newly-approved antituberculosis drugs impedes the successful eradication of *Mtb.* Bacteria commonly use two-component systems (TCS) to sense their environment and genetically modulate adaptive responses. The *prrAB* TCS is essential in *Mtb*, thus representing an auspicious drug target; however, the inability to generate an *Mtb* Δ*prrAB* mutant complicates investigating how this TCS contributes to pathogenesis. *Mycobacterium smegmatis*, a commonly used *M. tuberculosis* genetic surrogate was used here. This work shows that *prrAB* is not essential in *M. smegmatis*. During ammonium stress, the Δ*prrAB* mutant excessively accumulates triacylglycerol lipids, a phenotype associated with *M. tuberculosis* dormancy and chronic infection. Additionally, triacylglycerol biosynthetic genes were induced in the Δ*prrAB* mutant relative to the wild-type and complementation strains during ammonium stress. Next, RNA-seq was used to define the *M. smegmatis* PrrAB regulon. PrrAB regulates genes participating in respiration, metabolism, redox balance, and oxidative phosphorylation. The *M. smegmatis* Δ*prrAB* mutant is compromised for growth under hypoxia, is hypersensitive to cyanide, and fails to induce high-affinity respiratory genes during hypoxia. Furthermore, PrrAB positively regulates the hypoxia-responsive *dosR* TCS response regulator, potentially explaining the hypoxia-mediated growth defects in the Δ*prrAB* mutant. Despite inducing genes encoding the F_1F_0 ATP synthase, the Δ*prrAB* mutant accumulates significantly less ATP during aerobic, exponential growth compared to the wild-type and complementation strains. Finally, the *M. smegmatis* Δ*prrAB* mutant exhibited growth impairment in media containing gluconeogenic carbon sources. *M. tuberculosis* mutants unable to utilize these substrates fail to establish chronic infection, suggesting that PrrAB may regulate *Mtb* central carbon metabolism in response to chronic infection. In conclusion, 1) *prrAB* is not universally essential in mycobacteria; 2) *M. smegmatis* PrrAB regulates genetic responsiveness to nutrient and oxygen stress; and 3) PrrAB may provide feed-forward control of the DosRS TCS and dormancy phenotypes. The data

generated in these studies provide insight into the mycobacterial PrrAB TCS transcriptional regulon, PrrAB essentiality in *Mtb*, and how PrrAB may mediate stresses encountered by *Mtb* during the transition to chronic infection.

DEDICATION

To all the people who have helped shape the person I am. Whether they were positive or negative influences, I wouldn't be who I am without them. Special dedication to my family, because there's nothing more important than family and I'm one of the lucky ones to have incredibly supportive relatives.

ACKNOWLEDGMENTS

First and foremost, I need to acknowledge my father, Ron, whose constant support has been the single-most influential contribution toward my success in grad school and life in general. Through all my ups-and-downs, including too many years of uncertainty in my life's direction, he never gave up on me. There is no stronger person in my life and if I can become half the man he is, I'm confidant I'll be ok. I love you dad!

To my mother, who passed away from liver cancer when I was two years old. Though I never had the chance to grow up with this wonderful woman, her spirit permeates into every good thing I do. I don't fully believe or reject the existence of an afterlife, but I feel she is with me during my trials and tribulations. I'm trying to make you proud, mama.

Special thanks to my aunt Martha and uncle Stewart, who became my second parents after mom died. I wouldn't have achieved my successes without you. Martha, you filled mom's shoes better than anyone could have, and I know she's thanking you for doing so. Stewart, I will always be grateful for the lessons and morals you imparted to me during my youth, now, and in the future. Additionally, to my cousins (better yet, brothers) Rusty (Max), Cody, and Yari. Thanks for being the siblings I never had as an only child. We've done some stupid things in the past, but I wouldn't change a thing. Though our lives take us in different directions, for better or worse, I would be in a much worse place without you.

To Dr. Maneesha Muralinath (ASU mama), my first mentor at ASU who believed in me and helped me get my scientific "sea legs". To Dr. Valerie Stout, who's ever warming smile and advice provided me with a sense of calm and reassurance. To my committee, Dr. Heather Bean, Dr. Kenneth Roland, and Dr. Todd Sandrin: thank you for your advice and encouragement during my graduate school tenure. It's been a pleasure having your guidance and support throughout my graduate education.

Finally, to Dr. Shelley Haydel, my committee chair. You gave me the opportunity to work in a formal lab setting. I know I haven't always been your star student, but you showed ever-lasting patience and a refusal to give up on me. I wouldn't be the scientist I am today without your mentorship and guidance. Thanks for giving me the once-in-a-lifetime chance to make something

out of myself. I will do everything I can to make you proud in my future career and scientific endeavors.

To my girlfriend, Sam. You are my muse and gave me a reason not to quit during my last few years of grad school. Thanks for dealing with all my late nights and constant weekends working in the lab. I'm glad we had the chance to tackle the challenges of grad school together. I love you and will always be your support, friend, and partner.

Finally, to all the Haydel lab members of the present and past. Thanks to Dr. Caitlin Otto for the honest input regarding details of grad school. To Ryan Lamarca, my lab brother. We started our programs together and I couldn't have had a better lab mate. Your work ethic and intelligence will take you far! Rachell Barret, my first lab sister, whom I had the pleasure to mentor during my first year. I'll never forget our rides to-and-from the ASU West campus! I wish you and Nick a long, blissful marriage. To Michelle Stevens, the super smarty pants undergraduate and my second lab sister. It was an absolute pleasure seeing someone as young and talented as you mature in the lab. Thanks to my second lab sister, Rebecca Melo. I know you and Bryan are going to do well in California and best of luck during grad school! I'm excited to see lil' Grayson's pics when he's born! To everyone else (because there are too many to list), thanks for working hard to support Shelley's research goals. I know I can be intense sometimes, but please realize that I always had the lab's best interest in mind. Continue the proud Haydel lab tradition and take care of it well!

TABLE OF CONTENTS

LIST OF TABLES

LIST OF FIGURES

Figure Page

Figure Page

LIST OF ABBREVIATIONS

ADS	Albumin-dextrose-saline
BCG	Bacille Calmette-Guérin
CCM	Central carbon metabolism
COG	Cluster of orthologous groups
d	Day
DAG	Diacylglycerol
DEG	Differentially expressed gene
ESI	Electrospray ionization
FDR	False-discovery rate
FPKM	Fragments per kilobase per million mapped reads
GDH	Glutamate dehydrogenase
GO	Gene ontology
GOGAT	Glutamate synthase
GS	Glutamine synthetase
h	Hour
INFγ	Interferon gamma
LC	Liquid chromatography
M7H9	Middlebrook 7H9
MAME	Mycolic acid methyl ester
MDR-TB	Multi drug-resistant tuberculosis
MDS	Multi-dimensional scaling
min	Minute
MS	Mass spectrometry
MSX	Methionine-*S*-sulfoximine
OD_{600}	Optical density at 600 nm
PCA	Principal component analysis

PEP	Phosphoenolpyruvate
PLS-DA	Partial least squares discriminate analysis
PMF	Proton motive force
qRT-PCR	Quantitative real-time polymerase chain reaction
QTOF	Quadrapole time-of-flight
TAG	Triacylglycerol
TB	Tuberculosis
TCA	Tricarboxylic acid cycle
TCS	Two-component system
TLC	Thin-layer chromatography
VIP	Variable importance in projection
XDR-TB	Extremely drug-resistant tuberculosis

CHAPTER 1: INTRODUCTION

Mycobacterium tuberculosis and its Global Implications

Mycobacterium tuberculosis (*Mtb*), the etiologic agent of tuberculosis (TB), is the leading cause of mortality from an infectious disease and the 10th leading cause of all global deaths (WHO 2018). In 2017, 10 million incident TB cases and 1.6 million deaths attributed to TB were reported worldwide (WHO 2018). TB accounts for 22% of deaths in co-infected HIV patients. The majority of the disease burden lies in South-East Asia (44%), Africa (25%), and the West Pacific (18%) regions (WHO 2018). The actual global TB burden is likely higher, however, due to underreported incident cases in high-burden countries (e.g., India and Indonesia) that lack mandatory TB notification policies (WHO 2018).

Overall, the rates of infection and deaths due to TB in the United States have declined over the past 60 years (www.cdc.gov/tb/statistics/reports/2017/table2.htm). The consistent decrease in incident-reported TB cases reached a period of stagnation between 1983-1987, followed by a sudden resurgence until peaking in 1992 before resuming a downward trend (Small and Fujiwara 2001). High rates of TB infection in the United States are associated with specific ethnic groups, with Asian and Hispanic populations accounting for the majority of reported TB cases (36% and 28%, respectively) (www.cdc.gov/tb/statistics/reports/2017/table2.htm). Incident TB cases are greatest among foreign-born persons (70% of all reported TB cases in the United States), especially those of Asian descent (Stewart et al. 2018). In 2016, 92% of drug-resistant TB cases in the United States were diagnosed from foreign-born people (Stewart et al. 2018), implicating immigration as a positive contributor to the prevalence of drug-resistant incident TB cases in the United States.

The emergence of drug-resistant bacteria that are recalcitrant to commonly used antibiotics is complicating our current treatment regimens. For 25 years, clinics have experienced an increase in *Mtb* isolates resistant to front-line antituberculosis drugs, notably documented in the New York City TB epidemic of the early 1990s (Frieden et al. 1993). Multidrug-resistant TB (MDR-TB) is defined as *Mtb* resistant to rifampicin and isoniazid, two established front-line

antituberculosis drugs. Extensively drug-resistant TB (XDR-TB) is defined as MDR-TB plus resistance to a fluoroquinolone and an injectable second-line antibiotic (e.g. kanamycin, amikacin). In addition to prolonged patient care and morbidity, drug-resistant TB is estimated to cost countries with high prevalence of MDR-TB approximately $16.2 billion, many of which are financially burdened and possess inadequate health care infrastructures (WHO 2018).

Two-Component Regulatory Systems

All organisms must sense their immediate environment to enact appropriate biological responses. Environmental signaling in eukaryotic cells is dominated by serine/threonine (Ser/Thr) protein kinases (Hanks, Quinn, and Hunter 1988), tyrosine kinases (Schlessinger 2000), and G-protein coupled receptors (Rodbell 1980). Prokaryotes also utilize Ser/Thr protein kinase (Urabe, Ogawara, and Motojima 2015; Pan et al. 2017) and tyrosine kinase (C. Liu et al. 2017; Niesteruk et al. 2018) signal transduction mechanisms. Two-component systems (TCSs) are the most prevalent and well-studied signal transduction mechanisms in bacteria. The term “two-component system” was initially coined in the mid-1980s during investigations of nitrogen regulation in *Bradyrhizobium parasponia* (Nixon, Ronson, and Ausubel 1986), though seminal work on *Escherichia coli* OmpR provided the initial insights into bacterial environmental recognition (Hall and Silhavy 1981). A prototypical TCS consists of a membrane-bound histidine kinase sensor that transphosphorylates a cytoplasmic DNA-binding response regulator (Kofoid and Parkinson 1988). Deviations from this paradigm are exemplified by the CheY response regulator, which interacts with and modulates rotational direction of the flagellar apparatus (Sarkar, Paul, and Blair 2010), and the CheA (A. Stock et al. 1988) and NtrB (MacFarlane and Merrick 1985) histidine kinase, which are soluble cytoplasmic proteins.

TCS signaling is initiated when an appropriate environmental signal is recognized by the histidine kinase (Parkinson 1976; Hall and Silhavy 1981; Soncini, Vescovi, and Groisman 1995; Ioanoviciu et al. 2007). Upon activation, histidine kinase monomers dimerize and catalyze a transphosphorylation event on the opposing protein at a conserved histidine residue (Fig. 1.1). Interaction of the activated histidine kinase with its cognate response regulator stimulates

phosphotransfer from the histidine to a conserved aspartate residue on the response regulator in a reaction catalyzed by the response regulator (Lukat et al. 1992). Signal transduction between the histidine kinase and its cognate response regulator may involve direct phosphotransfer or occur by phosphorelay, in which one or more adaptor proteins sequentially transfer the phosphate from histidine kinase to response regulator (Burbulys, Trach, and Hoch 1991; Uhl and Miller 1996). Once phosphorylated, the response regulator interacts with its target, such as DNA (Mishra et al. 2017; Filippova et al. 2018), RNA (Ramesh et al. 2012; Luque-Almagro et al. 2013), or a cytoplasmic protein (Banno et al. 2004; Sarkar, Paul, and Blair 2010).

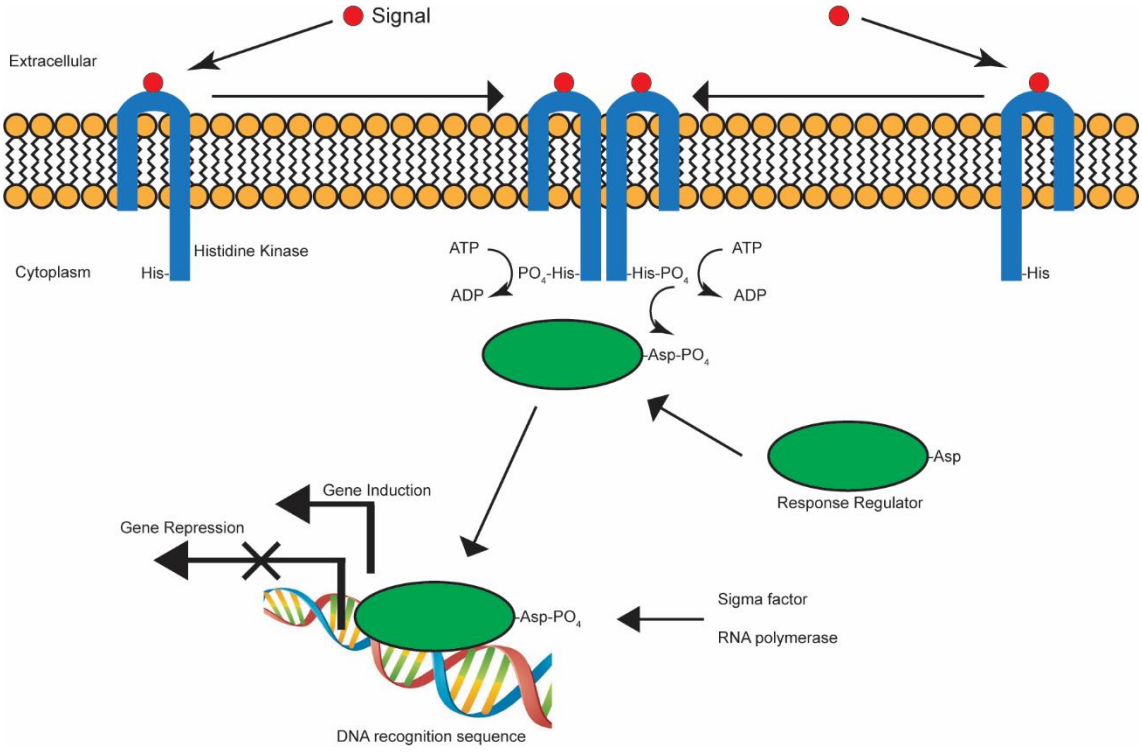

Figure 1.1. Diagram of a prototypical two-component signaling pathway.

Histidine kinases are modular proteins exhibiting distinct functional domains. Effector domains are located proximal to the C-terminus and show a high degree of sequence similarity, whereas the N-terminal sensor portion is highly variable, owing to diverse recognition of environmental stimuli (Georgellis and Kwon 2001; Hutchings, Hong, and Buttner 2006; A.I. Lee,

Delgado, and Gunsalus 1999). The orthodox histidine kinase, modeled after EnvZ of *E. coli*, is embedded in the cytoplasmic membrane through two N-terminal transmembrane helices located in the sensing domain (Forst et al. 1987). This feature is not universal, however, as some histidine kinases encode additional transmembrane segments, such as FixL of *Rhizobium meliloti* (Lois, Ditta, and Helinski 1993) and UhpB of *E. coli* (Kadner 1995), which possess four and eight transmembrane helices, respectively. Phosphorylation by each histidine kinase monomer is a bimolecular reaction accomplished by the C-terminal catalytic ATP-binding domain, which uses divalent cations and ATP to transfer the γ-phosphate to the conserved histidine of the adjacent monomer. The histidine kinase is now posed to interact with its cognate response regulator.

response regulators are cytoplasmic proteins that typically bind to specific DNA sequences and regulate gene expression (Aiba et al. 1989; Mizuno 1997). Exceptions to this model exist, as notably demonstrated with the *E. coli* CheY response regulator, which interacts with the flagellar motor protein, FliM, to modulate flagellar rotation (Welch et al. 1993). Response regulators catalyze transfer of the phosphohistidine phosphate from the histidine kinase to a conserved aspartate in the N-terminal regulatory domain of the response regulator (Lukat et al. 1992). This covalent modification induces conformational changes in the response regulator that allow the C-terminal effector region to act on its target. Intrinsic (Zapf et al. 1998) or auxiliary (Keener and Kustu 1988) phosphatase activity regulates the duration of phosphorylation to modulate temporal patterns of response regulator activity.

The PrrAB TCS of Mycobacteria

The *Mtb* genome harbors 12 TCSs, 11 of which are genetically linked, in addition to five orphaned response regulators and two orphaned histidine kinases (Table 1.1) (Bretl, Demetriadou, and Zahrt 2011). Of this repertoire, *prrAB* (*Rv0903-0902*) is one of four paired TCSs present in all fully-sequenced mycobacterial genomes, implying strong evolutionary retention for the *prrAB* TCS in mycobacteria. Additionally, *prrAB*, along with *mtrAB*, is essential for viability in *Mtb* (Zahrt and Deretic 2000; Haydel et al. 2012). Initial attempts to generate an *Mtb prrAB* mutant used transposon-based gene disruption (Ewann et al. 2002). Subsequent work by

Haydel et al. (Haydel et al. 2012), however, confirmed that the transposon mutant is actually a *prrAB* knockdown strain that expresses *prrA* and *prrB* at 30% and 42%, respectively, relative to the wild-type strain. Deletion of the native *prrAB* locus in the *Mtb* H37Rv strain was successful only after ectopic expression of *prrAB*, confirming the essentiality of the *Mtb prrAB* TCS (Haydel et al. 2012). Recently, Mishra et al. reported *prrAB* as essential in *M. smegmatis* (A.K. Mishra, Yabaji, et al. 2017); however, Maarsingh and Haydel later showed that *prrAB* is not universally essential in mycobacteria (Maarsingh and Haydel 2018).

The *prrAB* system was initially described and characterized using the selective capture of transcribed sequences (SCOTS) method whereby *Mtb* cDNA is generated and captured from *Mtb*-infected human macrophages (Graham and Clark-Curtiss 1999). In *Mtb, prrA* is expressed 48 h after infection in human peripheral blood monocyte-derived macrophages, suggesting that PrrAB may contribute to adaptation in the phagosomal environment (Graham and Clark-Curtiss 1999; Haydel and Clark-Curtiss 2004). However, *prrA* was not detected at 18 h or 110 h post-infection, indicating that expression is temporally restricted during macrophage infection (Haydel and Clark-Curtiss 2004). During in vitro culture, *prrAB* is upregulated upon nitrogen-limitation induced by the glutamine synthetase inhibitor, methionine *S*-sulfoximine (MSX), and repressed under hypoxia (Haydel et al. 2012). Though *prrAB* expression is greatest during exponential growth, the PrrA protein is stable throughout stationary phase, suggesting a maintenance role for PrrAB during later growth stages (Haydel et al. 2012). *prrAB* is autoregulated in both the *Mycobacterium bovis* Bacillus Calmette-Guérin (BCG) and *Mtb* Mt103 strains during growth in murine bone marrow-derived macrophages (Ewann, Locht, and Supply 2004). Purified 6XHis-PrrA binds to a 317 bp *prrAB* promoter fragment and binding affinity increases upon phosphorylation (Ewann, Locht, and Supply 2004). The *prrAB*/PrrA autoregulatory properties are consistent with other mycobacterial TCSs, including the *trcRS*/TrcR (Haydel et al. 2002), *phoPR*/PhoR (Gonzalo-Asensio et al. 2008), *senX3-regX3*/RegX3 (Himpens, Locht, and Supply 2000), *mtrAB*/MtrA (Curcic, Dhandayuthapani, and Deretic 1994*)*, *mprAB*/MprA (He and Zahrt 2005), *devRS*/DevRS (Bagchi et al. 2005), and *tcrXY*/tcrX (Bhattacharya and Das 2011).

Table 1.1. Paired TCSs and orphaned histidine kinases and response regulators in *Mtb* and *M. smegmatis* (*Msmeg*). NA, None available.

Name	*Mtb*	*Msmeg*	Function	Reference
Paired TCSs				
RegX3-SenX3	+	+	P_i response	(Namugenyi et al. 2017)
TcrA-Rv0600c/Rv0601c	+	-	Unknown	(Shrivastava, Ghosh, and Das 2009)
PhoP-PhoR	+	+	Lipid metabolism, respiration	(Goyal et al. 2011)
NarL-Rv0845	+	+	Nitrate metabolism (?)	(Schnell, Agren, and Schneider 2008)
PrrA-PrrB	+	+	Intracellular adaptation	(A.K. Mishra, Yabaji, et al. 2017)
MprA-MprB	+	+	Maintenance of persistent infection	(Zahrt et al. 2003)
KdpE-KdpD	+	+	K^+ homeostasis, osmotic balance	(Freeman, Dorus, and Waterfield 2013)
TrcR-TrcS	+	+	Unknown	(Pang et al. 2011)
DosR-DosS-DosT	+	+	Hypoxia and redox sensing	(Honaker et al. 2010; A. Kumar et al. 2007)
MtrA-MtrB	+	+	Cell division, cell wall maintenance	(Gorla et al. 2018)
TcrX-TcrY	+	+	Unknown	(Bhattacharya and Das 2011)
PdtaR-PdtaS	+	+	Unknown	(Preu et al. 2012)
Orphaned histidine kinase				
Rv3220c	+	+	Unknown	NA
Orphaned response regulators				
Rv0260c	+	+	Unknown	NA
Rv0818	+	+	Unknown	NA
Rv1626	+	+	Unknown	NA
Rv2884	+	-	Unknown	NA
Rv3143	+	+	Unknown	NA

PrrA is a 25.2 kDa response regulator belonging to the OmpR/PhoP family and bears a C-terminal DNA-binding winged-helix-turn-helix motif (Brennan 1993; Nowak et al. 2006). The N-terminal regulatory domain displays a prototypical $(\beta/\alpha)_5$ fold found in other OmpR/PhoP response regulators. PrrA is phosphorylated by PrrB at Asp-58, located in the α3 helix of the N-terminal regulatory domain (Mishra et al. 2017) (Fig. 1.2). The location and phosphorylation of Asp-58 in PrrA is consistent with other response regulators (Makino et al. 1989; Sanders et al. 1989; Lewis et al. 1999). The PrrA DNA-binding effector domain is found in the C-terminal region (Nowak, Panjikar, et al. 2006a) with the α3 helix of the helix-turn-helix motif likely involved in DNA

binding (Martinez-Hackert and Stock 1997; Blanco et al. 2002; Buckler, Zhou, and Stock 2002; Robinson, Wu, and Stock 2003).

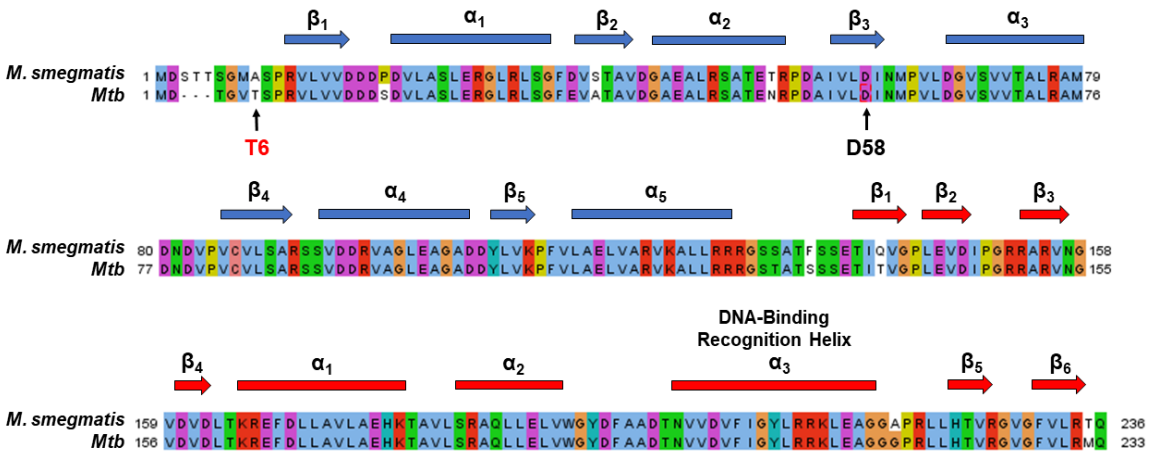

Figure 1.2. PrrA multiple-sequence alignment between *M. smegmatis* (top row) and *Mtb* (bottom row). Beta strands and alpha helices are indicted by arrows and rectangles, respectively. N-terminal receiver and C-terminal effector secondary structures are indicated by blue and red, respectively. The locations of the conserved phospho-receiving aspartate (D58; both *M. smegmatis* and *Mtb*) and phospho-receiving threonine (T6; *Mtb* only) are indicated at the bottom of the upper alignment.

PrrA is also phosphorylated by Ser/Thr protein kinases. The first evidence for auxiliary kinase action on PrrA came from analysis of the *Mtb* H37Rv phosphoproteome (Parandhaman et al. 2014). Western blot analysis using anti-phosphoserine antibodies and parallel mass spectrometry of in-gel trypsin digests confirmed that, during nitric oxide exposure, PrrA is phosphorylated in an *Mtb* Δ*pknE* mutant, but not in the wild-type background (Parandhaman et al. 2014). These data suggest that, during nitric oxide stress, PknE negatively regulates other Ser/Thr protein kinases that act on PrrA, however, evidence for direct interactions of PknE with Ser/Thr protein kinases is lacking. Purified recombinant *Mtb* PknG, PknK, and PknJ proteins phosphorylate *Mtb* and *M. bovis* BCG PrrA at Thr-6 (Mishra et al. 2017). Furthermore, phosphomimetic mutation at Thr-6 to Asp (T6D) enhances the DNA binding affinity of PrrA after phosphorylation by PrrB (Mishra et al. 2017). These data suggest that PrrA is subject to multiple levels of regulation, however, the effects on gene expression by differential phosphorylation is currently unknown.

Less is known about the 47.8 kDa PrrB histidine kinase. The crystal structure has been solved for a truncated C-terminal fragment bearing the catalytic activity domain; however, attempts to crystalize the full-length PrrB protein or other components of the polypeptide (i.e. HAMP and/or DHp domains) were unsuccessful (Nowak, Panjikar, Morth, et al. 2006b). Purified PrrB transphosphorylates the MprA response regulator in vitro, though whether this occurs in vivo and the relevance of such crosstalk transphosphorylation is unknown (Agrawal et al. 2015). The MprAB TCS responds to membrane and pH stress by inducing transcription of the *sigE* and *sigB* sigma factors (He et al. 2006). If physiological crosstalk occurs between PrrB and MprA, it would indicate that PrrB potentially integrates or augments stress responses independent from PrrA. In *M. smegmatis*, PrrA appears to be capable of acting independently from PrrB, as a Δ*prrAB* strain that constitutively expresses an *Mtb prrA* isoform from an ectopic chromosomal location phenotypically resembles the wild-type strain during growth in ammonium-limited medium (Maarsingh and Haydel 2018). Alternatively, an additional as-yet unidentified histidine kinase may be capable of transphosphorylating PrrA in this setting. Further work in *Mtb* is required to determine if both *prrA* and *prrB* are essential or whether the pathogen is viable in the absence of *prrB* (DeJesus et al. 2017).

Host-Pathogen Interactions and the *Mtb* PrrAB TCS

Macrophages employ a variety of receptors to promote *Mtb* phagocytosis (Hmama et al. 2015). Uptake through IgG receptors (type-I phagocytosis) is accompanied by activation of phagosome-associated NADPH oxidase (NOX2), which generates toxic superoxide radicals in an initial attempt to clear the pathogen (Bedard and Krause 2007; Lam, Huang, and Brumell 2010). Type II phagocytosis, mediated through complement (CR3), mannose, and scavenger receptors (among others), is not immediately associated with NOX2 activity (Hmama et al. 2015). It is likely that, in vivo, phagocytosis of *Mtb* by macrophages is accomplished through cooperative action of multiple receptors and the macrophage activation state influences receptor selectivity (Krauss et al. 1994; Chroneos and Shepherd 1995).

Upon internalization by the host macrophage, *Mtb* elicits defense mechanisms to evade phagosome maturation and host bactericidal attempts. Important examples include blocking phagosome-lysosome fusion (Ferrari et al. 1999; Fratti et al. 2003) and inhibiting phagosome recruitment of the vacuolar H^+/ATPase to prevent phagosome acidification and protease activation (Sturgill-Koszycki et al. 1994; Sturgill-Koszycki, Schaible, and Russell 1996). Tubercle bacilli that survive these initial bactericidal attempts must then adjust to long-term residence inside the phagosome, which is believed to represent a nutrient-poor environment (Schnappinger et al. 2003; Timm et al. 2003).

Mtb is capable of disrupting macrophage lipid metabolism by inducing the foamy macrophage phenotype. Foamy macrophages are characterized by significant accumulation of intracellular lipid droplets (Shi et al. 2017). These macrophages are frequently found at the periphery of the granuloma's necrotic center (Peyron et al. 2008). *Mtb* drives the foamy macrophage phenotype in processes requiring oxygenated mycolic acids (Peyron et al. 2008) and the ESX-1 secretion product, ESAT-6 (Singh et al. 2012). The inability to activate the bactericidal respiratory burst in addition to providing an energy-dense nutrient supply marks foamy macrophages as safe havens for long-term residence by *Mtb* during non-replicating persistence (Peyron et al. 2008).

Mtb-infected dendritic cells migrate to local lymph nodes to prime T-cell activation via *Mtb* antigen presentation (Wolf et al. 2007). Th1 T-cells secrete the proinflammatory cytokines, interferon gamma (IFNγ) (Herbst, Schaible, and Schneider 2011) and tumor necrosis factor (TNF) (He et al. 2010). These cytokines engage receptors at the macrophage cell membrane to activate nitric oxide production which exerts potent bactericidal activity (B.B. Mishra, Lovewell, et al. 2017). Activated macrophages secrete TNF and IL-12 which augment the Th1 response (Jung et al. 2011). Once internalized, *Mtb* elicits the macrophage cytosolic surveillance pathway to stimulate type I interferon production (Manzanillo et al. 2012) which inhibits T-cell Th1 responses and promotes bacterial survival (Manca et al. 2001). The Th1 adaptive immune response is therefore important for controlling *Mtb* infection (Redford et al. 2010).

During prolonged infection, activated T- and B-cells, epithelioid macrophages, and fibroblasts are recruited to local sites of pulmonary infection to stimulate granuloma development in attempts to constrain *Mtb* dissemination (Ulrichs and Kaufmann 2006). *Mtb* cells residing in these structures must then acclimate to the hypoxic (Tsai et al. 2006) and lipid-rich (Munoz-Elias and McKinney 2005) granuloma environment by modulating genetic programs to establish chronic infection (Shi et al. 2005; Schnappinger et al. 2003). From the outset of infection, *Mtb* is faced with repeated pernicious hurdles which require dynamic adaptive measures to survive in this hostile and ultra-narrow ecological niche.

The *Mtb prrAB* TCS is expressed after 2 d of macrophage infection (Graham and Clark-Curtiss 1999; Ewann et al. 2002; Haydel and Clark-Curtiss 2004), suggesting that PrrAB responds to cues encountered during the early infectious stages. Overexpressing *prrAB* or *prrA(T6D)prrB* (Figure 1.1) in *M. bovis* BCG improves viability after 1 and 2 d of infection in murine peritoneal macrophages (Mishra et al. 2017). An *Mtb prrAB* knockdown mutant grows poorly relative to the wild-type strain during the first 6 d of infection in murine bone marrow-derived macrophages (Ewann et al. 2002). Both strains are recovered in equal proportions after 9 d infection, indicating that PrrAB is not required for long-term infection in an *ex vivo* macrophage model. These data support the hypothesis that PrrAB provides adaptive measures during the early replicative stages within the host phagosome (Graham and Clark-Curtiss 1999; Haydel and Clark-Curtiss 2004; Ewann et al. 2002). In contrast, the *Mtb prrAB* knockdown mutant grew similar to wild-type over the course of 30 d infection in the lungs, liver, and spleen of C57BL/6J mice (Ewann et al. 2002), therefore highlighting the differences between *ex vivo* and in vivo infectious models and the putative interactions with the adaptive immune response. The combined data provide evidence for a protective role for the mycobacterial PrrAB TCS during the early stages of intracellular infection.

Important gaps in our knowledge remain regarding the environmental signals that activate PrrAB and the adaptive/responsive measures elicited by PrrAB during *Mtb* infection (Fig. 1.3). Is the *Mtb* PrrAB TCS responsive to phagosome acidification, energy status, and low oxygen tension, as suggested by transcriptomic data (Rohde, Abramovitch, and Russell 2007; Hards et

al. 2015; Bellale et al. 2014)? Does the *Mtb* PrrAB TCS regulate lipid metabolism (Maarsingh and Haydel 2018), respiratory pathways, and gluconeogenic carbon utilization, as demonstrated in *M. smegmatis* (unpublished data)? Further experimentation is required to answer these questions and the data gleaned from such studies will illuminate our currently dim understanding of the essential nature and virulence properties of the *Mtb* PrrAB TCS.

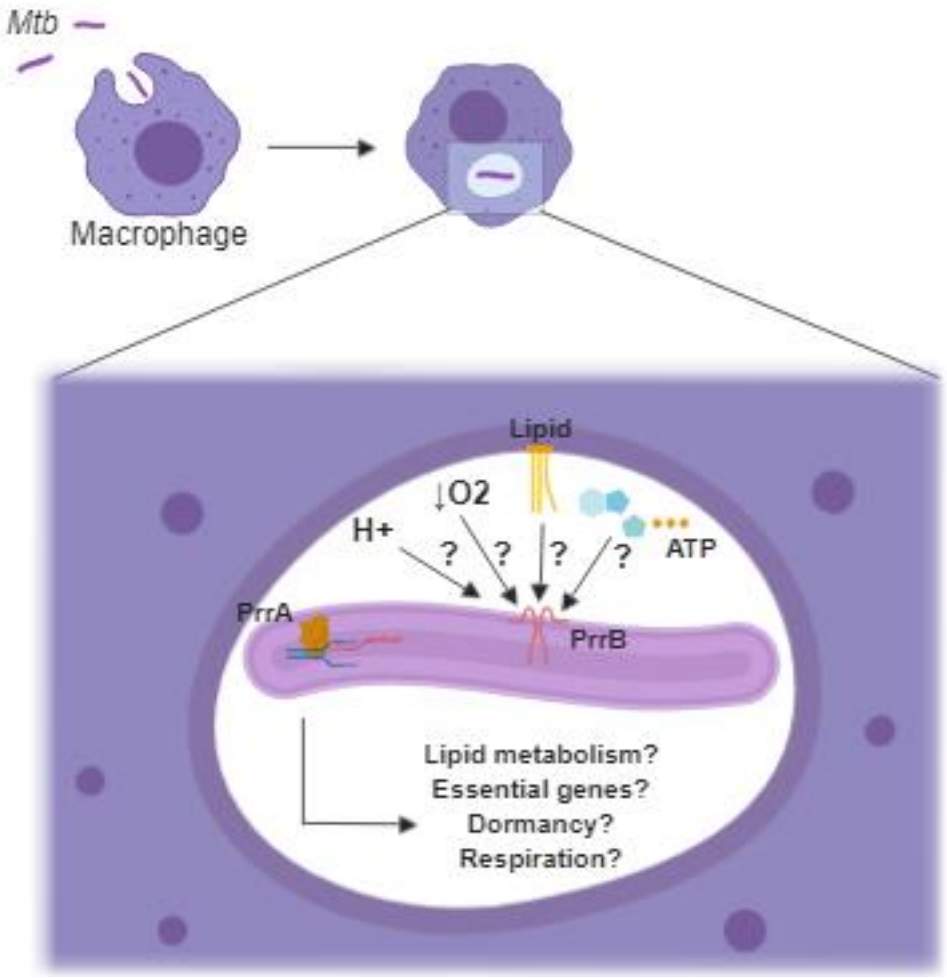

Figure 1.3. Putative PrrB environmental signals and PrrA genetic responses in *Mtb* during infection.

The *Mtb* PrrAB TCS as a Potential Therapeutic Target

The essential nature of the *Mtb prrAB* TCS suggests that its protein products, PrrA and PrrB, are promising drug targets. Diarylthiazole compounds possess antituberculosis activity in vitro and in

differentiated THP-1 monocytes (Bellale et al. 2014). *Mtb* diarylthiazole resistance correlates with mutations in *prrB* that map to the interface of the extracellular region near the second transmembrane helix (Bellale et al. 2014). Fatostatin, also a diarylthiazole compound (Choi et al. 2003), exerts antiobesity properties in mice by binding to and inhibiting sterol-cleavage activating protein (SCAP) in the endoplasmic reticulum. This event inhibits proteolytic release of sterol regulatory element-binding protein (SREBP), a transcription factor that modulates expression of fatty acid and cholesterol biosynthetic genes in human and murine cells. Fatostatin treatment in eukaryotic cells decreases tissue cholesterol levels (Kamisuki et al. 2009), which is required for *Mtb* phagocytosis by macrophages (Gatfield and Pieters 2000) and long-term persistence during infection (Pandey 2008). *Mtb* genes essential for cholesterol metabolism have been defined by *Himar1*-based transposon mutagenesis and highly-parallel deep sequencing (Griffin et al. 2011). *Mtb* exposed to diarylthiazoles upregulates genes participating in fatty acid catabolism, anaerobic/microaerophilic respiratory systems, and oxidoreductases while downregulating ribosomal protein, tRNA synthase, and RNA synthesis genes (Bellale et al. 2014). Additional work is needed to determine whether diarlythiazole compounds mediate antituberculosis activity through direct binding to PrrB or if diarylthiazole-resistant mutants harbor additional unreported chromosomal mutations that compensate for putative loss of PrrB activity.

M. smegmatis **as a Genetic Model for** ***Mtb***

M. smegmatis is a saprophytic bacterium initially isolated from human smegma, a secretion from sebaceous glands in human genitalia (T. Alvarez 1885), however, the bacterium naturally resides in soil deposits (Tsukamura 1976). *M. smegmatis* is infrequently associated with opportunistic infections in immunocompetent individuals. *M. smegmatis* has been implicated in soft tissue and endocardial infections, lymphadenitis, osteomyelitis (Wallace et al. 1988), and pneumonia (Cox, Heil, and Kleiman 1994; Ergan et al. 2004). To date, one fatality has been attributed to *M. smegmatis* infection in a 3-year old Italian child with interferon gamma receptor deficiency (Pierre-Audigier et al. 1997). Though it is generally accepted that *M. smegmatis* is a relatively non-pathogenic mycobacterium, sporadic cases has surfaced that implicate this

mycobacterium as capable of infecting immunocompetent individuals (Saffo and Ognjan 2016; Butt and Tirmizi 2019).

M. smegmatis is a commonly used mycobacterial model organism due to its safe handling (BSL-1) and rapid doubling time relative to *Mtb* (3 hours (h) vs. 24 h, respectively). Furthermore, *Mtb* and *M. smegmatis* share ~2,000 gene homologues, making *M. smegmatis* a popular surrogate model to study *Mtb* genetics (Reyrat and Kahn 2001). The *M. smegmatis* strain mc^2155 exhibits high transformation efficiency which promoted widespread use of this strain for plasmid-based genetic manipulation (Snapper et al. 1990). Studies using *M. smegmatis* promoted advances in plasmid (Knipfer, Seth, and Shrader 1997; Saviola and Bishai 2004), phage-based (Bardarov et al. 2002), and recombineering (van Kessel and Hatfull 2007) allelic-exchange methods and contributed to our modern toolbox of mycobacterial genetic manipulation techniques, thus revolutionizing our current understanding of *Mtb* pathogenesis.

M. smegmatis has been important for determining the targets and actions of antituberculosis drugs. *Mtb* isoniazid resistance was elucidated utilizing *M. smegmatis* isoniazid-resistant strains (Zhang et al. 1992; Payton et al. 1999; Larsen et al. 2002). *M. smegmatis* RNA polymerase was used to describe the mechanism of action and resistance to rifampicin (Levin and Hatfull 1993). The inhibitory action of pyrazinamide on mycobacterial fatty acid synthase I (FasI) was demonstrated by overexpressing *Mtb* or *M. bovis* BCG *fasI* in *M. smegmatis* (Zimhony et al. 2000). Activation of the pro-drug form of ethionamide was described using *M. smegmatis* to screen a genomic DNA library from ethionamide-resistant *Mtb* strains, which identified the *ethR* gene (Baulard et al. 2000). From a clinical standpoint, *M. smegmatis* has been an invaluable model organism to promote our understanding of the mechanisms of action and resistance of important antituberculosis drugs.

Despite the extensive use of *M. smegmatis* as an *Mtb* surrogate model, important differences between these species deserve attention. A salient distinction is reflected by the fact that *M. smegmatis* does not establish long-term infection in macrophages, owing in part to the inability to prevent phagolysosome fusion (Anes et al. 2006). The oxidative stress response, a crucial macrophage antituberculosis defense mechanism (MacMicking et al. 1997), is markedly

different between pathogenic and non-pathogenic mycobacteria (Sherman et al. 1995). Furthermore, *M. smegmatis* possesses additional iron acquisition mechanisms (De Voss et al. 1999) and is more resistant to the front-line antituberculosis drug, isoniazid (Larsen et al. 2002; Taneja and Tyagi 2007). Large-scale duplications in regions of the *M. smegmatis* chromosome harboring *Mtb* virulence gene homologues also complicate interpretation of comparative genetic studies (Galamba et al. 2001; Warner et al. 2006). Though information gleaned from studies in *M. smegmatis* have advanced our understanding of *Mtb* genetics and physiology, important disparities between these mycobacterial species exist which necessitates studies in *Mtb*.

Nitrogen Metabolism in Mycobacteria

Nitrogen and nitrogenous derivatives are ubiquitous and essential components of the cellular biochemical repertoire. DNA, RNA, and amino acids are traditional examples of nitrogenous molecules found in all organisms. Peptidoglycan, an essential polymer for maintaining the integrity of most bacterial cell walls, is composed of repeating amino sugars [*N*-glycolyl-muramic acid in mycobacteria (Petit et al. 1969)] crosslinked by a tetrapeptide. The mycobacterial inner membrane contains phosphatidylethanolamine, a nitrogenous phospholipid (Bansal-Mutalik and Nikaido 2014); therefore, nitrogen-containing biomolecules play important and diverse roles in both bacterial and eukaryotic organisms and are scrupulously regulated.

The ability to sense nitrogen levels and enact appropriate genetic responses are important for bacterial nitrogen homeostasis. Two transcription factors are recognized as important regulators of nitrogen metabolism in *M. smegmatis*: GlnR and AmtR (Jessberger et al. 2013; Amon et al. 2008). GlnR is the global regulator of intracellular nitrogen status in *M. smegmatis* whereas AmtR regulates far fewer genes in response to nitrogen limitation (Jenkins et al. 2013). In contrast, AmtR is the global regulator of nitrogen metabolism in corynebacteria (Walter et al. 2007), therefore highlighting discrepancies in regulatory control of nitrogen-responsive mechanisms between these genera, despite their evolutionary relatedness. The protective effects of GlnR on *M. smegmatis* viability during nitrogen limitation coincide with depletion of extracellular ammonium (Jenkins, Robertson, and Williams 2012). Currently, there is

a paucity of empirical evidence for genetic regulation of nitrogen metabolism in *Mtb*. The *Mtb* GlnR homologue (*Rv0818*) regulates the *nirBD* nitrite reductase genes (Malm et al. 2009) and is upregulated during *ex vivo* macrophage infection (Schnappinger et al. 2003), potentially in response to low intraphagosomal nitrogen status; however, this claim has not been substantiated. Furthermore, an *Mtb glnR* mutant fails to grow when nitrate is supplemented as the sole carbon source, supporting the positive regulation of *nirBD* by *Mtb* GlnR (Malm et al. 2009). Gene expression profiles of the *M. smegmatis* and *Mtb* GlnR regulons (i.e., the set of genes regulated by a common transcriptional regulator) overlap, therefore suggesting redundant regulatory properties between these species (Williams et al. 2015).

Mycobacteria exploit an impressive spectrum of substrates to maintain nitrogen homeostasis. Ammonium (NH_4^+) is the simplest nitrogen source utilized by mycobacteria (Williams, Bryant, et al. 2013) and ammonium assimilation is mediated by the GS/GOGAT system (see below) (Harper et al. 2010). While studies of ammonium transport proteins in mycobacteria are generally lacking, the *M. smegmatis* genome harbors homologs of the *Corynebacterium glutamicum amtA* and *amtB* ammonium transporters (Walter et al. 2008). The *amtA* and *amtB* genes are controlled by the AmtR (Beckers et al. 2005) and GlnR (Amon et al. 2008b) transcriptional regulators in *C. glutamicum* and *M. smegmatis*, respectively. The *C. glutamicum* AmtA ammonium transporter is only expressed during nitrogen-limited conditions (Siewe et al. 1996) and transport is driven by the transmembrane potential (Meier-Wagner et al. 2001). AmtB ammonium transport activity is regulated by GlnK, a P_{II}-like protein (see below) which senses intracellular ammonium concentrations (Strosser et al. 2004). *M. smegmatis* ammonium transporters may bear functional similarities as those seen in *C. glutamicum*, though empirical observations to support this hypothesis are lacking.

Mycobacteria are capable of assimilating nitrogenous substrates other than ammonium. *M. smegmatis* and *Mtb* can utilize nitrate (Khan et al. 2008; Malm et al. 2009) and urea (W. Lin, Mathys, Ang, Koh, Martinez Gomez, et al. 2012; Petridis et al. 2016) as sole nitrogen sources. The ability to assimilate multiple nitrogen sources benefits *M. smegmatis*, as nitrate (Ascott et al. 2017) and urea (Rochette et al. 2013) are constituents of soil, the saprophyte's natural ecological

niche. Nitric oxide produced by human macrophages infected with *Mtb* and *M. bovis* BCG may be oxidized and assimilated via nitrate reductase to serve as a nitrogen source within the host phagosome (Jung et al. 2013). *Mtb* urease mutants are not attenuated during murine infection, indicating that urea is not an important source of nitrogen in this setting (W.W. Lin, Mathys, Ang, Koh, Gomez, et al. 2012). *Mtb* and *M. smegmatis* can also utilize some amino acids as sole nitrogen sources (Lofthouse et al. 2013; Jessberger et al. 2013). Aspartate (Gouzy et al. 2013) and asparagine (Gouzy et al. 2014) are available nitrogen sources during *Mtb* infection. Mycobacteria therefore capitalize on a diverse range of nitrogenous substrates, possibly to promote growth when nutrients are limited or subject to oscillating availability. However, it's worth noting that nitrogen status and substrate availability in the natural environments that mycobacteria occupy have not been extensively explored and, hence, the available data derives from controlled in vitro or *ex vivo* studies. Future technological advances in culture conditions and detections systems are required to definitively translate laboratory conditions to real-world scenarios, especially in the context of *Mtb* infection.

Nitrogen metabolism in bacteria is subject to multiple regulatory checkpoints and control mechanisms. Glutamine synthetase (GS) is the key nitrogen-assimilating enzyme in bacteria. In *Escherichia coli*, GlnE reversibly adenylylates GS in a manner dependent on nitrogen availability: nitrogen sufficiency stimulates GS adenylylation (inhibition) whereas nitrogen limitation stimulates GS deadenylylation (activation) (Jaggi et al. 1997; Kingdon, Shapiro, and Stadtman 1967). GlnE adenylylation/deadenylylation activity is regulated through direct interactions with both GlnB (P_{II}) (Jiang, Mayo, and Ninfa 2007) and GlnK (Atkinson and Ninfa 1999). GlnD reversibly uridylylates GlnB and GlnK to promote GlnE-mediated activation of GS while GlnD deuridylylation activity on GlnB or GlnK stimulates GlnE-mediated inhibition of GS. *Mtb* GlnD differs from the *E. coli* isoform in that it possesses adenylyltransferase activity on GlnK, however, GS activity is independent of GlnD during nitrogen limitation, suggesting that GlnE may be regulated by another, currently unknown regulatory protein (Williams, Bennett, et al. 2013). See Fig. 1.4 for a visual depiction of this bicyclic regulatory cascade. *Mtb* lacks a *glnB* homologue and *glnK* is believed to serve as the sole P_{II}-like protein in this species (Cole et al. 1998; Williams, Bennett, et al. 2013). The *Mtb* GlnE

is a modular protein containing deadenylylation and adenylylation domains at the N- and C-terminal regions, respectively, and is essential for viability (Parish and Stoker 2000). Further studies are needed to decipher the upstream regulators, if any exist, of GlnE in mycobacteria.

Ammonium assimilation is accomplished through two enzymatic systems: glutamate dehydrogenase and glutamine synthase-glutamine oxoglutarate aminotransferase (GS/GOGAT). Each will be discussed in the following sections. In mycobacteria, the ATP-dependent, high-affinity GS/GOGAT system is the preferred route of ammonium assimilation during nitrogen limitation whereas glutamate dehydrogenase is relatively insensitive to the extracellular nitrogen status (Harper et al. 2010). As described above, GS activity is regulated by GlnE. GS assimilates nitrogen by incorporating ammonium into glutamate to form glutamine (Fig. 1.4). The *Mtb* genome harbors four GS homologues (Cole et al. 1998) but only the *glnA1* product is appreciably active and is an essential virulence factor (Tullius, Harth, and Horwitz 2003). Furthermore, an *Mtb glnA1* mutant is auxotrophic for glutamine (Tullius, Harth, and Horwitz 2003). In *M. smegmatis*, *glnA1* is transcriptionally regulated by GlnR and expression increases upon nitrogen deprivation (Amon et al. 2008). GS is secreted by pathogenic mycobacteria and generates poly-L-glutamate/glutamine, a constituent of the *Mtb* (Harth and Horwitz 1999) and *M. bovis* (Tripathi, Chandra, and Bhatnagar 2013) cell walls. MSX is a potent GS inhibitor (Manning et al. 1969) and inhibits growth of *Mtb*, *M. bovis*, and *Mycobacterium avium* (Harth and Horwitz 1999). Growth inhibition by MSX is likely mediated by disrupting synthesis of the poly-L-glutamate/glutamine component of the cell wall (Harth and Horwitz 1999). Intracellular GS activity is relatively unaffected by MSX, suggesting that MSX is unable to permeate into the cytoplasm (Harth and Horwitz 1999). These features are pathogen-specific, as non-pathogenic species, such as *M. smegmatis* and *Mycobacterium phlei,* are not inhibited by MSX, do not secrete GS, and lack poly-L-glutamate/glutamine cell wall structures (Harth and Horwitz 1999). The *M. smegmatis* genome harbors four annotated and three putative GS genes. GS activity is inversely related to ammonium availability (Harper et al. 2010), similar to the related Actinomycete, *C. glutamicum* (Schulz, Collett, and Reid 2001). GS is therefore an important ammonium assimilating enzyme in

both pathogenic and non-pathogenic mycobacteria and plays a pivotal role in nitrogen assimilatory processes.

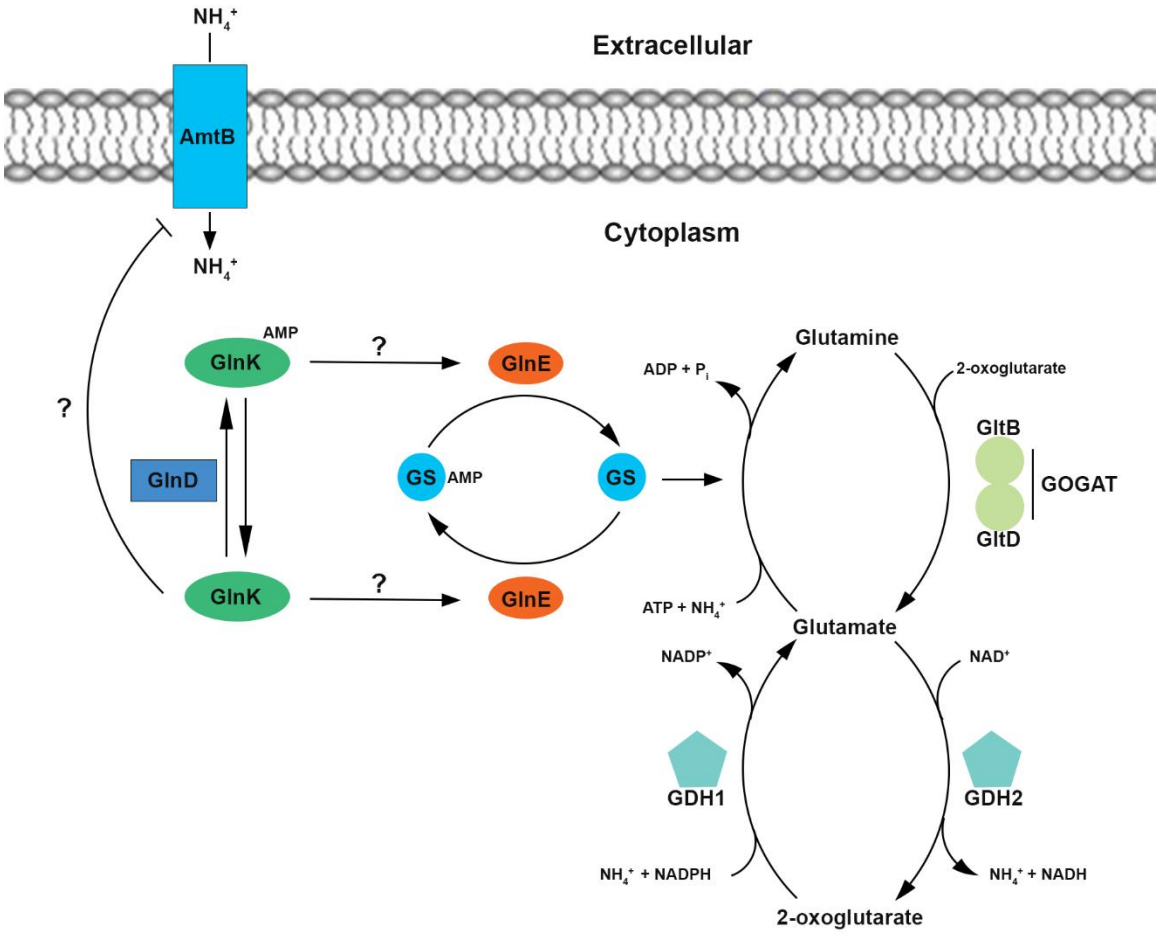

Figure 1.4. Regulation of nitrogen assimilatory pathways in mycobacteria. GlnD, Regulatory steps analogous to *E. coli* or *C. glutamicum* but not reported in mycobacteria are indicated by question marks (?). GlnD, GlnK adenylyltransferase; GlnK, P_{II}-like protein; GlnE, GS adenylyltransferase; GltB-GltD, Glutamate synthase (GOGAT); GDH, glutamate dehydrogenase. AmtB, ammonium transporter.

Glutamate synthase (GOGAT) is a heterodimeric enzyme composed of GltD and GltB subunits that are part of the GS/GOGAT system. GOGAT participates in nitrogen assimilation by incorporating ammonium from glutamine into 2-oxoglutarate to generate two molecules of glutamate (Fig. 1.4). The *C. glutamicum gltB* and *gltD* genes are upregulated during nitrogen limitation through relief of inhibition by AmtR (Beckers, Nolden, and Burkovski 2001). Similarly,

nitrogen starvation induces *gltB* and *gltD* expression in *M. smegmatis*, however, the transcriptional regulator responsible for this phenotype was not reported (Jessberger et al. 2013). Less evidence exists for GOGAT regulation in mycobacteria. *M. bovis* BCG GOGAT mutants and not viable in a medium containing ammonium as the sole nitrogen source and require glutamine supplementation for optimal growth (Viljoen et al. 2013). Further studies are needed to determine the fitness of *Mtb* GOGAT mutants during infection.

The second ammonium assimilation pathway in bacteria is performed by the low-affinity glutamate dehydrogenase (GDH). GDH exists as NADPH-dependent (GDH1) or NAD^+-dependent (GDH2) isoforms, which participate in glutamate anabolism and catabolism, respectively (Fig. 1.4). In *M. smegmatis*, the ammonium-assimilating activity of GDH1 is responsive during the first hour of in vitro ammonium limitation (3 mM NH_4^+) whereas the deaminating GDH2 activity remained unchanged after 4 h of ammonium limitation (Harper et al. 2010). An *M. bovis* BCG *gdh* mutant is severely impaired for growth in minimal 7H9 medium supplemented with L-glutamine and L-asparagine as sole nitrogen sources; ammonium supplementation is required to restore growth (Viljoen et al. 2013). *M. bovis* BCG cells require GDH to utilize glutamate as a sole carbon source and *gdh* mutants are hyper-susceptible to acid and nitrosative stress, which was reversed with ammonium supplementation (Gallant et al. 2016). Furthermore, the *M. bovis* BCG *gdh* mutant is attenuated during residence within macrophages, indicating a protective role for GDH during infection (Gallant et al. 2016). When phosphorylated by PknG, GarA (glycogen accumulation regulator) binds to and inhibits GDH activity, suggesting an additional layer of glutamate metabolic regulation in *M. smegmatis* (O'Hare et al. 2008). Though relatively fewer studies have addressed the biochemical roles of GDH relative to the GS/GOGAT system, GDH plays an important role in mycobacterial glutamate metabolism and promotes the infectious process in pathogenic mycobacteria.

Mycobacterial Lipids

Acid-fast mycobacteria are a lipid-rich genus of bacteria with up to 60% of the cellular dry weight represented by lipids (Wang et al. 2000). Mycobacteria are genetically classified as Gram-

positive bacteria, however, evidence for a relatively symmetrical outer membrane lipid bilayer and a periplasmic region analogous to Gram-negative organisms has been unambiguously identified (Hoffmann et al. 2008). The peptidoglycan layer is covalently linked to a linear chain of repeating 5- and 6-linked β-D-galactose polymers which in turn are bound to a network of branched arabinofuranose polysaccharides (Daffe, Brennan, and McNeil 1990). Arabinan polymerization is inhibited by ethambutol, a primary drug used to treat tuberculosis, thus highlighting the importance of arabinogalactan biosynthesis in mycobacterial physiology (Belanger et al. 1996). Mycolic acids are esterified to the terminal ends of the arabinofuranose chains (Daffe, Brennan, and McNeil 1990) to complete the mycolic acid-arabinogalactan-peptidoglycan complex.

Mycolic acids are long-chain fatty acids containing up to 90 carbon atoms in length (Barry et al. 1998). Mycolic acids fall into five main classes; α-mycolates, α'-mycolates, ketomycolates, epoxymycolates, and methyoxymycolates (Barry et al. 1998). *Mtb* and *M. smegmatis* both express α-mycolates; ketomycolates and methoxymycolates are restricted to *Mtb*; and α'-mycolates and epoxymycolates are found in *M. smegmatis* (Barry et al. 1998). Mycolic acids are essential in mycobacteria, as highlighted by the bactericidal action of the primary antituberculosis drug, isoniazid, an inhibitor of mycolic acid biosynthesis (Mdluli et al. 1998). Trehalose dimycolate, also known as "cord factor", is a non-covalently bound mycolic acid-containing glycolipid that possesses immunomodulatory properties (Indrigo, Hunter, and Actor 2003; Werninghaus et al. 2009). Trehalose dimycolate is synthesized by members of the antigen 85 (Ag85) complex (designated as Ag85-A, -B, and -C) which are promising vaccine candidates (Dhar, Rao, and Tyagi 2004; Giri, Verma, and Khuller 2006; Pabreja et al. 2016). Mycolic acids protect against desiccation (Harland et al. 2008), repel hydrophilic antibiotics (Nguyen, Chinnapapagari, and Thompson 2005), and are important virulence factors (Forrellad et al. 2013), thus contributing pivotal protective roles in both environmental and infectious settings.

The mycobacterial outer membrane consists of a diverse collection of readily extractable lipids. In *M. smegmatis*, these lipid species include phosphatidylinositol mannosides, glycopeptidolipids, free mycolic acids, and di- and triacylglycerols (DAGs and TAGs, respectively) (Bansal-Mutalik and Nikaido 2014). Few bacteria are capable of synthesizing TAGs and most

known species that accomplish this task belong to the Actinomycetes, such as *Gordonia* (Indest et al. 2015a), *Streptomyces* (Arabolaza et al. 2008b), *Nocardia* (H.M. Alvarez et al. 2001), *Rhodococcus* (Amara et al. 2016), and *Mycobacteria* (Daniel et al. 2004). The *Mtb* H37Rv and *M. smegmatis* mc^2155 genomes harbor 10 and 6 annotated *ws/dgat* (wax synthase/diacylglycerol acyl-CoA transferase) genes, respectively, compared to 17 and 14 *ws/dgat* homologues in *Rhodococcus opacus* and *Rhodococcus jostii*, respectively (Hernandez et al. 2013). Chromosomal enrichment of *ws/dgat* homologues in Actinomycetes is not universal, however, as demonstrated by the presence of only three and one *ws/dgat* genes in *Streptomyces coelicolor* (Arabolaza et al. 2008) and *Streptomyces avermitilis* (Kaddor et al. 2009), respectively. De novo TAG biosynthesis proceeds through the Kennedy pathway, which sequentially esterifies acyl-CoA intermediates of various chain lengths to a glycerol-3-phosphate backbone (Alvarez 2016). WS/DGATs are the key enzymes mediating TAG biosynthesis and are generally promiscuous regarding the specificity in the length of their fatty acyl-CoA substrates (Kalscheuer and Steinbuchel 2003).

TAG accumulation is a dormancy-associated phenotype in *Mtb* (Daniel et al. 2004; Deb et al. 2009; Daniel et al. 2011) and *M. smegmatis* (Chen et al. 2006; Nazarova et al. 2011; Purdy et al. 2013). TAGs may serve as a long-term energy storage molecule during macrophage infection (Daniel et al. 2011). Multiple in vitro stresses that mimic the activated macrophage phagosome environment, such as hypoxia, nitric oxide, and low pH, elicit TAG accumulation in *Mtb* and induce phenotypic drug tolerance that is genetically dependent on TAG biosynthesis (Deb et al. 2009). The hypervirulent *Mtb* W-Beijing strain accumulates TAGs under favorable conditions during exponential growth, which may reflect overexpression of the dormancy-associated DosR TCS response regulator in this strain (Reed et al. 2007). *Mtb* utilizes fatty acids liberated from the lipid-loaded macrophage host to generate intracellular TAG stores (Daniel et al. 2011). Collectively, TAG accumulation and biosynthesis promote and contribute to *Mtb* survival within the host macrophage during chronic infection.

The effect of nitrogen status on the ability to induce a TAG-accumulating phenotype in bacteria was first demonstrated in *Streptomyces lividans* (Olukoshi and Packter 1994). Nitrogen

limitation induces TAG accumulation in Actinomycetes, including *R. opacus* (Waltermann et al. 2000; Alvarez, Kalscheuer, and Steinbuchel 2000), *Nocardia globerula* (Alvarez et al. 2001), and *M. smegmatis* (Garton et al. 2002). This phenomenon may represent a survival strategy to provide nutrient-deprived cells with an energy-dense carbon storage depot without negatively disrupting the intracellular osmotic balance (TAGs are electrically neutral) until favorable environmental conditions are restored. Few studies have explored transcriptional regulation of TAG accumulation during nitrogen limitation. The NlpR transcriptional regulator of *R. opaccus* and *R. josti* is expressed during in vitro nitrogen limitation and promotes TAG accumulation under these conditions (Hernandez et al. 2017). *nlpR* homologues are present in the *M. smegmatis, M. abscessus,* and *Mtb* chromosomes (Hernandez et al. 2017); however, the effects of NlpR on TAG accumulation have not been verified in mycobacteria.

Respiration and Oxidative Phosphorylation in Mycobacteria

Mycobacteria are classified as obligate aerobes, although both *Mtb* and *M. smegmatis* genomes encode for anaerobic respiratory complexes capable of maintaining respiration through alternative electron acceptors (e.g., nitrate) during hypoxic conditions (Cook et al. 2014). In humans, *Mtb*-laden necrotic granulomas are believed to be hypoxic, as evidenced by lack of endothelial cell proliferation (Tsai et al. 2006) and the unique activity of metronidazole, which is inhibits *Mtb* only under hypoxic conditions (Wayne and Sramek 1994). Based on this evidence, it is proposed that *Mtb* expresses anaerobic/microaerophilic respiratory complexes to maintain redox balance and ATP homeostasis during periods of non-replicating dormancy (Voskuil, Visconti, and Schoolnik 2004). The precarious environments in which both pathogenic and saprophytic mycobacteria reside favor expressing multiple aerobic and anaerobic respiratory systems for maintaining respiratory capacity during uncertain periods of oxygen availability.

Mtb and *M. smegmatis* express two terminal aerobic respiratory branches: the cytochrome bc_1-aa_3 and cytochrome *bd* oxidases. In *M. smegmatis*, the bc_1 menaquinone-cytochrome c oxidoreductase (QcrCAB) forms a detergent-resistant supercomplex with the aa_3 cytochrome c oxidase (CtaBCDE) (Megehee, Hosler, and Lundrigan 2006). Similar interactions

between the bc_1-aa_3 complexes are found in the related species, *C. glutamicum* (Niebisch and Bott 2003). Cytochrome *bd* oxidase is a high-affinity respiratory complex composed of CydA and CydB subunits that are primarily active under low oxygen tensions (Kana et al. 2001). Both terminal respiratory branches couple the flow of electrons from NADH:menaquinone dehydrogenases (NDH-1 and NDH-2) or succinate dehydrogenases (SDH1 and SDH2) via reduced menaquinones to the reduction of molecular oxygen. The bc_1 and aa_3 oxidoreductases actively pump protons into the extracellular space to maintain the proton motive force (PMF), whereas for the cytochrome *bd* complex, protons are passively translocated across the cell membrane to generate a membrane potential (Belevich et al. 2005).

The menaquinone:cytochrome c bc_1 oxidoreductase and cytochrome c aa_3 oxidase form the principle terminal aerobic respiratory complex in mycobacteria (Matsoso et al. 2005) (Fig. 1.5). The cytochrome bc_1 and aa_3 complexes actively pump a combined $6H^+/2e^-$ into the extracellular space to maintain the PMF (Graf et al. 2016). This activity is accomplished through oxidation of the menaquinone pool by the bc_1 complex which subsequently transfers electrons to the aa_3 component with concomitant reduction of molecular oxygen to H_2O. The bc_1 complex is encoded by the *qcrCAB* operon in both *Mtb* and *M. smegmatis* (Matsoso et al. 2005). QcrA is a membrane-bound protein containing a Rieske iron-sulfur center; QcrB contains two *b*-type hemes; and QcrC contains one cytochrome c_1 heme (Cook et al. 2014). Both the *Mtb* and *M. smegmatis* genomes harbor single copies of the *qcrCAB* operon. In *Mtb*, a functional bc_1-aa_3 pathway is essential for viability (Matsoso et al. 2005). In contrast, *M. smegmatis* can sustain interruption of the *qcrCAB* operon and the resulting mutants exhibit growth deficiencies under atmospheric oxygen (Matsoso et al. 2005). The cytochrome c aa_3 oxidase is encoded by *ctaB, ctaC, ctaD,* and *ctaE* subunits, which are located in separate chromosomal regions. CtaB is a cytochrome c oxidase assembly factor; CtaC is a copper A-containing cytochrome c oxidase; CtaD contains *a*, a_3, and copper B-type hemes; and CtaE is a copper-containing cytochrome c oxidase (Cook et al. 2014). The *Mtb* genome encodes single copies of each cytochrome c aa_3 oxidase subunit whereas *M. smegmatis* harbors three *ctaD* alleles: two *ctaD1* genes and one

ctaD2 allele (Matsoso et al. 2005). At least one *ctaD1* gene is required for viability in *M. smegmatis*; however, the *ctaD2* allele is dispensable (Matsoso et al. 2005).

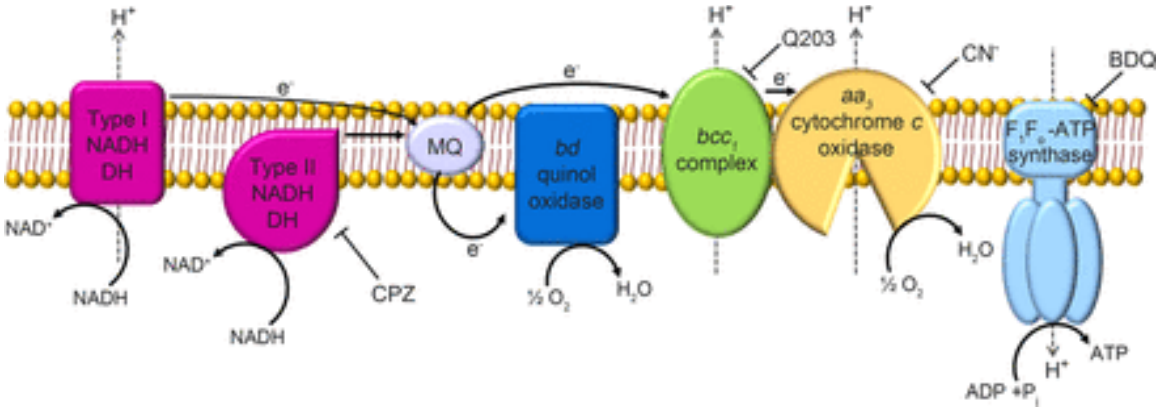

Fig. 1.5. The mycobacterial respiratory chain. BDQ, bedaquiline; CPZ, chlorpromazine; CN^-, cyanide; MQ, menaquinone. From Ji-A Jeong et al. Journal of Bacteriology. 2018; doi:10.1128/JB.00152-18.

The *Mtb* respiratory chain has garnered increased interest over the past decade as a therapeutic target. Inhibitors of the cytochrome bc_1 complex include the imidazopyridine analogs (Pethe et al. 2013; Arora et al. 2014), the human gastric proton pump inhibitor, lansoprazole (Rybniker et al. 2015), and 2-(quinolin-4-yloxy)acetamides (Phummarin et al. 2016). No pharmacologic inhibitors of the mycobacterial aa_3 cytochrome c oxidase have been reported to date.

Though classified as obligate aerobes, *Mtb* and *M. smegmatis* are capable of surviving hypoxic conditions by entering two sequential states of non-replicating persistence. These states are marked by downregulation of growth, DNA replication, and reduced RNA and ATP synthesis while maintaining basal levels of bacterial viability (Wayne and Hayes 1996). Additionally, states of non-replicating persistence are accompanied by induction of the DosR dormancy regulon (Voskuil, Visconti, and Schoolnik 2004), expression of nitrate transport (*narK2*) and nitrate reductase (*narGHJI*) genes, and upregulation of the cytochrome *bd* oxidase *cydA* and *cydB* genes (Shi et al. 2005).

During periods of hypoxia, *Mtb* and *M. smegmatis* can utilize alternative electron donors to maintain a transmembrane PMF for ATP generation via oxidative phosphorylation and to recycle NADH to NAD^+. Examples of alternative electron donors include malate (Mogi et al. 2009), H_2 (Berney and Cook 2010), proline (Tanner 2008), and nitrate (Sohaskey 2008), which are coupled to malate:menaquinone oxidoreductase, hydrogenase, proline dehydrogenase, and nitrate reductase, respectively. Nitrate promotes *Mtb* viability during rapid oxygen depletion, which otherwise results in significant loss of viability (Sohaskey 2008). *M. bovis* BCG mutants lacking nitrate reductase (*narGHJI*) fail to persist in BALB/c mice (Fritz et al. 2002). No information exists for a protective role of nitrate reductase in *Mtb* during in vivo infection; however, the *narX* nitrate reductase gene is upregulated in activated macrophages (Schnappinger et al. 2003), suggesting that *Mtb* enacts anaerobic respiratory programs in this setting and possibly during chronic infection in humans.

The cytochrome *bd* oxidase (CydAB) is a high-affinity terminal respiratory complex induced in *Mtb* (Voskiul 2004) and *M. smegmatis* (Kana et al. 2001) during microaerophilic and hypoxic conditions (Fig. 1.5). In many bacterial species, the cytochrome *bd* oxidase is relatively insensitive to inhibition by cyanide (Cunningham, Pitt, and Williams 1997; Kana et al. 2001; Voggu et al. 2006; Korshunov, Imlay, and Imlay 2016). In addition to its role in oxygen scavenging, the cytochrome *bd* oxidase also protects against oxidative (Borisov et al. 2013; Lu et al. 2015) and nitrosative (Giuffre et al. 2012) stresses. *Mtb* (Berney, Hartman, and Jacobs 2014) and *M. smegmatis* (Lu et al. 2015) cytochrome *bd* oxidase mutants are hypersensitive to the inhibitory effects of the ATP synthase inhibitor, bedaquiline. These findings suggest that cytochrome *bd* oxidase inhibitors, such as aurachin D (Lu et al. 2015), could be considered as adjunct therapy in combination with bedaquiline during *Mtb* infection.

Oxidative phosphorylation generates ATP through the free energy released by proton translocation across the membrane-bound F_1F_0 ATP synthase. Protons are pumped into the extracellular space by NDH-1 ($4H^+/2e^-$) and the bc_1-aa_3 cytochrome c oxidoreductase complex ($6H^+/2e^-$) under aerobic conditions to maintain the transmembrane PMF. At neutral extracellular pH (pH 7.0), actively growing aerobic cultures of *M. smegmatis*, *M. bovis* BCG, and *Mtb* maintain

a PMF of approximately -180 mV, -100 mV, and -115 mV, respectively (M. Rao et al. 2001; S.P. Rao et al. 2008). These values compare with -160 mV in the related Actinomycete, *C. glutamicum* (Bayan et al. 1993), and -240 mV in *E. coli* (Kashket 1981) cultured under similar conditions. The PMF is maintained in hypoxic, non-replicating *Mtb* cultures, despite the 5-fold decrease in intracellular ATP relative to aerobic cultures (S.P. Rao et al. 2008). Protons flow down the electrochemical gradient and through the F_1F_0 ATP synthase where ATP is generated from ADP and inorganic phosphate (P_i) using the free energy released from proton translocation.

The mycobacterial F_1F_0 ATP synthase is transcribed as an operon (*atpBEFHAGDC*) and is essential in *M. smegmatis* (Tran and Cook 2005) and, presumably, other mycobacteria. In mycobacteria, the F_1F_0 ATP synthase machinery does not exhibit ATP hydrolysis activity, indicating that ATP synthesis is a unidirectional process (Haagsma et al. 2010), similar to *B. subtilis* (Hicks, Cohen, and Krulwich 1994) and *Thermus thermophilus* (Nakano et al. 2008). *Mtb* downregulates expression of *atp* genes during in vitro non-replicating states (Shi et al. 2005; S.P. Rao et al. 2008; Gengenbacher et al. 2010) and murine infection (Tian, Bryk, Shi, et al. 2005), suggesting this dormancy-associated phenomenon is utilized to cope with limited nutrient and/or oxygen availability while maintaining basal ATP levels to sustain viability.

The *Mtb* F_1F_0 ATP synthase subunit c (AtpE) is the target of the recently-approved antituberculosis agent, bedaquiline (TMC207), which is active against drug-susceptible and drug-resistant *Mtb* (Worley and Estrada 2014) (Fig. 1.5). Bedaquiline is believed to inhibit ATP synthase by preventing rotary movement between subunits a and c, thereby precluding proton translocation (de Jonge et al. 2007; Haagsma et al. 2011). Hards et al. later demonstrated that the bactericidal action of bedaquiline is mediated by uncoupling proton movement through the ATP synthase (Hards et al. 2015). In this model, bedaquiline binds to AtpE and disrupts interactions between subunits a and c, therefore causing protons to leak into and acidify the cytoplasm without concomitant generation of ATP (Hards et al. 2015). While resistance to bedaquiline in *Mtb* was originally associated with mutations in the AtpE subunit (Andries et al. 2005; Petrella et al. 2006; Segala et al. 2012), mutations in the MmpL5 efflux pump (Hartkoorn, Uplekar, and Cole 2014) and, to a lesser degree, the PepQ aminopeptidase (Almeida et al. 2016)

confer cross resistance to both bedaquiline and clofazimine, indicating *Mtb* possesses multiple mutational routes to escape the bactericidal action of bedaquiline.

Mycobacterial Dormancy and the DosRS Two-Component Regulatory System

If *Mtb* escapes the bactericidal attempts of the host macrophage, the bacterium establishes latent infection, characterized by long-term persistence and entrance into a non-replicative state accompanied by clinical conversion to negative sputum smears (Wayne and Sohaskey 2001). Phenotypic traits of dormancy include loss of acid-fast staining (Seiler et al. 2003), TAG accumulation (Deb et al. 2009), and antibiotic tolerance (Wayne and Hayes 1996). Dormant *Mtb* cells downregulate genes involved in aerobic respiration, ATP synthase, and ribosomal proteins (Shi et al. 2005; Keren et al. 2011). In contrast, genes of microaerophilic/anaerobic respiratory complexes (Shi et al. 2005), glyoxylate shunt, and gluconeogenesis (Timm et al. 2003) are upregulated during dormancy.

Hypoxia (<2% O_2) is a potent inducer of the mycobacterial dormancy response which is relevant during infection, as human granulomas are believed to be hypoxic (Tsai et al. 2006). Wayne and colleagues developed an in vitro system of progressive oxygen depletion and demonstrated that *Mtb* transitions through two stages of non-replicating persistence. These stages are associated with metabolic shift-down (Wayne and Hayes 1996) and upregulation of isocitrate lyase and glycine dehydrogenase activities (Wayne and Lin 1982). *Mtb* cultures experience a significant loss of viability upon rapid oxygen depletion, suggesting that a concerted series of adaptations are required to successfully transition to non-replicating persistence (Wayne and Lin 1982). This phenomenon is not restricted to *Mtb,* as other mycobacteria exhibit similar patterns of hypoxia-induced dormancy, including *M. smegmatis* (Dick, Lee, and Murugasu-Oei 1998), *M. bovis* BCG (Boon et al. 2001), and *M. avium* spp. paratuberculosis (Gumber et al. 2009), indicating a conserved mycobacterial adaptive response to hypoxia, despite their classification as obligate aerobes.

Mtb responds to hypoxia by upregulating genes of the dormancy regulon achieved through activation of the hypoxia-responsive DosRS (and DosT) TCS (Park et al. 2003). DosR

(dormancy survival regulator), belongs to the LuxR family of TCS response regulators (Dasgupta et al. 2000) and is regulated by the DosS (Saini et al. 2004) and DosT (Roberts et al. 2004) histidine kinases (herein referred to as the DosRS-DosT TCS). The DosR regulon is composed of ~49 genes and is activated during hypoxia (Park et al. 2003), nitric oxide (Voskuil et al. 2003), carbon monoxide (Shiloh, Manzanillo, and Cox 2008), and perturbations of electron flux through respiratory systems (Honaker et al. 2010). The DosRS-DosT TCS promotes viability under hypoxic conditions (Boon and Dick 2002; O'Toole et al. 2003; Majumdar et al. 2012). Malhotra et al. demonstrated that an *Mtb devR* mutant (later renamed *dosR* by Boon and Dick (Boon and Dick 2002)) was attenuated in a guinea pig infectious model (Malhotra et al. 2004). Converse et al. reported similar results in guinea pigs and additionally demonstrated that an *Mtb dosR* mutant was attenuated in mice and, to a lesser extent, rabbits (Converse et al. 2009). Signaling through the DosRS-DosT TCS constitutes an important virulence factor in *Mtb* and provides protective measures during transitions to hypoxic environments encountered during chronic infection.

Carbon Metabolism in Mycobacteria

Mycobacteria are heterotrophic bacteria that utilize organic compounds for energy demands, cellular constituents, and biosynthetic processes. The *Mtb* (Cole et al. 1998) and *M. smegmatis* (https://mycobrowser.epfl.ch/) genomes harbor all genes necessary for glycolysis, the pentose phosphate pathway, and a near-complete tricarboxylic acid (TCA) cycle (Fig. 1.6). A surprising feature of the *Mtb* genome was the extensive enrichment of lipid degradative genes, suggesting the pathogen was genetically adapted to thriving on a lipid-rich diet (Cole et al. 1998). Evidence for this hypothesis came decades earlier when Segal and Bloch demonstrated that when *Mtb* isolated from infected mice was cultured in vitro, the bacilli failed to thrive on glucose and glycerol, yet multiplied in the presence of fatty acids (Bloch and Segal 1956).

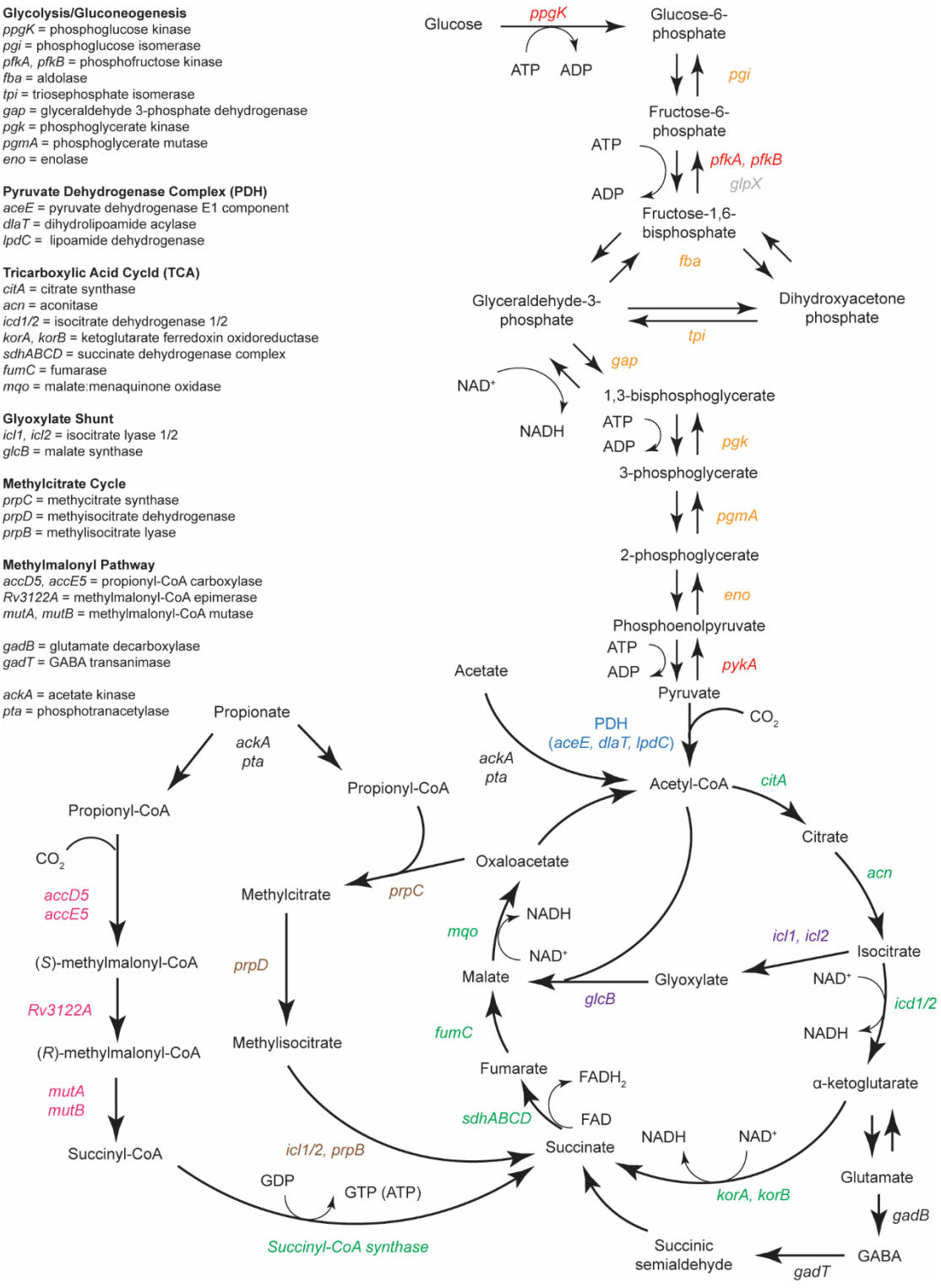

Figure 1.6. Central carbon metabolism in mycobacteria. Enzyme abbreviation color schemes are as follows: red, dedicated reactions of glycolysis; grey, dedicated enzymes of gluconeogenesis; orange, reversible reactions of glycolysis; blue, pyruvate dehydrogenase (PDH) complex; green, TCA cycle; black, GABA shunt; purple, glyoxylate shunt; brown, methylcitrate cycle; pink, methylmalonyl-CoA pathway. Adapted from (Rhee et al. 2011).

To survive on a lipolytic diet, bacteria must enzymatically convert fatty acid catabolites to essential biosynthetic intermediates normally generated through glycolysis. Gluconeogenesis, the formation of glucose from non-glycolytic metabolites, is especially important for *Mtb* during infection (Marrero et al. 2010), as is the glyoxylate shunt, a metabolic bypass of the TCA cycle during growth on fatty acids (Munoz-Elias and McKinney 2005). Propionyl-CoA, an end-product of odd-chain fatty acid and cholesterol metabolism, has its own dedicated metabolic pathway (methylcitrate cycle) which prevents accumulation of toxic intermediates (Upton and McKinney 2007). Bacteria have therefore evolved distinct central carbon metabolic pathways to subsist on a variety of organic substrates to cope with changing and often uncertain periods of nutrient availability.

Glycolysis, also known as the Embden-Myerhof pathway, is the preferred route of glucose catabolism in most organisms (Fig. 1.6). The first step of glycolysis is the ATP-dependent phosphorylation, or “activation”, of glucose by glucokinase to generate glucose-6-phosphate (G6P) (Marrero et al. 2013). *Mtb* expresses two glucokinase isoforms: PPGK (polyphosphate glucokinase, *Rv2702*) and GLKA (glucokinase, *Rv0650*) (Marrero et al. 2013), both of which have homologues in *M. smegmatis*. PPGK is the predominantly active glucokinase in *Mtb* (Marrero et al. 2013). An *Mtb* Δ*ppgK*Δ*glkA* double-knockout mutant is attenuated after 60 d post-infection in the lungs, but not the spleens, of C57BL/6 mice (Marrero et al. 2013). However, the presence of either glucokinase alone restore virulence in a murine infection model (Marrero et al. 2013). G6P is then isomerized to fructose-6-phosphate by phosphoglucose isomerase (*pgi)*. *M. smegmatis* Δ*pgi* mutants are auxotrophic for glucose and fail to grow on glycerol, fructose, ribose, and succinate (Tuckman et al. 1997), suggesting an important role for Pgi during gluconeogenesis (see below). In the first committed ATP-dependent step in glycolysis, fructose-6-phosphate is phosphorylated by phosphofructokinase-1 (*pfk*) to generate fructose-1,6-bisphosphate. The *Mtb* genome harbors two *pfk* isoforms (*pfkA* and *pfkB*), but only PFKA is active in vitro (Phong et al. 2013). In *Mtb*, PFKA is necessary for growth on glucose as a sole carbon source, but not glycerol or acetate (Phong et al. 2013). Furthermore, PFKA is not required for *Mtb* virulence in BALB/c mice but is essential for long-term survival under in vitro hypoxia (Phong et al. 2013). Fructose-

1,6-bisphophate is cleaved by fructose-1,6-bisphosphate aldolase (*fba*) to generate two triose phosphates: glyceraldehyde-3-phosphate (G3P) and dihydroxyacetone phosphate (DHAP). *Mtb fba* is essential for virulence in C57BL/6 mice and bone marrow-derived murine macrophages, likely as a consequence of its role in gluconeogenesis (Puckett et al. 2014). DHAP is reversibly converted to G3P by triose phosphate isomerase (*tpi*). TPI represents a metabolic branch point between glycolysis, gluconeogenesis, the pentose phosphate pathway, and is the entry point for metabolites of glycerol entering glycolysis. *Mtb tpi* mutants require co-supplementation of glycolytic and gluconeogenic carbon sources to maintain viability in vitro (Trujillo et al. 2014). *Mtb* Δ*tpi* mutants fail to establish infection are rapidly cleared from the lungs of C57BL/6 mice (Trujillo et al. 2014). The two molecules of G3P generated per molecule of glucose completes the energy input phase of glycolysis, expending two molecules of ATP. G3P then enters the payoff phase of glycolysis where net generation of ATP occurs. G3P dehydrogenase (*gap*) oxidizes G3P to generate 1,3-bisphosphoglycerate (BPG) with the concomitant reduction of NAD^+ to NADH. *Mtb gap* is downregulated during in vitro nutrient starvation (Betts et al. 2002) and is predicted to be essential (Griffin et al. 2011). BPG is converted to 3-phosphoglycerate by phosphoglycerate kinase (*pgk*) with concomitant generation of ATP by substrate level phosphorylation. 3-phosphoglycerate is an important biosynthetic precursor of serine, glycine, and cysteine. *Mtb* PGK is Mg^{2+}-dependent and indispensable for growth (Griffin et al. 2011). 3-phosphoglycerate is isomerized to 2-phosphoglycerate by phosphoglycerate mutase. The *Mtb* genome harbors two phosphoglycerate mutase homologues: *Rv0489* (*gpm*) and *Rv3086c* (*pgmA*), the former of which is essential (Griffin et al. 2011). 2-phosphoglycerate is dehydrated by enolase (*Rv1023, eno*) to generate phosphoenolpyruvate (PEP), a key intermediate used in a variety of metabolic processes. Eno is an essential surface-exposed protein in *Mtb* that provides protective immunity in C57BL/6 mice after intravenous challenge with *Mtb*, suggesting its potential use as a vaccine candidate (Rahi et al. 2017). The final step in glycolysis is the transfer of P_i from PEP to ADP to generate pyruvate and ATP by pyruvate kinase (*pyk*), an essentially irreversible and rate-limiting reaction. Pyruvate kinase (PK) is inactive in some members of the *Mtb* complex, such as *M. bovis, Mycobacterium africanum*, and *Mycobacterium microti,* each of which require pyruvate

supplementation for in vitro growth (Keating et al. 2005). The *M. bovis pyk* gene has a single nucleotide polymorphism at the enzyme's active site (Glu220Asp) that renders PK inactive (Keating et al. 2005). *Mtb* Δ*pykA* mutants upregulate lipid degradation (β-oxidation) and downregulate lipid biosynthetic pathways (Chavadi et al. 2009). *Mtb* PK activity is indifferent to carbon availability (acetate or glucose), is required for co-catabolism of mixed carbon substrates, and is allosterically activated by G6P and AMP (adenosine monophosphate) (Noy et al. 2016) in a synergistic manner (Zhong et al. 2017). *Mtb* Δ*pykA* mutants are equally virulent as the wild-type strain in C57BL/6 mice (Noy et al. 2016). In summary, *Mtb* expresses a full complement of enzymes participating in glycolysis. Though fewer studies of this pathway have been conducted in *M. smegmatis*, the presence of genetic homologues for all genes of glycolysis suggest similar pathways operate in this nonpathogenic mycobacterium.

The TCA cycle, also known as the citrate cycle or the Krebs cycle from its discoverer, Hans Krebs, is an important metabolic pathway for utilizing pyruvate generated from glycolysis for energy production (Fig. 1.6). The TCA cycle is present in species from all kingdoms of life. An equally important function of the TCA cycle is its role in anaplerosis (Greek for "to fill"), which replenishes key metabolic intermediates and precursors for a variety of biosynthetic reactions. The pyruvate dehydrogenase complex (PDH) generates acetyl-CoA from pyruvate, the end-product of glycolysis. The *E. coli* PDH is a large multienzyme complex composed of E1 (pyruvate decarboxylase, AceE), E2 (lipoate acyltransferase, AceF), and E3 (lipoamide dehydrogenase, Lpd) subunits (Bates et al. 1977). In *E. coli,* the PDH genes are arranged in an operon (*aceE-aceF-lpd*), whereas in *Mtb*, *aceE* (*Rv2241*), *dlaT* (*Rv2215,* homologous to *aceF* in *E. coli*), and *lpdC* (*Rv0462*) are located in separate genomic regions (Tian, Bryk, Shi, et al. 2005). *Mtb* harbors a second set of annotated PDH genes (*pdhABC*), however, the gene products do not exhibit PDH activity when reconstituted in vitro (Tian, Bryk, Shi, et al. 2005). Furthermore, LpdC and DlaT are subunits of alkyl hydroperoxide reductase (AhpC) (Bryk et al. 2002) indicating these proteins have dual roles in both metabolism (Tian, Bryk, Shi, et al. 2005) and antioxidant defense (Bryk et al. 2002). In a highly exergonic reaction catalyzed by citrate synthase, acetyl-CoA is condensed with oxaloacetate to generate free CoA and citrate. The *Mtb* genome encodes for two citrate

synthases (*citA/Rv0889c* and *gltA2/Rv0896*), the latter of which is essential in *Mtb* (Griffin et al. 2011). Aconitase (*acn, Rv1475c*) catalyzes the reversible formation of isocitrate from citrate via a *cis*-aconitate intermediate followed by decarboxylation of isocitrate by isocitrate dehydrogenase to generate α-ketoglutarate. In a prototypical TCA cycle, succinate is generated from α-ketoglutarate via the α-ketoglutarate dehydrogenase complex; however, activity from this complex is not found in *Mtb* cell lysates (Tian, Bryk, Shi, et al. 2005). Instead, α-ketoglutarate decarboxylase produces succinic semialdehyde from α-ketoglutarate followed by sequential action of succinic semialdehyde dehydrogenase to form succinate, which re-enters the TCA cycle (Tian, Bryk, Itoh, et al. 2005). Succinate donates electrons to the respiratory chain through the membrane-bound succinate dehydrogenase complex. Succinate oxidation generates fumarate, which is hydrated by fumarase to form malate (Ruecker et al. 2017). Malate is oxidized by malate dehydrogenase to generate oxaloacetate, which is now available to condense with an additional molecule of acetyl-CoA and thus completes the TCA cycle.

As described above, the *Mtb* genome harbors an extensive repertoire of genes participating in β-oxidation, suggesting that the bacillus is well suited for metabolizing fatty acids as a carbon source during infection (Cole et al. 1998; Bloch and Segal 1956). To subsist on a lipolytic diet, *Mtb* utilizes the glyoxylate shunt (isocitrate lyase and malate synthase) (Munoz-Elias and McKinney 2005), and the methylcitrate cycle (methylcitrate synthase, methylcitrate dehydrogenase, and isocitrate lyase) (Munoz-Elias et al. 2006) to metabolize acetyl-CoA and propionyl-CoA, respectively (Fig. 1.6). In *Mtb,* and possibly *M. smegmatis*, isocitrate lyase serves a redundant role in both the glyoxylate shunt and methylcitrate cycle (Munoz-Elias et al. 2006). In contrast, *M. smegmatis* expresses a dedicated methylcitrate lyase which acts at the final step of the methylcitrate cycle. Important anapleurotic metabolites are generated by each pathway. The end-products of the glyoxylate shunt are succinate and malate, while the methylcitrate cycle generates pyruvate and succinate. Succinate and pyruvate are important biosynthetic precursors and the latter metabolite can also enter the TCA cycle or proceed through gluconeogenesis. A functional glyoxylate shunt (Munoz-Elias and McKinney 2005), but not methylcitrate cycle (Munoz-Elias et al. 2006), is required for *Mtb* virulence in mice. *Mtb* expresses enzymes of the

vitamin B_{12}-dependent methylmalonyl pathway—an alternative route for propionate metabolism that incorporates carbon into methyl-branched lipids and generates succinyl-CoA (Savvi et al. 2008). The *M. smegmatis* genome also harbors orthologues of the methylmalonyl pathway that have not been studied to date.

Growth on fatty acids via the glyoxylate shunt or methylcitrate cycle generates anapleurotic metabolites and directs electron flux through respiratory systems for ATP generation by oxidative phosphorylation. In the absence of glucose, gluconeogenesis is important for maintaining carbon flux through the pentose phosphate pathway, which generates pentose intermediates and NADPH. Pentose sugars are components of RNA, DNA, and some coenzymes (e.g., ATP, NADH, $FADH_2$, coenzyme-A), while NADPH provides reducing equivalents for anabolic reactions. Enzymes of gluconeogenesis provide a means to generate G6P during growth on fatty acids (Marrero et al. 2010). Phosphoenolpyruvate carboxykinase (PEPCK) is the first committed step of gluconeogenesis which forms PEP from oxaloacetate (Marrero et al. 2010). PEP is then sequentially routed through gluconeogenesis using most of the enzymes of glycolysis in a reverse manner until reaching fructose-1,6-bisphosphate. At this point, the second dedicated enzyme of gluconeogenesis, fructose-1,6-bisphosphatase (GlpX), unidirectionally generates fructose-1-phosphate from fructose-1,6-bisphosphate (Gutka et al. 2011). GPM2 (*Rv3214*) also exhibits fructose-1,6-bisphosphatase activity. Disruptions in both *glpX* and *gpm2* are required to prevent in vitro growth on gluconeogenic carbon substrates and attenuation during murine infection (Ganapathy et al. 2015). For *Mtb* to thrive on non-glycolytic carbon sources (e.g., acetate, propionate), as is believed occur during chronic infection, a functional gluconeogenic pathway must be operational. Therefore, enzymes of gluconeogenesis represent attractive drug targets.

Bacterial central carbon metabolic pathways are regulated at the transcriptional and post-translational levels. Catabolite repression is perhaps the most well-studied regulatory mechanism of central carbon metabolism (CCM) in prokaryotes. In this model, when two-or-more utilizable carbon sources are available, the substrate that provides the most rapid growth (often glucose, if available) is utilized first (Bettenbrock et al. 2006). Upon exhausting the favored substrate, the

bacterium adapts by exploiting the next most favorable carbon source to maximize growth potential, a phenomenon called diauxic growth (Bettenbrock et al. 2006). This shift in metabolic programing is modulated by protein-protein interactions of the phosphotransferase system (Deutscher, Francke, and Postma 2006) followed by transcriptional activation of genes required to utilize the secondary carbon source (F.L. Liu et al. 2005). However, *Mtb* does not exhibit catabolite repression and simultaneously utilizes multiple organic substrates that feed different metabolic pathways (e.g., glucose and acetate), termed co-compartmentalization, presumably to maximize growth potential during stringent nutrient availability inside the host phagosome (de Carvalho et al. 2010).

TCSs have been shown to regulate CCM. The *Salmonella enterica* spp. Typhimurium BarA-SirA TCS promotes intestinal epithelial cell invasion in an acetate-dependent manner (Lawhon et al. 2002). In *E. coli,* the BarA-UvrY TCS regulates expression of the carbon storage regulatory system (Pernestig et al. 2003) which controls metabolic switching from glycolytic to gluconeogenic carbon sources (Sabnis, Yang, and Romeo 1995). The CrbSR and AcsRS TCSs of *Vibrio cholerae* and *Vibrio vulnificus*, respectively, induce expression of genes participating in acetate activation and transport (Hang et al. 2014; Kim et al. 2015). Similar genetic targets are regulated by the *Pseudomonas aeruginosa* and *Pseudomonas entomophila* CrbSR homologues and the *Shewanella oneidensis* SO_2742/2648 TCS (unnamed) and the corresponding mutants are defective for in vitro growth on acetate (Jacob et al. 2017). Phosphofructokinase II (*pfkB*) is induced by the *Mtb* DosRS TCS (Park et al. 2003) and is predicted to be essential during hypoxic growth (Fang, Wallqvist, and Reifman 2012), however, the contributions of PfkB during hypoxia remain obscure (Phong et al. 2013; Shi et al. 2010).

In *Mtb* and *M. smegmatis*, genetic regulation of CCM is primarily mediated by non-TCS transcriptional regulators. The TetR-family transcriptional repressors, KstR and KstR2, regulate genes participating in lipid and cholesterol uptake and β-oxidation in a cholesterol-dependent manner (Kendall et al. 2007; Kendall et al. 2010). RamB, an XRE-family transcription factor in *Mtb*, represses isocitrate lyase 1 (*icl1*), a key gene of the glyoxylate shunt, during growth on glucose (Micklinghoff et al. 2009). RamB was initially identified in the related Actinomycete, *C.*

glutamicum (Gerstmeir et al. 2004), where it serves as a global regulator of acetate metabolism in cooperation with RamA (Auchter et al. 2011), however, *ramA* homologues are not found in mycobacteria. The *Mtb* and *M. smegmatis* PrpR is a transcriptional activator of the methylcitrate cycle operon (*gltA1*) and *icl1* while repressing *ramB* and *dnaA* (DNA replication initiator) during growth on propionate (Masiewicz et al. 2012; Masiewicz et al. 2014). The stress-responsive sigma factors, SigE and SigB, also regulate the *gltA1* operon and *icl1* through feed-forward loops that interact with PrpR and RamB, respectively, adding an additional layer of complexity to genetic regulation of acetate and propionate metabolism (Datta et al. 2011).

Mycobacterial CCM is also subject to regulation at the post-translational level. The GarA protein of *M. smegmatis* inhibits α-ketoglutarate dehydrogenase, therefore reducing flux through the TCA cycle (Ventura et al. 2013). The *M. smegmatis garA* mutant grows on propionate, acetate, and succinate as sole carbon sources only when ammonium-donating amino acids are present (Ventura et al. 2013). PK activity is upregulated upon phosphorylation by the *Mtb* Ser/Thr protein kinase, PknJ, and confers a survival advantage when ectopically expressed in *M. smegmatis* during infection in differentiated THP-1 monocytes (Singh et al. 2014). An *M. bovis* BCG lysine acetyltransferase prevents accumulation of toxic propionyl-CoA metabolites by inhibiting acyl-CoA synthetase, an activator of acetate and propionate (Nambi et al. 2013). Furthermore, isocitrate dehydrogenase isoform 1, but not isoform 2, is inhibited through acetylation by an *Mtb* GCN5-like acetyltransferase (Rv2170) to inhibit carbon flux through the TCA cycle during growth on fatty acids (W. Lee et al. 2017). Mycobacteria therefore employ numerous post-translational enzymatic modifications help fine tune CCM, presumably to maximize growth potential and reduce toxic metabolite accumulation.

The studies described above demonstrate that mycobacteria exert strict regulatory control of CCM. Efficient management of central metabolism has likely evolved to provide growth and survival benefits in the diverse environmental niches occupies by mycobacteria. The host macrophage phagosome is believed to be a nutrient-restricted environment and *Mtb* utilizes fatty acids as primary carbon sources during chronic infection (Bloch and Segal 1956; Timm et al. 2003; Schnappinger et al. 2003). As a saprophytic organism, *M. smegmatis* likely encounters

similar nutrient stresses due to the unpredictability of its natural environment, such as periods of drought, availability of decaying organic matter, temperature extremes, and competition for resources by co-inhabiting microorganisms. It is therefore unsurprising that mycobacteria have evolved intricate regulatory programs to efficiently utilize multiple organic substrates to sustain survival in their natural environments.

CHAPTER 2

MYCOBACTERIUM SMEGMATIS PRRAB TWO-COMPONENT SYSTEM INFLUENCES TRIACYLGLYCEROL ACCUMULATION DURING AMMONIUM STRESS

Publication Note

The research reported in this chapter was previously published in an altered format in *Microbiology*. Jason D. Maarsingh and Shelley E. Haydel. 2018. *Mycobacterium smegmatis* PrrAB two-component system influences triacylglycerol accumulation during ammonium stress. *Microbiology*. **164**:1276-1288. doi:10.1099/mic0.000705.

Abstract

The PrrAB two-component system is conserved across all sequenced mycobacterial species and is essential for viability in *Mycobacterium tuberculosis*, thus making it a promising drug target. The *prrAB* operon was successfully deleted in nonpathogenic *Mycobacterium smegmatis*, and the Δ*prrAB* mutant strain exhibited clumping in ammonium-limited medium and significantly reduced growth during ammonium and hypoxic stress. To assess the influence of *M. tuberculosis* PrrA overexpression, we constructed a recombinant *M. smegmatis* Δ*prrAB* mutant strain which overexpresses *M. tuberculosis prrA*. *M. smegmatis prrAB* and *M. tuberculosis prrA* complemented the *M. smegmatis* Δ*prrAB* deletion mutant in Middlebrook M7H9 and ammonium-limited media and during hypoxic and ammonium stress. Based on quantitative untargeted mass spectrometry-based lipidomics, triacylglycerol lipid species were significantly upregulated in the Δ*prrAB* mutant strain compared to wild-type when cultured in ammonium-limited medium, revealing that *M. smegmatis* PrrAB influences triacylglycerol levels during ammonium stress. These results were qualitatively corroborated by thin-layer chromatography. Furthermore, the Δ*prrAB* mutant significantly upregulated expression of several genes (*glpK, GPAT, WS/DGAT, accA3, accD4, accD6,* and *Ag85C*) that participate in triacylglycerol and lipid biosynthetic pathways, thus corroborating the lipidomics analyses.

Introduction

Mycobacterium tuberculosis infects one-third of the world's population and causes approximately nine million new disease cases and 1.5 million fatalities each year (World Health 2014). Since treatment options for multi-drug resistant and extensively-drug resistant tuberculosis are limited (Haydel 2010), new therapeutic intervention strategies are needed. Antimicrobial agents traditionally target pathways and/or processes that are essential for viability or survivability within the human host. Therefore, regulatory proteins that are essential for viability or control critical virulence factors represent auspicious targets for the development of novel antimicrobial therapeutics. TCSs embody such regulatory models as they are ubiquitous among bacteria, but not found in humans; have conserved structural homologies, particularly surrounding catalytic sites (Gao and Stock 2009); are essential for viability in several pathogens (Fabret and Hoch 1998; Martin et al. 1999; Caimano et al. 2011; Zahrt and Deretic 2000b); are critical for bacterial virulence (Guzman-Verri et al. 2002; Walters et al. 2006); and are required for bacterial adaptation in various disease processes (Saini et al. 2004; Pflock et al. 2006).

TCSs provide an efficient means for prokaryotes to sense and respond to environmental stimuli [reviewed in (A.M. Stock, Robinson, and Goudreau 2000)]. A prototypical TCS consists of a membrane-bound histidine sensor kinase and a cytoplasmic DNA-binding response regulator which acts as a transcriptional regulator. Upon recognition of an appropriate environmental signal by the sensor kinase, a series of phosphotransfer reactions occur which end with phosphorylation of the response regulator at a conserved aspartate and subsequent modulation of activity (Hoch 2000). Diffusion of the response regulator and binding to its DNA recognition sequence induce or repress gene expression in response to the activating environmental signal(s) (Karimova, Bellalou, and Ullmann 1996; Bajaj et al. 1996).

The *M. tuberculosis prrAB* two-component system is essential for viability (Haydel et al. 2012). The *M. tuberculosis* PrrB histidine kinase and PrrA response regulator represent a functional and highly specific cognate TCS signal transduction circuit (Nowak, Panjikar, et al. 2006; Morth et al. 2005). Importantly, diarylthiazole compounds exhibit potent bactericidal activity against drug-susceptible and drug-resistant *M. tuberculosis* (Bellale et al. 2014). Laboratory-

generated diarylthiazole-resistant mutants harbored *prrB* point mutations, thus indicating that diarylthiazole potentially functions through the action of the PrrAB system and highlighting PrrB as a bona fide therapeutic target (Bellale et al. 2014).

Although Mishra et al. (Mishra et al. 2017) recently reported that *prrAB* is essential for viability in *M. smegmatis*, in this study, we deleted the *M. smegmatis prrAB* genes, establishing that the PrrAB system is not universally essential in pathogenic and nonpathogenic mycobacteria. Since the *M. tuberculosis* and *M. smegmatis* PrrA and PrrB proteins exhibit 97% and 81% identities, respectively, it is possible that commonly-regulated genes exist within the two species. Therefore, we began mechanistically understanding PrrAB functionality and its role in mycobacterial physiology and growth. Upon exposure to ammonium stress, the *M. smegmatis* Δ*prrAB* mutant grew similarly to the wild-type strain, but exhibited an excessive clumping during prolonged incubation, thereby prompting mass spectrometry-based lipidomic and thin layer chromatography (TLC) analyses that revealed accumulation of apolar lipids, TAG and DAGs in the Δ*prrAB* mutant. To complement the lipidomics data, qRT-PCR demonstrated that, relative to wild-type, the Δ*prrAB* mutant strain significantly upregulates key genes that contribute to TAG, DAG, and lipid biosynthetic processes. Furthermore, the *prrAB* is necessary for growth when *M. smegmatis* is cultured in both ammonium-limiting conditions and hypoxia.

Methods

Bacterial Strains, Media, and Culture Conditions

Escherichia coli strains (Table 2.1) used for maintenance of recombinant clones and plasmid transformation and isolation were cultured in Luria-Bertani broth (LB) at 37°C. *M. smegmatis* strains (Table 2.1) were cultured in Middlebrook 7H9 broth supplemented with albumin-dextrose-saline (ADS), 0.2% glycerol, and 0.05% Tween 80 with pH 6.8 (herein referred to as M7H9). To mimic nitrogen-limited conditions, nitrogen sources were provided in modified SR-1 defined medium (20 g/L glucose, 0.5 g/L $MgSO_4 \cdot 7H_2O$, 0.5 g/L NaCl, 0.5 g/L $K_2H_2PO_4$, 0.5 mg/L $CaCl_2$, supplemented with 0.05% Tween 80) as either 2 mM $NH_4H_2PO_4$ (SR-1-lowNH_4), 2 mM KNO_3 (SR-1-lowNO_3), 2 mM L-glutamine (SR-1-lowGln), or 2 mM L-asparagine (SR-1-

lowAsn) with pH 6.8 (Anuchin et al. 2009). The SR-1 medium includes 3 mM K_2HPO_4, thus avoiding simultaneous limitation for nitrogen and phosphorus. SR-1 medium was also supplemented with 10 mM $NH_4H_2PO_4$ (SR-1-highNH_4) to evaluate restoration of growth in ammonium sufficiency. Middlebrook 7H10 agar supplemented with ADS and 0.5% glycerol (M7H10) was used for CFU quantification. Modified SR-1-lowNH_4 agar [SR-1-lowNH_4 medium (without 0.05% Tween 80) and 1.5% Noble agar] and M7H10 agar were used to evaluate colony morphologies. Colony morphology was monitored daily and images were collected using a Fisher Scientific Stereomaster microscope and Micron v1.08 software.

Genetic Manipulations

M. smegmatis prrAB deletion mutants were generated via mycobacteriophage-mediated allelic exchange (Bardarov et al. 2002). The 5'- and 3'-flanking sequences of *M. smegmatis prrAB* were amplified and cloned on either side of the *res*-Hyg-*res* cassette within pYUB854 (Bardarov et al. 2002) to generate pSH667. The ligation mixture of *Pac*I-digested pSH667 and *Pac*I-digested concatemerized phAE87 (phSH680) was packaged using GigaPack III packaging extracts (Stratagene, La Jolla, CA) and transduced into *E. coli* HB101. Phasmid DNA was prepared from pooled Hyg-resistant transductants, restriction enzyme-digested to verify the presence of the desired insert, electroporated into *M. smegmatis* mc^2155, and plated for mycobacteriophage plaques at 30°C. A high-titer mycobacteriophage stock was generated from a confirmed temperature-sensitive phage plaque and was used to infect *M. smegmatis* mc^2155 at 37°C as previously described (Bardarov et al. 2002). Hygromycin-resistant colonies were selected after 6 d of growth at 37°C and screened by PCR for deletion of the *prrAB* genes (*prrA*Δ*53-611-prrB*Δ*1-414*). After Southern analysis to confirm the *M. smegmatis* Δ*prrAB*::Hyg deletion, the helper plasmid pYUB870 expressing *tnpR* resolvase was transformed into the *M. smegmatis* Δ*prrAB*::Hyg deletion strain to generate an unmarked *prrAB* deletion.

Table 2.1. Strains, mycobacteriophages, and plasmids used in this study.

Strains	Description	Reference or source
Mycobacterium smegmatis		
mc^{2}155	Wild-type, electroporation-competent strain	(Snapper et al. 1990)
FDL7	Δ*prrAB* deletion complemented with *M. tuberculosis prrA* (mc^{2}155::Δ*prrAB*::P$_{myc1}$-*tetO*-3XFLAG-*prrA*^{Mtb}-6XHis)	This work
FDL10	Δ*prrAB* knockout mutant (mc^{2}155::Δ*prrAB*)	This work
FDL15	Δ*prrAB* knockout mutant with integrated *M. smegmatis prrAB* (complemented mutant) (mc^{2}155::Δ*prrAB*::*prrAB*^{Msmeg})	This work
Escherichia coli		
HB101	Cloning and storage strain	Laboratory collection
JM109	Cloning and storage strain	Laboratory collection
GC10	Cloning and storage strain	Laboratory collection
DH5α	Cloning and storage strain	Laboratory collection
Mycobacteriophages		
phAE87	Temperature-sensitive mycobacteriophage used for generating phSH680 allelic exchange	(Bardarov et al. 2002)
phSH680	phAE87::Δ*prrAB*^{Msmeg}::*hyg*	This work
Plasmids		
pYUB854	Cosmid vector with *res* sites flanking the Hyg^R gene	(Bardarov et al. 2002)
pYUB870	Helper plasmid harboring □□-*tnpR* for generating unmarked mutations; *sacB*; Km^R	(Bardarov et al. 2002)
pSH667	pYUB854::Δ*prrAB*::*res*-Hyg^R-*res*	This work
pSE100	pMS2 derivative containing P$_{myc1}$-*tetO*; Hyg^R	(Ehrt et al. 2005)
pTZ842	pET24b::3XFLAG-6XHis; Km^R	(White et al. 2011)
pMV306	Site-specific (*att*) integrating *E. coli* – mycobacterial shuffle vector; Km^R	(Stover et al. 1991)
pSH492	pMV306::*aacC41*; Am^R	(Haydel and Clark-Curtiss 2006)
pSH695	pMV306::*prrAB*^{Msmeg}; Km^R	This work

Transformants were screened by a pick-and-patch method on LB agar with and without hygromycin (50 □g/ml) for loss of the *res-hyg-res* cassette and hygromycin sensitivity. Hygromycin-sensitive strains were analyzed via Southern blot for loss of the *res*-Hyg-*res* cassette. Confirmed Hyg^S clones were then cultured in the presence 10% sucrose to induce expression of *sacB* and provide negative selection for loss of the pYUB870 plasmid. The *M. smegmatis* Hyg^S Km^S unmarked *prrAB* mutant, FDL10, was confirmed via Southern blot analysis (Fig. 2.1).

Table 2.2. Oligonucleotide primers used in this study.

PCR Primers		
Primer	**Sequence**	**Target/Product**
SH192	5'-GCTCTAGAAGTGCCGACATCAGCGTCAG-3'	*prrA* 5' flanking
SH193	5'-GCACCGGTGTCATCCACCACAAGCACCC-3'	*prrA* 5' flanking
SH194	5'-GCCCATGGGGCTGTTGTTGAGGCTGCCG-3'	*prrB* 3' flanking
SH195	5'-GCCAGATCTGGCTCACCAGGTACGAGTAG-3'	*prrB* 3' flanking
SH390	5'-GGATCGATAATGGCCAGAGGGCGAAAC-3'	*attP_int_aacC41* from pMV306
SH391	5'-GGTCGCGAGTCTGACGCCTCAGTGGAAC-3'	*attP_int_aacC41* from pMV306
qRT-PCR Primers		
Primer	**Sequence**	**Target/Product**
SH571	5'-TGTCATGCAGTCGTATGTGG-3'	*MSMEG 4757* (*fas*)
SH572	5'-TGCCGAGCTTGATCTTGTC-3'	*MSMEG 4757* (*fas*)
SH579	5'-TGCTGATGGATCTGGAGAC-3'	*MSMEG 6759* (*glpK*)
SH580	5'-AGACCTGACCGAACATGG-3'	*MSMEG 6759* (*glpK*)
SH583	5'-TCAGCTTCGACCAGTTGC-3'	*MSMEG 4703* (*GPAT*)
SH584	5'-GGGAAGCGGACATAGATCTTG-3'	*MSMEG 4703* (*GPAT*)
SH585	5'-TTTTCAAGTTCGTCCTGTTGG-3'	*MSMEG 4248* (*AGPAT*)
SH586	5'-GTAGAAACTGTCCATCACCG-3'	*MSMEG 4248* (*AGPAT*)
SH587	5'-CGACATCACTTATCACATCCG-3'	*MSMEG 1882* (*WS/DGAT*)
SH588	5'-CTGATGTGACTTGGTGTAGAC-3'	*MSMEG 1882* (*WS/DGAT*)
SH589	5'-GAATCATGGGCGTCGAAC-3'	*MSMEG 4705* (*WS/DGAT*)
SH590	5'-TGGTAGTCGAGGTTGAAGTC-3'	*MSMEG 4705* (*WS/DGAT*)
SH593	5'-TTTTCCCGTCCTGGTCTG-3'	*MSMEG 3580* (*Ag85C*)
SH594	5'-AGCCGTTGTAGTCATCCTG-3'	*MSMEG 3580* (*Ag85C*)
SH599	5'-CAAAGATCTCCAAGGTGCTG-3'	*MSMEG 1807* (*aacA3*)
SH600	5'-CTTCTCGAAGACCAGGTAGG-3	*MSMEG 1807* (*accA3*)
SH603	5'-ACAGCAAGATTTTCGTCACC-3'	*MSMEG 4329* (*accD6*)
SH604	5'-GCAGAACAATCCGACCAG-3'	*MSMEG 4329* (*accD6*)
SH605	5'-GATCAGGGCTACATGTTCATC-3'	*MSMEG 6391* (*accD4*)
SH606	5'-CAGGAAGCTCAGGTAGTCG-3'	*MSMEG 6391* (*accD4*)
SH611	5'-TCAACATGCCCGTCCTC-3'	*MSMEG 5662* (*prrA*)
SH612	5'-TTTCACCAGGTAGTCGTCG-3'	*MSMEG 5662* (*prrA*)

To create integrative, expression vectors, *M. tuberculosis prrA* was cloned between the 5'-3XFLAG and 3'-6XHis tags present in pTZ842 (White et al. 2011) prior to cloning downstream of P_{myc1}-*tetO* in pSE100 (Ehrt et al. 2005). The Hyg resistance gene in pSE100 was replaced with *attP_int_aacC41* from pSH492 (pMV306::*aacC41*) to generate integrative, expression plasmids conferring apramycin (Am) resistance (Consaul and Pavelka 2004). This construct was electroporated into the Δ*prrAB* background and integrated at the chromosomal *attB* site to generate FDL7. To complement the mutation, *M. smegmatis prrAB* with 166 bp of upstream DNA and 76 bp downstream of the *prrB* stop codon was cloned into pMV306, a site-specific integrating mycobacterial vector, to generate pSH695. This construct was electroporated into the Δ*prrAB*

background and integrated at the chromosomal *attB* site to generate the complementation strain, FDL15. Plasmids were electroporated into *M. smegmatis* FDL10, and recombinants were selected on LB agar with Am (10 □g/ml) or Km (50 □g/ml). All strains, mycobacteriophages, plasmids, and PCR primers used in this study are presented in Tables 2.1 and 2.2.

Growth Curves

Growth of the *M. smegmatis* strains was assessed in M7H9, SR-1-lowNO_3, SR-1-lowNH_4, SR-1-highNH_4, SR-1-lowGln, and SR-1-lowAsn. Cultures were grown at 37°C with orbital shaking at 100 rpm for 96 h. Absorbance readings and samples for CFU quantitation were collected every 24 h.

MAME Extraction and TLC Analysis

MAMEs were prepared as previously described (Slayden and Barry 2001). Briefly, cultures were grown in SR-1-lowNH_4 or SR-1-highNH_4 for 48 h, and cells were harvested by centrifugation. Cell pellets were lysed in 5 ml tetrabutylammonium hydroxide (TBAH) for 3 h at 100ºC and methylated with 200 □l iodomethane in 2 ml dichloromethane. The organic layer was collected after centrifugation at 6000 x *g*, washed in 2 ml 0.1 M HCl, and evaporated. MAMEs were eluted in 2 ml diethyl ether, dried, and resuspended in dichloromethane. Equal quantities of MAMEs were applied to 6.5 x 10 cm aluminum-backed silica gel TLC plates and developed 3X in petroleum ether:diethyl ether (9:1). MAMEs were visualized by spraying plates with 10% ethanolic sulfuric acid followed by charring at 110°C for 15 min.

Apolar Lipid Extraction and TLC Analysis

Apolar lipids were harvested (Slayden and Barry 2001) from cultures grown to early stationary phase in SR-1-lowNH_4 or SR-1-highNH_4. Briefly, cells were collected by centrifugation, washed in PBS, and resuspended in 20 ml methanol:0.3% NaCl (10:1) to which 10 ml petroleum ether was added and stirred for 15 min at room temperature. After phase separation, the upper petroleum ether layer containing apolar lipids was removed, and the extraction was repeated with

an additional 10 ml petroleum ether. Following evaporation of petroleum ether, dried apolar lipids were dissolved in dichloromethane.

TAGs were analyzed by qualitative 1D TLC using a development system of hexane:diethyl ether:acetic acid (80:20:1) and were visualized with iodine vapor. Triacylglycerol standards (Sigma-Aldrich, St. Louis, MO) were developed with mycobacterial apolar lipids to identify TAG-specific bands. All experiments were performed in triplicate, and two technical replicates per biological replicate were processed for each strain.

Sample Preparation for Lipidomics Analysis

M. smegmatis strains were cultured in 500 ml SR-1-lowNH_4 for 48 h at 37°C, 100 rpm. Cells were harvested by centrifugation at 4225 x *g* for 10 min and resuspended in PBS (25 ml). Each sample was adjusted to ~ 10^8 cells/ml, and 1 ml of each sample was harvested by centrifugation. Cell pellets were stored at –70°C prior to lipidomics analysis. Three biological replicates, each bearing two technical replicates, were prepared per strain.

Lipid extraction was performed by the University of California, Davis West Coast Metabolomics Center as described by Matyash *et al*. (Matyash et al. 2008) using a bi-phasic solvent system of cold methanol, methyl *tert*-butyl ether, and water with slight modifications. Specifically, cold methanol (225 µl) containing a mixture of odd chain and deuterated lipid internal standards [lysoPE(17:1), lysoPC(17:0), PC(12:0/13:0), PE(17:0/17:0), PG(17:0/17:0), sphingosine (d17:1), d_7-cholesterol, SM(17:0), C17 ceramide, d_3-palmitic acid, MG(17:0/0:0/0:0), DG(18:1/2:0/0:0), DG(12:0/12:0/0:0), and d_5-TG(17:0/17:1/17:0)] was added to 10^7 cells and vortexed for 10 sec. Next, cold methyl *tert*-butyl ether (750 µl) containing CE(22:1) (internal standard) was added, followed by vortexing for 10 sec and shaking for 6 min at 4°C. Phase separation was induced by adding mass spectrometry-grade H_2O (188 µl). After vortexing for 20 sec, the sample was centrifuged at 14,000 rpm for 2 min. The upper organic phase (300 µl) was collected and evaporated to dryness in a SpeedVac. Dried extracts were resuspended using a mixture of methanol/toluene (9:1, v/v) (60 µl) containing an internal standard (12-[[(cyclohexylamino)carbonyl]amino]-dodecanoic acid) for quality control.

LC/MS Parameters for Lipidomics

The LC/QTOF-MS analyses were performed using an Agilent 1290 Infinity LC system (G4220A binary pump, G4226A autosampler, and G1316C Column Thermostat) coupled to either an Agilent 6530 (positive ion mode) or an Agilent 6550 mass spectrometer equipped with an ion funnel (iFunnel) (negative ion mode). Lipids were separated on an Acquity UPLC CSH C18 column (100 x 2.1 mm; 1.7 µm) maintained at 65°C at a flow-rate of 0.6 ml/min. Solvent pre-heating (Agilent G1316) was used. The mobile phases consisted of 60:40 acetonitrile:water with 10 mM ammonium formate and 0.1% formic acid (A) and 90:10 propan-2-ol:acetonitrile with 10 mM ammonium formate and 0.1% formic acid. The gradient was as follows: 0 min 85% (A); 0–2 min 70% (A); 2–2.5 min 52% (A); 2.5–11 min 18% (A); 11–11.5 min 1% (A); 11.5–12 min 1% (A); 12–12.1 min 85% (A); 12.1–15 min 85% (A). A sample volume of 3 µl was used for the injection. Sample temperature was maintained at 4°C in the autosampler.

The quadrupole/time-of-flight (QTOF) mass spectrometers were operated with electrospray ionization (ESI) performing full scan in the mass range *m*/*z* 65–1700 in positive (Agilent 6530, equipped with a JetStreamSource) and negative (Agilent 6550, equipped with a dual JetStream Source) modes producing both unique and complementary spectra. Instrument parameters were as follows: (positive mode) Gas Temp 325°C, Gas Flow 8 l/min, Nebulizer 35 psig, Sheath Gas 350°C, Sheath Gas Flow 11, Capillary Voltage 3500 V, Nozzle Voltage 1000V, Fragmentor 120V, Skimmer 65V. Data (both profile and centroid) were collected at a rate of 2 scans per sec. In negative ion mode, all parameters were identical to the positive ion mode except for the following: Gas Temp 200°C, Gas Flow 14 l/min, and Fragmentor 175V. For the 6530 QTOF, a reference solution generating ions of 121.050 and 922.007 *m/z* in positive mode and 119.036 and 966.0007 *m/z* in negative mode were used for continuous mass correction. For the 6550 QTOF, the reference solution was introduced via a dual spray ESI, with the same ions and continuous mass correction. Samples were injected with a needle wash solvent (isopropanol) for 20 sec for sample normalization.

Lipidomics Data Analysis

For data processing, the MassHunter software was used, and a unique ID was given to each lipid based on its retention time and exact mass (RT_*mz*), thus allowing the report of peak areas/heights or concentration of lipids based on the use of particular internal standards. Lipids were identified based on their unique MS/MS fragmentation patterns using the LipidBlast software. Using complex lipid class-specific internal standards, this approach was used to quantify >400 lipid species including: mono-, di- and triacylglycerols, glycerophospholipids, sphingolipids, cholesterol esters, ceramides, and fatty acids. This approach is highly reproducible, displaying a relative standard deviation of 0.1% for the retention time and 1.7% for peak area based on replicate analysis of plasma samples (*n*=10). An average shot-to-shot carryover of less than 0.1% was observed.

RNA Isolation and qRT-PCR

After 24 h *in vitro* growth in SR-1-lowNH_4, RNA was isolated from *M. smegmatis* using Trizol reagent according to the manufacturer's instructions and following a previously published protocol (Rustad et al. 2010). Total RNA (2 µg) was digested with DNase (Thermo Scientific) for 30 min at 37°C. Residual DNase was removed by phenol:chloroform extraction and resuspended in nuclease-free H_2O. Total RNA (2 µg) was converted to cDNA using an iScript cDNA synthesis kit (Bio-Rad). Gene expression profiling was performed using a MyiQ thermocycler and reactions with 5 ng cDNA, 300 nM primers, and iQ SYBR Green Supermix (Bio-Rad). Relative expression was calculated using the comparative C_T method ($\Delta\Delta C_T$) (Livak and Schmittgen 2001) with mc^2155 as the calibrator strain and 16S rRNA gene as an internal control. Gene expression was determined for three independent biological replicates, each with two technical replicates. All qRT-PCR primers used in this study are presented in Table 2.2.

Stress Assays

All stress assays were performed in 96-well microtiter plates using SR-1-lowNH_4 with the following adjustments. For acid stress, SR-1-lowNH_4 medium was adjusted to pH 5.5 (compared

to pH 6.8 for control experiments). Cell wall stress was tested with or without 0.05% SDS. Hypoxic conditions were generated using the GasPak EZ anaerobic system in sealed bags (Becton Dickinson, Franklin Lakes, NJ) with colorimetric indicator strips (Thermo Scientific, Waltham, MA) to monitor O_2 depletion. To assess antibiotic sensitivity, all strains were exposed to 2-fold decreasing concentrations of isoniazid (4 – 0.125 µg/ml) for 48 h. All incubations were performed in triplicate at 37°C with gentle agitation (100 rpm) in a humidified incubator. Cell growth (OD_{600}) was measured an M2 SpectraMax 96-well plate reader (Molecular Devices, San Jose, CA).

Statistical Analyses

We used unpaired Student t tests to assess significant differences in growth curves and gene expression and one-way ANOVA to assess differences for the stress assays. Statistical analyses were performed using GraphPad Prism 6 (GraphPad Software, San Diego, CA), and *p* values of < 0.05 were considered statistically significant. Lipidomic datasets were statistically analyzed using unpaired Students t tests, univariate ANOVA, Tukey's multiple comparisons tests, and principle component analysis. For volcano plot data, the -log(*p*) of each species was plotted against the ratio of the mean $\log_2$ fold-change of lipid intensities between FDL10 and mc^2155.

Results

The M. smegmatis prrAB Two-Component System is not Essential for Viability

While *prrAB* is essential for *in vitro* viability in *M. tuberculosis* (Haydel et al. 2012), we successfully constructed the *M. smegmatis* Δ*prrAB* mutant using the specialized transducing mycobacteriophage system (Bardarov et al. 2002). The hygromycin resistance cassette flanked by *res* sites replaced 96% of the *prrAB* coding sequences, leaving only the first 55 bp of *prrA* and the last 32 bp of *prrB*. After removing the hygromycin resistance cassette to generate *M. smegmatis* FDL10, a plasmid harboring the *M. tuberculosis prrA* gene controlled by the P_{myc1}-*tetO* promoter, a highly active mycobacterial promoter (*rpsA*) flanked by TetR-operator sites (Ehrt et al. 2005), was integrated into the chromosome via the L5 *attB* locus to create *M. smegmatis* FDL7.

To generate the *M. smegmatis prrAB* complement strain (FDL15), an integrative plasmid (pMV306::*prrAB*^{Msmeg}) expressing *M. smegmatis prrAB* under control of its native promoter was introduced into the Δ*prrAB* background at the chromosomal *attB* site. All recombinant *M. smegmatis* strains were confirmed by Southern analysis (Figs. 2.1A), and wild-type and recombinant PrrA expression in M7H9 and SR-1-lowNH_4 was confirmed via western analysis (Figs. 2.1B, C). Agitated *in vitro* growth of all recombinant *M. smegmatis* strains in M7H9 was similar to wild-type mc^{2}155, except for slight decreased viability (CFU) of the FDL7 *prrA*^{Mtb} complementation and FDL10 Δ*prrAB* strains at 96 h (Fig. 2.2A). Additionally, colony morphology was assessed by monitoring growth of *M. smegmatis* strains on M7H10 agar plates for 5 d. All colonies displayed wrinkled morphologies and yellow pigmentation (Fig. 2.2B), indicating that *M. smegmatis* PrrAB does not influence growth under these conditions.

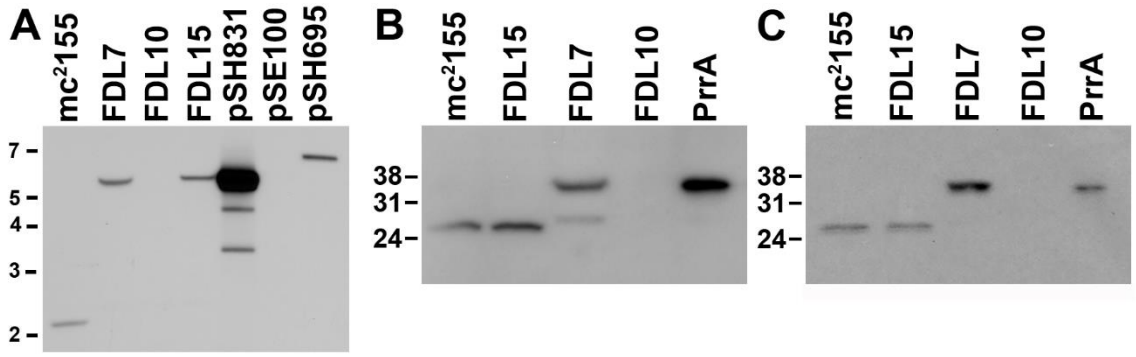

Figure 2.1. Southern blot and western blot analyses of the *M. smegmatis* wild-type (mc^{2}155), *prrAB* deletion mutant (FDL10), and genetic complementation strains (FDL7 and FDL15). (A) Genomic DNA was digested with *Bsa*AI, and pSH831, pSE100, and pSH695 plasmids were digested with *Xba*I, followed by hybridization with *prrA*. Molecular weight (MW) markers (kb) are shown on the left. (B) Soluble protein fractions were collected during M7H9 growth and detected using α-PrrA^{Mtb} polyclonal antisera. (C) Soluble protein fractions were collected during SR-1-lowNH_4 growth and detected using α-PrrA^{Mtb} polyclonal antisera. Purified recombinant 3XFLAG-PrrA-6XHis protein is shown as a control and MW markers (kDa) are shown on the left. Predicted MW of *M. smegmatis* PrrA is 25.3 kDa (mc^{2}155 and FDL15). Predicted MW of recombinant *M. tuberculosis* 3XFLAG-PrrA-6XHis (FDL7 and purified PrrA) is 30.6 kDa.

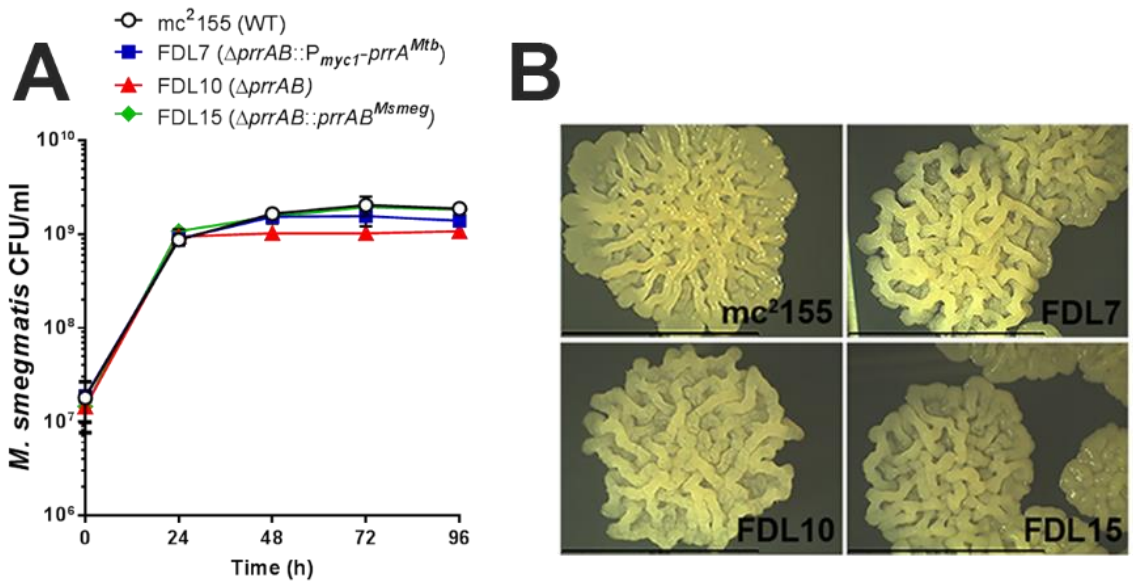

Figure 2.2. Growth characteristics of the *M. smegmatis* strains in M7H9 broth and colony morphologies on M7H10 ADS agar. (A) Growth characteristics of mc²155 (open circles), FDL7 (closed, blue squares), FDL10 (closed, red diamonds), and FDL15 (closed, green diamonds) were assessed during aerated growth in M7H9 at 37ºC. At specified times, samples were plated on M7H10 agar and incubated at 37ºC to determine viable c.f.u. Values represent the mean ± SEM of data collected from three independent cultures. (B) Images (2X magnification) of c.f.u. morphology were taken on day 5. Scale bar, 6 mm.

The M. smegmatis ΔprrAB Mutant Forms Aggregates During Growth in NH_4-Limited Medium

Expression of *prrAB* is induced when *M. tuberculosis* is cultured in the presence of 200 □M MSX, an inhibitor of glutamine synthetase which mimics a state of nitrogen limitation (Pace and McDermott 1952; Amon et al. 2008). Since ammonium is the preferred nitrogen source for *M. smegmatis* (Williams, Bryant, et al. 2013) and *M. smegmatis* assimilates nitrate (Khan et al. 2008), we assessed whether deletion of *prrAB* with and without expression of episomal *M. tuberculosis prrA* altered growth of *M. smegmatis* in SR-1-lowNH_4 and SR-1-lowNO_3 media (see Materials and Methods). Viability of the Δ*prrAB* mutant in SR-1-lowNO_3 was lower compared to wild-type mc²155 at 24 h and 96 h (Fig. 2.3A), indicating that the Δ*prrAB* mutant exhibits time-dependent (mid-log and stationary phase) growth defects with limited nitrate (2 mM) as a sole nitrogen source. In SR-1-lowNH_4 with limited ammonium as the sole nitrogen source, the *M. smegmatis* Δ*prrAB* mutant (FDL10) did not exhibit the early-stage (24 h) growth defects (Fig. 2.4A) that were evident in SR-1-lowNO_3 medium (Fig. 2.3A). After 72 h of growth, the FDL10

culture in SR-1-lowNH_4 exhibited extensive clumping (Fig. 2.4C). Attempts were made to disperse cells by thorough agitation, however, the discrepancy in viability between mc^{2}155 and the Δ*prrAB* mutant at 96 h (Fig. 2.4A) could be masked by residual cell clumps not visible to the naked eye. All strains displayed similar growth kinetics in SR-1-highNH_4 medium (Fig. 2.4B), and no visible clumping patterns were detected in any strain under these conditions.

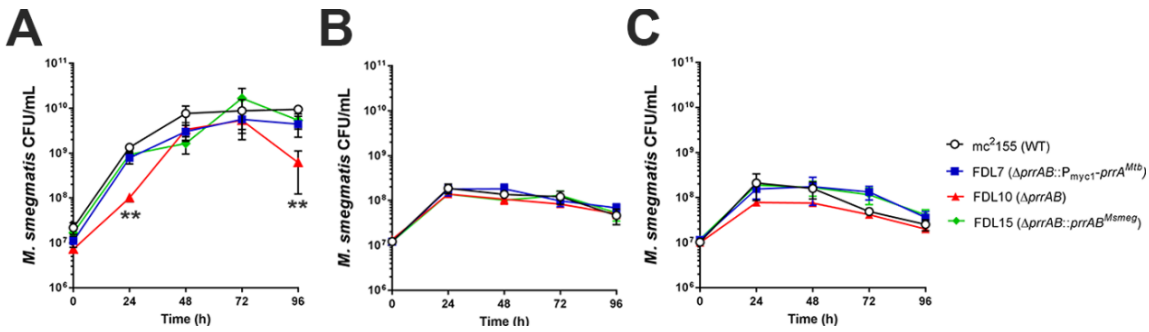

Figure 2.3. Growth characteristics of the *M. smegmatis* strains in (A) SR-1-lowNO_3, (B) SR-1-lowAsn, and (C) SR-1-lowGln. Growth characteristics of mc^{2}155 (open circles), FDL7 (closed, blue squares), FDL10 (closed, red triangles), and FDL15 (closed, green diamonds) were assessed during aerated growth in SR-1 broth containing at 37°C. At specified times, samples were plated on M7H10 agar and incubated at 37°C to determine viable c.f.u. Values represent the mean ± SEM of data collected from three independent cultures. **, P<0.01; Student's *t*-test.

Complementation of Δ*prrAB* with *M. smegmatis prrAB* (FDL15) and *M. tuberculosis prrA* (FDL7) restored wild-type growth characteristics similar to mc^{2}155 (Fig. 2.4A, B). Since FDL7 lacks *prrB*, these data suggest that PrrB is dispensable during ammonium stress conditions, *M. tuberculosis* PrrA can functionally replace the native PrrAB in *M. smegmatis*, or another histidine kinase may be capable of transphosphorylating PrrA. After incubation on modified SR-1-lowNH_4 agar for 5 days, wild-type mc^{2}155 and FDL7 colonies were smooth on the outer edges with a central "cracked" appearance, while the Δ*prrAB* mutant and FDL15 both displayed smooth colony morphologies (Fig. 2.4D). Although the colony morphologies of mc^{2}155 and the FDL15 complementation strain differed on modified SR-1-lowNH_4 agar, FDL15 did not clump in SR-1-lowNH_4 broth (Fig. 2.4C), suggesting *prrAB* complementation.

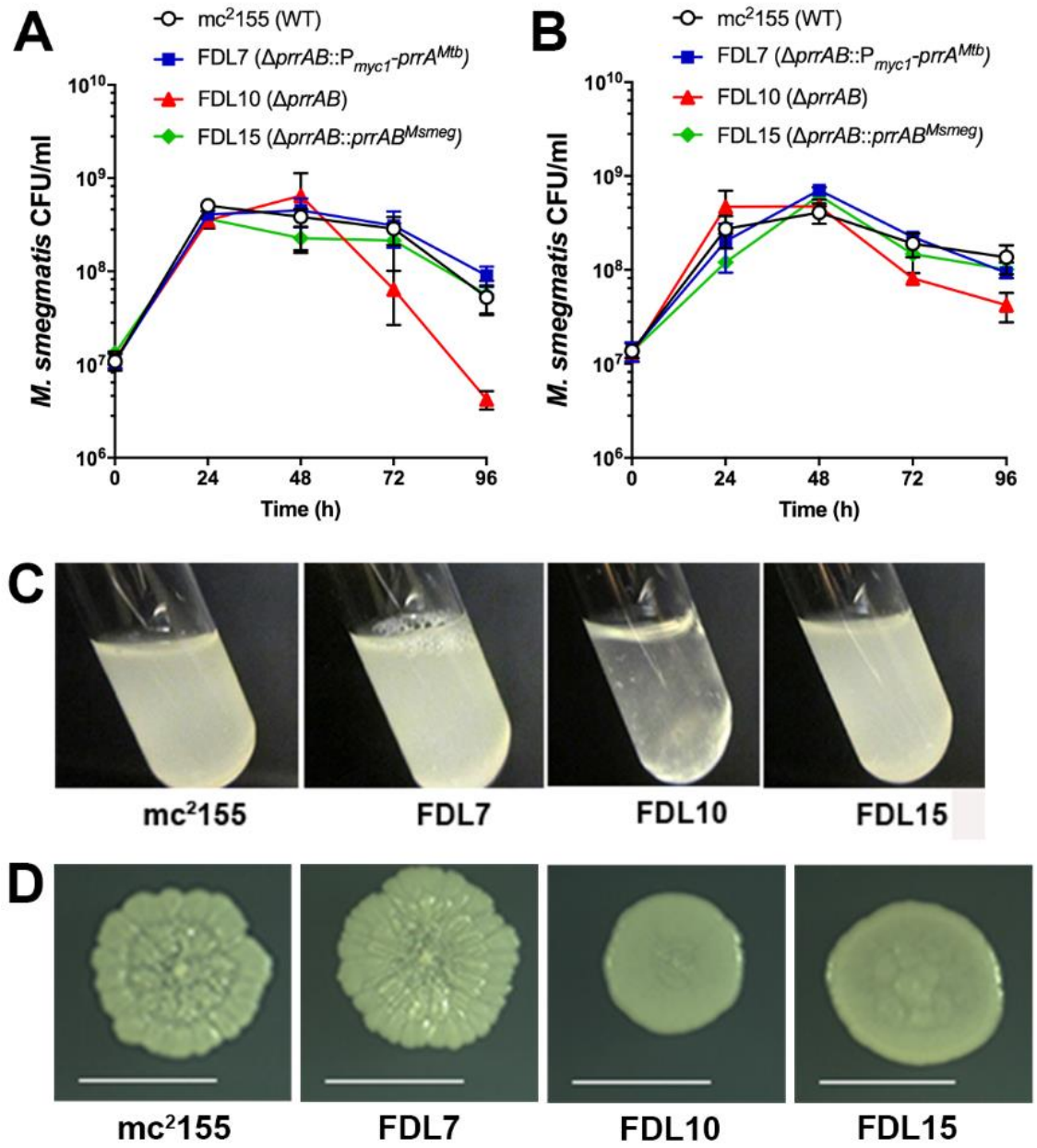

Figure 2.4. Growth characteristics of the *M. smegmatis* strains in SR-1 media supplemented with ammonium as the sole nitrogen source. Viability of mc^{2}155 (open circles), FDL7 (closed, blue squares), FDL10 (closed, red triangles), and FDL15 (closed, green diamonds) was assessed during aerated growth in SR-1 broth containing (**A**) 2 mM NH_4 or (**B**) 10 mM NH_4 at 37ºC. At specified times, samples were plated on M7H10 agar and incubated at 37ºC to determine viable CFU. Values represent the mean ± SEM of data collected from three independent cultures. (**C**) *M. smegmatis* cultures during growth in low ammonium (SR-1-lowNH_4). Relative to mc^{2}155, FDL7, and FDL15, the *M. smegmatis* Δ*prrAB* strain (FDL10) exhibited a clumping phenotype after 72 h growth in SR-1 medium with 2 mM NH_4. (**D**) Images (2X magnification) of CFU morphology on modified SR-1-lowNH_4 agar were taken on day 5. Scale bar, 2 mm.

Growth of the M. smegmatis ΔprrAB Mutant with Different Nitrogen Sources

To determine the growth characteristics of the *M. smegmatis* strains cultured under alternative nitrogen sources, growth curves were performed in SR-1 medium supplemented with 2 mM L-asparagine (SR-1-lowAsn) or L-glutamine (SR-1-lowGln). All strains grew similarly in SR-1-lowAsn (Fig. 2.3B). While CFU levels of the Δ*prrAB* mutant were slightly lower than wild-type mc^{2}155 in SR-1-lowGln at 24 and 48 h, the two strains were similar at 72 h and 96 h (Fig. 2.3C). While the mc^{2}155 growth rate was approximately 3X greater than the Δ*prrAB* mutant during the initial 24 h in SR-1-lowGln medium, mc^{2}155 declined at a greater rate than the Δ*prrAB* mutant with continued growth (Fig. 2.3C). The data suggests that despite the more robust growth potential achieved in mc^{2}155 during growth in SR-1-lowGln, the Δ*prrAB* mutant resisted the deleterious effects of glutamine depletion in a time-dependent manner. Cell clumping was not observed in either SR-1-lowAsn or SR-1-lowGln media.

Ammonium Stress Does Not Alter prrA Transcription in M. smegmatis

Since *prrA* is upregulated in *M. tuberculosis* in response to *in vitro* nitrogen-limiting conditions (Haydel et al. 2012), *M. smegmatis prrA* transcriptional activity during ammonium stress was characterized. *prrA* transcription was similar in mc^{2}155 and the complemented Δ*prrAB* mutant (FDL15) in SR-1-lowNH_4 medium (Fig. 2.5), revealing that ammonium stress does not alter *prrA* transcription.

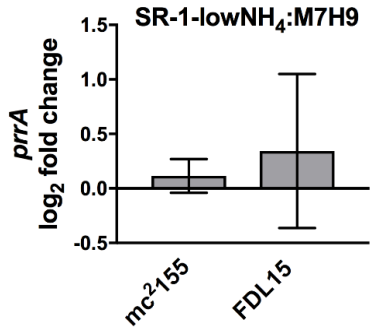

Figure 2.5. Quantitative analysis of *prrA* transcription in mc^{2}155 and FDL15 when cultured in SR-1-lowNH_4 (2 mM NH_4) relative to M7H9. Log_2-fold change calculated using the comparative C_T method ($\Delta\Delta C_T$). *P*=0.7675, unpaired Student's *t*-test.

Mycolic Acid Methyl Esters (MAMEs) Profiles of the ΔprrAB Mutant During Ammonium Stress

Since the *M. smegmatis ΔprrAB* mutant clumped during prolonged growth in SR-1-lowNH_4, we used alkaline methanolysis to generate MAMEs and analyzed these key lipid constituents of the mycobacterial envelope by qualitative 1D TLC. MAMEs isolated from the *M. smegmatis* strains grown in SR-1-lowNH_4 or SR-1-highNH_4 and visualized with ethanolic sulfuric acid produced similar profiles with regards to the major α, α', and epoxy mycolate species (Fig. 2.6). Quantitative assessments with radiolabeled lipids and mass spectrometry are necessary to determine and further explore the influence of PrrAB on MAME production.

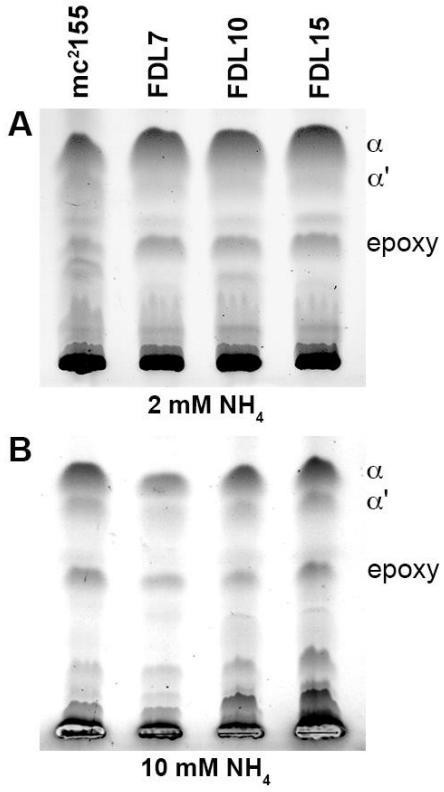

Figure 2.6. Qualitative TLC analyses of mycolic acid/fatty acid methyl esters (MAMEs/FAMEs) from *M. smegmatis* cultured in (A) SR-1-lowNH_4 and (B) SR-1-highNH_4. Mycolic acids and fatty acids were extracted by alkaline methanolysis and derivatized with CH_3I to generate methyl esters. MAME/FAME species were resolved using petroleum ether:diethyl ether (9:1) and visualized by charring with 10% ethanolic sulfuric acid at 110°C for 15 min. The major MAME species (α, α', and epoxy) are as indicated.

M. smegmatis Δ*prrAB* Mutant Accumulates TAGs, DAGs, and Lipids in Ammonium Stress

To begin globally profiling lipids in an untargeted manner, we subjected the *M. smegmatis* cultures grown in SR-1-lowNH_4 to high-resolution liquid chromatography followed by ESI-QTOF. Univariate ANOVA revealed 319 significantly expressed ($p < 0.05$) lipid species between mc^2155 and FDL10, with the vast majority (309 species) elevated in FDL10 compared to mc^2155 (Fig. 2.7A). LC/QTOF-MS analyses revealed a series of positive molecular ions, *m/z* 834.76 – 963.84, which correspond to TAGs ranging from 49 to 58 carbons, with relative peak heights that were significantly elevated in the FDL10 Δ*prrAB* mutant compared to wild-type mc^2155 (Fig. 2.7B). Of these significantly-elevated lipid species, nine were identified as TAGs (Fig. 2.8). Quantitative lipidomics analyses revealed that TAG species with 49, 50, 51, and 58 total carbons exhibited median fold increases of 4.9 (3.9 – 6.4 range), 6.2 (3.2 – 8.4 range), 5.5 (4.1 – 6.9 range), and 4.8, respectively, in the FDL10 Δ*prrAB* mutant compared to wild-type mc^2155 (Fig. 2.8). Principal component analysis categorized mc^2155, FDL7, and FDL15 as a separate group from FDL10 (Fig. 2.9). Univariate ANOVA comparing mc^2155 to FDL7 or FDL15 revealed only 29 and 15 differentially-expressed positive molecular ion lipid species, respectively, further confirming the principal component analysis. While complementation with *M. smegmatis prrAB* (FDL15) did not completely restore lipid abundance to wild-type mc^2155 levels (Fig. 2.7B), 1,996 out of 2,089 positively-charged molecular ion lipid species were not significantly different.

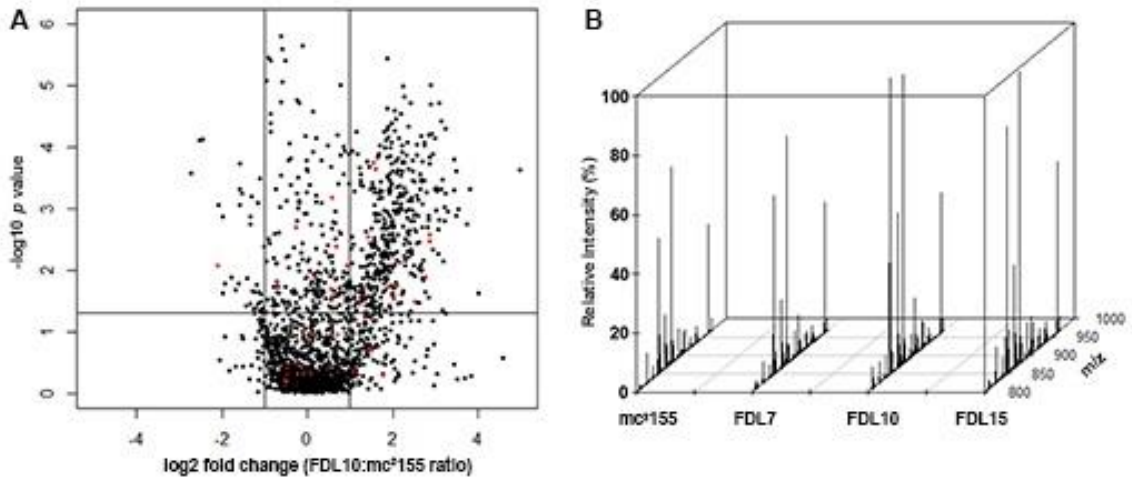

Figure 2.7. LC/QTOF-MS analysis of positively-charged ion lipid species. (A) Volcano plot of mc^{2}155 and FDL10 lipid species identified in positive ion mode. Vertical lines represent FDL10 lipid species exhibiting a $\log_2$ fold change of ± 1 relative to mc^{2}155. All species above the horizontal line represent $p < 0.05$. Red dots indicate TAG species. (**B**) 3D spectra and *M. smegmatis* strain comparison of lipid species within the *m/z* range of TAG species. All mass spectra were displayed after normalization to the base peak present in FDL15. *m/z*, mass-to-charge ratio.

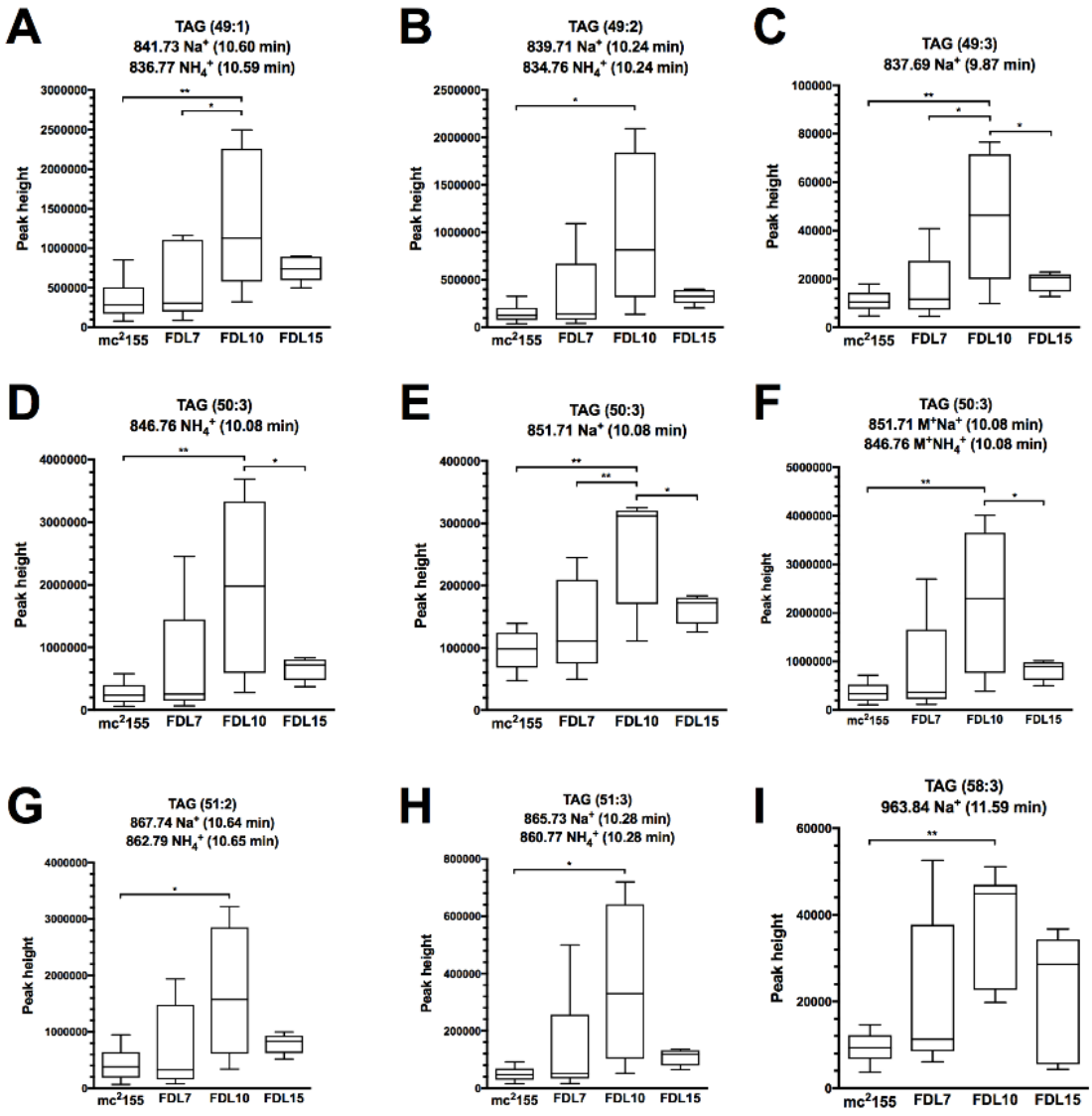

Figure 2.8. LC/QTOF-MS peak heights of TAGs significantly elevated in the FDL10 Δ*prrAB* mutant compared to mc^{2}155. Na^+, molecular ion of target lipid species plus sodium; NH_4^+, molecular ion of target lipid species plus ammonium. Values represent the peak heights of positive molecular ions analyzed from three independent cultures, each with two technical replicates. Boxplots with median lines extend from the 25th to 75th percentiles and show Tukey whiskers. *, adjusted $p < 0.05$; **, adjusted $p < 0.01$; two-way ANOVA, Tukey's multiple comparisons.

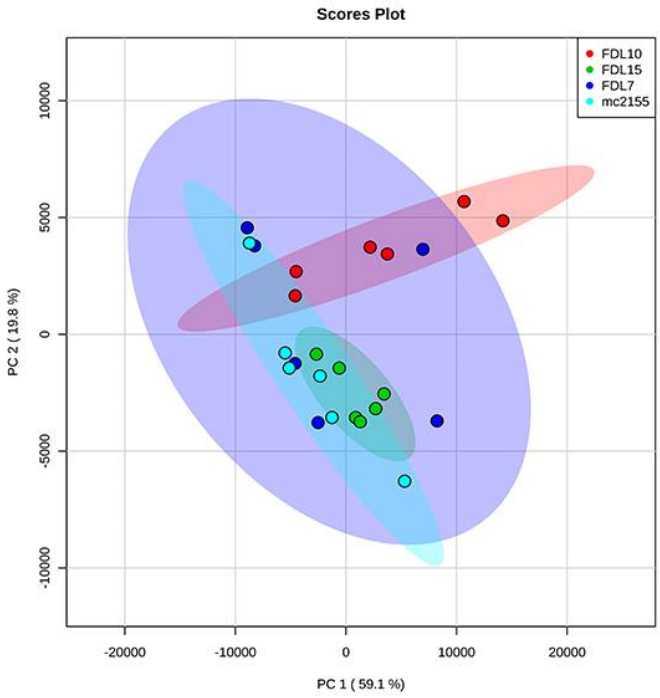

Figure 2.9. Principal component analysis (PCA) of *M. smegmatis* mc^{2}155, FDL7, FDL10, and FDL15 strains subjected to untargeted lipid analysis via LC/QTOF-MS.

Qualitative Assessment of TAGs and DAGs in the M. smegmatis ΔprrAB Mutant During Ammonium Stress

To support the LC/QTOF-MS quantitative TAG analyses (Fig. 2.8), apolar lipids were extracted, separated by TLC, and visualized with iodine vapor. Qualitative TLC analysis revealed slightly higher levels of TAGs, DAGs, and other apolar lipids in the Δ*prrAB* mutant compared with wild-type mc^{2}155 when cultured in SR-1-lowNH_4 (Fig. 2.10, Fig. 2.11). The relative levels of TAGs, DAGs, and apolar lipids were similar in mc^{2}155, FDL7, and FDL15 compared to FDL10 during growth in SR-1-lowNH_4, revealing reproducibility in three biological (Fig. 2.10) and two technical replicates (Fig. 2.11). These qualitative TLC analyses corroborated the LC/QTOF-MS lipidomics results (Fig. 2.7) and the associated TAG quantitative levels shown in Figure 2.8 and further indicate that PrrAB influences TAG and DAG production.

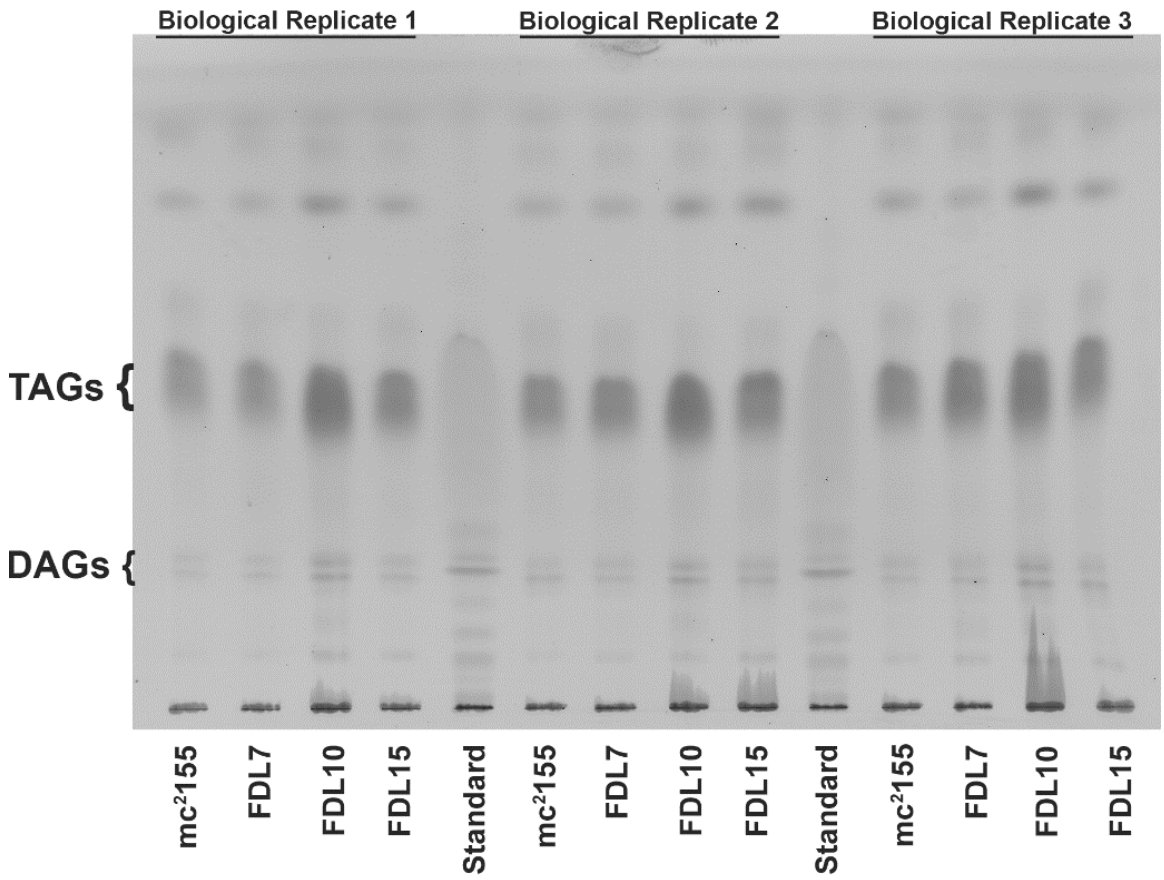

Figure 2.10. Qualitative TLC analysis of TAG and DAG lipid species isolated from *M. smegmatis* cultures grown in SR-1-lowNH_4 (2 mM NH_4). *M. smegmatis* apolar lipids (75 □g) from three independent biological replicates and TAG standards (Std; 500 □g) were separated, and TLC plates were developed using hexane:diethyl ether:acetic acid (80:20:1). Apolar lipids were visualized with I_2 vapor.

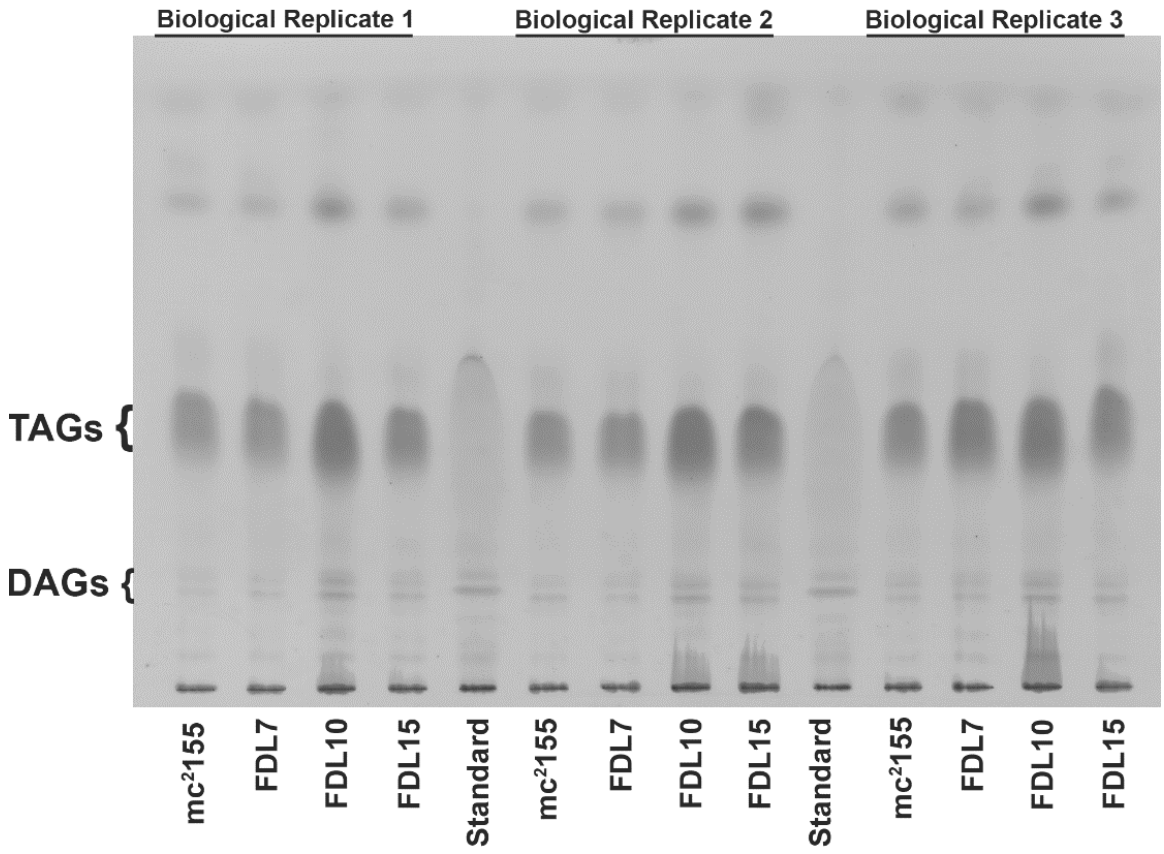

Figure 2.11. Second technical replicate of qualitative TLC analysis of TAG and DAG lipid species from *M. smegmatis* cultures grown in SR-1-lowNH_4. *M. smegmatis* apolar lipids (75 □g) from three independent biological replicates and TAG standards (Std; 500 □g) were separated, and TLC plates were developed using hexane:diethyl ether:acetic acid (80:20:1). Apolar lipids were visualized with I_2 vapor.

TAG Accumulation is a PrrAB-Dependent Phenotype During Ammonium Stress

We next sought to determine if TAG accumulation was a PrrAB-dependent phenotype during *M. smegmatis* ammonium stress. Culturing the strains under ammonium sufficient conditions (SR-1-highNH_4) and resolving the apolar lipid fractions containing TAG and DAG species revealed no consistent qualitative differences in TAG accumulation in the *M. smegmatis* strains (Fig. 2.12). Compared to mc^{2}155, FDL7, and FDL15, DAG species appeared elevated in the Δ*prrAB* mutant in one biological replicate (Fig. 2.12). These results further indicate that *M. smegmatis* PrrAB contributes to TAG regulation specifically in response to ammonium stress conditions.

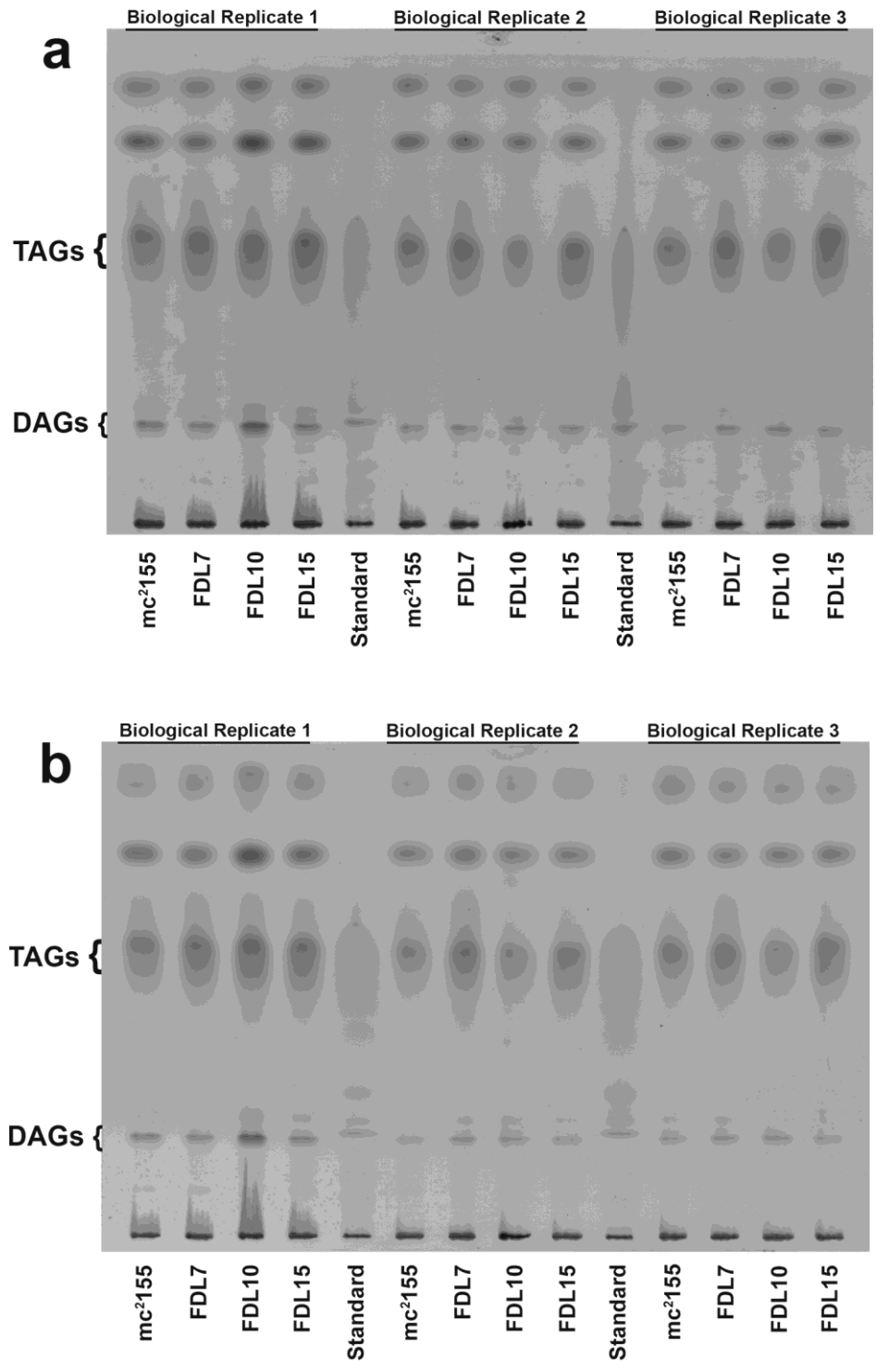

Figure 2.12. Qualitative TLC analysis of TAG and DAG lipid species isolated from *M. smegmatis* cultures grown in SR-1-highNH_4. *M. smegmatis* apolar lipids (75 µg) from three independent biological replicates and TAG standards (Std; 500 µg) were separated, and TLC plates were developed using hexane:diethyl ether:acetic acid (80:20:1). Apolar lipids were visualized with I_2 vapor. Panels (a) and (b) shows the first and second technical replicates, respectively, of the three independent biological replicates.

M. smegmatis Lipid and TAG Biosynthesis Genes are Regulated by PrrAB During Ammonium Stress

To examine the genetic basis for the lipid-accumulating phenotype in the Δ*prrAB* mutant, total RNA was isolated from mc^{2}155, FDL10, and FDL15 strains cultured for 24 h in SR-1-lowNH_4. We analyzed transcript profiles of genes belonging to the Kennedy pathway of TAG biosynthesis (Fig. 2.13A) and fatty acid biosynthesis (Fig. 2.13B). As shown in Fig. 2.13A, transcriptional profiles for glycerol kinase (*glpK, MSMEG_6759*) and glycerol-3 phosphate acyl transferase (*GPAT, MSMEG 4703*), whose enzyme products catalyze the first two steps in TAG biosynthesis (Fig. 2.14A), were upregulated >4-fold in the Δ*prrAB* mutant. Two wax ester synthase/acyl-CoA:diacylglycerol acyltransferase (WS/DGAT) genes, which catalyze the final TAG biosynthetic reaction (Fig. 2.14A), were upregulated >2 fold in the Δ*prrAB* mutant (Fig. 2.13A). The *accD6* and *accA3* acetyl-CoA carboxylase genes were also highly upregulated (>2 fold each) in the Δ*prrAB* mutant (Fig. 2.13B), indicating that PrrAB may influence de novo lipid biosynthesis (Fig. 2.14B). In the Δ*prrAB* mutant, Ag85C (*fbpC, MSMEG 3280*) transcripts were upregulated >4 fold (Fig. 2.13B), indicating that PrrAB is involved in regulating genes involved in mycolic acid biosynthesis (Fig. 2.14B) despite qualitative TLC revealing similar MAME profiles in the *M. smegmatis* strains (discussed above; Fig. 2.6a). Collectively, these quantitative transcriptional results revealed that PrrAB directly or indirectly represses genes involved in TAG and lipid biosynthesis, corroborating the LC/QTOF-MS lipidomics results (Fig. 2.7) data and lipid-accumulating phenotype in the Δ*prrAB* mutant (Figs. 2.8, 2.10).

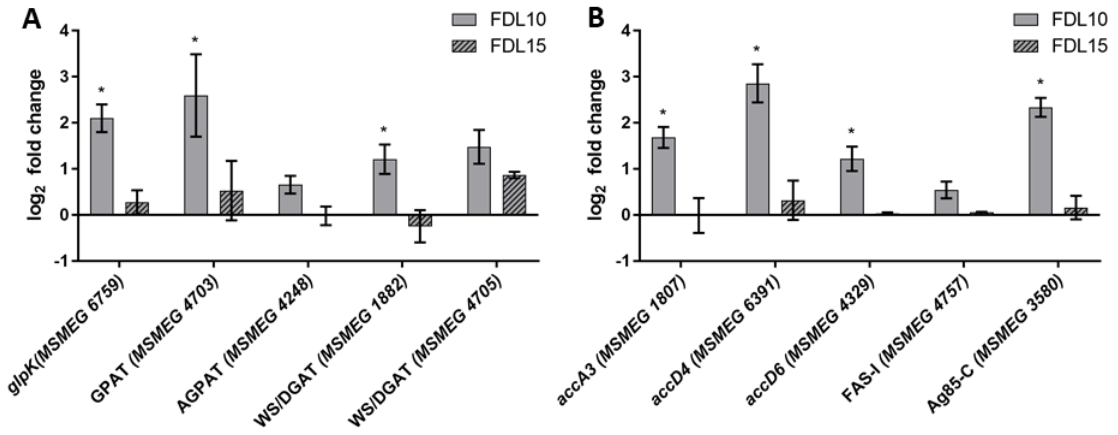

Figure 2.13. TAG and fatty acid biosynthetic genes were upregulated in the Δ*prrAB* mutant during growth in low ammonium (SR-1-lowNH_4). (A) Transcriptional profiles of key genes participating in TAG and (**B**) fatty acid biosynthesis. Log_2 expression values compare the FDL10 Δ*prrAB* mutant (solid bars) and the FDL15 complemented mutant (hatched bars) relative to mc^2155 ($\Delta\Delta C_t$ method using 16S rRNA as a reference gene). *, $p < 0.05$; unpaired t test.

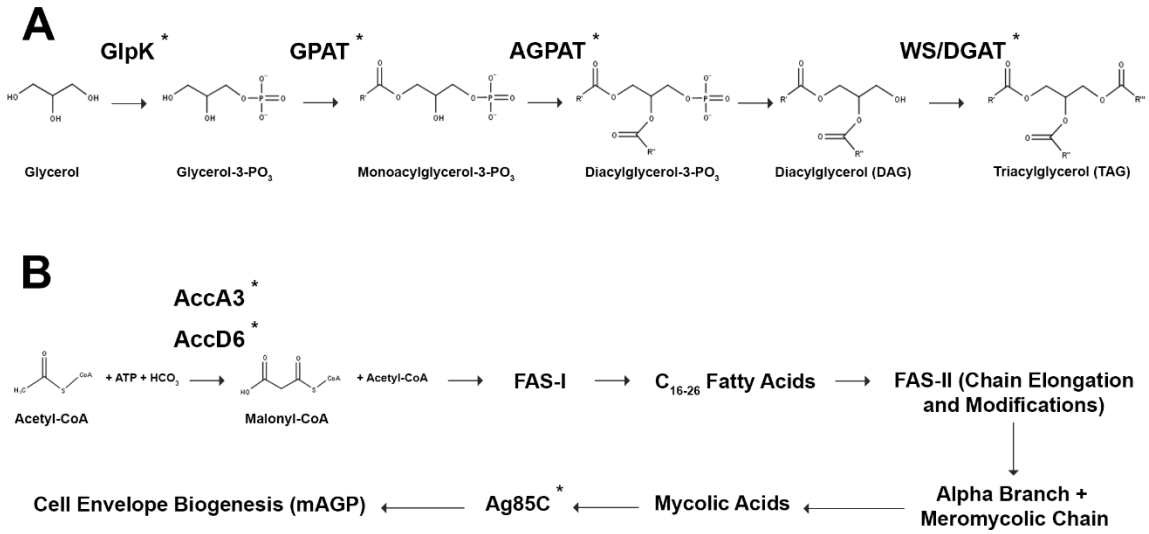

Figure 2.14. Pathways for (A) TAG and (B) lipid biosynthesis in *M. smegmatis.* TAG and fatty acid biosynthetic genes upregulated in the Δ*prrAB* mutant during growth in low ammonium (SR-1-lowNH_4) (Fig. 2.13) are marked with an asterisk.

The M. smegmatis ΔprrAB Mutant is Sensitive to Hypoxia in Ammonium-Limited Medium

To determine if the Δ*prrAB* mutant exhibits sensitivity or resistance to environmental stresses in the presence of low ammonium, we monitored growth of the *M. smegmatis* strains in the presence of isoniazid (INH) and upon exposure to acidic (pH 5.5), SDS (0.05%), and hypoxic stresses for 48 h. In SR-1-lowNH_4 medium, the Δ*prrAB* mutant grew poorly during hypoxia for 48

h, exhibiting 70% reduced growth, compared to mc^{2}155 ($p < 0.0001$) (Fig. 2.15). After 48 h incubation in SR-1-lowNH_4 medium, wild-type mc^{2}155 and the Δ*prrAB* mutant grew similarly in the presence of acidic (pH 5.5) and detergent (0.05% SDS) stress and upon exposure to isoniazid (data not shown).

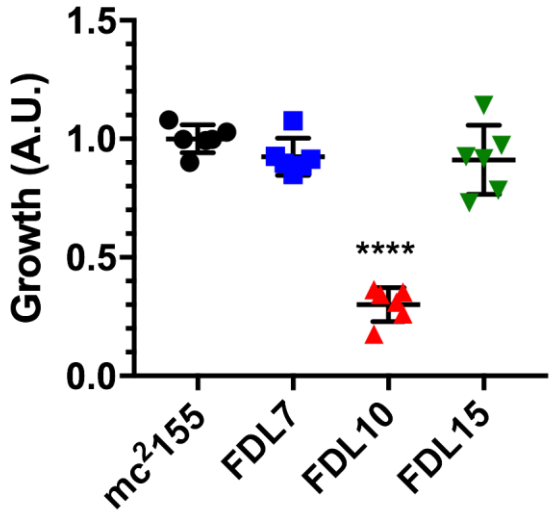

Figure 2.15. *M. smegmatis* growth in SR-1-lowNH_4 media during hypoxia. Growth (OD_{600}) of mc^{2}155, FDL7, FDL10, and FDL15 was assessed during hypoxia in SR-1-lowNH_4 media for 48 h. Values were normalized to the average OD_{600} of mc^{2}155 replicates at 48 h and represent the mean ± SD of data collected from six independent cultures. A.U., arbitrary units; ****, $p < 0.0001$; ANOVA.

Discussion

The *M. tuberculosis prrAB* two-component system is expressed during infection in human peripheral blood-derived macrophages (Graham and Clark-Curtiss 1999; Haydel and Clark-Curtiss 2004) and is required for early intracellular infection in murine bone-derived macrophages (Ewann et al. 2002). Additionally, *prrAB* is essential for viability in *M. tuberculosis* and is significantly upregulated under nitrogen-limited conditions (Haydel et al. 2012). In addition to PrrAB, the MtrAB TCS is also essential in *M. tuberculosis* (Zahrt and Deretic 2000). The essential nature of *prrAB* in *M. tuberculosis* implicates this TCS as a bona fide target for development of novel classes of antituberculosis drugs (Bellale et al. 2014), and the transcriptional

responsiveness to nitrogen availability provides a platform for experimentally determining the physiological role of PrrAB.

Due to the inability to generate a targeted *prrAB* gene deletion in *M. tuberculosis* (Haydel et al. 2012), we questioned if the conserved PrrAB system was universally essential in pathogenic and nonpathogenic mycobacteria. In this report, we show that *prrAB* was not essential in *M. smegmatis* (Figs. 2.1, 2.2), contrary to a recent study describing *prrAB* essentiality in *M. smegmatis* (Mishra et al. 2017). Generation of the *M. smegmatis* Δ*prrAB* mutant strain prompted us to explore the physiological contributions of this TCS in mycobacteria. PrrAB was necessary for maintaining a dispersed cell phenotype in ammonium-limiting growth conditions during stationary phase (Fig. 2.4C), likely through coordinated lipid expression patterns. Growth of the *M. smegmatis* Δ*prrAB* mutant displayed early (24 h) and late (96 h) growth deficiencies when nitrate was present at limiting (2 mM) concentrations (Fig. 2.3A), however, no clumping phenotype was observed in this growth medium. To test amino acid-derived nitrogen sources, *M. smegmatis* strains were cultured in minimal media supplemented with 2 mM L-asparagine or 2 mM L-glutamine. In a limited L-glutamine environment, Δ*prrAB* mutant growth was slightly decreased at 24 h but subsequently mimicked the growth rate of wild-type *M. smegmatis* (Fig. 2.3C).

Overexpression of *M. tuberculosis prrA* in the *M. smegmatis* Δ*prrAB* background restored growth to *M. smegmatis* wild-type levels *in vitro* (Fig. 2.4; Fig. 2.2A), possibly due to the *M. smegmatis* and *M. tuberculosis* PrrA proteins exhibiting 97% overall identity and 100% identity in the □8 DNA-binding recognition helix. Genetic complementation in the absence of PrrB suggests that in vivo cross talk occurs or that PrrA is functional in vivo in a non-phosphorylated state. Although genetic complementation and growth phenotype restoration occurs in the absence of the PrrB cognate histidine kinase, in vitro phosphorylation reactions reveal that PrrA is specifically transphosphorylated by PrrB (Agrawal et al. 2015).

Mycobacteria produce an extensive repertoire of lipids, many of which are virulence factors, including phthiocerol dimycocerosate (Goren, Brokl, and Schaefer 1974), sulfolipids (Goren, Brokl, and Schaefer 1974), and trehalose dimycolate (Behling et al. 1993). Additionally,

M. tuberculosis accumulates TAGs in response to various physical stresses that mimic the phagosomal environment of activated macrophages, including hypoxia (Daniel et al. 2004), acidic conditions, and nitric oxide exposure (Sirakova et al. 2006). Accumulation of large quantities of TAGs in the highly virulent W-Beijing *M. tuberculosis* strain correlates with upregulation of the DosR dormancy regulon (Reed et al. 2007), a 48-gene regulon associated with latent tuberculosis infection (Sherman et al. 2001). In *M. smegmatis*, TAGs accumulated during *in vitro* culture growth in a low nitrogen medium (Garton et al. 2002). Clearly, upregulation of TAG biosynthetic pathways and accumulation of TAGs are strategies which allow mycobacteria to cope with environmental stresses and provide *M. tuberculosis* with an energy source during dormancy (Garton et al. 2002; Daniel et al. 2011).

While TAG accumulation in prokaryotes is a relatively rare phenomenon, numerous members of the Actinomycetes, including *Gordonia, Mycobacteria, Streptomyces,* and *Nocardia* (Indest et al. 2015; Daniel et al. 2004; Arabolaza et al. 2008; H.M. Alvarez et al. 2001), share this phenotype. TAGs accumulate in *M. tuberculosis* during periods of dormancy induced by hypoxia and nitric oxide (Daniel et al. 2004) and during *in vitro* nitrogen limitation in *M. smegmatis* (Garton et al. 2002). Additionally, TAGs are located in the cell envelope (Bansal-Mutalik and Nikaido 2014) and as intracellular inclusions during nutrient starvation (Wu, Gengenbacher, and Dick 2016) in *M. smegmatis*. In the absence of PrrAB and during growth in an ammonium-limiting environment, *M. smegmatis* clumped excessively (Fig. 2.4C) and accumulated TAGs (Figs. 2.7, 2.8, and 2.10). Since low ammonium levels generate dormancy-associated signals that induce accumulation of TAGs (Garton et al. 2002), these results could link PrrAB to particular dormancy phenotypes (Daniel et al. 2011).

Genes of the Kennedy TAG biosynthesis pathway (Fig. 2.14A) were universally upregulated in the Δ*prrAB* mutant compared to wild-type mc^{2}155 and the *prrAB* complementation strain, FDL15. Genes participating in the first two steps of TAG biosynthesis, catalyzed by glycerol kinase (*MSMEG 6759*) and glycerol-3 phosphate acyltransferase (*MSMEG 4703*), and two *WS/DGAT* genes (*MSMEG 4705*, *MSMEG 1882*) (Fig. 2.14A) were significantly upregulated in the Δ*prrAB* mutant (Fig. 2.13A). Overall, transcriptional profiling of genes participating in

numerous steps in the Kennedy pathway for TAG biosynthesis genetically corroborates the LC/QTOF-MS lipidomics data (Fig. 2.7) and quantitative TAG analyses (Fig. 2.8), indicating that PrrAB indirectly or directly contributes to regulating TAG biosynthesis.

The first reaction in fatty acid biosynthesis is the irreversible carboxylation of acetyl-CoA with bicarbonate to generate malonyl-CoA, catalyzed by acetyl-CoA carboxylase (ACCase) (Fig. 2.14B). The *accD6* and *accA3* genes, encoding two biosynthetic ACCase subunits, were significantly upregulated in the Δ*prrAB* mutant relative to wild-type mc^{2}155 (Fig. 2.13B). Although differences in α, α', and epoxy mycolic acid species were not observed via qualitative TLC (Fig. 2.6), deletion of *prrAB* resulted in upregulation of the Ag85C mycolyl transferase gene, which is important for incorporation of mycolic acids into the cell envelope (Belisle et al. 1997), further implicating PrrAB in lipid metabolism regulation. Global transcriptomics analyses of the Δ*prrAB* mutant are currently underway and will further link PrrAB and *M. smegmatis* metabolism (Maarsingh and Haydel, unpublished data).

M. tuberculosis modulates its transcriptional programming to adapt to the phagosomal environment during infection (Schnappinger et al. 2003; Rohde et al. 2012). We have demonstrated that an *M. smegmatis* Δ*prrAB* mutant accumulates TAGs (Fig. 2.8) and increases transcription of several TAG and fatty acid biosynthetic genes in an ammonium-limited environment (Fig. 2.13A). The *M. smegmatis* genome is annotated with six WS/DGAT genes which catalyze the final and committed step in TAG biosynthesis. The abundance of these enzymes in *M. smegmatis* complicates enzymatic studies to mechanistically determine the contributions of specific WS/DGAT isoforms to explain the upregulated TAG phenotype in the Δ*prrAB* mutant. The *M. smegmatis* PrrAB TCS may serve to repress transcription of one or more of the less active WS/DGAT genes during ammonium limitation, as our qRT-PCR data suggests (Fig. 2.13A). TAGs accumulate in *M. tuberculosis* during residence in macrophages grown under hypoxic conditions (Daniel et al. 2011) and upon exposure to *in vitro* stress responses that mimic the phagosome environment (Sirakova et al. 2006). Additional studies are needed determine if other *in vitro* stresses produce an exacerbated TAG accumulation phenotype in the Δ*prrAB* mutant. Since *M. tuberculosis prrAB* is expressed during early infection in macrophages (Graham

and Clark-Curtiss 1999; Haydel and Clark-Curtiss 2004; Ewann et al. 2002) and is significantly upregulated under nitrogen-limited conditions (Haydel et al. 2012), PrrAB could serve to repress transcriptional adaptive responses during early stages of macrophage infection.

As *M. tuberculosis* advances into a persistent state during infection, it must adapt to the nutritionally-deprived and anoxic environment of the granulomatous lesion (Timm et al. 2003). Additionally, nutrient starvation is associated with tolerance to rifampicin and isoniazid (Betts et al. 2002). Although exposure to low pH, cell wall (detergent) stress, or isoniazid did not affect the *M. smegmatis* Δ*prrAB* mutant in ammonium-limiting media, hypoxic conditions significantly compromised Δ*prrAB* mutant growth (Fig. 2.15). The *M. tuberculosis* DosRS TCS is required for long-term *in vitro* survival during anaerobic conditions (Park et al. 2003; Leistikow et al. 2010), and *dosR* and *dosS* mutants fail to establish persistent infection and hypoxic granulomas in rhesus macaques (Mehra et al. 2015). Given that *M. tuberculosis* accumulates TAGs and lipids and shifts nitrogen metabolic pathways during hypoxia (Leistikow et al. 2010; Baek, Li, and Sassetti 2011; Akhtar et al. 2013) and that the DosRS system is inextricably linked to *M. tuberculosis* hypoxic responsiveness and persistence (Park et al. 2003; Leistikow et al. 2010; Mehra et al. 2015), our results suggest PrrAB TCS also contributes to mycobacterial metabolic responsiveness and changes.

To better understand the essential nature of the *M. tuberculosis* PrrAB TCS and its potential role in tuberculosis disease progression, efforts to generate a titratable *prrAB* knockdown mutant using a tetracycline-responsive repression system (Ehrt et al. 2005) are underway. Additionally, *M. tuberculosis* PrrA site-specific mutations will be generated to investigate transcriptional and phenotypic responses of this essential TCS. While additional studies are necessary to explore the role of PrrAB in pathogenesis, mechanistic and metabolic understanding of the essential *M. tuberculosis* PrrAB system and investigations into how diarylthiazoles functionally disrupt PrrAB (Bellale et al. 2014) or PrrAB-regulated pathways are necessary to help combat the ongoing epidemic of drug-resistant tuberculosis.

CHAPTER 3

COMPARATIVE TRANSCRIPTOMICS REVEALS PRRAB-MEDIATED CONTROL OF METABOLIC, RESPIRATION, ENERGY-GENERATING, AND DORMANCY PATHWAYS IN MYCOBACTERIUM SMEGMATIS

Publication Note: This article was submitted for publication in an altered format to *BMC Genomics* on April 5, 2019.

Abstract

Background

Mycobacterium smegmatis is a saprophytic bacterium frequently used a as a genetic surrogate to study pathogenic *Mycobacterium tuberculosis*. The PrrAB two-component genetic regulatory system is essential in *M. tuberculosis* and represents an attractive therapeutic target. In this study, transcriptomic analysis (RNA-seq) of an *M. smegmatis* Δ*prrAB* mutant was used to define the PrrAB regulon and provide insights into the essential nature of PrrAB in *M. tuberculosis*.

Results

RNA-seq differential expression analysis of *M. smegmatis* wild-type (WT), Δ*prrAB* mutant, and complementation strains revealed that during in vitro exponential growth, PrrAB regulates 683 genes, 62% of which are repressed in the WT background. Gene ontology and cluster of orthologous groups analyses showed that PrrAB regulates genes participating in ion homeostasis, redox balance, metabolism, and energy production. PrrAB induced transcription of *dosR* (*devR*), a response regulator gene that promotes latent infection in *M. tuberculosis*. Compared to the WT and complementation strains, the Δ*prrAB* mutant exhibited an exaggerated delayed growth phenotype upon exposure to potassium cyanide and respiratory inhibition. Gene expression profiling correlated with these growth deficiency results, revealing that PrrAB induces transcription of the high-affinity cytochrome *bd* oxidase genes under both aerobic and hypoxic

conditions. ATP synthesis was ~64% lower in the Δ*prrAB* mutant relative to WT strain, further demonstrating that PrrAB regulates energy production.

Conclusions

The *M. smegmatis* PrrAB two-component system regulates respiratory and oxidative phosphorylation pathways, potentially to provide tolerance against the dynamic environmental conditions experienced in its natural ecological niche. PrrAB positively regulates ATP levels during exponential growth, presumably through transcriptional activation of both terminal respiratory branches (cytochrome c bc_1-aa_3 and cytochrome *bd* oxidases), despite transcriptional repression of ATP synthase genes. Additionally, PrrAB positively regulates expression of the dormancy-associated *dosR* response regulator in an oxygen-independent manner, which may serve to fine-tune sensory perception of environmental stimuli associated with metabolic repression.

Background

TCSs participate in signal transduction pathways and are ubiquitously found in bacteria, archaea, some lower eukaryotes and plants (Zschiedrich, Keidel, and Szurmant 2016; Krell 2018; Schaap et al. 2015; Liu et al. 2018). TCSs recognize specific environmental stimuli (A. Kumar et al. 2007) and integrate an adaptive response, frequently by modulating transcription (Richmond et al. 2016). A prototypical TCS consists of a membrane-bound histidine kinase sensor and a cytoplasmic DNA-binding response regulator. In pathogenic bacteria, TCSs act as virulence factors that regulate diverse survival mechanisms, such as antibiotic resistance (Gebhardt and Shuman 2017), phosphate limitation (Kelliher, Radin, and Kehl-Fie 2018), low oxygen tension (Mehra et al. 2015), and evasion of immune responses (Herrera et al. 2014). Though mammalian proteins bearing histidine kinase sequence motifs and activity (Srivastava et al. 2006) have been identified, response regulators appear absent in humans, opening the possibility for development of inhibitors targeting virulence-related or essential bacterial TCSs as novel therapeutic approaches.

Mycobacterium tuberculosis, the causative agent of tuberculosis, is an ancient disease of mankind and the leading cause of death from an infectious agent (WHO 2017). The *M. tuberculosis* genome harbors 11 paired TCSs, two orphaned histidine kinases, and six orphaned response regulators (Haydel and Clark-Curtiss 2004). Of these TCSs, only MtrAB (Zahrt and Deretic 2000) and PrrAB (Haydel et al. 2012) are essential for *M. tuberculosis* viability. The *prrAB* genes are conserved across all fully-sequenced mycobacterial genomes, suggesting an evolutionary selective pressure to retain this TCS. The *M. tuberculosis prrAB* is upregulated during the early stages of human macrophage infection (Haydel and Clark-Curtiss 2004) and under in vitro nitrogen limitation (Haydel et al. 2012). During infection in murine macrophages, *prrAB* is required for early replication and adaptation to the intracellular environment (Ewann et al. 2002). Capitalizing on findings that diarylthiazole compounds inhibit *M. tuberculosis* growth via the PrrAB TCS, Bellale et al. (Bellale et al. 2014) exposed *M. tuberculosis* cultures to diarylthiazole and found that PrrAB modulates transcription of genes enabling metabolic adaptation to a lipid-rich environment, responsiveness to reduced oxygen tension, and production of essential ribosomal proteins and amino acid tRNA synthases.

Mycobacterium smegmatis strain mc^2155 (Snapper et al. 1990) is a non-pathogenic, rapid-growing, saprophytic mycobacterium that is used as a surrogate model to study *M. tuberculosis* genetics and mycobacterial TCSs. We recently demonstrated that *prrAB* is not essential in *M. smegmatis* and that PrrAB differentially regulates triacylglycerol biosynthetic genes during ammonium limitation (Maarsingh and Haydel 2018). The inability to generate an *M. tuberculosis prrAB* knockout mutant (Haydel et al. 2012), the high degree of PrrA sequence identity (95%) between *M. tuberculosis* and *M. smegmatis*, and the presence of over 2,000 homologous genes (51% of total genes in *M. tuberculosis* H37Rv) shared between these species prompted use of the *M. smegmatis* Δ*prrAB* mutant to better understand PrrAB transcriptional regulatory properties. A comprehensive profiling of the genes and pathways regulated by PrrAB in *M. smegmatis* would provide insights into the genetic adaptations that occur during *M. tuberculosis* infection and open new avenues for discovering novel therapeutic targets to treat tuberculosis.

In this study, we used RNA-seq-based transcriptomics analysis to obtain a global profile of the genes regulated by PrrAB in *M. smegmatis*. We compared the transcriptomic profiles of *M. smegmatis* WT, Δ*prrAB* mutant, and *prrAB* complementation strains during mid-logarithmic growth under standard laboratory conditions. PrrAB primarily functioned as repressor, decreasing transcription of twice as many genes as it induced. Down-regulated genes were associated with nitrogen, nucleotide, and fatty acid metabolism, while PrrAB-induced genes were implicated in ATP synthesis, respiration, and ion homeostasis. These data provide seminal information into the transcriptional regulatory properties of the mycobacterial PrrAB TCS and how PrrAB may be controlling molecular processes important in *M. tuberculosis* and other mycobacteria.

Results

Phylogenetic Analyses of PrrA and PrrB in Mycobacteria

Since *prrAB* orthologues are present in all mycobacterial species and *prrAB* is essential for viability in *M. tuberculosis* (Haydel et al. 2012), it is reasonable to believe that PrrAB fulfills important regulatory properties in mycobacteria. We therefore questioned the evolutionary relatedness or distance between PrrA and PrrB proteins in mycobacteria. The *M. tuberculosis* H37Rv and *M. smegmatis* mc^2155 PrrA and PrrB amino acid sequences share 93% and 81% identity, respectively. Maximum-likelihood phylogenetic trees, based on PrrA (Fig. 3.1a) and PrrB (Fig. 3.1b) multiple sequence alignments, were generated. Using the Gupta et al. (Gupta, Lo, and Son 2018) recent reclassification of mycobacterial species, the results suggested that, with a few exceptions, PrrA and PrrB evolved with specific mycobacterial clades (Fig. 3.1). While subtle differences in the PrrA or PrrB sequences may represent evolutionary changes as mycobacterial species of the same clade adapted to similar environmental niches, additional experiments are needed to determine if *prrAB* is essential in other pathogenic mycobacteria.

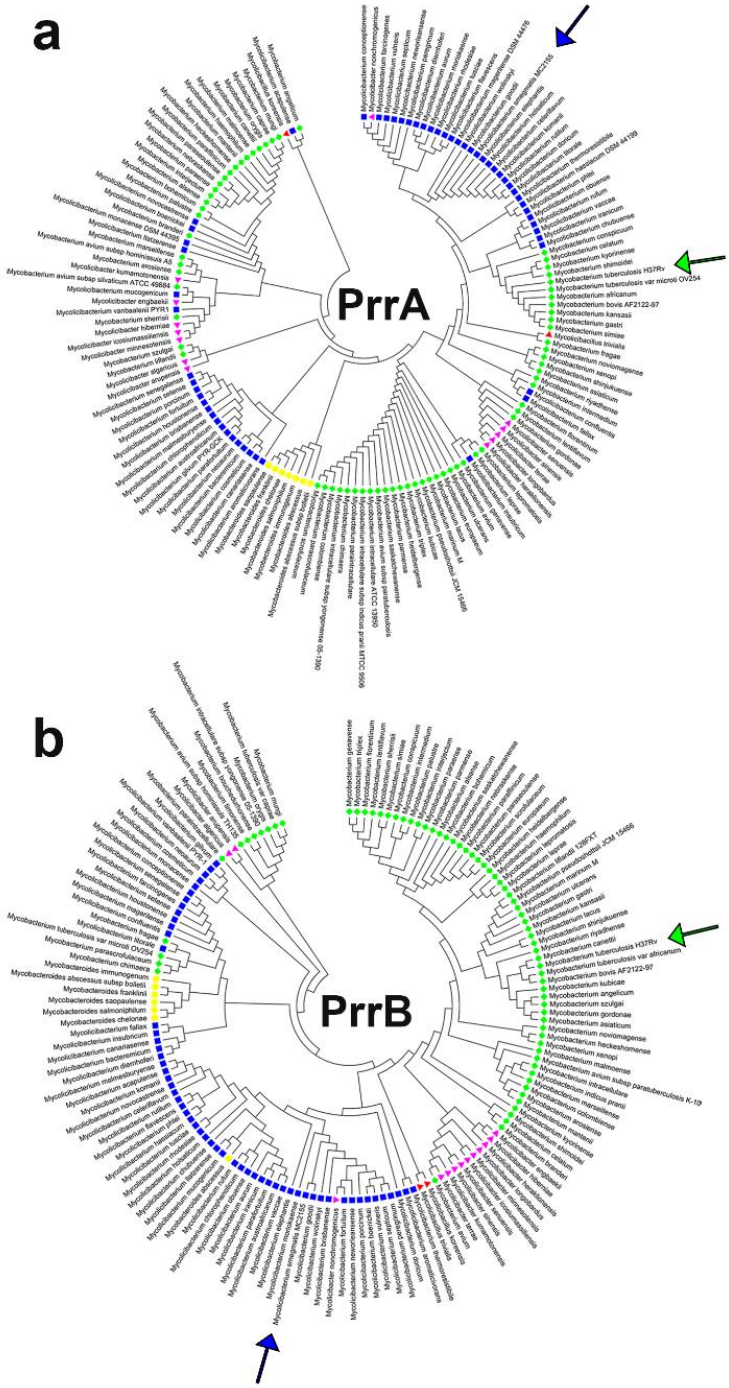

Figure 3.1. Maximum-likelihood phylogenetic analyses of mycobacterial (a) PrrA and (b) PrrB sequences based on the recent reclassification of mycobacterial species by Gupta et al. (Gupta, Lo, and Son 2018). Blue squares, *Fortuitum-Vaccae* clade. Red triangles, *Trivale* clade. Green diamonds, *Tuberculosis-Simiae* clade. Yellow circles, *Abscessus-Chelonae* clade. Purple triangles, *Terrae* clade. *M. smegmatis* mc^{2}155 and *M. tuberculosis* H37Rv are indicated by blue and green arrows, respectively. PrrA and PrrAB sequences were aligned using default MUSCLE algorithms (Edgar 2004) and phylogenetic tree was generated in MEGA 7 (S. Kumar, Stecher, and Tamura 2016).

We next questioned if the distinct phylogenetic separations between clades could be mapped to specific PrrA or PrrB amino acid residues. We separately aligned mycobacterial PrrA and PrrB sequences in JalView using the default MUSCLE algorithm (Edgar 2004). Within species of the *Abscessus-Chelonae* clade, two unique PrrA signatures were found: asparagine and cysteine substitutions relative to serine 38 (S38) and serine 49 (S49), respectively, of the *M. smegmatis* PrrA sequence (Fig. 3.2). These *Abscessus-Chelonae* clade PrrA residues were not found at similar aligned sites in other mycobacteria (Fig. 3.2). Similarly, members of the *Abscessus-Chelonae* clade (except *Mycobacteriodes abscessus*) harbored unique amino acid substitutions in PrrB, including glutamate, valine, lysine, aspartate, lysine, and valine corresponding to threonine 42 (T42), glycine 67 (G67), valine 90 (V90), methionine 318 (M318), alanine 352 (A352), and arginine (R371), respectively, of the *M. smegmatis* PrrB sequence (Fig. 3.3).

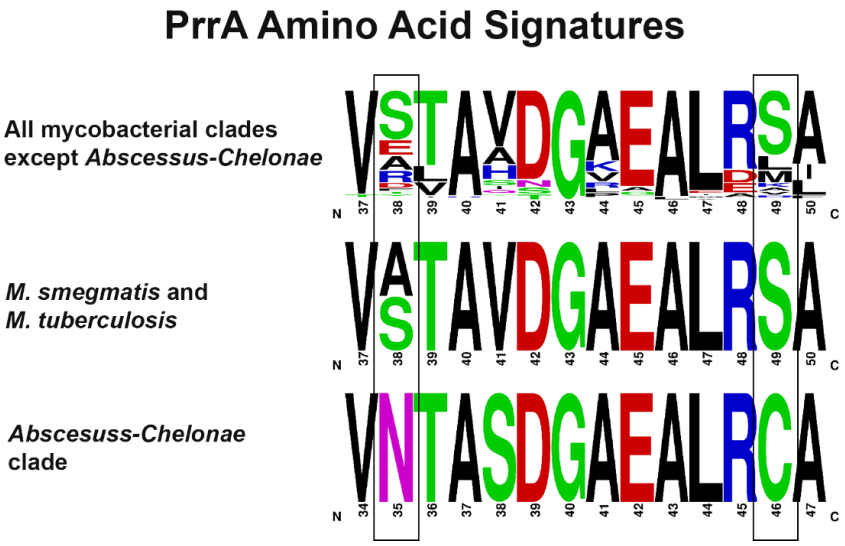

Figure 3.2. Members of the mycobacterial *Abscessus-Chelonae* clade harbor unique PrrA amino acid "signatures". Boxed residues correspond to amino acid residues only found in mycobacterial species belonging to the *Abscessus-Chelonae* clade (bottom row) compared to all other mycobacterial clades (top row) or *M. smegmatis* mc^{2}155 and *M. tuberculosis* H37Rv (middle row). Numerical system below single-letter amino acid codes correspond to the residue position in *M. smegmatis* (top and middle rows) or *M. abscessus* (bottom row). Left box corresponds to PrrA residue S38 of *M. smegmatis* (top and middle rows) and N35 of *M. abscessus*. Right box corresponds to PrrA residue S49 of *M. smegmatis* (top and middle rows) and C46 of *M. abscessus*.

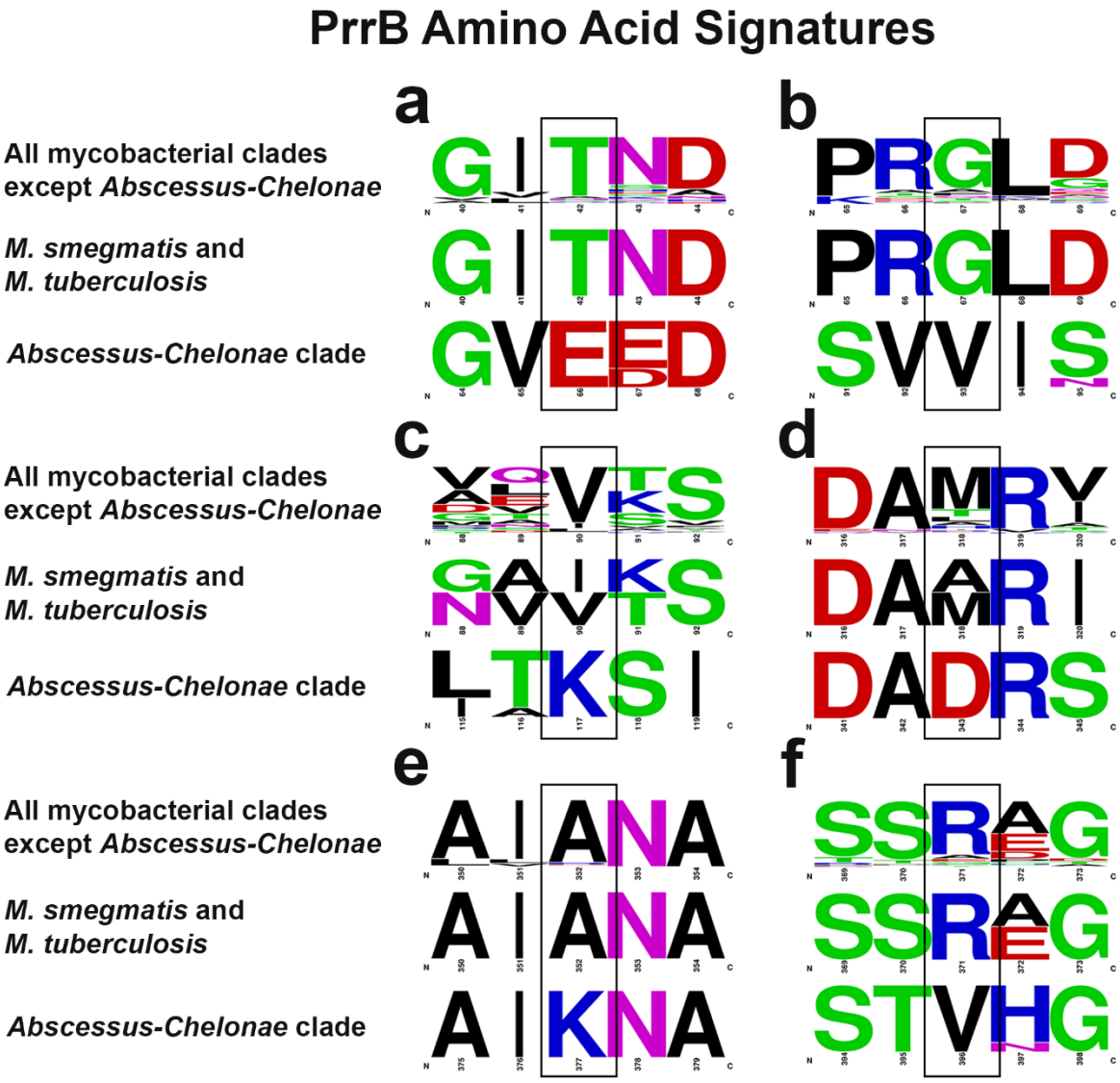

Figure 3.3. Members of the mycobacterial *Abscessus-Chelonae* clade harbor unique PrrB amino acid "signatures". Boxed residues correspond to amino acid residues only found in mycobacterial species belonging to the *Abscessus-Chelonae* clade (bottom row) compared to all other mycobacterial clades (top row) or *M. smegmatis* mc^{2}155 and *M. tuberculosis* H37Rv (middle row). Numerical system below single-letter amino acid codes correspond to the residue position in *M. smegmatis* (top and middle rows) or *M. abscessus* (bottom row). (a) PrrB residue T42 of *M. smegmatis* (top and middle rows) and E66 of *M. abscessus*. (b) PrrB residue G67 of *M. smegmatis* (top and middle rows) and V93 of *M. abscessus*. (c) PrrB residue V90 of *M. smegmatis* (top and middle rows) and 117 of *M. abscessus*. (d) PrrB residue M318 of *M. smegmatis* (top and middle rows) and D343 of *M. abscessus*. (e) PrrB residue A352 of *M. smegmatis* (top and middle rows) and K377 of *M. abscessus*. (f) PrrB residue R371 of *M. smegmatis* (top and middle rows) and V396 of *M. abscessus*.

Transcriptomics Analysis of the M. smegmatis WT, prrAB Mutant, and Complementation Strains

We previously generated an *M. smegmatis* mc^{2}155 *prrAB* deletion mutant (mc^{2}155::Δ*prrAB*; FDL10) and its complementation strain (mc^{2}155::Δ*prrAB*::*prrAB*; FDL15) (Maarsingh and Haydel 2018). Since the *prrAB* regulon and the environmental cue which stimulates PrrAB activity are unknown, a global transcriptomics approach was used to analyze differential gene expression in standard laboratory growth conditions. RNA-seq was used to determine transcriptional differences between the Δ*prrAB* mutant, mc^{2}155, and the complementation strains during mid exponential growth, corresponding to an OD_{600} of ~0.6 (Fig. 3.4), in supplemented Middlebrook 7H9 (M7H9) broth. Total RNA was isolated from three independent, biological replicates of each *M. smegmatis* strain. Based on multidimensional scaling (MDS) plot, one mc^{2}155 biological replicate which was deemed an outlier and excluded from subsequent analyses (details in Methods, Fig. 3.5). Principal component analysis (PCA) of the global expression patterns of the samples (excluding the mc^{2}155 outlier) demonstrated that samples from the mc^{2}155 and FDL15 complementation strains clustered together, apart from those of the FDL10 Δ*prrAB* strain with the majority of variance occurring along PC1 (Fig. 3.6), indicating complementation with ectopically-expressed *prrAB* in the Δ*prrAB* background.

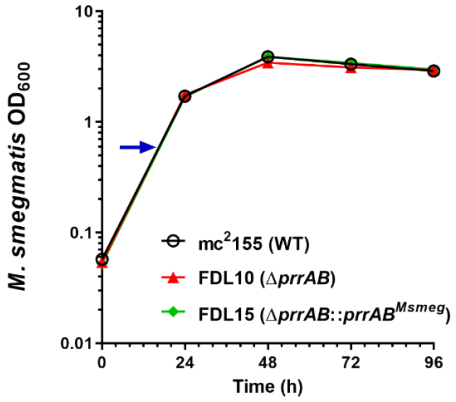

Figure 3.4. *M. smegmatis* growth characteristics in M7H9 broth. Optical density (OD_{600}) of mc^{2}155 (open circles), FDL10 (red triangles), and FDL15 (green diamonds). The blue arrow shows the OD_{600} (~0.6) when cultures were collected for RNA isolation. Values represent the mean ±SEM of data collected from three independent cultures.

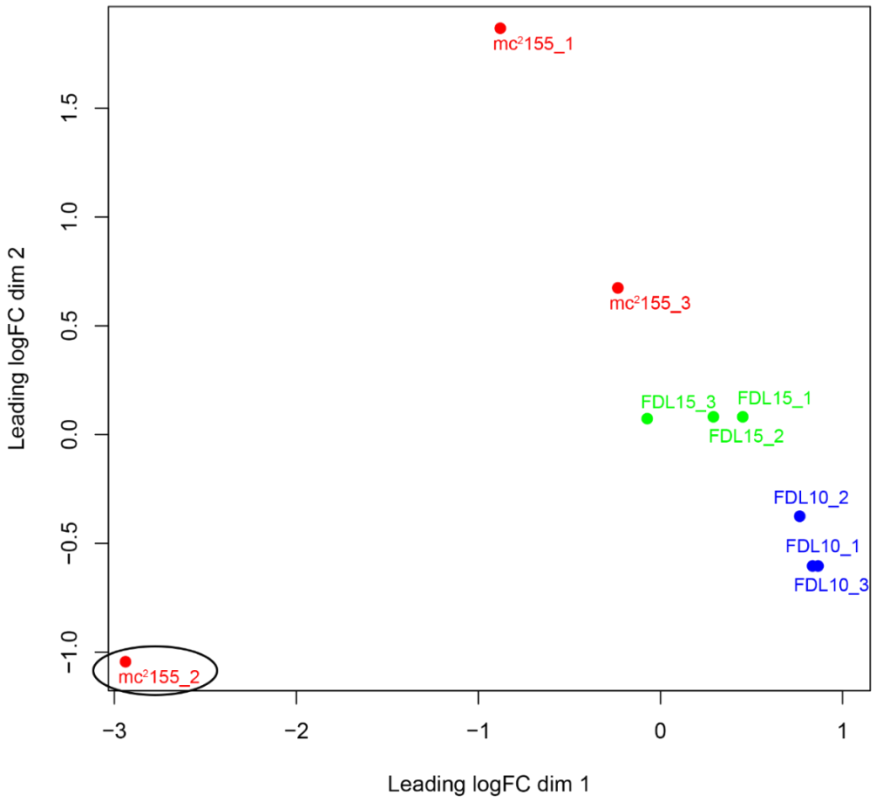

Figure 3.5. Multidimensional scaling (MDS) plot of triplicate *M. smegmatis* RNA-seq samples. Given the MDS-based distance separation of the mc²155_2 sample (circled in the bottom-left corner of plot) from other mc²155 replicates, the mc²155_2 sample was removed from differential expression analysis.

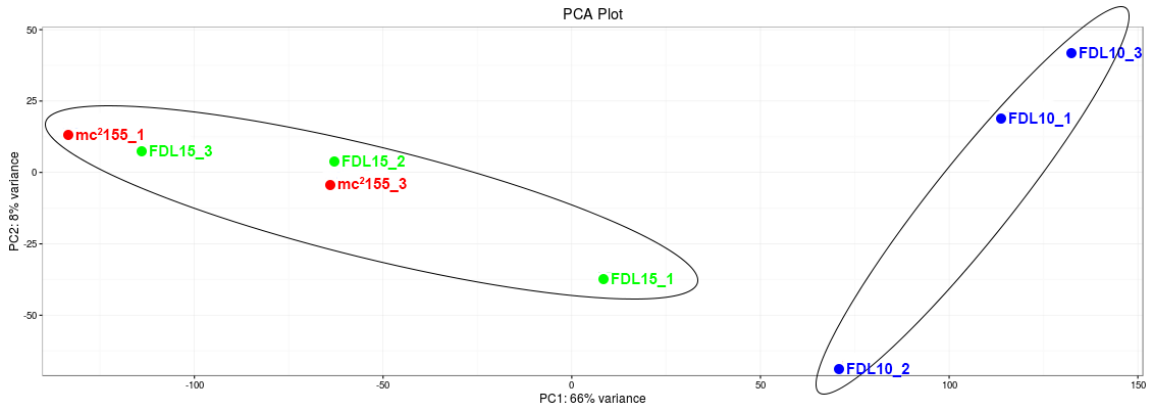

Figure 3.6. Principal component analysis (PCA) of *M. smegmatis* strains used for RNA-seq DEG analyses.

Identifying the PrrAB regulon

To identify differentially-expressed genes (DEGs), pair-wise comparisons of normalized read counts between the □*prrAB* mutant and WT (FDL10 vs. mc^{2}155) as well as the □*prrAB* mutant and *prrAB* complementation (FDL10 vs. FDL15) datasets were performed using EdgeR. Deletion of *prrAB* resulted in induction of 426 genes and repression of 257 genes ($p < 0.05$), representing 683 transcriptional targets (Fig. 3.7a) that are repressed and induced, respectively, by PrrAB in the WT background (Fig. 3.7c). More conservative FDR-based comparisons revealed 167 DEGs ($q < 0.05$) between the WT and □*prrAB* mutant strains (Fig. 3.8a). Between the□*prrAB* complementation and□□*prrAB* mutant strains, 578 DEGs ($p < 0.05$) were identified (Fig. 3.7b), representing 412 repressed and 166 induced genetic targets by the complementation of PrrAB (Fig. 3.7c), while FDR-based comparisons revealed 67 DEGs (Fig. 3.8a). Overall, pair-wise DEG analyses revealed that during mid-logarithmic *M. smegmatis* growth, PrrAB primarily functions to transcriptionally repress genes via direct or indirect mechanisms. In addition, comparison between the two DEG sets (i.e., for mc^{2}155 vs. FDL10 and FDL15 vs. FDL10) datasets revealed 226 (Fig. 3.7e) and 40 (Fig. 3.8b) overlapping DEGs at the significance levels of $p < 0.05$ and $q < 0.05$, respectively. Hierarchical clustering with the overlapping DEGs further illustrated that gene expression changes induced by the *prrAB* deletion were partially recovered by *prrAB* complementation (Fig. 3.7d). We randomly selected six DEGs for qRT-PCR analyses and verified the RNA-seq results for five genes, thus strengthening the transcriptomics data (Fig. 3.9).

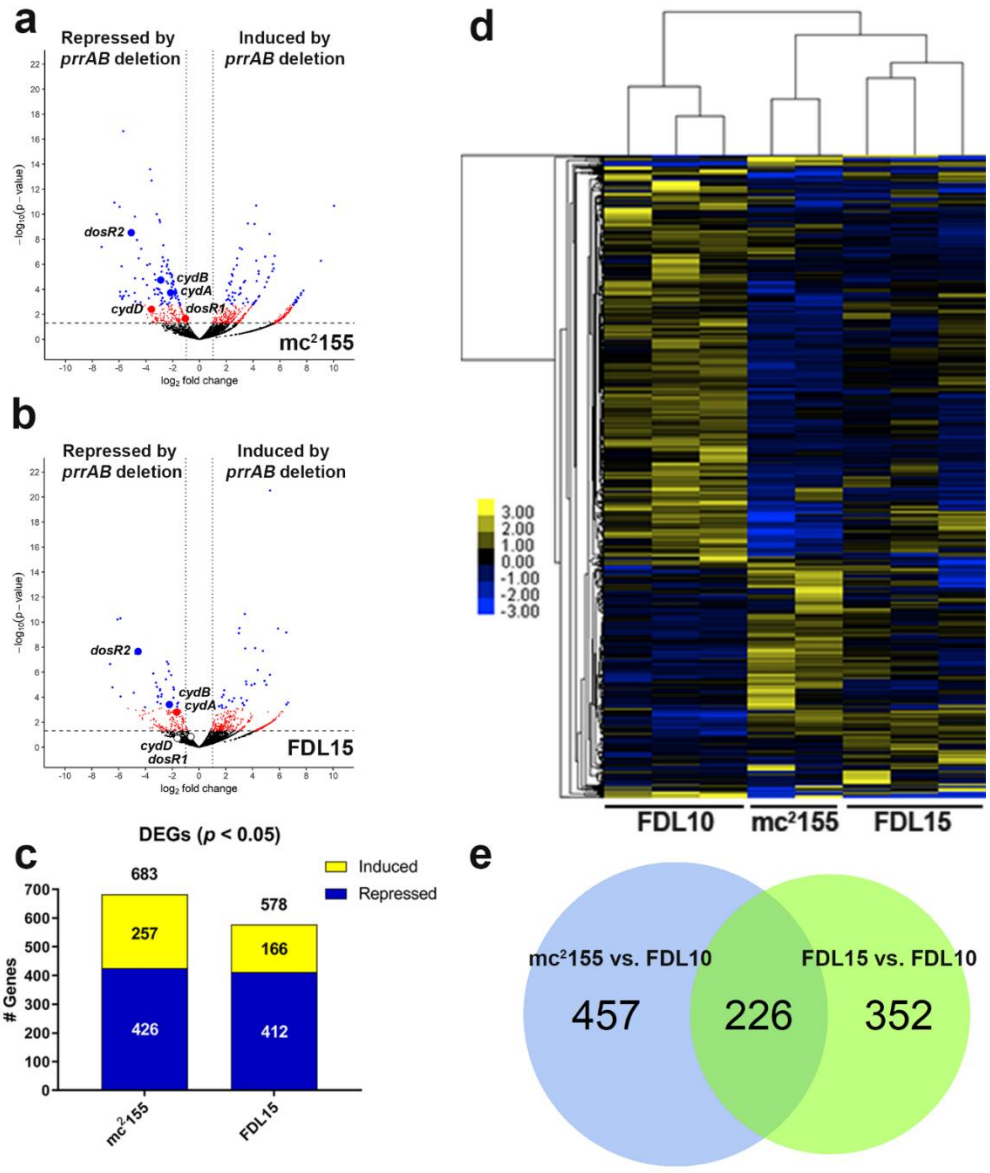

Figure 3.7. Global DEG profiles ($p < 0.05$) between the mc²155 vs. FDL10 and FDL15 vs. FDL10 RNA-seq comparisons. Volcano plots of (a) FDL10 vs. mc²155 and (b) FDL10 vs. FDL15 group comparisons with red and blue dots representing differentially-expressed genes with $p < 0.05$ and $q < 0.05$, respectively. The horizontal hatched line indicates $p = 0.05$ threshold, while the left and right vertical dotted lines indicate $\log_2$ fold change of -1 and +1, respectively. (c) Repressed (blue) and induced (yellow) DEGs in mc²155 (WT) and FDL15 (*prrAB* complementation strain) compared to the FDL10 Δ*prrAB* mutant. (d) Average hierarchical clustering (FPKM +1) of individual RNA-seq sample replicates. (e) Venn diagrams indicating 226 overlapping DEGs between mc²155 vs. FDL10 (WT vs. Δ*prrAB* mutant) and FDL15 vs. FDL10 (*prrAB* complementation strain vs. Δ*prrAB* mutant) strain comparisons.

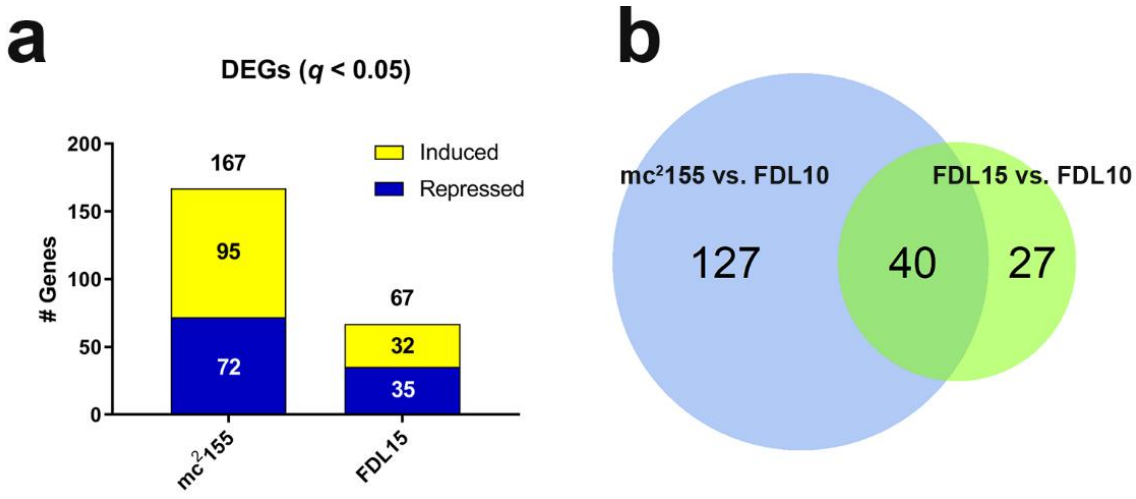

Figure 3.8. Global expression profile of DEGs (q <0.05). (a) Total DEGs (q < 0.05) induced (yellow) or repressed (blue) by PrrAB in mc^{2}155 (WT) and FDL15 (Δ*prrAB* complementation) backgrounds (RNA-seq pair-wise comparisons to the Δ*prrAB* mutant). (b) Venn diagrams of DEGs (q < 0.05) demonstrating that 40 DEGs (q < 0.05) overlapped between RNA-seq pair-wise comparisons.

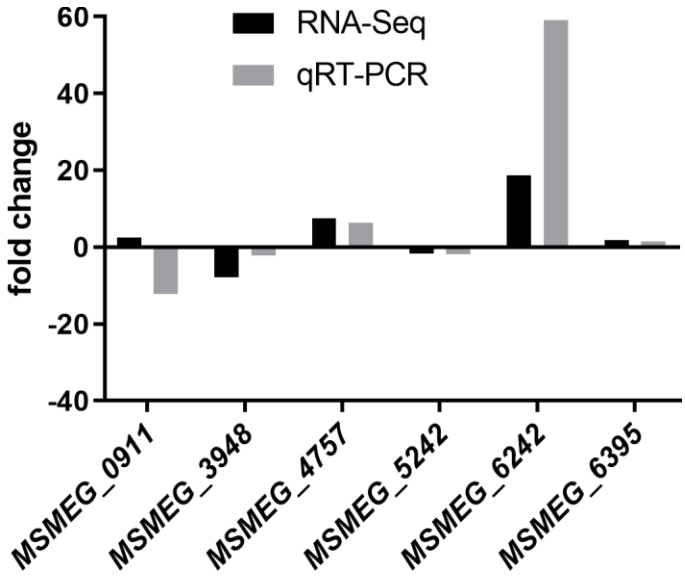

Figure 3.9. qRT-PCR verification of six randomly selected genes from the RNA-seq FDL10 vs. mc^{2}155 comparison. All qRT-PCR measurements were performed from the same RNA samples used for RNA-seq analyses and each gene was tested in triplicate. Absolute fold-change ratios were calculated using the $2^{-\Delta\Delta Ct}$ method (Livak and Schmittgen 2001).

Gene Ontology and Clustering Analyses

To infer function of the genes regulated by PrrAB, enrichment of gene ontology (GO) terms (biological processes and molecular functions) in the DEGs of the mc^{2}155 vs. FDL10

comparison was assessed by the DAVID functional annotation tool. The two sets of DEGs from the mc^{2}155 vs. FDL10 comparison (Fig. 3.7c), were examined. In general, genes repressed by PrrAB were associated with numerous metabolic processes (Fig. 3.10a) and nucleotide binding (Fig. 3.10b), while PrrAB-induced genes were associated with ion or chemical homeostasis (Fig. 3.10c) and oxidoreductase, catalase, and iron-sulfur cluster binding activities (Fig. 3.10d). The GO enrichment analyses suggested that during *M. smegmatis* exponential growth in M7H9 medium, PrrAB negatively regulates genes associated with diverse components of phosphorus, nitrogen, carbohydrate, and nucleotide metabolic and biosynthetic processes and positively regulates expression of genes participating in cation (particularly, iron) homeostasis, redox mechanisms, and gluconeogenesis (Fig. 3.10).

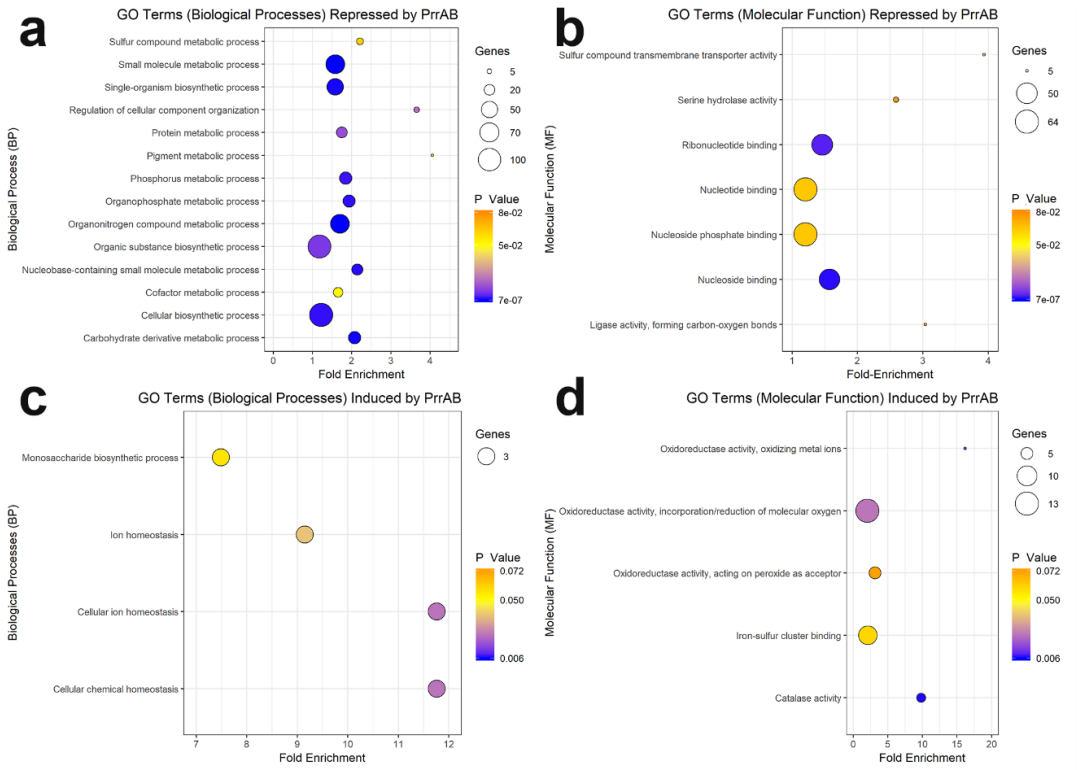

Figure 3.10. GO term enrichment associated with DEGs ($p < 0.05$) that are (a, b) repressed (c, d) or induced by PrrAB in the WT background. GO terms categorized by (a, c) biological processes (BP) or (b, d) molecular function (MF).

Classification of genes based on clusters of orthologous groups (COGs) analyses were then performed using the online eggNOG mapper program. Of all COG categories in each gene list, 39% (N=146) and 28% (N=59) of genes repressed or induced by PrrAB, respectively, participate in diverse aspects of metabolism (Fig. 3.11), thus corroborating the GO results. Of the COG categories induced by PrrAB, 17% (N=36) were associated with energy production and conversion (COG Category C). The relatively even proportions of COG categories associated with PrrAB-induced and repressed genes (Fig. 3.11) suggest that this TCS, as both transcriptional activator and repressor, fine-tunes diverse cellular functions to maximize and/or optimize growth potential during exponential replication.

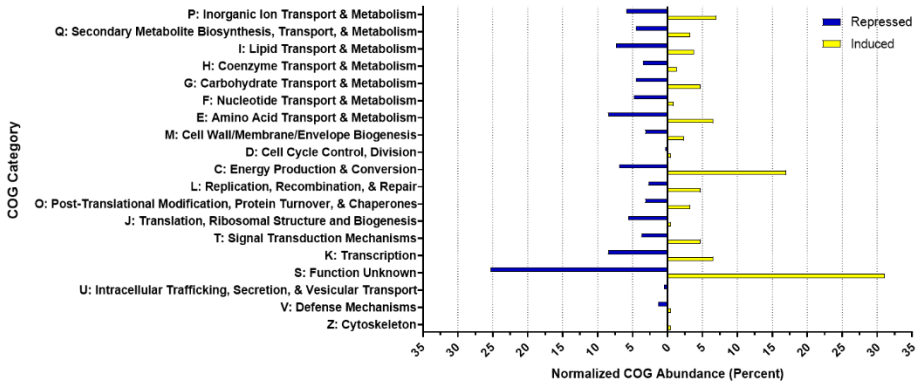

Figure 3.11. COG analysis of DEGs ($p < 0.05$) induced (yellow) or repressed (blue) by PrrAB in the WT background. COGs from each category were normalized to represent the percent abundance of each category to all COGs returned in the induced or repressed analyses, respectively.

PrrAB Regulates dosR Expression in M. smegmatis

Differential expression analysis revealed significant repression of *MSMEG 5244* and *MSMEG 3944*, two paralogues of the *dosR* (*devR*) response regulator gene, in the Δ*prrAB* mutant strain (Fig. 3.7a). In *M. tuberculosis*, the hypoxia-responsive DosRS (DevRS) TCS (along with the DosT histidine kinase) induces transcription of ~50 genes that promote dormancy and chronic infection (Park et al. 2003). Here, we designate *MSMEG 5244* as *dosR1* (due to its genomic proximity to *dosS*) and *MSMEG 3944* as *dosR2*. Among the 25 *M. smegmatis* homologues of the *M. tuberculosis* DosRS regulon genes, 23 genes were differentially expressed

(+/- 2-fold changes) in pair-wise comparisons among the three strains (Fig. 3.12). Importantly, 21 of the 25 *M. smegmatis* DosRS regulon homologues were induced by PrrAB in the WT and complementation backgrounds, corroborating the activity of the DosR as a positive transcriptional regulator (Park et al. 2003).

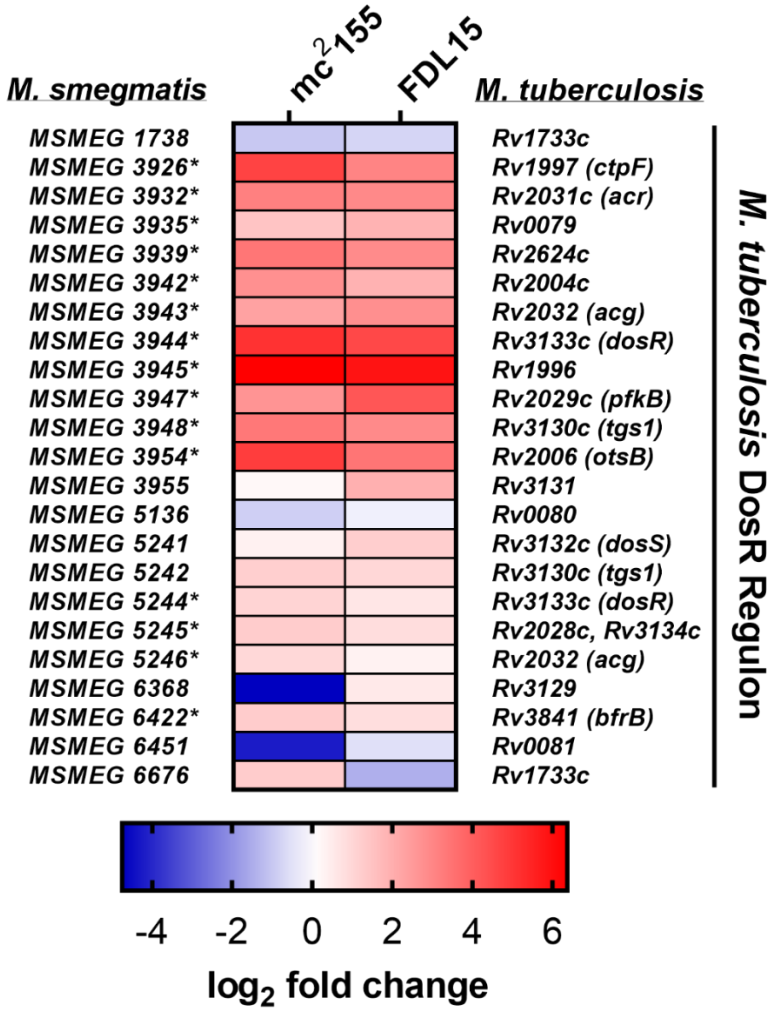

Figure 3.12. *M. smegmatis* PrrAB regulates dormancy-associated genes of the DosR regulon. Heatmap of *M. smegmatis* RNA-seq DEGs associated with *M. tuberculosis dosR* regulon homologues. Color bar indicates $\log_2$ fold change values corresponding to mc^{2}155 vs. FDL10 (left tiles) and FDL15 vs. FDL10 (right tiles) DEGs. *MSMEG* genes differentially regulated ($p < 0.05$) are denoted by asterisks.

PrrAB is Necessary for M. smegmatis Adaptation to Hypoxia

The cytochrome *bd* oxidase respiratory system is a high-affinity terminal oxidase that is important for *M. smegmatis* survival under microaerophilic conditions (Kana et al. 2001). Because the *cydA, cydB,* and *cydD* genes were repressed in the in the Δ*prrAB* mutant during aerobic growth (Fig. 3.7a), we questioned if the Δ*prrAB* mutant was more sensitive to hypoxia than the WT strain. Compared to WT and the *prrAB* complementation strains, the Δ*prrAB* mutant exhibited reduced viability (Fig. 3.13a) and produced smaller colonies (Fig. 3.13b) after 24 h hypoxia exposure. In contrast, cell viability and colony sizes were similar for all strains cultured under aerobic growth conditions (Fig. 3.13a, b).

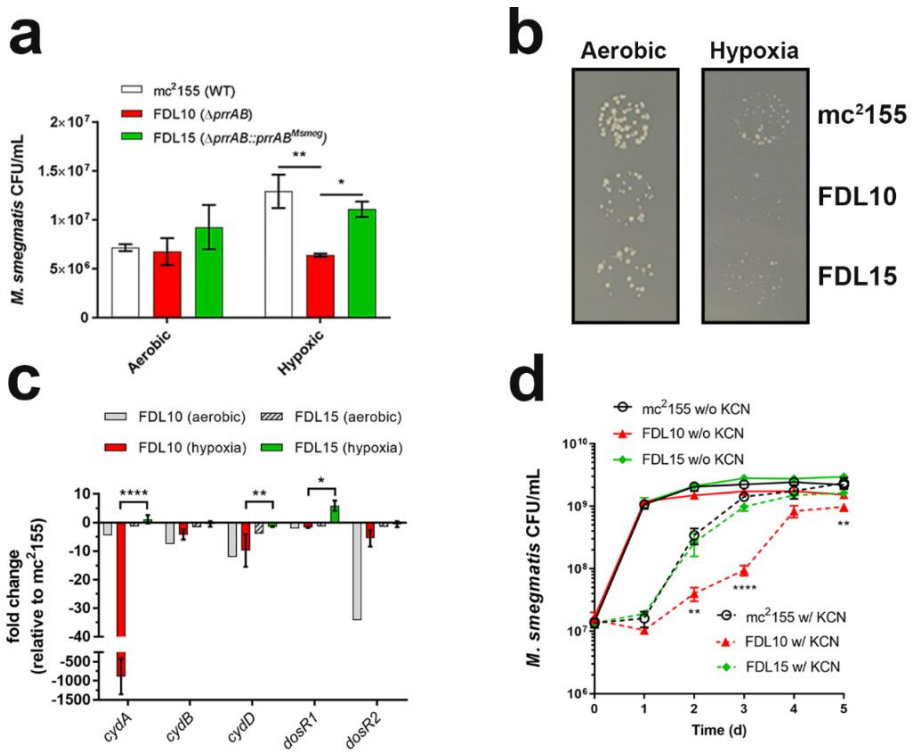

Figure 3.13. PrrAB is protective during hypoxia and cyanide-mediated respiratory inhibition and regulates cytochrome *bd* and *dosR* expression. (a, b) Viability of *M. smegmatis* strains after 24 h incubation in hypoxic or aerobic environments at 37ºC. *, $p = 0.04$; **, $p = 0.0099$; one-way ANOVA, Dunnett's multiple comparisons. (**c**) qRT-PCR of *cydA* (*MSMEG 3233*)*, cydB* (*MSMEG 3232*)*, cydD* (*MSMEG 3231*), *dosR1* (*MSMEG 5244*), and *dosR2* (*MSMEG 3944*) RNA isolated from *M. smegmatis* after exposure to hypoxia for 24 h. Relative fold change in gene expression was calculated using the $2^{\Delta\Delta Ct}$ method. *, $p = 0.0103$; **, $p = 0.0013$; ****, $p < 0.0001$; unpaired Student's t tests. (**d**) *M. smegmatis* growth in the presence (dashed lines) or absence (solid lines) of 1 mM cyanide (KCN). **, $p < 0.01$; ****, $p < 0.0001$; unpaired Student's t tests. Values represent the mean ±SEM of data collected from three independent cultures.

Next, we questioned if differential expression of *cydA, cydB,* and *cydD* correlated with growth deficiencies in the Δ*prrAB* mutant. We compared transcriptional profiles of *cydA, cydB,* and *cydD* by qRT-PCR from each strain incubated in M7H9 broth and hypoxic conditions for 24 h. Expression levels of *cydA, cydB,* and *cydD* were universally reduced in the Δ*prrAB* mutant relative to the WT strain (Fig. 3.13c). Furthermore, both *dosR1* and *dosR2* were also downregulated in the Δ*prrAB* mutant after 24 h hypoxia (Fig. 3.13c), demonstrating that PrrAB is required for activating *dosR* under hypoxic conditions. Complementation with *M. smegmatis prrAB* restored expression of *cydA, cydB, cydD,* and *dosR2* to levels similar to WT, while the *dosR1* paralogue was expressed approximately 6-fold higher in the complementation strain relative to WT after 24 h hypoxia (Fig. 3.13c). Overall, the gene expression profiles correlated with in vitro growth characteristics, indicating that PrrAB expression is necessary for *M. smegmatis* survival under hypoxic conditions and confirms that PrrAB induces *cydA, cydB, cydD, dosR1*, and *dosR2* in both oxygen-rich and oxygen-poor environmental conditions.

The ΔprrAB Mutant is Hypersensitive to Cyanide Exposure

Cyanide is a potent inhibitor of the aa_3 cytochrome c oxidase in bacteria. Conversely, cytochrome *bd* oxidases in *Escherichia coli* (Korshunov, Imlay, and Imlay 2016), *Pseudomonas aeruginosa* (Cunningham, Pitt, and Williams 1997), some staphylococci (Voggu et al. 2006), and *M. smegmatis* (Kana et al. 2001) are relatively insensitive to cyanide inhibition. In the absence of alternative electron acceptors (e.g., nitrate and fumarate), aerobic respiratory capacity after cyanide-mediated inhibition of the *M. smegmatis* aa_3 terminal oxidase would be provided by the cytochrome *bd* terminal oxidase (CydAB). Because *cydA, cydB,* and *cydD* were significantly repressed in the Δ*prrAB* mutant (Fig. 3.7a), as were most subunits of the cytochrome c $bc_1 - aa_3$ respiratory oxidase complex, we hypothesized that the Δ*prrAB* mutant would be hypersensitive to cyanide relative to the WT and complementation strains. Cyanide inhibited all three strains during the first 24 h (Fig. 3.13d). While the WT and complementation strains entered exponential growth after 24 h of cyanide exposure, the Δ*prrAB* mutant exhibited significantly delayed and slowed growth between 48-72 h (Fig. 3.13d). These data demonstrated that the Δ*prrAB* mutant strain had

defects in alternative cytochrome *bd* terminal oxidase pathways, further supporting that genes controlling cytochrome c bc_1 and aa_3 respiratory oxidases are induced by PrrAB.

PrrAB Positively Regulates ATP Levels

KEGG pathway analysis of DEGs ($p < 0.05$) induced by PrrAB revealed oxidative phosphorylation as a significantly enriched metabolic pathway (enrichment = 3.78; $p = 0.017$). Further examination of the RNA-seq data generally revealed that genes of the terminal respiratory complexes (cytochrome c bc_1-aa_3 and cytochrome *bd* oxidases) were induced by PrrAB, whereas F_1F_0 ATP synthase genes were repressed by PrrAB (Fig. 3.14a). Therefore, we hypothesized that ATP levels would be greater in the Δ*prrAB* mutant relative to the WT and complementation strains despite the apparent downregulation of terminal respiratory complex genes (except *ctaB*) in the Δ*prrAB* mutant (Fig. 3.14a). While viability was similar between strains at the time of sampling (Fig. 3.14b), ATP levels ([ATP] pM/CFU) were 36% and 76% in the Δ*prrAB* mutant and complementation strains, respectively, relative to the WT strain (Fig. 3.14c). Ruling out experimental artifacts, we confirmed sufficient cell lysis with the BacTiter-Glo reagent (See Methods) and that extracellular ATP in cell-free supernatants were similar in all three strains (Fig. 3.15). These data suggested that PrrAB positively regulates ATP levels during aerobic logarithmic growth, although *prrAB* complementation did not fully restore ATP to WT levels (Fig. 3.14c). Additionally, ATP levels correlated with PrrAB induction of respiratory complex genes rather than PrrAB-mediated repression than F_1F_0 ATP synthase genes (Fig. 3.14a).

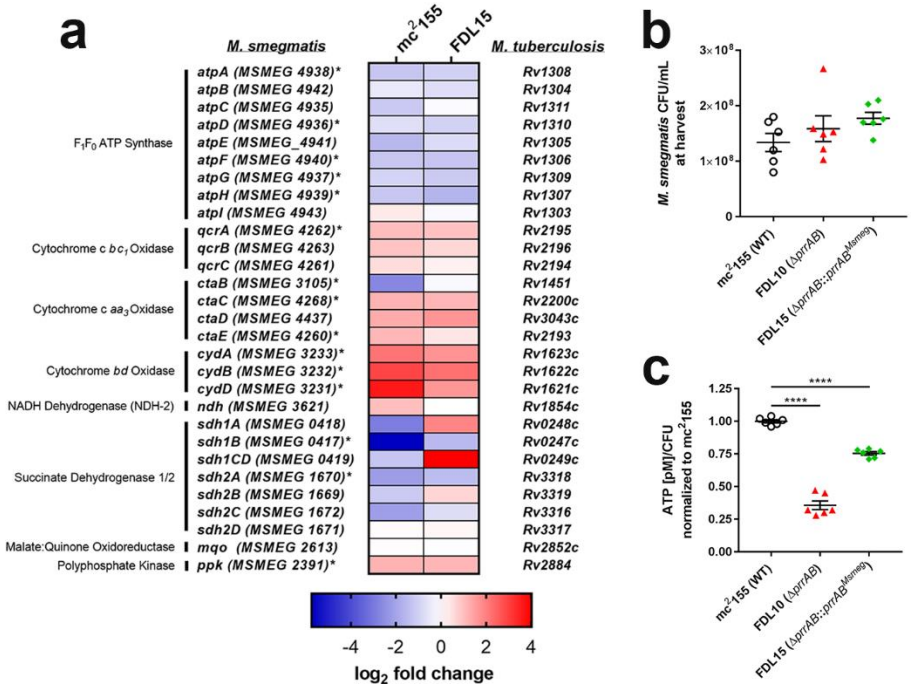

Figure 3.14. PrrAB regulates oxidative phosphorylation genes and ATP levels in *M. smegmatis*. (a) Heatmap of genes participating in oxidative phosphorylation. Color bar indicates $\log_2$ fold change of gene expression between mc^{2}155 vs. FDL10 (left column) and FDL15 vs. FDL10 (right column). *MSMEG* genes significantly regulated ($p < 0.05$) are indicated with asterisks. (b) *M. smegmatis* viability (CFU/ml) at harvest and (c) corresponding ATP levels (pM/CFU) normalized to mc^{2}155 were measured from exponentially-growing (OD_{600} ~0.6) aerobic cultures in M7H9 broth. ****, $p < 0.0001$; one-way ANOVA, Dunnett's multiple comparisons.

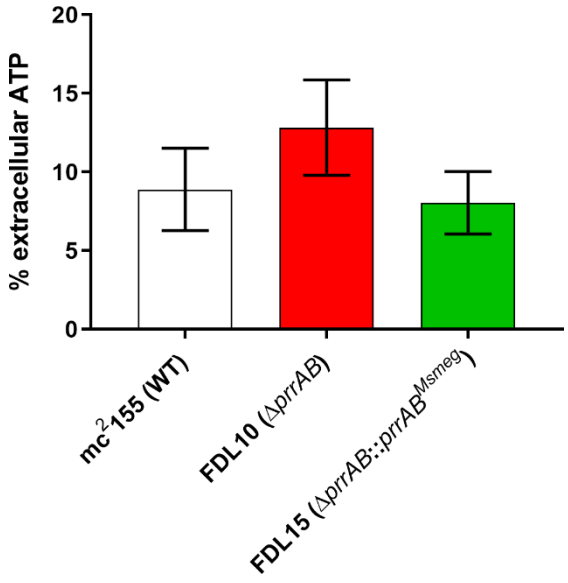

Figure 3.15. *M. smegmatis* extracellular ATP (supernatant) expressed as a percentage of whole culture normalized ATP (pM/CFU). Values represent the mean ±SEM of data collected from three independent cultures.

Discussion

TCSs provide transcriptional flexibility and adaptive responses to specific environmental stimuli in bacteria (Calva and Oropeza 2006). The mycobacterial PrrAB TCS is conserved across most, if not all, mycobacterial lineages and is essential for viability in *M. tuberculosis* (Haydel et al. 2012), thus representing an attractive therapeutic target (Bellale et al. 2014). Here, we use an *M. smegmatis* Δ*prrAB* mutant (Maarsingh and Haydel 2018) as a surrogate to provide insights into the essential nature and regulatory properties associated with the PrrAB TCS in *M. tuberculosis*. Our rationale for this approach is founded on the high degree of identity between the *M. smegmatis* and *M. tuberculosis* PrrA and PrrB sequences, including 100% identity in the predicted DNA-binding recognition helix of PrrA (Fig. 3.16) (Nowak et al. 2006).

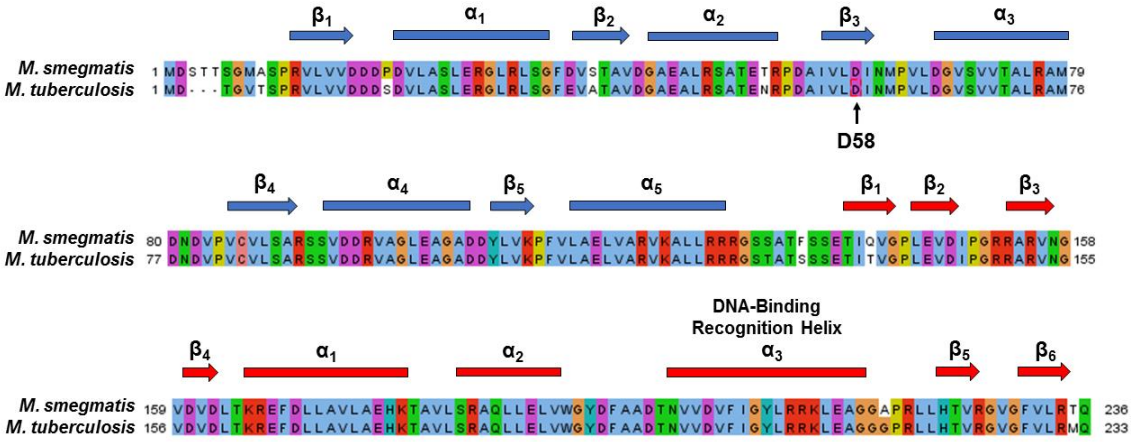

Figure 3.16. Multiple sequence alignment comparing the *M. smegmatis* and *M. tuberculosis* PrrA amino acid sequences. Secondary structures are represented by arrows (β-sheets) or bars (α-helices). Secondary structures colored in blue correspond to the N-terminal receiver domain while red corresponds to the C-terminal effector domain. The conserved phosho-receiving aspartate (D58) and DNA-binding recognition helix are labeled. Multiple sequence alignments were performed in JalView using default MUSCLE algorithms (Edgar 2004). Secondary structure and DNA-binding recognition helix designations were adapted from Nowak et al. (Nowak et al. 2006a).

Using BLAST queries of *M. smegmatis* PrrA and PrrB against 150 recently reclassified mycobacterial species, as proposed by Gupta et al. (Gupta, Lo, and Son 2018), all fully-sequenced mycobacterial genomes harbored *prrA* and *prrB* homologues, implying strong evolutionary conservation for the PrrAB TCS. Likely due to the incomplete genomic sequences

(Gupta, Lo, and Son 2018), *prrA* was not found in *Mycobacterium timonense* and *Mycobacterium bouchedurhonense* genomes, while a *prrB* homolog was not identified in *Mycobacterium avium* subsp. silvaticum. Phylogenetic analyses showed that PrrA and PrrB sequences grouped closely, but not perfectly, within members of specific mycobacterial clades (Fig. 3.1), and members of the *Abscessus-Chelonae* clade harbored unique PrrA and PrrB amino acid substitutions (Figs. 3.2, 3.3). While it is unclear if these residues impact PrrA or PrrB functionality in the *Abscessus-Chelonae* clade, it may be possible to develop *prrAB*-based single nucleotide polymorphism genotyping or proteomic technologies for differentiating mycobacterial infections. Multiple sequence alignments of the *M. smegmatis* and *M. tuberculosis* PrrA DNA-binding recognition helices revealed 100% sequence conservation (Fig. 3.16), suggesting a shared set of core genes regulated by PrrA in mycobacteria. Incorporation of a global approach, such as ChIP-seq, will be valuable for identifying and characterizing the essential genes directly regulated by PrrA in *M. tuberculosis* and other mycobacterial species.

We used RNA-seq-based transcriptomics analyses to define the *M. smegmatis* PrrAB regulon during exponential growth under standard laboratory conditions. We showed that in *M. smegmatis,* PrrAB deletion led to differential expression of 683 genes ($p < 0.05$), corresponding to ~10% of chromosomal genes, of which 257 genes are induced and 426 are repressed in the WT background (Fig. 3.7). Importantly, PrrAB differentially regulated genes involved in aerobic and microaerophilic respiration. The cytochrome c terminal oxidase bc_1 (*qcrCAB)* and aa_3 (*ctaC*) genes are essential in *M. tuberculosis,* but not in *M. smegmatis*, and mutants in the latter species are attenuated during exponential phase growth (Matsoso et al. 2005). If *M. tuberculosis* PrrAB also regulates genes of the cytochrome c bc_1 and/or aa_3 respiratory complex, it could partially explain *prrAB* essentiality. Further, to corroborate the key findings from comparison between the□*prrAB* mutant and WT strains, we included the *prrAB* complementation strain in our RNA-seq analyses. Of the 683 DEGs that were affected by the□*prrAB* mutation, expression changes of 226 genes were variably reversed ($p < 0.05$) in the□*prrAB* complementation strain (Fig. 3.7e). For example, three genes (*MSMEG 5659*, *MSMEG 5660*, and *MSMEG 5661*) located upstream of the *prrAB* genes were overexpressed in the complementation strain compared to WT, suggesting

imperfect transcriptional complementation. We previously demonstrated similar *prrA* transcription and PrrA protein levels in the WT and complementation strains during aerobic mid-logarithmic growth in M7H9 broth (Maarsingh and Haydel 2018). The lack of full complementation seen in our RNA-seq results may have associated with sequencing artifacts. For example, the average number of uniquely mapped reads in the WT strain was 68% of the average in the complementation strain. These results were unlikely due to poor RNA quality, as RNA integrity numbers were consistently high. Global DEG regulation, however, was similar between mc^2155 vs. FDL10 and FDL15 vs. FDL10 pairwise comparisons. In both pairwise comparisons, 32% and 36% of all DEGs were induced by PrrAB in the WT and complementation backgrounds, respectively, while 68% and 64% of all DEGs were repressed by PrrAB in the WT and complementation backgrounds, respectively. These data indicate that complementation with *prrAB* in the deletion background restored global transcriptomic profiles to WT levels. Future studies are warranted to explore the utility of incorporating sequencing data from both WT and complementation strains to improve the reliability of transcriptomics experiments.

M. tuberculosis acclimates to an intramacrophage environment and the developing granuloma by counteracting the detrimental effects of hypoxia (Aly et al. 2006), nutrient starvation (Schnappinger et al. 2003), acid stress (Rohde et al. 2012), and defense against reactive oxygen and nitrogen species (Voskuil, Visconti, and Schoolnik 2004). Adaptive measures to these environmental insults include activation of the dormancy regulon and upregulation of the high-affinity cytochrome *bd* respiratory oxidase (Voskuil, Visconti, and Schoolnik 2004), induction of the glyoxylate shunt and gluconeogenesis pathways (Timm et al. 2003), asparagine assimilation (Gouzy et al. 2014), and nitrate respiration (Tan et al. 2010). As a saprophytic bacterium, *M. smegmatis* could encounter similar environmental stresses as *M. tuberculosis*, despite their drastically different natural environmental niches. Conserving the gene regulatory circuit of the PrrAB TCS for adaptive responses would thus be evolutionarily advantageous.

The hypoxia-responsive DosRS TCS controls the dormancy regulon in both *M. tuberculosis* (Park et al. 2003) and *M. smegmatis* (Mayuri et al. 2002; Bagchi, Mayuri, and Tyagi 2003; O'Toole et al. 2003). The *M. smegmatis* DosRS TCS regulates dormancy phenotypes

similar to *M. tuberculosis*, including upregulation of the *dosRS* TCS (Mayuri et al. 2002), gradual adaptation to oxygen depletion (Dick, Lee, and Murugasu-Oei 1998), and upregulation of alanine dehydrogenase (Feng et al. 2002). DosR is required for optimal viability in *M. smegmatis* after the onset of hypoxia (O'Toole et al. 2003). Our RNA-seq and qRT-PCR data revealed that PrrAB induces both *M. smegmatis dosR* paralogues (*dosR1* and *dosR2*) during aerobic and hypoxic growth (Fig. 3.7a, and Fig. 3.13c). Additionally, the RNA-seq data revealed that PrrAB induces genes associated with the *M. tuberculosis* DosR regulon (Park et al. 2003; Voskuil et al. 2003) (Fig. 3.12). Thus, it is possible that PrrAB also positively regulates *dosR* expression in *M. tuberculosis*, which would provide additional mechanisms of *dosR* control as previously demonstrated with PknB (Bae et al. 2017), PknH (Chao et al. 2010), NarL (Malhotra et al. 2015), and PhoP (Vashist et al. 2018).

The *M. tuberculosis* respiration and oxidative phosphorylation pathways have increasingly gained attention as promising anti-tuberculosis therapeutic targets. Bedaquiline (TMC207), a recent FDA-approved mycobacterial F_1F_0 ATP synthase inhibitor, is active against drug-sensitive and drug-resistant *M. tuberculosis* strains (Diacon et al. 2009; Andries et al. 2005), as is Q203, a cytochrome c bc_1 inhibitor, which has advanced to phase-I clinical trials (Butler, Blaskovich, and Cooper 2017). Accumulating evidence suggests that the alternative terminal cytochrome *bd* oxidase system, encoded by the *cydABDC* operon in *M. tuberculosis*, is important during chronic infection and may represent a novel drug target. *M. tuberculosis cydA* mutants are hypersensitive to the bactericidal activity of bedaquiline (Berney, Hartman, and Jacobs 2014), suggesting that combined therapeutic regimens simultaneously targeting the F_1F_0 ATP synthase and cytochrome *bd* oxidase represent promising anti-tuberculosis treatment strategies. Analysis of the DEGs ($p < 0.05$) induced by PrrAB revealed significant enrichment of the oxidative phosphorylation KEGG pathway, including genes encoding the cytochrome c bc_1 (*qcrA*), cytochrome c aa_3 (*ctaC, ctaE*), and cytochrome *bd* (*cydB*, *cydD*) terminal respiratory branches. We showed that the Δ*prrAB* mutant was more sensitive to hypoxic stress and cyanide inhibition relative to the WT and complementation strains (Fig. 3.13), thus corroborating the transcriptomics results. Bacterial cytochrome *bd* oxidases are relatively insensitive to cyanide inhibition compared

to the cytochrome c oxidase respiratory branch (Megehee, Hosler, and Lundrigan 2006; Hammer et al. 2016; Hirai et al. 2016). Growth of the Δ*prrAB* mutant in the presence of 1 mM potassium cyanide was similar to *M. smegmatis cydA* mutant growth under similar conditions (Kana et al. 2001). Our data demonstrates that the *M. smegmatis* PrrAB TCS controls expression of aerobic and microaerophilic respiratory genes, and it should be noted that, to date, a master transcriptional regulator of respiratory systems has not been discovered in *M. tuberculosis*.

ATP is required for all living organisms and serves as the cellular energy currency. We found increased expression of the F_1F_0 ATP synthase genes, including *atpA, atpD, atpF, atpG,* and *atpH,* in the Δ*prrAB* mutant strain compared to WT (Fig. 3.14a), leading us to hypothesize that ATP levels would be elevated in the Δ*prrAB* mutant. Conversely, ATP levels were lower in Δ*prrAB* mutant strain compared to the WT and complementation strains (Fig. 3.14c). Induction of *atp* genes in the Δ*prrAB* mutant may indicate a compensatory measure to maintain ATP homeostasis due to repression of the bc_1-aa_3 terminal respiratory complex (except *ctaB*) and hence, disruption of the transmembrane proton gradient.

Via comprehensive transcriptomics analyses, we demonstrated that PrrAB regulates expression of genes involved in respiration, environmental adaptation, ion homeostasis, oxidoreductase activity, and metabolism in *M. smegmatis*. The inability to induce transcription of the *cydA, cydB, cydD, dosR1*, and *dosR2* genes likely led the Δ*prrAB* mutant to grow poorly after 24 h hypoxia exposure. An important goal of our RNA-seq study was to provide insight into the essential nature of PrrAB in *M. tuberculosis* using an *M. smegmatis* Δ*prrAB* mutant as a surrogate model while recognizing differences in their natural environmental niches, pathogenic potential, and genetic composition. From a therapeutic perspective, PrrAB could influence the sensitivity of *M. tuberculosis* to Q203 and/or bedaquiline by controlling expression of cytochrome *bd* oxidase, cytochrome c bc_1 oxidase, and ATP synthase genes. Furthermore, it remains unknown whether diarylthiazoles directly target PrrB (Bellale et al. 2014) or whether the *prrB* mutations associated with diarylthiazole resistance are compensatory in nature. Taken together, our study provides seminal information regarding the mycobacterial PrrAB TCS regulon as well

as a powerful surrogate platform for in-depth investigations of this essential TCS in *M. tuberculosis*.

Conclusions

We used RNA-seq-based transcriptomics as an experimental platform to provide insights into the essential *M. tuberculosis prrAB* TCS using an *M. smegmatis* Δ*prrAB* mutant as a genetic surrogate. In *M. smegmatis*, PrrAB regulates high-affinity respiratory systems, intracellular redox and ATP balance, and the *dosR* TCS response regulator genes, all of which promote infectious processes in *M. tuberculosis*. Using these results, we may be able to exploit diarylthiazole compounds that putatively target the PrrB histidine kinase as synergistic therapies with bedaquiline. These results are informing the basis of *prrAB* essentiality in *M. tuberculosis* and advancing our understanding of regulatory systems that control metabolic, respiration, energy-generating, and dormancy pathways in mycobacteria. Exploitation of PrrAB as a drug target through development of small molecule inhibitors will advance the discovery and development of novel therapeutics to combat the global tuberculosis epidemic.

Methods

Bacterial Strains and Culture Conditions

Genetic construction of the *M. smegmatis* FDL10 Δ*prrAB* deletion mutant and the FDL15 complementation strain was previously described (Maarsingh and Haydel 2018). All *M. smegmatis* strains (mc^{2}155, FDL10, and FDL15) were routinely cultured in M7H9 broth (pH 6.8) supplemented with 10% ADS, 0.2% glycerol (v/v), and 0.05% Tween 80 (v/v), herein referred to as M7H9. *M. smegmatis* was incubated on Middlebrook 7H10 agar supplemented with 10% ADS and 0.5% glycerol, herein referred to as M7H10 agar, for CFU/ml enumeration.

Hypoxic Growth Conditions

M. smegmatis strains were cultured in M7H9 medium at 37°C, 100 rpm to an OD_{600} ~0.6. Cells were diluted into fresh, pre-warmed M7H9 to an OD_{600} ~0.05, serially diluted in PBS (pH

7.4), and spot-plated onto M7H10 agar. Hypoxic cultures were transferred to a GasPak chamber containing two anaerobic GasPak sachets (Beckon Dickinson, Franklin Lakes, NJ, USA), sealed, and incubated at 37°C for 24 h after the onset of hypoxia (~6 h), as indicated by decolorization of an oxygen indicator tablet included with the sachet. Plates were then incubated aerobically for an additional 48 h to allow colony outgrowth. Control plates were cultured under aerobic conditions for 48 h prior to counting and documenting colonies. Colonies were visualized using a dissecting microscope (Stereomaster, Fisher Scientific). All experiments were performed in triplicate.

Cyanide Inhibition Assays

M. smegmatis strains were grown in the presence of potassium cyanide (KCN) as described by (Kana et al. 2001) with modifications. Briefly, cultures were inoculated into prewarmed M7H9 broth to an OD_{600} ~0.05 and incubated at 37°C, 100 rpm for 30 min. KCN, prepared in M7H9 broth, was then added to a final concentration of 1 mM and growth was allowed to resume. Negative control cultures using M7H9 broth without KCN addition were performed concurrently. Cultures were grown for 5 d with samples collected at 24 h intervals for OD_{600} measurements and CFU quantitation on M7H10 agar. All experiments were performed in triplicate.

ATP Assays

M. smegmatis strains were cultured in M7H9 broth at 37°C, 100 rpm. Cultures were sampled in 100 µl aliquots upon reaching an OD_{600} ~0.6, flash-frozen in a dry ice-ethanol bath, and stored at -70°C for 7 d. Cells were thawed at room temperature and ATP quantification was performed using the BacTiter-Glo kit (Promega, Madison, WI, USA). 50 µl of cells were mixed with equal volumes of BacTiter-Glo reagent in opaque 96-well plates and incubated at room temperature for 5 min. ATP standard curves were included in the same plate. Relative luminescence was measured in a SpectraMax M5 plate reader (Molecular Devices, San Jose, CA, USA). To assess lysis efficiency, viability of all samples was confirmed after both freeze-thaw and processing in the BacTiter-Glo reagent by plating serial dilutions onto M7H10 agar followed

by incubation at 37°C for 48-72 h. Lysis efficiencies collected from three independent culture of mc^{2}155, FDL10, and FDL15 were 99.97% (± 0.03), 99.99% (± 0.04), and 99.99% (± 0.02), respectively. Cell viability was quantified for each sample at the time of harvest by plating serial dilutions onto M7H10 agar followed by incubation at 37°C for 48 h before enumerating CFU/ml. All strains were analyzed in triplicate with two technical replicates each.

RNA Isolation

M. smegmatis strains mc^{2}155, FDL10, and FDL15 were grown in 30 ml M7H9 at 37°C, 100 rpm until mid-logarithmic phase (OD_{600} ~0.6). Culture aliquots (15 ml) were harvested by centrifugation at 4,000 rpm for 10 min at 4°C. The supernatant was discarded, and the cell pellet was resuspended in 1 ml TRIzol (Invitrogen), transferred to 2 ml screw cap tubes containing 500 mg of zirconia-silicate beads (0.1-0.15 mm), and placed on ice. Cells were mechanically disrupted 3X by bead beating (BioSpec Products) at the highest setting for 40 s and incubated on ice for at least 1 min between disruptions. The cell lysates were incubated at room temperature for 5 min, centrifuged at 13,000 x *g* for 1 min to separate cell debris, and the supernatant was transferred to a new microcentrifuge tube. Chloroform (200 µl) was added, and samples were vortexed for 15 s followed by 5 min incubation at 4°C. The homogenate was centrifuged at 13,000 x *g* for 15 min at 4°C and the upper, aqueous phase was transferred to a new microcentrifuge tube. RNA was precipitated with 500 µl isopropanol overnight at 4°C. Total RNA was pelleted by centrifugation at 13,000 x *g* for 15 min at 4°C, and the supernatant was discarded. RNA pellets were washed 2X with 70% ethanol and centrifuged at 13,000 x *g* for 5 min at 4°C between washes. After evaporation of residual ethanol by air-drying, total RNA was resuspended in 100 µl nuclease-free H_2O. Total RNA (10 µg) was treated with TURBO-DNase (Invitrogen, Carlsbad, CA) for 20 min at 37°C to degrade residual genomic DNA. RNA samples were purified using the RNeasy Mini Kit (Qiagen, Germany) and eluted in 50 µl nuclease-free H_2O. RNA yields were quantified by Nanodrop (Thermo Scientific, Waltham, MA), and quality was assessed by agarose gel electrophoresis and a 2100 Bioanalyzer (Agilent, Santa Clara, CA).

RNA (250 ng) was subjected to PCR using primers directed at the *16S* rRNA gene to confirm lack of residual genomic DNA.

RNA-seq Library Preparation

cDNA was generated from RNA using the Nugen Ovation RNA-seq System via single primer isothermal amplification and automated on the BRAVO NGS liquid handler (Agilent, Santa Clara, CA, USA). cDNA was quantified on the Nanodrop (Thermo Fisher Scientific) and was sheared to approximately 300 bp fragments using the Covaris M220 ultrasonicator. Libraries were generated using the Kapa Biosystem's library preparation kit (Kapa Biosystems, Wilmington, MA, USA). Fragments were end-repaired and A-tailed and individual indexes and adapters (Bioo, catalogue #520999) were ligated on each separate sample. The adapter-ligated molecules were cleaned using AMPure beads (Agencourt Bioscience/Beckman Coulter, La Jolla, CA, USA), and amplified with Kapa's HIFI enzyme (Kapa Biosystems, Wilmington, MA, USA). Each library was then analyzed for fragment size on an Agilent Tapestation and quantified by qPCR (KAPA Library Quantification Kit, Kapa Biosystems, Wilmington, MA, USA) using Quantstudio 5 (Thermo Fisher Scientific) prior to multiplex pooling.

Sequencing and Data Processing

Sequencing was performed on a 1x75 bp flow cell using the NextSeq500 platform (Illumina) at the ASU Genomics Core facility. The total number of 101,054,986 Illumina NextSeq500 paired-end reads were generated from nine RNA samples (i.e., triplicates for each strain). The total number of reads generated for each sample ranged from 7,729,602 to 14,771,490. RNA-seq reads for each sample were quality checked using FastQC v 0.10.1 and aligned to the *Mycolicibacterium smegmatis* MC2155 assembly obtained from NCBI (https://www.ncbi.nlm.nih.gov/assembly/GCF_000015005.1/) using STAR v2.5.1b. Cufflinks v2.2.1 was used to report FPKM (Fragments Per Kilobase of transcript per Million mapped reads) values and the read counts. As a quality check for the biological replicates, overall similarity of gene expression profiles were then assessed by MDS, in which distances correspond to leading

log-fold changes between samples. The MDS analysis demarcated clearly one of the three mc^{2}155 samples as an outlier that did not cluster with the other two mc^{2}155 samples and the three FDL15 samples (See Fig. 3.5), and the sample was thus excluded from further analysis. Average genome-wide expression (FPKM) was 6.76 for the WT strain, 5.88 for the Δ*prrAB* mutant, and 6.38 for the complementation strain.

Bioinformatics Analysis

Differential expression analysis was performed with EdgeR package from Bioconductor v3.2 in R 3.2.3. EdgeR applied an overdispersed Poisson model to account for variance among biological replicates. Empirical Bayes tagwise dispersions were also estimated to moderate the overdispersion across transcripts. Then, a negative binomial generalized log-linear model was fit to the read counts for each gene for all comparison pairs. For each pairwise comparison, genes with p values <0.05 were considered significant and $\log_2$-fold changes of expression between conditions (logFC) were reported. False discovery rate (FDR) was calculated following the Benjamini and Hochberg procedure (Benjamini and Hochberg 1995), the expected proportion of false discoveries amongst the rejected hypotheses.

PCA was done on the scaled data using the prcomp function in R. Clustering analysis was done using Cluster 3.0 software, in which normalized expression (FPKM +1) values were $\log_2$ transformed and grouped using uncentered Pearson's correlation distance and average linkage hierarchal clustering (Eisen et al. 1998). Data matrices and tree dendrograms were visualized in Java TreeView. Gene ontology (GO) term enrichment, KEGG pathways, and statistical analyses of differentially expressed genes (DEGs, $p < 0.05$) were performed using the DAVID functional annotation tool (https://david.ncifcrf.gov/summary.jsp). Clusters of orthologous groups (COGs) were obtained by querying DEGs ($p < 0.05$) against the eggNOG Mapper database (http://eggnogdb.embl.de/#/app/emapper).

Quantitative RT-PCR (qRT-PCR)

cDNA libraries from each sample were generated by reverse transcription of 1 µg total RNA using the iScript cDNA Synthesis Kit (Bio-Rad, Hercules, CA, USA), according to the manufacturer's instructions. Primer efficiency was validated against 10-fold dilution standard curves using a cutoff criterion for acceptable efficiency of 90-110% and coefficient of determination (R^2) ≥ 0.997. Relative gene expression was calculated using the $2^{-\Delta\Delta Ct}$ method (Livak and Schmittgen 2001) using the *16S* gene as an internal normalization reference.

Phylogenetic Analyses

The *M. smegmatis* mc^2155 PrrA and PrrB sequences were separately queried in BLASTp (https://blast.ncbi.nlm.nih.gov/Blast.cgi) against all Mycobacteriacea (taxid: 1762). Sequences corresponding to the revised mycobacterial phylogenetic clade classification (Gupta, Lo, and Son 2018) were selected for further analysis. When multiple hits were returned from the same species, those corresponding to the lowest E-value were selected for alignment. Compiled PrrA and PrrB sequences were separately aligned in MEGA 7 (https://www.megasoftware.net/) using default MUSCLE algorithms. Maximum-likelihood phylogenetic trees were generated in MEGA 7 and visualized by iTOL (Letunic and Bork 2016).

Statistical Analyses

We used one-way ANOVA to assess significant differences in cell viability and ATP quantification assays. Student's t tests were used to assess differences in qRT-PCR gene expression. Statistical analyses were performed using GraphPad Prism 7 (GraphPad Software, San Diego, CA) and *p*-values of <0.05 were considered statistically significant. For volcano plot data, the $-\log_{10}$ *p*-value of each DEG was plotted against the ratio of the mean $\log_2$-fold change of each differential expressed gene between FDL10 vs. mc^2155 or FDL10 vs. FDL15.

CHAPTER 4

MYCOBACTERIUM SMEGMATIS PRRAB REGULATES ACETATE AND PROPIONATE METABOLISM: CURRENT RESEARCH AND FUTURE DIRECTIONS

Introduction

CCM feeds a multitude of biological processes, including energy production via oxidative phosphorylation (Munoz-Elias and McKinney 2006), replenishment of anapleurotic intermediates (Xu et al. 2012), and carbon assimilation (Baughn et al. 2009). Saprophytic mycobacteria, such as *Mycobacterium smegmatis*, are genetically well-equipped to metabolize a diverse collection of carbon sources (Titgemeyer et al. 2007; Chopra et al. 2014) relative to the highly pathogenic *Mycobacterium tuberculosis*, which is specialized to reside within the nutrient-poor host macrophage phagosome (Schnappinger et al. 2003; Rohde, Abramovitch, and Russell 2007; Rohde et al. 2012). The *M. tuberculosis* chromosome is highly enriched in fatty acid degradative genes (Cole et al. 1998) which are upregulated during infection in activated macrophages (Schnappinger et al. 2003; Rohde et al. 2012) . It is widely-believed that *M. tuberculosis* persists on a diet of fatty acids and host cholesterol during chronic infection and mutants unable to utilize fatty acids are severely attenuated (Munoz-Elias and McKinney 2005; Pandey and Sassetti 2008; Hu et al. 2010).

CCM is orchestrated through a variety of regulatory checkpoints, owing to the fluxuating physiologic demands and intricate control of metabolic homeostasis. Enzymes of microbial CCM are allosterically regulated by metabolic intermediates (Link, Kochanowski, and Sauer 2013; Noy et al. 2016; Wagner et al. 2011), cofactors (Stokke et al. 2007; Zheng et al. 2014; Willquist and van Niel 2010) and protein-protein interactions (Ventura et al. 2013). In the presence of two utilizable carbon sources, many bacteria will first metabolize the substrate that provides the most rapid growth before utilizing the other substrate. This phenomenon, termed catabolite repression, involves the reversible induction of genes required to catabolize each carbon source (Gorke and Stulke 2008). Mycobacteria do not appear to exhibit catabolite repression and instead, simultaneously utilize mutliple organic substrates in a process termed co-compartmentalization

(de Carvalho et al. 2010). Cues within the host phagosome activate signaling pathways that stimulate the tubercle bacilli to modulate gene transcription to adapt to long-term residence wihin the host macrophage. To date, little is known regarding the transcriptional machinery that regulates CCM genes in mycobacteria. In *M. tuberculosis*, PrpR (*Rv1129c*) induces expression of the methycitrate operon (*prpDC*) and is required for optimal growth on propionate as a sole carbon source (Masiewicz et al. 2012). RamB (*Rv0465c*) represses isocitrate lyase 1 (*Rv0467, icl1*) during growth on glucose, but does not influence *icl1* expression during growth on acetate (Micklinghoff et al. 2009). PrpR and RamB work in feed-forward loops with the sigma factors SigE and SigB, respectively, to positively regulate *prpDC* and *icl1* during hypoxic growth (Datta et al. 2011). KstR (Kendall et al. 2007) KstR2 (Kendall et al. 2010) are transcriptional regulators of genes participating in lipid and cholesterol metabolism, including a small subset of five β-oxidation genes. In contrast, no information is available describing specific transcriptional regulators that control expression of genes participating in gluconeogenesis or acetate and propionate activation. Given that fatty acid metabolism plays a pivotal role in *M. tuberculosis* pathogenesis and mycobacterial metabolism, a comprehensive description of the regulatory circuits that control these physiological processes would be beneficial and would aid in the development of novel small-molecule inhibitors against essential pathways.

TCSs are signal-transducing proteins extensively utilized by prokaryotes to sense their immediate environment and generate appropriate adaptive responses (Alvarez et al. 2016). A prototypical TCS is composed of a membrane-bound histidine kinase sensor and a cytoplasmic DNA-binding response regulator. Upon activation by a specific environmental stimulus, histidine kinase proteins dimerize and propogate the signal through a series of phosphorylation events which culminate on the response regulator. The phosphorylated response regulator then generates an adaptive response, frequently through modulating gene expression (Stock, Robinson, and Goudreau 2000). Some TCSs have been demonstrated to regulate CCM pathways. The *Escherichia coli* BarA-UvrY TCS regulates metabolic shifting from glycolytic to gluconeogenic carbon metabolism (Pernestig et al. 2003). Acetate and formate are the physiologic stimuli for activating BarA-UvrY, which in turn induce expression of the acetate

activating genes, acetate kinase (*ack*) and phosphotranacetylase (*pta*) (Chavez et al. 2010). In *Vibrio cholerae*, the CrbRS TCS promotes colonization of the host intestines by activating genes that metabolize acetate (Hang et al. 2014). It is likely that other bacterial TCSs regulate additional CCM pathways, however, little information is currently known.

The *M. tuberculosis* genome harbors 11 genetically linked TCSs, two orphaned histidine kinases, and five orphaned response regulators (Bretl, Demetriadou, and Zahrt 2011). Of this repertiore, the *M. tuberculosis mtrAB* (Zahrt and Deretic 2000) and *prrAB* (Haydel et al. 2012) TCSs are essential for viabilty. We recently constructed an *M. smegmatis* Δ*prrAB* mutant, therefore demonstrating that *prrAB* is not universally essential in mycobacteria (Maarsingh and Haydel 2018). During in vitro ammonium limitation, the Δ*prrAB* mutant accumulates triacylglycerol lipids (Maarsingh and Haydel 2018), which is a hallmark of *M. tuberculosis* (Deb et al. 2009) and *M. smegmatis* (Nazarova et al. 2011) dormancy. Preliminary growth experiments in our lab revealed the *M. smegmatis* Δ*prrAB* mutant experiences early stage growth defects in a medium supplemented with glycerol as the primary carbon source. This prompted us to explore the growth potential of the Δ*prrAB* mutant in the presence of other organic substrates. In this paper, we demonstrate that PrrAB is required for optimal growth on gluconeogenic carbon sources. We took a global untargeted metabolomics approach to precisely locate the metabolic discrepencies between the Δ*prrAB* mutant, wild-type, and complementation strains. Our studies provide evidence that the *M. smegmatis* PrrAB TCS participates in CCM by regulating assimilation of gluconeogenic carbon sources known to be important during *M. tuberculosis* chronic infection (Munoz-Elias and McKinney 2005).

Materials and Methods

Bacterial Media and Culture Conditions

M. smegmatis strains were routinely cultured in M7H9 medium supplemented with 10% ADS, 0.2% glycerol (v/v), and 0.05% Tween 80 and adjusted to pH 6.8. Carbon-defined experiments were performed in M7H9 medium supplemented with 10% albumin-saline, 0.05% Tyloxapol, and 0.2% of the described carbon sources (herein referred to as M7H9-glucose,

M7H9-acetate, and M7H9-propionate) and adjusted to pH 6.8. All cultures were incubated at 37°C on a platform rotary shaker (100 rpm) for the indicated times. Media supplements were included at 100 µg/ml where specified.

Growth Curves

To assess growth kinetics, *M. smegmatis* overnight cultures (2 ml) were harvested by centrifugation at 10,000 rpm for 2 min in a microcentrifuge. The cell pellets were washed twice in PBS (pH 7.4) (1 ml) to remove residual carbon sources. Cell pellets were resuspended in prewarmed medium (1 ml) and used to inoculate same medium (30 ml) to an OD_{600} ~0.05. Cultures were grown at 37°C, 100 rpm for the indicated times. Absorbance (OD_{600}) and viability (CFU/ml) measurements were performed at 24 h intervals. To assess viability, cultures were serially diluted in sterile PBS (pH 7.4) and plated in 5 µl aliquots onto M7H10 agar supplemented with 10% ADS and 0.5% glycerol (herein referred to as M7H10 agar), and colonies were enumerated after 48 h growth at 37°C. For supplementation experiments, FDL10 was initially grown as overnight cultures in M7H9-ADS-glycerol-TW80. Cells were harvested by centrifugation, washed twice in PBS (pH 7.4) to remove residual carbon sources, and resuspended in pre-warmed M7H9-acetate (1 ml) or M7H9-propionate (1 ml). Samples were inoculated into M7H9-acetate (3 ml) or M7H9-propionate (3 ml) to an OD_{600}~0.05 and cultures were grown on a rotary drum at 37°C. Absorbance (OD_{600}) values were measured at 24 h intervals for 3 d.

RNA Isolation

Samples were collected from *M. smegmatis* strains cultured in M7H9-glucose, M7H9-acetate, and M7H9-propionate at 1 and 4 d growth. Cells were harvested by centrifugation at 4,000 rpm for 10 min at 4°C, resuspended in Trizol (Thermo Scientific) (1 ml), and flash frozen until future use. Upon RNA isolation, samples were thawed on ice and mechanically disrupted by bead beating (BioSpec Products, Bartlesville, OK, USA) using 0.1 mm diameter glass beads. Each sample was disrupted for 30 s, three times each, at the highest setting and intermittently cooled on ice for at least 1 min between disruptions. Cell debris was separated by centrifugation

at 10,000 rpm for 1 min and the Trizol-containing supernatant was transferred to a fresh microfuge tube. Chloroform (200 µl) was added and the samples were homogenized by vortexing for 15 s followed by 5 min incubation at room temperature. Samples were centrifuged at 13,000 x *g*, the upper aqueous phase was transferred to a fresh microfuge tube, and RNA was precipitated with isopropanol (500 µl) overnight at 4°C. RNA was pelleted by centrifugation at 4°C for 15 min, 13,000 x *g*, washed twice with 70% ethanol (1 ml), air-dried for 10 min at room temperature, and resuspended in nuclease-free H_2O (50 µl). Total RNA (10 µg) was treated with TURBO DNase-*free* (Ambion) for 20 min at 37°C and cleaned using the RNeasy mini kit (Qiagen, Germany) according to the manufacturer's instructions. RNA quality was assessed by agarose gel electrophoresis and lack of contaminating genomic DNA was evaluated by PCR using *16S* gene primers.

Quantitative RT-PCR (qRT-PCR)

cDNA was prepared from total RNA (1 µg) using the iScript cDNA synthesis kit (Bio-Rad, Hercules, CA, USA) according to the manufactures' instructions. Gene expression was measured by qRT-PCR using iQ SYBR Green Supermix (Bio-Rad, Hercules, CA, USA), 300 nM primers, and cDNA (5 ng) per reaction on a MyiQ thermocycler (Bio-Rad, Hercules, CA, USA). The *M. smegmatis 16S* gene was used for internal normalization before calculating fold-change expression values between test and calibrator samples using the comparative C_T method (Livak and Schmittgen 2001).

ATP Quantification

Cultures were harvested at 24 h intervals in 100 µl aliquots, flash-frozen in an ethanol-dry ice slurry and stored at -70°C until further use. Upon ATP measurement, culture samples were thawed at room temperature and aliquoted in 50 µl samples in an opaque 96-well plate. Serially-diluted ATP samples were included in the same plate to generate standard curves. Equal volumes of BacTiter-Glo reagent (Promega, Madison, WI, USA) were added to experimental wells; samples were thoroughly mixed by pipetting and allowed to incubate at room temperature

for 5 min. Relative luminescence (RLU) was measured on a SpectraMax M5 plate reader (Molecular Devices, San Jose, CA, USA) using an integration time of 0.5 s.

Metabolite Extraction

M. smegmatis strains were grown in M7H9-glucose, M7H9-acetate, or M7H9-propionate and samples (5 ml) were collected at 1 and 4 d growth. All samples were kept on ice or at -72°C in an ethanol/dry ice slurry unless stated otherwise. Culture aliquots were harvested by centrifugation at -4°C at 7,800 x *g*, the supernatant was discarded, and the pellet was washed with ice-cold PBS (pH 7.4) (1 ml) and transferred to pre-chilled 2 ml screw-cap tubes. Cells were harvested at 10,622 x *g* for 1 min in a pre-chilled microcentrifuge set to 0°C. The supernatant was discarded and cells were immediately resuspended in pre-chilled quenching solution (1 ml) consisting of acetonitrile:methanol:H_2O (40:40:20) (Marrero et al. 2010). Metabolism was quenched by incubating samples at -72°C for 30 min. To extract intracellular metabolites, 0.1 mm diameter glass beads (BioSpec Products, Bartesville, OK) (500 mg) were added to each sample, and cells were disrupted twice by bead beating (BioSpec Products, Bartlesville, OK) at the highest speed for 30 s each. Samples were incubated at -72°C for at least 4 min between disruptions. The lysate was centrifuged at 10,622 x *g* for 1 min at 0°C, and the lysate was transferred to a fresh microcentrifuge tube. Samples were centrifuged for 20 min, 20,817 x *g*, at -4°C to separate the protein fraction, and the supernatant containing intracellular metabolites were transferred to a fresh microfuge tube. This process was repeated once, and the lysate was clarified through 0.22 µm-pore filtration devices. Metabolites were evaporated to dryness and stored at -70°C until analysis by LC-MS. Protein fractions were analyzed via BCA assay (Thermo Scientific) in microplate format according to the manufacture's protocol and quantified based on a simultaneously-generated BSA standard curve. Prior to LC-MS, metabolites were reconstituted in PBS:acetonitrile (4:6) (150 µl) and centrifuged at 20,817 x *g* for 10 min at 4°C. Metabolites (100 µl) were aliquoted into 2 ml glass vials containing 300 µl glass capillary tubes. Each metabolite sample (50 µl) was pooled and analyzed by LC-MS as a quality control.

Liquid Chromatography-Mass Spectrometry

Metabolites were resolved on an XBridge BEH Amide XP column (Waters Corporation, Milford, MA). An Agilent 6490 triple quadrapole mass spectrometer (Agilent Technologies, Santa Clara, CA) was coupled to an Agilent UHPLC liquid chromatography system. Each sample (4 µl) was resolved at a column temperature of 40°C. The mobile phase consisted of the following: solvent A [H_2O:acetonitrile (95:5), 10 mM ammonium acetate, and 10 mM ammonium hydroxide] and solvent B [H_2O:acetonitrile (95:5)].

Statistical Analyses

Comparative gene expression and inter-strain ATP levels were statistically analyzed using two-way ANOVA in GraphPad Prism 7.0 (GraphPad Software, San Diego, CA, USA). Partial least squared discriminate analysis (PLS-DA) was used to discriminate metabolites based on variable importance in projection values (VIP >1). Univariate testing was performed using SPSS 22.0 (SPSS Inc., Chicago, IL). Multivariate statistical analyses were performed using open-source R software and SIMCA-P (Umetrics, Umeå, Sweden). The data were log_{10}-transformed prior to model construction. Pathway analysis and integrating enrichment analysis were performed and visualized using MetaboAnalyst software.

Results

PrrAB is Required for Early Growth on Gluconeogenic Carbon Sources

Preliminary experiments revealed that the Δ*prrAB* mutant experienced early-stage growth defects in M7H9 medium containing glycerol as the primary carbon source (Fig. 4.1A). Co-supplementation with glucose restored the growth defect, however, the Δ*prrAB* mutant reached stationary phase earlier than the wild-type and complementation strains (Fig. 4.1B). All strains grew similarly during growth with glucose alone (Fig. 4.1C). We then questioned if the Δ*prrAB* mutant exhibited other carbon-specific growth defects. We found that the Δ*prrAB* mutant experienced an extended lag phase growth (early-stage growth) in the presence of acetate, propionate, butyrate (Figs. 4.2A, B, C), and succinate (Fig. 4.1D) as primary carbon sources.

Supplementing M7H9-propionate medium with vitamin B_{12} (10 µg/ml), which activates an alternative route of propionate utilization via the methylmalonyl pathway (Savvi, 2008), did not rescue the Δ*prrAB* mutant growth defects (Fig. 4.2D). In the presence of pyruvate and oxaloacetate, the Δ*prrAB* mutant was only slightly compromised for early-stage growth relative to the wild-type and complementation strains (Figs. 4.1E, F). Furthermore, the Δ*prrAB* mutant was not hypersensitive to acetate or propionate toxicity, as demonstrated by comparable growth between all strains during co-supplementation with glucose-acetate or glucose-propionate (Fig. 4.3). Co-supplementation experiments were terminated after 24 h due to excessive clumping in all which prevented accurate measurements of viability. Collectively, the data demonstrates that PrrAB is required for early growth when the gluconeogenic substrates acetate, propionate, and succinate (and glycerol, a mixed glycolytic/gluconeogenic metabolite) are provided as primary carbon sources.

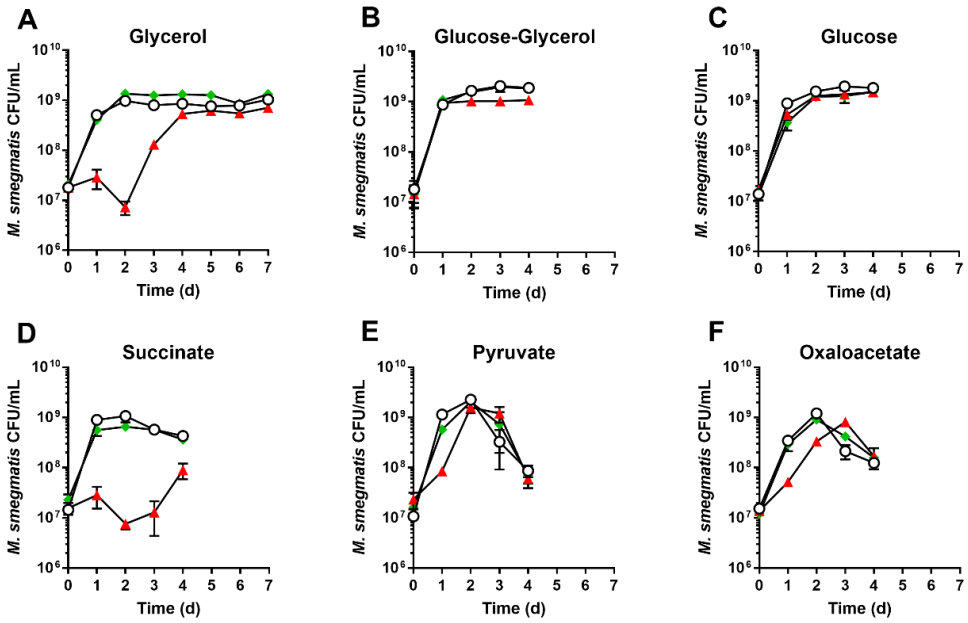

Figure 4.1. *M. smegmatis* mc²155 (○), FDL10 (▲), and FDL15 (♦) growth curves in different carbon sources (0.2%). Note that only growth in M7H9-glycerol was performed over 7 d period, whereas all other experiments were terminated after 4 d. Values represent the mean ± SEM of data collected from three independent cultures.

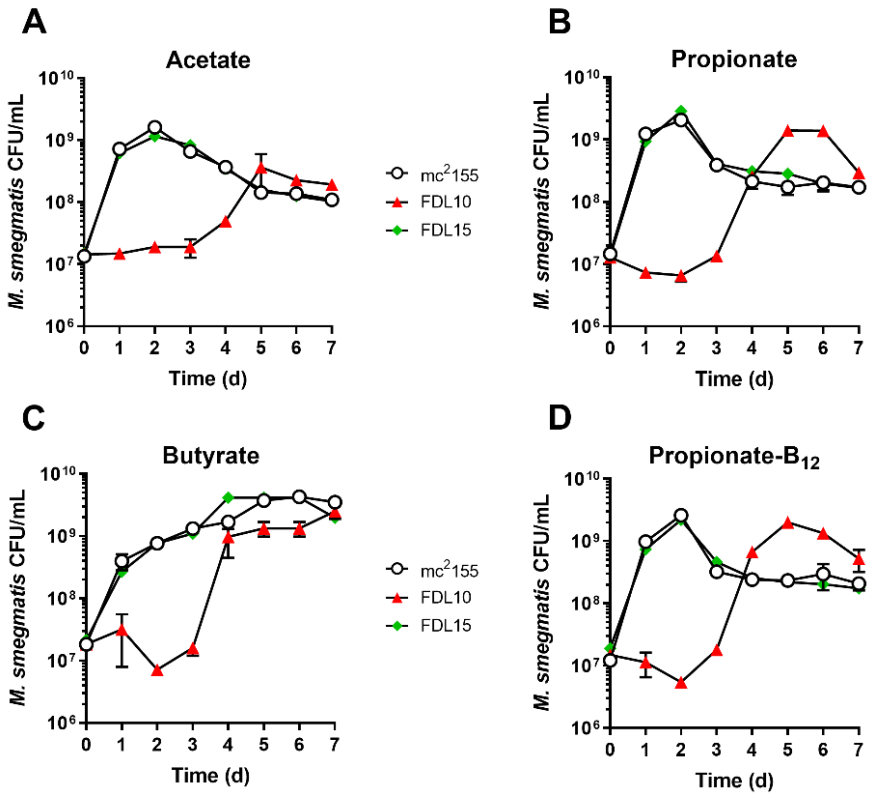

Figure 4.2. *M. smegmatis* growth curves in gluconeogenic carbon sources (0.2%). Values represent the mean ± SEM of data collected from three independent cultures.

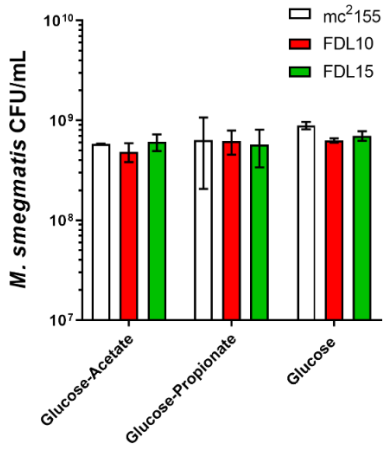

Figure 4.3. FDL10 is not hypersensitive to acetate or propionate toxicity. Strains were cultured for 24 h in M7H9 co-supplemented with 0.2% glucose and acetate or propionate or glucose alone. Values represent the mean ± SEM of data collected from three independent cultures.

prrA is Upregulated During Growth on Propionate and Acetate

Since PrrAB is required for optimal growth in short time periods on acetate and propionate, we questioned if *prrA* expression was upregulated during growth on these organic substrates. We measured relative expression values of the wild-type and complementation strains during exponential growth in M7H9-acetate and M7H9-propionate relative to M7H9-glucose. *prrA* was upregulated by ~1.5 and ~3.5 log_2 fold change in the wild-type strain during growth on acetate and propionate, respectively (Fig. 4.4). Similarly, *prrA* was upregulated by ~2 log_2 fold in the complementation strain during growth on propionate, however, *prrA* expression was not different in the complementation strain relative to mc^2155 during growth on acetate (-0.18 log_2 fold change), indicating lack of *prrAB* complementation in this setting (Fig. 4.4). These results suggested that propionate and, possibly, acetate, are environmental stimuli that activate *prrA* expression.

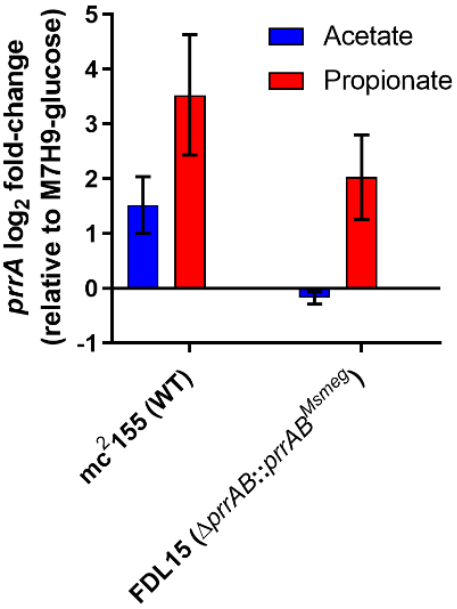

Figure 4.4. *prrA* is upregulated in the presence of acetate and propionate. qRT-PCR comparative gene expression profiling of *prrA* transcripts in mc^2155 (wild-type) and FDL15 (complementation strain) during growth in acetate (blue bars) or propionate (red bars). Log_2 fold change values are relative to growth in glucose. Relative *prrA* expression values were not significantly different between M7H9-acetate and M7H9-propionate (two-tailed Student's t test) or between strains (two-way ANOVA).

Isocitrate Lyase is Upregulated in the ΔprrAB Mutant During Growth on Acetate and Propionate

Isocitrate lyase (Icl) is the first enzyme of the glyoxylate cycle and *M. tuberculosis icl* (annotated as *aceA1* in *M. smegmatis*) mutants are defective for growth on acetate and fatty acids (and to a lesser extent, propionate) as sole carbon sources (Munoz-Elias and McKinney 2005). To determine if PrrAB regulates isocitrate lyase, we compared *aceA1* (*MSMEG 0911*) expression in the Δ*prrAB* mutant during exponential growth on acetate and propionate relative to the wild-type strain. *aceA1* was minimally upregulated in the Δ*prrAB* mutant during growth on glucose (Fig. 4.5A), however, expression was upregulated by ~1 $\log_2$ fold and ~3.5 $\log_2$ fold during growth on acetate and propionate, respectively (Fig. 4.5A and B). *aceA1* levels were similar in FDL15 relative to mc^2155, indicating complementation (Fig. 4.5). The results suggested that the growth defects in the Δ*prrAB* mutant during growth on acetate and propionate were not due to insufficient expression of *aceA1*.

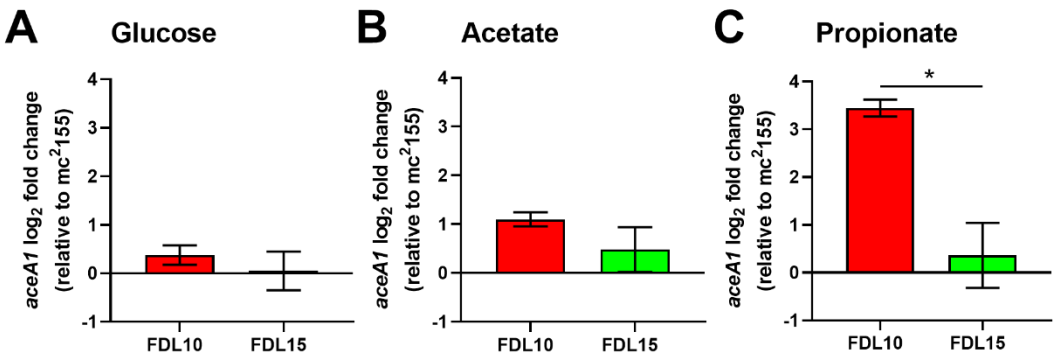

Figure 4.5. Isocitrate lyase 1 (*aceA1*) is upregulated during growth on acetate or propionate. qRT-PCR results from samples harvested after 1 d in (A) M7H9-glucose, (B) M7H9-acetate, and (C) M7H9-propionate. Log_2 fold change expression values are relative to mc^2155 samples taken from same carbon source, as indicated. All measurements were performed in biological triplicate. Error bars represent ±SEM. *, p = 0.0119, Student's t test.

Pantothenic Acid Partially Rescues Growth in Acetate and Propionate

We sought to determine if the growth defects experienced by Δ*prrAB* mutant during growth on acetate or propionate could be rescued by specific cellular metabolites. Supplementation with glucose and media-only samples were included as positive and negative

controls, respectively. Pantothenic acid (vitamin B_5) rescued growth over the course of 3 d in both media tested (Fig. 4.6). Phenylalanine also provided a slight growth advantage after 2 d culture in M7H9-propionate, however, the results were transient (Fig. 4.6B). All other supplements tested inhibited growth relative to the media only controls. The results suggest that defects in coenzyme-A (CoA) metabolism may contribute to the growth defects in the Δ*prrAB* mutant during culture under acetate and propionate.

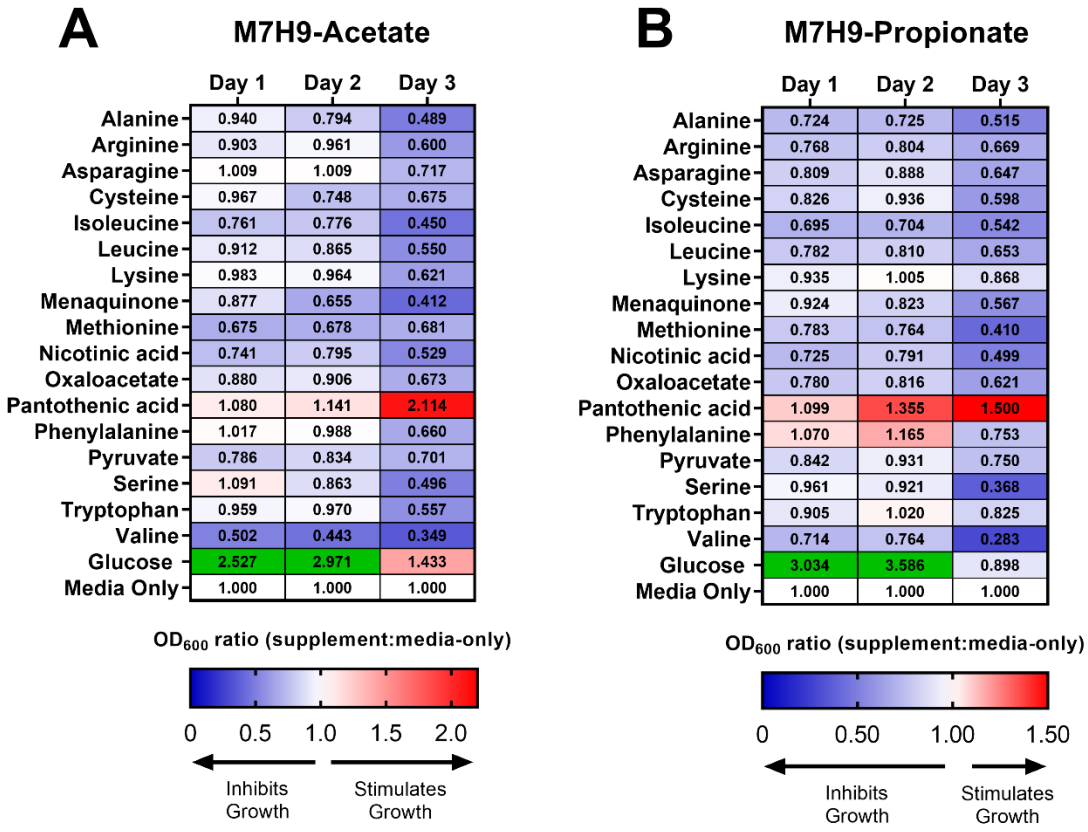

Figure 4.6. Pantothenic acid partially rescued the Δ*prrAB* mutant growth in acetate and propionate. (A) Three-day cultures in M7H9-acetate. (B) 3 d cultures in M7H9-propionate. Values within heatmap cells indicate mean OD_{600} values. Absorbance values normalized to media-only samples at each day. Red and blue colored cells indicate increased and decreased growth, respectively, compared to media-only samples. Green cells indicate supplement/media-only ratios >2.5. Data is representative of the mean values of triplicate, independently-grown cultures.

The M. smegmatis ΔprrAB Mutant Accumulates ATP in the Presence of Acetate and Propionate

To determine if FDL10 displays an energy imbalance during growth in carbon-defined conditions, we measured ATP levels in all strains after 1 and 4 d of growth. During growth in propionate, average ATP levels were 66-fold and 48-fold greater in FDL10 relative to mc^{2}155 and FDL15 ($p < 0.01$), respectively, during early growth (Fig. 4.7C). In the presence of acetate, average ATP levels were 21-fold and 23-fold greater in FDL10 compared to mc^{2}155 and FDL15 ($p = 0.0011$), respectively, after 1 d of growth (Fig. 4.7B). Average ATP levels remained greater in FDL10 after 4 d of growth in acetate and propionate relative to mc^{2}155 and FDL15 (Fig. 4.7B, C). In the presence of glucose, ATP levels were slightly lower in FDL10 compared to mc^{2}155 and FDL15, respectively, at 1 d, whereas ATP levels were slightly, but significantly ($p < 0.003$), greater in FDL10 relative to mc^{2}155 and FDL15 after 4 d of growth (Fig. 4.7A). The results demonstrated that the early growth defects in FDL10 during growth on acetate and propionate are not due to insufficient ATP levels and that FDL10 accumulates ATP during culture in these carbon sources relative to mc^{2}155 and FDL15.

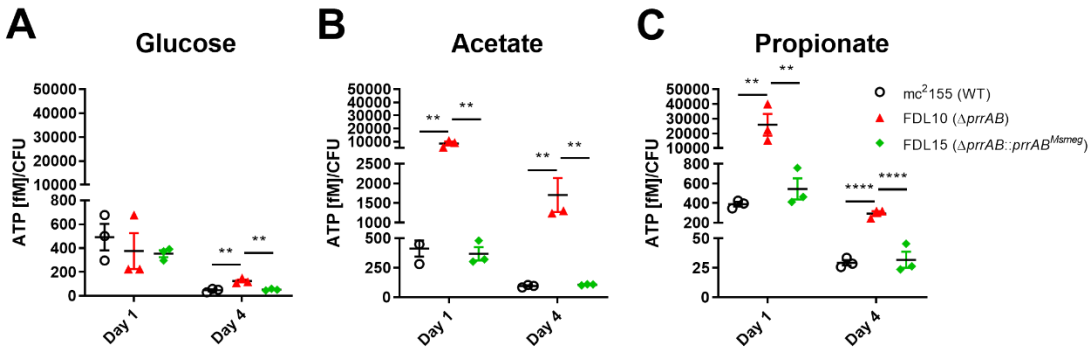

Figure 4.7. FDL10 accumulates ATP during growth in M7H9-acetate or M7H9-propionate. Relative ATP (fM/CFU) was calculated at 1 and 4 d growth in (A) M7H9-glucose, (B) M7H9-acetate, and (C) M7H9-propionate media. Values are representative of triplicate, independently-grown cultures. Error bars represent ±SEM. **, $p < 0.01$; ****, $p < 0.0001$; one-way ANOVA (within each day) with Dunnett's multiple comparisons.

Untargeted Metabolomics Analyses

To understand dysregulation in metabolite levels in FDL10, we utilized an untargeted LC-MS/MS metabolomics approach. Of 278 metabolites detected in both positive and negative ionization modes, 109 metabolites were reliably identified, as defined by counts greater than 1000 in ≥80% of samples and a QC coefficient of variation <20%. Of this cohort, 28, 64, and 63 metabolites were significant between the strain, carbon source, and time point multivariate general linear models, respectively. Hierarchical cluster analysis comparing reliably detected metabolites demonstrated different metabolite profiles in FDL10 relative to mc^2155 and FDL15 (Fig. 4.8). These effects were readily evident at 1 d in acetate or propionate (Fig. 4.8). VIP scores based on partial least squares models identified 20 and 25 metabolites in the carbon source and time point models, respectively, with VIP scores >1; 9 metabolites with VIP scores >1 were shared between both models (Fig. 4.9). No metabolites with VIP scores >1 were found in the strain model.

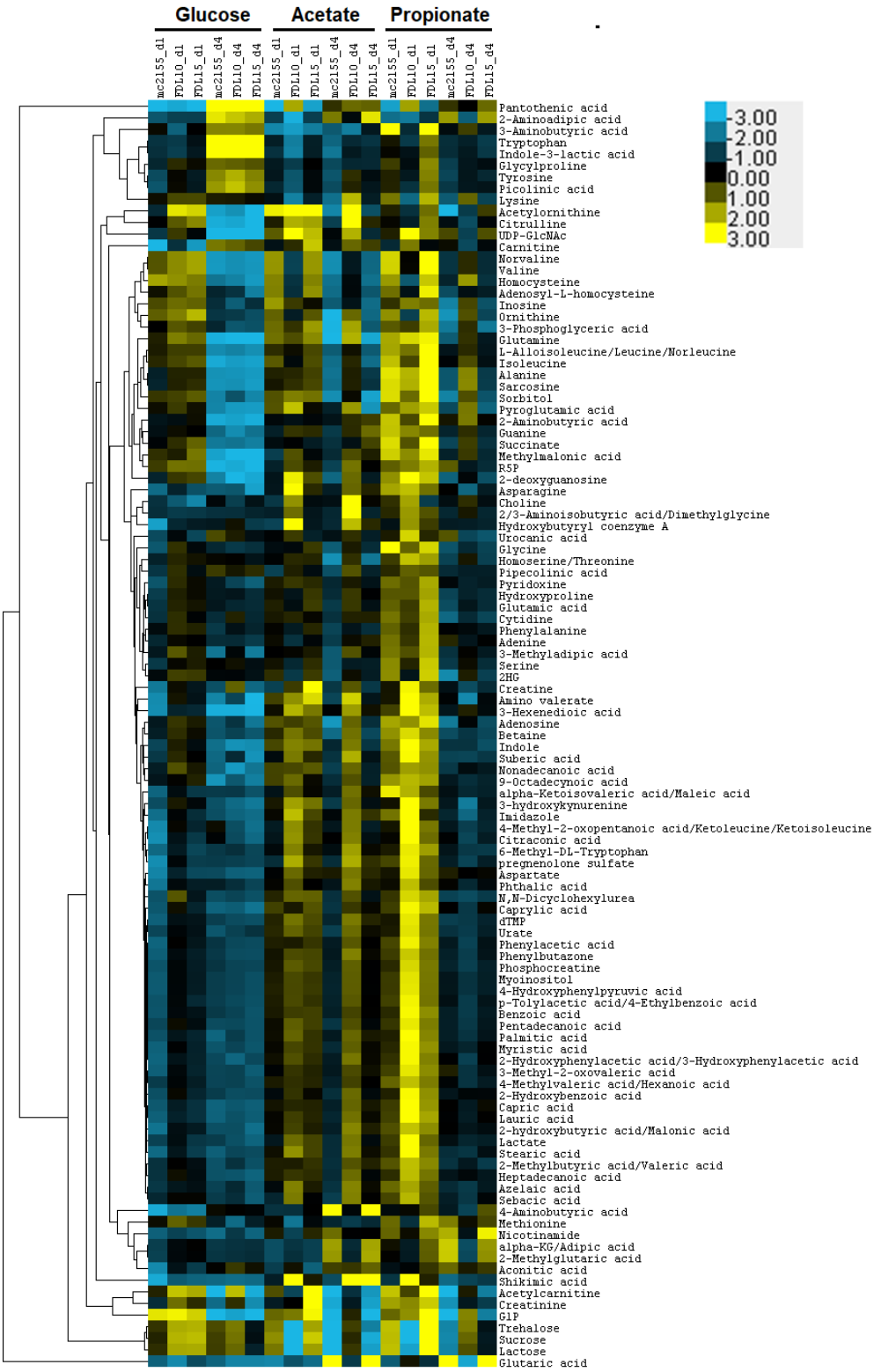

Figure 4.8. Average linkage hierarchical cluster heatmap of 109 reliably detected metabolites by LC-MS/MS in all samples tested. Individual strains and time points are listed at the top of the heatmap under each respective carbon source tested.

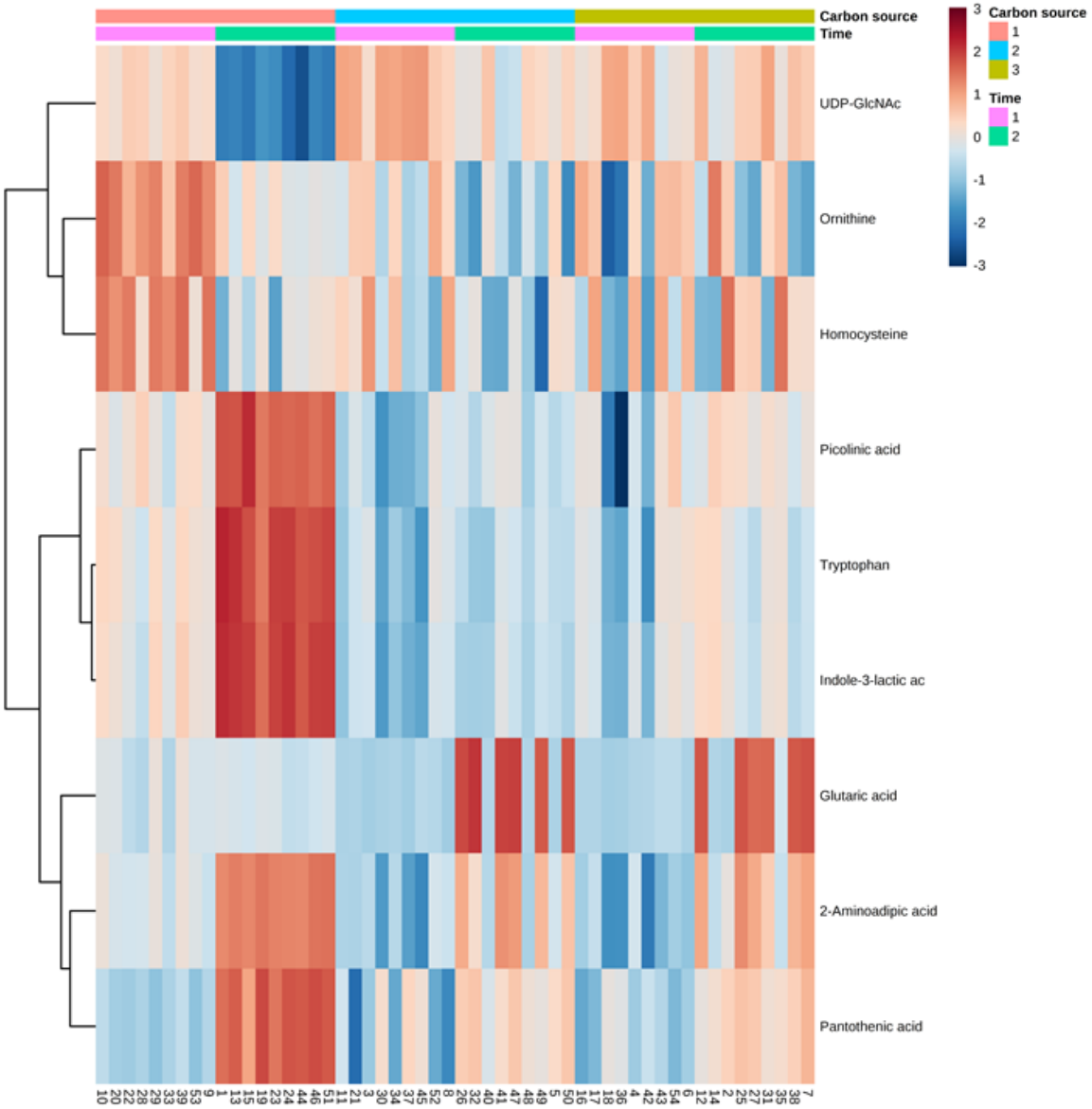

Figure 4.9. Hierarchical cluster heat map of metabolites with a VIP score >1 shared between both carbon source and time point statistical models. Carbon source: 1, glucose (pink); 2, acetate (blue), 3, propionate (yellow). Time: 1, 1 d (purple); 2, 4 d (green).

Comparative Metabolomic Profiles by Carbon Source

To help explain the Δ*prrAB* mutant growth defects during early-stage growth in acetate or propionate, we compared normalized relative abundances of 109 reliably detected metabolites in each strain at 1 and 4 d growth. Since we specifically sought to identify metabolites that were accumulated or depleted in FDL10, metabolite abundances ratios were calculated in FDL10

relative to mc^{2}155 or FDL15. We defined accumulated metabolites as a ratio >2 and depleted metabolites as a ratio <0.5 when present between both pair-wise strain comparisons. Only metabolites that were present in at least one-of-two online data bases (Metacyc and KEGG) and found in the *M. smegmatis* search criteria were retained for further analysis. See Tables 4.1 and 4.2 for all relevant information.

Comparative Metabolomes in M7H9-Glucose

Since all strains grew similarly in M7H9-glucose over the 7 d growth period, we expected to find similar comparative metabolomes. Consistent with this hypothesis, the metabolite profiles of each strain were mostly similar after 1- and 4-d growth in M7H9-glucose (Fig. 4.8). One metabolite (urocanic acid) accumulated in FDL10 at 1 d, while three metabolites (creatine, creatinine, and cytidine) accumulated and one metabolite (methionine) was depleted at 4 d. The results corroborated the growth data and suggest that glucose metabolism is not genetically regulated by PrrAB.

Comparative Metabolomes in M7H9-Acetate

We found 10 metabolites accumulated and 13 metabolites depleted in FDL10 after one day of growth in M7H9-acetate. Notably, pantothenic acid was elevated 53- and 25-fold in FDL10 relative to mc^{2}155 and FDL15, respectively, at 1 d in M7H9-acetate (Table 4.1). Pantothenic acid levels were similar in FDL10 relative to mc^{2}155 and FDL15 at 4 d. Other highly-accumulated metabolites in FDL10 at 1 d include asparagine, hydroxybutyryl-CoA, and shikimic acid (Table 4.1). At 4 d culture, 52 metabolites accumulated and 4 metabolites were depleted in FDL10 in M7H9-acetate. The accumulation of metabolites at day 4 was likely due to the opposing growth stages of FDL10 (exponential growth) relative to mc^{2}155 and FDL15 (death/early stationary phase) (Fig. 4.1A). Three disaccharides (lactose, sucrose, and trehalose) were severely depleted in FDL10 at 1 d, suggesting defects in carbohydrate storage metabolism.

Comparative Metabolomes in M7H9-Propionate

We found 27 metabolites accumulated and 20 depleted metabolites in FDL10 at 1 d culture in M7H9-propionate. There were 21 accumulated and 9 depleted metabolites in FDL10 after 4 d culture in M7H9-propionate. During growth in M7H9-propionate, pantothenic acid accumulated 24- and 14-fold greater in FDL10 relative to mc^{2}155 and FDL15, respectively. These results were similar to those seen in M7H9-acetate, however, pantothenic acid accumulated to a lesser degree in M7H9-propionate. Shikimic acid and UDP-GlcNAc also accumulated to high levels in FDL10 at d 1 in M7H9-propionate (Table 4.1). Fewer metabolites accumulated in FDL10 at d 4 in M7H9-Prp relative to M7H9-acetate, potentially reflecting different end products of acetate (malate and succinate) and propionate (pyruvate and succinate) metabolism. Lactose, sucrose, and trehalose were also severely depleted in FDL10 at d 1, similar to the results seen at d 1 in M7H9-acetate (Table 4.2).

Table 4.1. Accumulated metabolites in FDL10 relative to mc^{2}155 and FDL15 in each carbon source tested.

M7H9-Glucose

	Day 1		Day 4	
Metabolite	**FDL10/mc^{2}155**	**FDL10/FDL15**	**FDL10/mc^{2}155**	**FDL10/FDL15**
Creatine	-	-	5.567	7.389
Creatinine	-	-	5.01	7.244
Cytidine	-	-	2.211	2.102
Urocanic acid	2.115	2.044	-	-

M7H9-Acetate

	Day 1		Day 4	
Metabolite	**FDL10/mc^{2}155**	**FDL10/FDL15**	**FDL10/mc^{2}155**	**FDL10/FDL15**
Dimethylglycine	3.541	3.149	16.993	16.36
2-deoxyguanosine	8.943	3.716	7.581	3.26
2-hydroxybutyric acid	-	-	4.258	2.338
2/3-Hydroxyphenylacetic acid	-	-	3.647	2.483
3-Phosphoglyceric acid	-	-	30.314	10.637
4-Hydroxyphenylpyruvic acid	-	-	3.269	2.206
Ketoleucine/Ketoisoleucine	4.393	2.113	3.581	3.883
Acetylornithine	-	-	38.646	20.754
Aconitic acid	2.363	3.51	-	-
Adenosine	-	-	13.07	3.876
Adenosyl-L-homocysteine	-	-	3.131	2.44
Alanine	-	-	4.837	2.491
2-Ketoisovaleric acid	-	-	3.556	2.235
Asparagine	31.396	17.531	-	-
Betaine	-	-	8.625	5.794
Choline	6.277	3.805	18.33	14.664

Citrulline	-	-	20.114	7.016
Creatine	-	-	3.836	3.925
Creatinine	-	-	5.062	4.649
dTMP	-	-	4.218	2.018
G1P	-	-	10.553	22.127
Glutamine	-	-	35.873	29.322
Glycine	-	-	3.587	2.048
Heptadecanoic acid	-	-	4.005	2.602
Homocysteine	-	-	3.321	3.27
Homoserine/Threonine	-	-	7.803	5.787
Hydroxybutyryl-CoA	27.858	16.851	7.511	3.356
Indole	-	-	4.254	5.036
Inosine	-	-	2.274	2.763
Isoleucine	-	-	4.814	4.797
Lactate	-	-	4.42	3.02
Lactose	-	-	34.127	9.518
Leucine	-	-	3.275	3.216
Lauric acid	-	-	3.952	2.355
Lysine	-	-	16.538	6.422
Methylmalonic acid	3.977	2.112	-	-
Myoinositol	-	-	3.233	2.21
Myristic acid	-	-	3.562	2.059
Nonadecanoic acid	-	-	4.8	3.351
Ornithine	-	-	20.346	7.736
Pantothenic acid	52.591	25.448	-	-
Pentadecanoic acid	-	-	3.529	2.07
Phenylacetic acid	-	-	2.81	2.05
Phosphocreatine	-	-	3.099	2.248
Pipecolinic acid	-	-	4.992	2.933
R5P	-	-	5.572	2.64
Sarcosine	-	-	4.61	2.314
Shikimic acid	13.792	7.969	83.991	2.721
Sorbitol	-	-	5.513	6.999
Stearic acid	-	-	4.697	2.531
Sucrose	-	-	16.651	9.736
Trehalose	-	-	24.19	7.234
UDP-GlcNAc	-	-	4.656	7.043
Urate	-	-	4.958	2.177
Valine	-	-	3.815	2.467

M7H9-Propionate

	Day 1		**Day 4**	
Metabolite	**FDL10/mc^{2}155**	**FDL10/FDL15**	**FDL10/mc^{2}155**	**FDL10/FDL15**
2-Aminobutyric acid	-	-	2.284	2.637
2-deoxyguanosine	5.401	3.502	2.878	2.35
2-hydroxyglutarate	-	-	6.147	2.665
2/3-Hydroxyphenylacetic acid	5.092	2.649	-	-
3-Methyl-2-oxovaleric acid	3.917	2.118	-	-
3-Phosphoglyceric acid	-	-	5.818	5.726
4-Hydroxyphenylpyruvic acid	4.121	2.536	-	-
Ketoleucine/Ketoisoleucine	11.139	4.974	-	-
Adenosine	-	-	3.807	2.283
Alanine	-	-	8.097	5.884
Aspartate	5.646	2.892	-	-
Benzoic acid	5.487	2.4	-	-

Capric acid	5.329	2.555	-	-
Choline	2.589	7.646	-	-
Creatine	6.366	3.1	-	-
dTMP	5.604	2.51	-	-
G1P	-	-	32.424	12.5
Guanine	-	-	2.173	2.239
Homocysteine	-	-	5.257	6.235
Homoserine/Threonine	-	-	2.582	2.522
Hydroxybutyryl-CoA	4.174	2.09	-	-
Indole	4.041	2.695	-	-
Inosine	-	-	7.997	4.556
Lactate	6.302	4.513	-	-
Lactose	-	-	8.744	2.509
Lauric acid	5.283	2.296	-	-
Lysine	-	-	6.417	4.923
Methylmalonic acid	-	-	2.34	2.527
Myoinositol	4.004	2.448	-	-
Myristic acid	5.513	2.294	-	-
Ornithine	-	-	10.571	4.279
Palmitic acid	6.309	2.726	-	-
Pantothenic acid	23.705	13.616	-	-
Pentadecanoic acid	4.369	2.436	-	-
Phenylacetic acid	4.103	2.523	-	-
Phosphocreatine	4.161	2.159	-	-
Sarcosine	-	-	8.299	6.144
Shikimic acid	49.223	20.196	-	-
Sorbitol	-	-	8.531	4.973
Stearic acid	6.427	3.636	-	-
Succinate	-	-	3.685	2.932
Sucrose	-	-	10.91	3.107
Trehalose	-	-	12.733	3.428
UDP-GlcNAc	17.414	7.723	-	-
Urate	5.123	2.427	-	-
Urocanic acid	4.629	4.201	-	-
Valine	-	-	2.577	2.324

Table 4.2. Depleted metabolites in FDL10 relative to mc^{2}155 and FDL15 in each carbon source tested.

M7H9-Glucose

	Day 1		Day 4	
Metabolite	**FDL10/mc^{2}155**	**FDL10/FDL15**	**FDL10/mc^{2}155**	**FDL10/FDL15**
Methionine	-	-	0.42	0.42

M7H9-Acetate

	Day 1		Day 4	
Metabolite	**FDL10/mc^{2}155**	**FDL10/FDL15**	**FDL10/mc^{2}155**	**FDL10/FDL15**
2-Aminoadipic acid	0.276	0.271	0.331	0.137
2-hydroxyglutarate	0.356	0.321	-	-
4-Aminobutyric acid	-	-	0.065	0.044
Adenosyl-L-homocysteine	0.205	0.18	-	-
α-ketoglutarate	-	-	0.166	0.158
Glutaric acid	-	-	0.013	0.006
Homocysteine	0.188	0.19	-	-

Indole-3-lactic acid	0.393	0.314	-	-
Isoleucine	0.433	0.48	-	-
Lactose	0.027	0.02	-	-
Lysine	0.273	0.332	-	-
Methionine	0.243	0.285	-	-
Nicotinamide	0.368	0.337	-	-
Ornithine	0.321	0.354	-	-
Sucrose	0.016	0.01	-	-
Trehalose	0.019	0.014	-	-
Tryptophan	0.332	0.336	-	-
Tyrosine	0.487	0.411	-	-
Valine	0.136	0.134	-	-

M7H9-Propionate

	Day 1		Day 4	
Metabolite	**FDL10/mc^{2}155**	**FDL10/FDL15**	**FDL10/mc^{2}155**	**FDL10/FDL15**
2-Aminoadipic acid	-	-	0.096	0.094
2-Aminobutyric acid	0.359	0.172	-	-
2-hydroxyglutarate	0.248	0.145	-	-
2/3-Hydroxyphenylacetic acid	-	-	0.49	0.49
Acetylornithine	0.436	0.23	-	-
Adenosyl-L-homocysteine	0.327	0.114	-	-
α-ketoglutarate	-	-	0.077	0.12
Asparagine	-	-	0.312	0.439
Carnitine	-	-	0.39	0.474
Citrulline	-	-	0.482	0.446
Glutaric acid	-	-	0.004	0.004
Glycine	0.101	0.389	-	-
Homocysteine	0.102	0.071	-	-
Isoleucine	0.366	0.171	-	-
Lactose	0.032	0.019	-	-
Lysine	0.113	0.068	-	-
Methionine	0.243	0.124	-	-
Nicotinamide	0.487	0.364	0.191	0.112
Ornithine	0.146	0.105	-	-
Picolinic acid	0.426	0.214	-	-
Serine	0.429	0.256	-	-
Sorbitol	0.392	0.294	-	-
Succinate	0.321	0.245	-	-
Sucrose	0.01	0.006	-	-
Trehalose	0.006	0.003	-	-
Tryptophan	0.427	0.191	-	-
UDP-GlcNAc	-	-	0.261	0.247
Valine	0.185	0.105	-	-

Discussion

The natural environments that saprophytic bacteria reside are subject to uncertain periods of nutrient availability and may experience periods of starvation. For instance, deep freezes may delay decomposition of fallen foliage; extended periods of drought prevent optimal enzymatic activity and cellular growth; or leaching of nutrients from the soil depletes organic and

inorganic matter. Pathogenic bacteria, such as *M. tuberculosis*, are believed to experience nutrient-limitation during prolonged residence within the host macrophage (Schnappinger et al. 2003; Rohde et al. 2012; Timm et al. 2003). The ability to capitalize on a diverse collection of organic substrates to fuel energetic and biosynthetic demands is therefore evolutionarily advantageous to both pathogenic and non-pathogenic mycobacteria in their natural ecological niches.

CCM is an intricate and highly interactive network of anabolic and catabolic reactions that fulfills many of the metabolic pathways that sustain life. As heterotrophic organisms, mycobacteria assimilate organic compounds available in their environment for immediate use or as metabolic intermediates. As a saprophytic mycobacterium, *M. smegmatis* is genetically equipped to metabolize a wide range of carbon sources, including, but not limited to, sterols (Fernandez-Cabezon et al. 2017), TAGs (Nakagawa, Kashiwabara, and Matsuki 1976), propionate (Upton and McKinney 2007), and acetate (Hayden et al. 2013), in addition to a wide variety of sugars (Titgemeyer et al. 2007). It is believed that *M. tuberculosis* utilizes fatty acids as primary carbon sources during chronic infection (Bloch and Segal 1956; Timm et al. 2003) and mutants defective in these pathways are attenuated during infection (Munoz-Elias and McKinney 2005; Marrero et al. 2010). Though the natural ecological niche that each species occupies is profoundly different, *M. smegmatis* and *M. tuberculosis* both exhibit redundancy in the pathways employed to exploit available organic substrates.

A paucity of information is available regarding transcriptional regulation of CCM in mycobacteria. In *M. tuberculosis*, RamB represses isocitrate lyase-1 (*icl1*) during growth on glucose (Micklinghoff et al. 2009); PrpR acts as a transcriptional activator of the methylcitrate operon (Masiewicz et al. 2012); the RegX3 and DosR TCS response regulators induce the citrate synthase (*gltA1*) (Roberts et al. 2011) and phosphofructokinase (*pfk*) (Park et al. 2003) genes, respectively, during hypoxic growth. In this study, we add to the current body of knowledge by demonstrating that the *M. smegmatis* PrrAB TCS promotes early growth in the presence of acetate, butyrate, propionate, and succinate as primary carbon sources. However, it currently

remains unknown the precise gene(s) regulated by PrrAB that enable utilizing these gluconeogenic substrates.

Utilizing acetate or propionate as primary carbon sources requires an intact gluconeogenesis pathway. Phosphoenolpyruvate carboxykinase (PEPCK) represents the first committed step of gluconeogenesis. PEPCK generates phosphoenolpyruvate from oxaloacetate and is required for *M. tuberculosis* in vitro growth on acetate and to establish infection in mice (Marrero et al. 2010). The second committed enzyme of gluconeogenesis is fructose-1,6-bisphosphatase (GlpX), which generates fructose-6-phosphate from fructose-1,6-bisphosphate. *M. tuberculosis* mutants lacking two enzymes with fructose-1,6-bisphosphatase activity fail to grow on fatty acids and are severely attenuated in mice (Ganapathy et al. 2015). Fructose-6-phosphate is a precursor of UDP-*N*-acetylglucosamine (UDP-GlcNAc), an integral component of the essential peptidoglycan cell wall structure (Moraes et al. 2015), or is reversibly isomerized to glucose-1-phosphate. Glucose-1-phosphate can then enter the pentose phosphate pathway to generate essential pentose intermediates for nucleotide and cofactor synthesis and NADPH as reducing power for anabolic reactions. It seems unlikely that PrrAB positively regulates PEPCK, as FDL10 is only slightly compromised for growth when oxaloacetate is supplemented as the primary carbon source and follows the same overall growth pattern relative to the wild-type and complementation strains (Fig. 4.1F). Additionally, the accumulation of UDP-GlcNAc in FDL10 after 1 d growth on acetate and propionate suggests that fructose-6-phosphate is generated through the action of GlpX. If PrrAB regulates downstream genes of peptidoglycan biosynthesis, then FDL10 should also be compromised for growth on glucose, a phenomenon which is not seen on this carbon source (Figs. 4.1B, C).

The accumulation of ATP in FDL10, relative to mc^2155 and FDL15, after 1 d culture on acetate and propionate was unexpected, since FDL10 was severely inhibited for growth under these conditions. We currently hypothesize that genes of the glyoxylate shunt and methylcitrate cycle are repressed by PrrAB in the wild-type setting and hence, are active in FDL10. This premise is first based on evidence for the accumulated ATP levels in FDL10, which suggests that acetate and propionate are metabolized to succinate through the glyoxylate shunt and

methylcitrate cycles, respectively. Succinate would then be oxidized by succinate dehydrogenase, with subsequent transfer of electrons through the respiratory chain to generate ATP through oxidative phosphorylation. Our previous RNA-seq data shows that both succinate dehydrogenase operons (*MSMEG 0420-sdh1DAB-MSMEG 0416* and *sdh2CDAB*) are overexpressed in FDL10 relative to mc^{2}155 (except *sdh2D*) during mid-logarithmic growth in M7H9-ADS-glycerol-TW80 (Maarsingh et al., unpublished data). Overexpression of the SDH1 and SDH2 complexes may at least partially explain the accumulated ATP seen in FDL10 relative to mc^{2}155 and FDL15 during growth on acetate and propionate. Second, we show that isocitrate lyase (*aceA1*), a key enzyme of the glyoxylate shunt, is upregulated in the Δ*prrAB* mutant during growth on acetate and propionate (Figs. 4.5B, C), indicating that PrrAB represses *aceA1* in the wild-type background. RNA-seq data shows that *glcB, prpB,* and *prpC* are expressed at similar levels in FDL10 relative to mc^{2}155 and *prpD* expression is ~2-fold lower in FDL10 relative to mc^{2}155; however, none of the differential expression values were statistically significant. Gene expression profiling of malate synthase (*glcB*), the second enzyme of the glyoxylate shunt, and genes of the methylcitrate cycle (*prpDBC*), in addition to measuring enzymatic activity, are required to support to this hypothesis (Fig. 4.10).

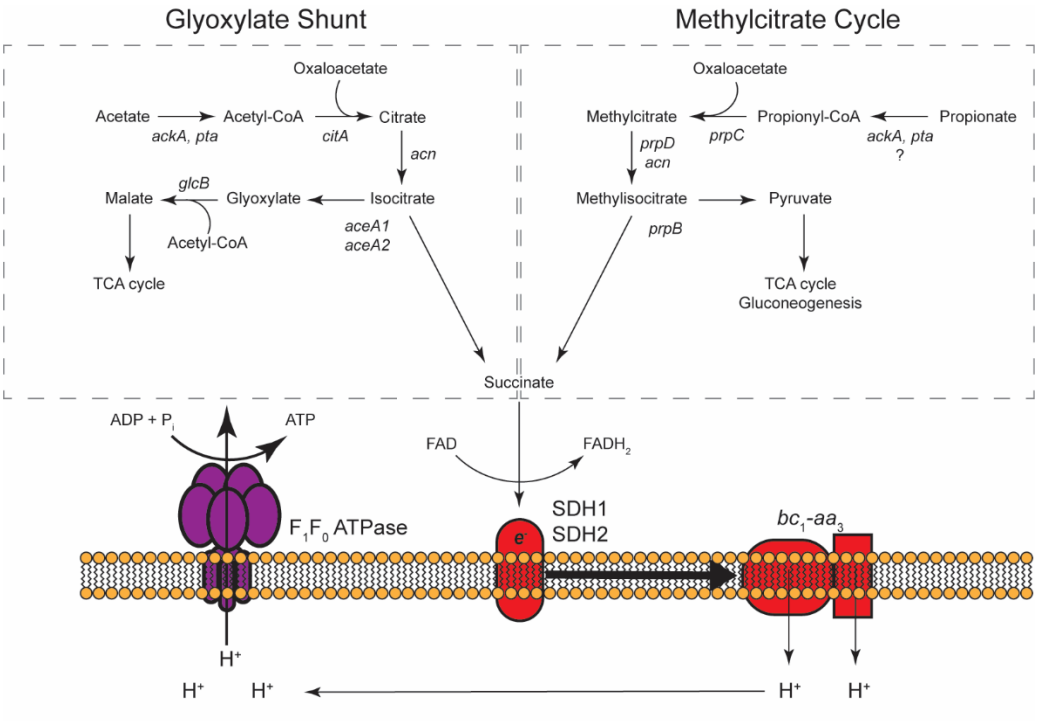

Figure 4.10. The metabolic fate of acetate and propionate as sole carbon sources via the glyoxylate shunt and methylcitrate cycle, respectively, in *M. smegmatis*. *ackA*, acetate kinase; *aceA1/aceA2,* isocitrate lyase1/2; *acn*, aconitase; *citA*, citrate synthase; *glcB*, malate synthase; *prpB,* methylisocitrate lyase; *prpC*, methylcitrate synthase; *prpD*, methylcitrate dehydratase; *pta*, phosphotranacetylase; SDH1/SDH2, succinate dehydrogenase complex; bc_1-aa_3, cytochrome *c*:menaquinol oxidase-cytochrome *c* oxidase respiratory complex; FAD, flavin adenine dinucleotide.

It is possible that FDL10 is unable to utilize acetate or propionate for energy-demanding biosynthetic pathways during early growth stages. An intriguing postulate is that PrrAB regulates lipid or mycolic acid biosynthesis, both of which are energetically expensive processes and use acetate (Zimhony, Vilcheze, and Jacobs 2004) or propionate (Gago et al. 2006) as building blocks for fatty acid chain elongation. Fatty acid biosynthesis requires the input of energy from both ATP and NADPH. Though we demonstrated that ATP accumulates to high levels in FDL10 during growth on acetate and propionate (Figs. 4.7B, C), intracellular redox balance (NAD^+:NADH and $NADP^+$:NADPH) remains unknown and should be measured under the growth conditions employed in these studies. The severe depletion of trehalose seen in FDL10 after 1 d in M7H9-acetate and M7H9-propionate suggests a modified hypothesis that mycolic acid incorporation into the outer membane may be regulated by PrrAB. Trehalose is a non-reducing disaccharide

composed of 1,1-linked α-glucose molecules and is essential in *M. smegmatis* (Woodruff et al. 2004). Trehalose dimycolate, also known as cord factor, is an important *M. tuberculosis* virulence factor (Hunter, Venkataprasad, and Olsen 2006) and both trehalose dimycolate and trehalose monomycolate are present in the *M. smegmatis* outer membrane (Bansal-Mutalik and Nikaido 2014). MmpL3 transports trehalose monomycolate to the outer membrane for synthesis of the mycolyl-arabinogalactan-peptidoglycan cell wall structure (Takayama, Wang, and Besra 2005; Xu et al. 2017). RNA-seq analysis shows that *mmpL3* (*MSMEG 0250*) is expressed at similar levels between the FDL10 and mc^{2}155 (+1.24 fold, p = 0.5204) or FDL15 (+1.23 fold, p = 0.4901) pair-wise comparisons, suggesting that PrrAB does not regulate mycolic acid transport across the inner membrane via MmpL3. Defects in trehalose synthesis would decrease incorporation of mycolic acid into the outer membrane and may explain the growth defects seen in FDL10 during growth on acetate and propionate. However, further investigations are required to determine the enzymatic pathways from acetate to trehalose synthesis putatively interrupted in FDL10. Isotopically-labeled acetate or propionate could be used to quantitatively investigate lipid biosynthetic activity between strains during growth in the presence of different carbon sources. These results may provide insight into the choice of genes to pursue in efforts to correlate the transcriptional deficiencies with the carbon-specific growth defects seen in FDL10. Furthermore, this would provide valuable information for exploring PrrAB redundancy in *M. tuberculosis*.

Pantothenic acid is a precursor to CoA biosynthesis, an important cofactor for many biological processes (Begley, Kinsland, and Strauss 2001). Free acetate is activated to acetyl-CoA by acetyl-CoA synthetase (Noy, Xu, and Blanchard 2014) or the acetate kinase-phosphotransacylase pathway (Rucker et al. 2015). The key lipid and mycolic acid biosynthetic enzymes, fatty acid synthase and polyketide synthase, are activated from their inactive apo- to the active holo-forms through covalent attachment of the 4'-phosphopantetheine moiety of CoA by phosphopantetheinyl transferase (Chalut et al. 2006). Comparative metabolomic profiles revealed that FDL10 accumulates pantothenic acid by 53- and 24-fold after 1 d growth in M7H9-acetate and M7H9-propionate, respectively, relative to mc^{2}155 (Table 4.1). Paradoxically, supplementing M7H9-acetate or M7H9-propionate with pantothenic acid rescued growth, albeit

modestly, in FDL10 after 2 d culture relative to media-only controls (Fig. 4.6). Previous RNA-seq data shows that phosphopantetheine adenylyltransferase (*coaD, MSMEG 2414*) is expressed at -3.37-fold in FDL10 relative to mc^2155 (p = 0.0246) during exponential growth in M7H9-ADS-glycerol-TW80 (unpublished data). CoaD catalyzes the transfer of ATP to pantetheine to generate dephospho-CoA, representing the penultimate step in CoA biosynthesis. If FDL10 under-expresses CoaD during growth on M7H9-acetate or M7H9-propionate, it could explain the accumulation of pantothenate and thus represent a metabolic bottleneck that hinders optimal CoA biosynthesis. Desphospho-CoA kinase (CoaE) generates CoA from desphspho-CoA, however, the *M. smegmatis* genome (https://mycobrowser.epfl.ch/) lacks an annotated *coaE* gene and an *Mtb coaE* (*Rv 1631*) homologue is not found in *M. smegmatis*. Free CoA or propionyl-CoA was not detected by LC-MS/MS (acetyl-CoA was not reliably detected), therefore, it is uncertain how intracellular levels of these metabolites correlate with FDL10 growth in M7H9-acetate or M7H9-propionate. However, as described above, the elevated ATP levels in FDL10 suggest that activation of acetate and propionate to their CoA derivatives, which are required to enter the glyoxylate shunt and methylcitrate cycle, respectively, is not responsible for the growth defects seen in FDL10. It is possible that import of exogenous pantothenic acid activates an alternative pathway that promotes CoA synthesis or utilization that is independent of regulation by PrrAB.

The chorismate pathway for aromatic amino acid biosynthesis (phenylalanine, tryptophan, and tyrosine) is essential in mycobacteria (Parish and Stoker 2002). Chorismate is a precursor for the biosynthesis of two other important molecules: folic acid (Bermingham and Derrick 2002) and menaquinones (Dhiman et al. 2009). Shikimic acid, a metabolic intermediate of the chorismate pathway, was highly accumulated in FDL10 at day 1 in both M7H9-acetate and M7H9-propionate, suggesting blockade of downstream biosynthetic reactions leading to chorismate (chorismate itself was not detected by LC-MS/MS). In FDL10, two VIP metabolites of tryptophan catabolism (indole-3-lactic acid and pipecolinic acid), including tryptophan itself (Fig. 4.9), were depleted at day 1 in M7H9-acetate and M7H9-propionate (Table 4.2). Other products of phenylalanine and tyrosine metabolism were depleted or accumulated in FDL10 at day 1 during growth in M7H9-acetate or -propionate, suggesting that PrrAB regulates numerous

pathways of aromatic amino acid metabolism (Tables 4.1, 4.2). Tryptophan supplementation inhibited FDL10 during growth on acetate, but not propionate, compared to media-only controls, while phenylalanine supplementation only produced a modest growth inhibition after 3 d growth on both acetate and propionate (Fig. 4.6). It is possible that accumulation of these aromatic amino acids contributed to the growth inhibition seen in FDL10 under the conditions employed. Further investigations are required to determine if PrrAB regulates one or more genes involved in the chorismite, shikimate, or aromatic amino acid metabolism pathways.

In conclusion, we have identified numerous metabolic abnormalities between the *M. smegmatis* Δ*prrAB* mutant (FDL10) relative to the wild-type (mc^2155) and *prrAB* complementation strain (FDL15). The highly complex nature of CCM complicates precisely locating the genes responsible for the growth defects seen in the Δ*prrAB* mutant during early growth on acetate or propionate. Ideally, integrating next-generation transcriptomic sequencing (RNA-Seq) with the LC-MS/MS metabolomic techniques described in this report will elucidate the transcriptional regulatory defects that ultimately are at the root of the carbon-specific growth deficiencies seen in FDL10. Preliminary work in our lab demonstrates that an *M. tuberculosis prrAB* knockdown mutant is compromised for in vitro growth on glycerol and acetate in a manner similar to that seen in *M. smegmatis* (unpublished data). It therefore appears that PrrAB functional redundancy exists between these species and, hence, *M. smegmatis* is an appropriate surrogate model to approach understanding the phenotypes and genetics influenced by PrrAB in *M. tuberculosis*. Since *prrAB* deletion mutants are not viable in *M. tuberculosis* (Haydel et al. 2012), generating a conditional *prrAB* knockdown mutant appears the best option for deciphering the essential nature of this TCS.

CHAPTER 5: FINAL SUMMARY AND IMPLICATIONS OF THE RESEARCH PRESENTED

Infections by *M. tuberculosis*, the etiological cause of tuberculosis, constitutes a global health crisis. Tuberculosis is the 10th leading cause of death worldwide, and *M. tuberculosis* is the most deadly infectious agent (WHO 2017). For decades, isoniazid, rifampicin, pyrazinamide, and ethambutol have proven to be effective antituberculosis drugs. However, the increasing rates of multiple drug-resistant *M. tuberculosis* clinical isolates necessitate discovery of new antibiotics. The development of bedaquiline for treating drug sensitive and -resistant *M. tuberculosis* represents the first antituberculosis drug approved worldwide in the past 40 years (Worley and Estrada 2014). Other promising drug candidates in clinical phase testing include Q203 (Lu et al. 2018), delamanid (von Groote-Bidlingmaier et al. 2019), and pretomanid (Diacon et al. 2012). Increased efforts are needed to reveal essential and promising drug targets in *M. tuberculosis* to stay ahead of the evolutionary arms race between us and this global scourge.

Two-component systems (TCSs) represent important, and in some instances, essential (Haydel et al. 2012; Zahrt and Deretic 2000; Yan et al. 2011; Howell et al. 2003) signal transduction pathways in bacteria. TCSs allow bacteria to sense their immediate environment and enact appropriate adaptive responses. Disrupting signal transduction pathways has led to the development of new approaches for treating many human diseases (Noble, Endicott, and Johnson 2004). It therefore surprising that relatively less effort has been dedicated toward inhibiting essential signaling pathways in pathogenic bacteria. However, small molecules have been discovered that inhibit TCSs. Examples include walkmycin B inhibition of the essential WalK histidine kinase of *Bacillus subtilis* and *Staphylococcus aureus* (Okada et al. 2010); LED209 inhibition of the QseC histidine kinase of *Salmonella enterica* spp. Typhimurium (Rasko et al. 2008); and diarylthiazole inhibition via the *M. tuberculosis* PrrB histidine kinase (Bellale et al. 2014). In our current period of increasing prevalence of antibiotic-resistant bacterial pathogens, investing in the discovery and development of novel and unorthodox essential targets, such as TCSs, represent promising therapeutic modalities.

Our lab previously demonstrated that the *M. tuberculosis prrAB* TCS is essential for viability (Haydel et al. 2012). Subsequent work by Bellale et al. reported that the *M. tuberculosis* growth inhibition exerted by diarylthiazole compounds is mediated through the PrrB histidine kinase (Bellale et al. 2014). Fatostatin is a representative diarylthiazole compound and has previously been demonstrated to act as an antiobesity agent in mice and prevents fatty acid biosynthesis in human cell lines (Kamisuki et al. 2009). Furthermore, fatostatin exhibits anticancer properties (Gholkar et al. 2016) and prevents bone loss (Inoue and Imai 2015). The pleiotropic effects of fatostatin may complicate its clinical use for treating tuberculosis. Efforts to repurpose this small molecule by rationale pharmacological design may alleviate the eukaryotic mechanisms of action and direct use towards antituberculosis activity. However, it is imperative that we reveal the genetic cause of the essential nature of PrrAB in *M. tuberculosis*. Furthermore, this information will provide us with a more comprehensive understanding of the transcriptional programs that make *M. tuberculosis* an extremely successful intracellular pathogen.

Since we are currently unable to construct a Δ*prrAB* mutant in *M. tuberculosis*, we have directed our efforts toward the non-pathogenic relative, *Mycobacterium smegmatis*. In the studies reported here, we have shown that *prrAB* is not universally essential in mycobacteria, evidenced by the Δ*prrAB* mutant generated in *M. smegmatis* (Maarsingh and Haydel 2018). PrrAB is responsive to at least two in vitro stress conditions: ammonium limitation and hypoxia. PrrAB represses excessive triacylglycerol (TAG) accumulation during ammonium limitation in *M. smegmatis* (Maarsingh and Haydel 2018) (Fig. 5.1). We corroborated these data using gene expression profiling (qRT-PCR) which showed that the Δ*prrAB* mutant overexpresses numerous TAG and fatty acid biosynthetic genes (Maarsingh and Haydel 2018). The TAG accumulating phenotype under this condition is believed to provide bacteria with a long-term carbon storage molecule which the cell can utilize upon return of favorable nitrogen availability. *M. tuberculosis* also accumulates TAGs during in vitro stresses that mimic the host macrophage phagosome (Deb et al. 2009). Additionally, the *M. tuberculosis* W-Beijing lineage, which constitutively expresses the dormancy-associated *dosRS* TCS, accumulates TAGs under favorable laboratory growth conditions (Reed et al. 2007).

We also demonstrate that the *M. smegmatis* PrrAB TCS positively regulates the *dosR* TCS response regulator during aerobic and hypoxic growth, (Maarsingh et al., submitted for review) (Fig. 5.1). Hypoxia is an activating environmental signal of the DosRS-DosT TCS in *M. tuberculosis* (A. Kumar et al. 2007) and *M. smegmatis* (Lee et al. 2008) and induces the dormancy regulon in *M. tuberculosis* (Park et al. 2003). PrrAB therefore provides an additional layer of genetic regulation for the hypoxic response in *M. smegmatis* and likely serves to fine-tune regulation of *dosR* in this species. To corroborate this data, we showed that the Δ*prrAB* mutant is deficient, compared to the wild-type and complementation strains, during hypoxic growth and cyanide inhibition (Maarsingh et al., manuscript in preparation). The hypersensitivity of the Δ*prrAB* mutant to cyanide inhibition correlated with the data revealing that PrrAB positively regulates expression of the cytochrome *bd* oxidase genes (*cydABD*), the products of which serve as important respiratory complexes during microaerophilic/hypoxic conditions (Kana et al. 2001). Unexpectedly, ATP levels were ~64% lower in the Δ*prrAB* mutant compared to the wild-type strain, despite upregulation of the ATP F_1F_0 synthase genes in the former strain (Maarsingh et al., manuscript submitted for review) (Fig. 5.1). We hypothesize that this phenotype is due to downregulated expression of the bc_1-aa_3 aerobic terminal respiratory complexes in the Δ*prrAB* mutant. The bc_1-aa_3 respiratory complexes are essential in *M. tuberculosis* and genes encoding these proteins are found in multiple copies in *M. smegmatis*. If PrrAB functional redundancy exists between *M. tuberculosis* and *M. smegmatis*, this may, at least in part, explain the essential nature of PrrAB in the former species.

Lastly, the research presented here implicates PrrAB in utilization of acetate, propionate, butyrate, and succinate as primary carbon sources during early growth stages. These nutrients are gluconeogenic substrates and *M. tuberculosis* mutants unable to metabolize these metabolites are severely attenuated during infection (Munoz-Elias and McKinney 2005; Marrero et al. 2010; Ganapathy et al. 2015). Though we currently lack a genetic explanation for the growth defects seen in the Δ*prrAB* mutant during growth on these carbon sources, comparative metabolomics suggests that PrrAB may regulate aromatic amino acid metabolism, lipid biosynthesis, or cell well biosynthesis. Further experiments are forthcoming that will

comparatively measure expression of genes involved in these metabolic pathways. *M. tuberculosis* central carbon metabolism has attracted great attention over the past decade, and these data provide novel insights into a putative master regulator of essential central metabolism during chronic infection.

In summary, we provide the first biochemical evidence for metabolic regulation of triacylglycerol lipids and gluconeogenic carbon sources by PrrAB in *M. smegmatis*. Our results provide seminal data that have advanced our understanding of this essential TCS in *M. tuberculosis*. Furthermore, these studies further support diarylthiazole compounds as novel therapeutic agents that add to our arsenal of antituberculosis therapies. We believe that these molecules will also prove invaluable towards development of a more comprehensive understanding of the detailed regulatory mechanisms imparted on the physiology of *M. tuberculosis*.

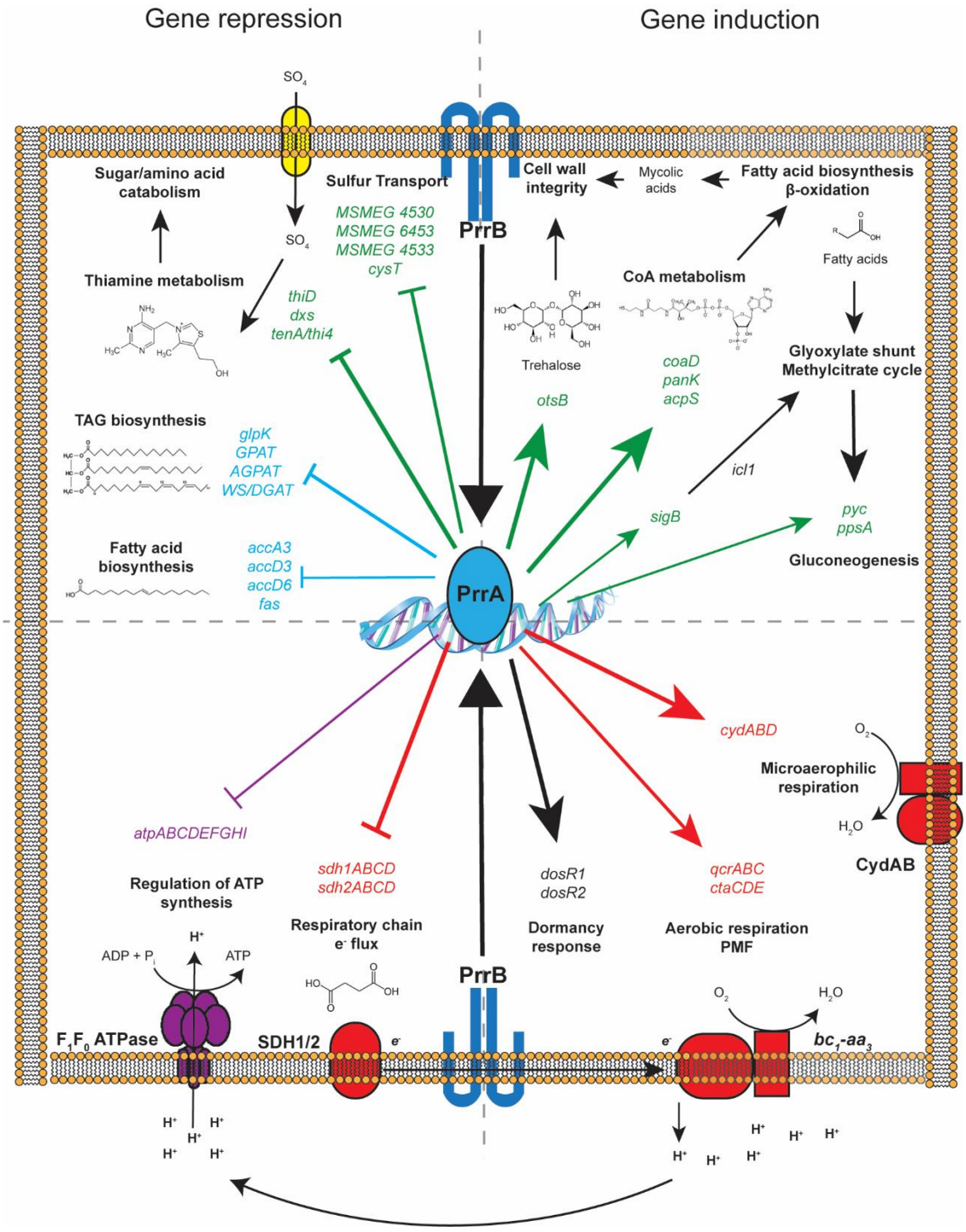

Figure 5.1. Overview of the *M. smegmatis* PrrAB TCS regulatory properties. Genes to the left of the vertical dashed line are repressed by PrrAB in the wild-type background whereas genes to the right of the vertical dashed line are induced by PrrAB in the wild-type background. Metabolic pathways are represented above the horizontal dashed line and respiratory pathways are indicated below the horizontal dashed line. Green lines, central metabolism genes; blue lines, genes affected during ammonium limitation; red lines, respiratory genes; purple line, ATP synthase genes.

REFERENCES

Agrawal, R., A. Pandey, M. P. Rajankar, N. M. Dixit, and D. K. Saini. 2015. "The Two-Component Signalling Networks of *Mycobacterium tuberculosis* Display Extensive Cross-Talk in vitro." *Biochemical Journal* 469 (1): 121-134. https://doi.org/10.1042/BJ20150268

Aiba, H., F. Nakasai, S. Mizushima, and T. Mizuno. 1989. "Phosphorylation of a Bacterial Activator Rrotein, OmpR, by a Protein Kinase, EnvZ, Results in Stimulation of its DNA-Binding Ability." *Journal of Biochemistry* 106 (1): 5-7.

Akhtar, S., A. Khan, C. D. Sohaskey, C. Jagannath, and D. Sarkar. 2013. "Nitrite Reductase NirBD is Induced and Plays an Important Role During in vitro Dormancy of *Mycobacterium tuberculosis*." *Journal of Bacteriology* 195 (20): 4592-9. https://doi.org/10.1128/JB.00698-13.

Almeida, D., T. Ioerger, S. Tyagi, S. Y. Li, K. Mdluli, K. Andries, J. Grosset, J. Sacchettini, and E. Nuermberger. 2016. "Mutations in *pepQ* Confer Low-Level Resistance to Bedaquiline and Clofazimine in *Mycobacterium tuberculosis*." *Antimicrobial Agents and Chemotherapy* 60 (8): 4590-4599. https://doi.org/10.1128/aac.00753-16.

Alvarez, H. M. 2016. "Triacylglycerol and Wax Ester-Accumulating Machinery in Prokaryotes." *Biochimie* 120: 28-39. https://doi.org/10.1016/j.biochi.2015.08.016.

Alvarez, H. M., R. Kalscheuer, and A. Steinbuchel. 2000. "Accumulation and Mobilization of Storage Lipids by *Rhodococcus opacus* PD630 and *Rhodococcus ruber* NCIMB 40126." *Applied Microbiology and Biotechnology* 54 (2): 218-223. https://doi.org/10.1007/s002530000395.

Alvarez, H. M., M. F. Souto, A. Viale, and O. H. Pucci. 2001a. "Biosynthesis of Fatty Acids and Triacylglycerols by 2,6,10,14-Tetramethyl Pentadecane-Grown Cells of *Nocardia globerula* 432." *FEMS Microbiology Letters* 200 (2): 195-200. https://doi.org/S0378109701002245 .

Alvarez, T. 1885. "Recherches sur le Bacille de Lustgarten." *Archives Physiologica Normal Pathological* 2: 303-321.

Amara, S., N. Seghezzi, H. Otani, C. Diaz-Salazar, J. Liu, and L. D. Eltis. 2016. "Characterization of Key Triacylglycerol Biosynthesis Processes in rhodococci." *Scientific Reports* 6. https://doi.org/10.1038/srep24985.

Amon, J., T. Brau, A. Grimrath, E. Hanssler, K. Hasselt, M. Holler, N. Jessberger, *et al*. 2008. "Nitrogen Control in *Mycobacterium smegmatis*: Nitrogen-Dependent Expression of Ammonium Transport and Assimilation Proteins Depends on the OmpR-Type Tegulator GlnR." *Journal of Bacteriology* 190 (21): 7108-7116. https://doi.org/10.1128/JB.00855-08.

Andries, K., P. Verhasselt, J. Guillemont, H. W. H. Gohlmann, J. M. Neefs, H. Winkler, J. Van Gestel, *et al*. 2005. "A Diarylquinoline Drug Active on the ATP Synthase of *Mycobacterium tuberculosis*." *Science* 307 (5707): 223-227. https://doi.org/10.1126/science.1106753.

Anes, E., P. Peyron, L. Staali, L. Jordao, M. G. Gutierrez, H. Kress, M. Hagedorn, *et al*. 2006. "Dynamic Life and Death Interactions Between *Mycobacterium smegmatis* and J774 Macrophages." *Cellular Microbiology* 8 (6): 939-960. https://doi.org/10.1111/j.1462-5822.2005.00675.x.

Anuchin, A. M., A. L. Mulyukin, N. E. Suzina, V. I. Duda, G. I. El-Registan, and A. S. Kaprelyants. 2009. "Dormant Forms of *Mycobacterium smegmatis* with Distinct Morphology." *Microbiology* 155 (Pt 4): 1071-1079. https://doi.org/10.1099/mic.0.023028-0.

Arabolaza, A., E. Rodriguez, S. Altabe, H. Alvarez, and H. Gramajo. 2008a. "Multiple Pathways for Triacylglycerol Biosynthesis in *Streptomyces coelicolor*." *Applied Environmental Microbiology* 74 (9): 2573-82. https://doi.org/10.1128/AEM.02638-07.

Arora, K., B. Ochoa-Montano, P. S. Tsang, T. L. Blundell, S. S. Dawes, V. Mizrahi, T. Bayliss, *et al*. 2014. "Respiratory Flexibility in Response to Inhibition of Cytochrome c Oxidase in *Mycobacterium tuberculosis*." *Antimicrobial Agents and Chemotherapy* 58 (11): 6962-6965. https://doi.org/10.1128/aac.03486-14.

Ascott, M. J., D. C. Gooddy, L. Wang, M. E. Stuart, M. A. Lewis, R. S. Ward, and A. M. Binley. 2017. "Global Patterns of Nitrate Storage in the Vadose Zone." *Nature Communications* 8. https://doi.org/10.1038/s41467-017-01321-w.

Asensio, J. G., C. Maia, N. L. Ferrer, N. Barilone, F. Laval, C. Y. Soto, N. Winter, *et al*. 2006. "The Virulence-Associated Two-Component PhoP-PhoR System Controls the Biosynthesis of Polyketide-Derived Lipids in *Mycobacterium tuberculosis*." *Journal of Biological Chemistry* 281 (3): 1313-1316. https://doi.org/10.1074/jbc.C500388200.

Atkinson, M. R., and A. J. Ninfa. 1999. "Characterization of the GlnK Protein of *Escherichia coli*." *Molecular Microbiology* 32 (2): 301-313. https://doi.org/10.1046/j.1365-2958.1999.01349.x.

Auchter, M., A. Cramer, A. Huser, C. Ruckert, D. Emer, P. Schwarz, A. Arndt, *et al*. 2011. "RamA and RamB are Global Transcriptional Regulators in *Corynebacterium glutamicum* and Control Genes for Enzymes of the Central Metabolism." *Journal of Biotechnology* 154 (2-3): 126-139. https://doi.org/10.1016/j.jbiotec.2010.07.001.

Baek, S. H., A. H. Li, and C. M. Sassetti. 2011. "Metabolic Regulation of Mycobacterial Growth and Antibiotic Sensitivity." *PLoS Biology* 9 (5): e1001065. https://doi.org/10.1371/journal.pbio.1001065.

Bagchi, G., S. Chauhan, D. Sharma, and J. S. Tyagi. 2005. "Transcription and Autoregulation of the *Rv3134c-devR-devS* Operon of *Mycobacterium tuberculosis*." *Microbiology-Sgm* 151: 4045-4053. https://doi.org/10.1099/mic.0.28333-0.

Bajaj, V., R. L. Lucas, C. Hwang, and C. A. Lee. 1996. "Co-Ordinate Regulation of *Salmonella typhimurium* Invasion Genes by Environmental and Regulatory Factors is Mediated by Control of *hilA* Expression." *Molecular Microbiology* 22 (4): 703-714.

Banno, S., D. Shiomi, M. Homma, and I. Kawagishi. 2004. "Targeting of the Chemotaxis Methylesterase/Deamidase CheB to the Polar Receptor-Kinase Cluster in an *Escherichia coli* Cell." *Molecular Microbiology* 53 (4): 1051-1063. https://doi.org/10.1111/j.1365-2958.2004.04176.x.

Bansal-Mutalik, R., and H. Nikaido. 2014. "Mycobacterial Outer Membrane is a Lipid Bilayer and the Inner Membrane is Unusually Rich in Diacyl Phosphatidylinositol Dimannosides." *Proceedings of the National Academy of Sciences of the United States of America* 111 (13): 4958-4963. https://doi.org/10.1073/pnas.1403078111.

Bardarov, S., S. Bardarov Jr, Jr., M. S. Pavelka Jr, Jr., V. Sambandamurthy, M. Larsen, J. Tufariello, J. Chan, G. Hatfull, and W. R. Jacobs, Jr. 2002. "Specialized Transduction: an

Efficient Method for Generating Marked and Unmarked Targeted Gene Disruptions in *Mycobacterium tuberculosis*, *M. bovis* BCG and *M. smegmatis*." *Microbiology (Reading, England)* 148 (Pt 10): 3007-3017. https://doi.org/10.1099/00221287-148-10-3007.

Barry, C. E., III, R. E. Lee, K. Mdluli, A. E. Sampson, B. G. Schroeder, R. A. Slayden, and Y. Yuan. 1998. "Mycolic acids: Structure, Biosynthesis and Physiological Functions." *Progress in Lipid Research* 37 (2-3): 143-179. https://doi.org/10.1016/s0163-7827(98)00008-3.

Bates, D. L., M. J. Danson, G. Hale, E. A. Hooper, and R. N. Perham. 1977. "Self-Assembly and Catalytic Activity of the Pyruvate Dehydrogenase Multienzyme Complex of *Escherichia coli*." *Nature* 268 (5618): 313-316.

Baulard, A. R., J. C. Betts, J. Engohang-Ndong, S. Quan, R. A. McAdam, P. J. Brennan, C. Locht, and G. S. Besra. 2000. "Activation of the Pro-Crug Ethionamide is Regulated in Mycobacteria." *The Journal of Biological Chemistry* 275 (36): 28326-28331. https://doi.org/10.1074/jbc.M003744200.

Bayan, N., S. Schrempp, G. Joliff, G. Leblon, and E. Shechter. 1993. "Role of the Proton Motive Force and the State of the Lipids in the in vivo Protein Secretion in *Corynebacterium glutamicum*, a Gram-Positive Bacterium." *Biochimica Et Biophysica Acta* 1146 (1): 97-105. https://doi.org/10.1016/0005-2736(93)90343-x.

Beckers, G., L. Nolden, and A. Burkovski. 2001. "Glutamate synthase of *Corynebacterium glutamicum* is not Essential for Glutamate Synthesis and is Regulated by the Nitrogen Status." *Microbiology (Reading, England)* 147 (Pt 11): 2961-2970. https://doi.org/10.1099/00221287-147-11-2961.

Beckers, G., J. Strosser, U. Hildebrandt, J. Kalinowski, M. Farwick, R. Kramer, and A. Burkovski. 2005. "Regulation of AmtR-Controlled Gene Expression in *Corynebacterium glutamicum*: Mechanism and Characterization of the AmtR Regulon." *Molecular Microbiology* 58 (2): 580-595. https://doi.org/10.1111/j.1365-2958.2005.04855.x.

Bedard, K., and K. H. Krause. 2007. "The NOX Family of ROS-Generating NADPH Oxidases: Physiology and Pathophysiology." *Physiological Reviews* 87 (1): 245-313. https://doi.org/10.1152/physrev.00044.2005.

Behling, C. A., R. L. Perez, M. R. Kidd, G. W. Staton, Jr., and R. L. Hunter. 1993. "Induction of Pulmonary Granulomas, Macrophage Procoagulant Activity, and Tumor Necrosis Factor-Alpha by Trehalose Glycolipids." *Annals of Clinical and Laboratory Science* 23 (4): 256-266.

Belanger, A. E., G. S. Besra, M. E. Ford, K. Mikusova, J. T. Belisle, P. J. Brennan, and J. M. Inamine. 1996. "The *embAB* Genes of *Mycobacterium avium* Encode an Arabinosyl Transferase Involved in Cell Wall Arabinan Biosynthesis that is the Target for the Antimycobacterial Drug Ethambutol." *Proceedings of the National Academy of Sciences of the United States of America* 93 (21): 11919-11924. https://doi.org/10.1073/pnas.93.21.11919.

Belevich, I., V. B. Borisov, J. Zhang, K. Yang, A. A. Konstantinov, R. B. Gennis, and M. I. Verkhovsky. 2005. "Time-Resolved Electrometric and Optical Studies on Cytochrome *bd* Suggest a Mechanism of Electron-Proton Coupling in the Di-Heme Active Site." *Proceedings of the National Academy of Sciences of the United States of America* 102 (10): 3657-3662. https://doi.org/10.1073/pnas.0405683102.

Belisle, J. T., V. D. Vissa, T. Sievert, K. Takayama, P. J. Brennan, and G. S. Besra. 1997. "Role of the Major Antigen of *Mycobacterium tuberculosis* in Cell Wall Biogenesis." *Science* 276 (5317): 1420-2. https://www.ncbi.nlm.nih.gov/pubmed/9162010.

Bellale, E., M. Naik, B. V. V, A. Ambady, A. Narayan, S. Ravishankar, V. Ramachandran, P. Kaur, *et al*. 2014. "Diarylthiazole: an Antimycobacterial Scaffold Potentially Targeting PrrB-PrrA Two-Component system." *Journal of Medicinal Chemistry* 57 (15): 6572-6582. https://doi.org/10.1021/jm500833f.

Berney, M., and G. M. Cook. 2010. "Unique Flexibility in Energy Metabolism Allows Mycobacteria to Combat Starvation and Hypoxia." *PLoS One* 5 (1). https://doi.org/10.1371/journal.pone.0008614.

Berney, M., T. E. Hartman, and W. R. Jacobs, Jr. 2014. "A *Mycobacterium tuberculosis* Cytochrome *bd* Oxidase Mutant is Hypersensitive to Bedaquiline." *mBio* 5 (4): e01275-14. https://doi.org/10.1128/mBio.01275-14.

Bettenbrock, K., S. Fischer, A. Kremling, K. Jahreis, T. Sauter, and E. D. Gilles. 2006. "A Quantitative Approach to Catabolite Repression in *Escherichia coli*." *Journal of Biological Chemistry* 281 (5): 2578-2584. https://doi.org/10.1074/jbc.M508090200.

Betts, J. C., P. T. Lukey, L. C. Robb, R. A. McAdam, and K. Duncan. 2002. "Evaluation of a Nutrient Starvation Model of *Mycobacterium tuberculosis* Persistence by Gene and Protein Expression Profiling." *Molecular Microbiology* 43 (3): 717-31. https://www.ncbi.nlm.nih.gov/pubmed/11929527.

Bhattacharya, M., A. Biswas, and A. K. Das. 2010. "Interaction Analysis of TcrX/Y Two Component System from *Mycobacterium tuberculosis*." *FASEB Journal* 24.

Bhattacharya, M., and A. K. Das. 2011. "Inverted Repeats in the Promoter as an Autoregulatory Sequence for TcrX in *Mycobacterium tuberculosis*." *Biochemical and Biophysical Research Communications* 415 (1): 17-23. https://doi.org/10.1016/j.bbrc.2011.09.143.

Blanco, A. G., M. Sola, F. X. Gomis-Ruth, and M. Coll. 2002. "Tandem DNA Recognition by PhoB, a Two-Component Signal Transduction Transcriptional Activator." *Structure (London, England : 1993)* 10 (5): 701-713. https://doi.org/S096921260200761X.

Bloch, H., and W. Segal. 1956. "Biochemical Differentiation of *Mycobacterium tuberculosis* Grown in vivo and in vitro." *Journal of Bacteriology* 72 (2): 132-141.

Boon, C., and T. Dick. 2002. "*Mycobacterium bovis* BCG Response Regulator Essential for Hypoxic Dormancy." *Journal of Bacteriology* 184 (24): 6760-6767. https://doi.org/10.1128/jb.184.24.6760-6767.2002.

Boon, C., R. Li, R. Qi, and T. Dick. 2001. "Proteins of *Mycobacterium bovis* BCG Induced in the Wayne Dormancy Model." *Journal of Bacteriology* 183 (8): 2672-2676. https://doi.org/10.1128/jb.183.8.2672-2676.2001.

Borisov, V. B., E. Forte, A. Davletshin, D. Mastronicola, P. Sarti, and A. Giuffre. 2013. "Cytochrome *bd* Oxidase from *Escherichia coli* Displays High Catalase Activity: An Additional Defense Against Oxidative Stress." *FEBS Letters* 587 (14): 2214-2218. https://doi.org/10.1016/j.febslet.2013.05.047.

Brennan, R. G. 1993. "The Winged-Helix DNA-Binding Motif: Another Helix-Turn-Helix Takeoff." *Cell* 74 (5): 773-776. https://doi.org/0092-8674(93)90456-Z.

Bretl, D. J., C. Demetriadou, and T. C. Zahrt. 2011. "Adaptation to Environmental Stimuli within the Host: Two-Component Signal Transduction Systems of *Mycobacterium tuberculosis*." *Microbiology and Molecular Biology Reviews* 75 (4): 566-582. https://doi.org/10.1128/MMBR.05004-11.

Bryk, R., C. D. Lima, H. Erdjument-Bromage, P. Tempst, and C. Nathan. 2002. "Metabolic Enzymes of Mycobacteria Linked to Antioxidant Defense by a Thioredoxin-Like Protein." *Science (New York, N.Y.)* 295 (5557): 1073-1077. https://doi.org/10.1126/science.1067798.

Buckler, D. R., Y. Zhou, and A. M. Stock. 2002. "Evidence of Intradomain and Interdomain Flexibility in an OmpR/PhoB Homolog from *Thermotoga maritima*." *Structure (London, England : 1993)* 10 (2): 153-164. https://doi.org/S0969212601007067.

Burbulys, D., K. A. Trach, and J. A. Hoch. 1991. "Initiation of Sporulation in *B. subtilis* is Controlled by a Multicomponent Phosphorelay." *Cell* 64 (3): 545-552. https://doi.org/0092-8674(91)90238-T.

Caimano, M. J., M. R. Kenedy, T. Kairu, D. C. Desrosiers, M. Harman, S. Dunham-Ems, D. R. Akins, U. Pal, and J. D. Radolf. 2011. "The Hybrid Histidine Kinase Hk1 is Part of a Two-Component System that is Essential for Survival of *Borrelia burgdorferi* in Feeding *Ixodes scapularis* Ticks." *Infection and Immunity* 79 (8): 3117-3130. https://doi.org/10.1128/IAI.05136-11.

Chavadi, S., E. Wooff, N. G. Coldham, M. Sritharan, R. G. Hewinson, S. V. Gordon, and P. R. Wheeler. 2009. "Global Effects of Inactivation of the Pyruvate Kinase Gene in the *Mycobacterium tuberculosis* Complex." *Journal of Bacteriology* 191 (24): 7545-7553. https://doi.org/10.1128/JB.00619-09.

Chen, J. M., G. J. German, D. C. Alexander, H. P. Ren, T. Tan, and J. Liu. 2006. "Roles of Lsr2 in Colony Morphology and Biofilm Formation of *Mycobacterium smegmatis*." *Journal of Bacteriology* 188 (2): 633-641. https://doi.org/10.1128/jb.2.633-641.2006.

Choi, Y., Y. Kawazoe, K. Murakami, H. Misawa, and M. Uesugi. 2003. "Identification of Bioactive Molecules by Adipogenesis Profiling of Organic Compounds." *The Journal of Biological Chemistry* 278 (9): 7320-7324. https://doi.org/10.1074/jbc.M210283200.

Chroneos, Z., and V. L. Shepherd. 1995. "Differential Regulation of the Mannose and SP-A Receptors on Macrophages." *American Journal of Physiology-Lung Cellular and Molecular Physiology* 269 (6): L721-L726.

Cole, S. T., R. Brosch, J. Parkhill, T. Garnier, C. Churcher, D. Harris, S. V. Gordon, *et al*. 1998. "Deciphering the Biology of *Mycobacterium tuberculosis* from the Complete Genome Sequence." *Nature* 393 (6685): 537-544. https://doi.org/10.1038/31159.

Consaul, S. A., and M. S. Pavelka, Jr. 2004. "Use of a Novel Allele of the *Escherichia coli aacC4* Aminoglycoside Resistance Gene as a Genetic Marker in Mycobacteria." *FEMS Microbioogy Letters* 234 (2): 297-301. https://doi.org/10.1016/j.femsle.2004.03.041.

Converse, P. J., P. C. Karakousis, L. G. Klinkenberg, A. K. Kesavan, L. H. Ly, S. S. Allen, J. H. Grosset, *et al*. 2009. "Role of the *dosR-dosS* Two-Component Regulatory System in *Mycobacterium tuberculosis* Virulence in Three Animal Models." *Infection and Immunity* 77 (3): 1230-1237. https://doi.org/10.1128/IAI.01117-08.

Cook, G. M., Hards, K., Vilcheze, C., Hartman, T., and Berney ,M. 2014. "Energetics of Respiration and Oxidative Phosphorylation in Mycobacteria." *Microbiology Spectrum* 2 (3): 1-20.

Cox, E. G., S. A. Heil, and M. B. Kleiman. 1994. "Lipoid Pneumonia and *Mycobacterium smegmatis*." *Pediatric Infectious Disease Journal* 13 (5): 414-415.

Cunningham, L., M. Pitt, and H. D. Williams. 1997. "The *cioAB* Genes from *Pseudomonas aeruginosa* Code for a Novel Cyanide-Insensitive Terminal Oxidase Related to the Cytochrome *bd* Quinol Oxidases." *Molecular Microbiology* 24 (3): 579-591.

Curcic, R., S. Dhandayuthapani, and V. Deretic. 1994. "Gene Expression in Mycobacteria: Transcriptional Fusions Based on *xylE* and Analysis of the Promoter Region of the Response Regulator *mtrA* from *Mycobacterium tuberculosis*." *Molecular Microbiology* 13 (6): 1057-1064.

Daffe, M., P. J. Brennan, and M. McNeil. 1990. "Predominant Structural Features of the Cell Wall Arabinogalactan of *Mycobacterium tuberculosis* as Revealed Through Characterization of Oligoglycosyl Alditol Fragments by Gas Chromatography-Mass Spectrometry and by H1 and C13 NMR Analyses." *Journal of Biological Chemistry* 265 (12): 6734-6743.

Daniel, J., C. Deb, V. S. Dubey, T. D. Sirakova, B. Abomoelak, H. R. Morbidoni, and P. E. Kolattukudy. 2004. "Induction of a Novel Class of Diacylglycerol Acyltransferases and Triacylglycerol Accumulation in *Mycobacterium tuberculosis* as it Goes Into a Dormancy-Like State in Culture." *Journal of Bacteriology* 186 (15): 5017-5030. https://doi.org/10.1128/JB.186.15.5017-5030.2004.

Daniel, J., H. Maamar, C. Deb, T. D. Sirakova, and P. E. Kolattukudy. 2011. "*Mycobacterium tuberculosis* Uses Host Triacylglycerol to Accumulate Lipid Droplets and Acquires a Dormancy-Like Phenotype in Lipid-Loaded Macrophages." *PLoS Pathogens* 7 (6): e1002093. https://doi.org/10.1371/journal.ppat.1002093.

Dasgupta, N., V. Kapur, K. K. Singh, T. K. Das, S. Sachdeva, K. Jyothisri, and J. S. Tyagi. 2000. "Characterization of a Two Component System, *devR-devS*, of *Mycobacterium tuberculosis*." *Tubercle and Lung Disease* 80 (3): 141-159. https://doi.org/10.1054/tuld.2000.0240.

Datta, P., L. Shi, N. Bibi, G. Balazsi, and M. L. Gennaro. 2011. "Regulation of Central Metabolism Genes of *Mycobacterium tuberculosis* by Parallel Feed-Forward Loops Controlled by Sigma Factor E (σ^E)." *Journal of Bacteriology* 193 (5): 1154-1160. https://doi.org/10.1128/JB.00459-10.

de Carvalho, L. P., S. M. Fischer, J. Marrero, C. Nathan, S. Ehrt, and K. Y. Rhee. 2010. "Metabolomics of *Mycobacterium tuberculosis* Reveals Compartmentalized Co-Catabolism of Carbon Substrates." *Chemistry & Biology* 17 (10): 1122-1131. https://doi.org/10.1016/j.chembiol.2010.08.009.

de Jonge, M. R., L. H. H. Koymans, J. E. G. Guillemont, A. Koul, and K. Andries. 2007. "A Computational Model of the Inhibition of *Mycobacterium tuberculosis* ATPase by a New Drug Candidate R207910." *Proteins-Structure Function and Bioinformatics* 67 (4): 971-980. https://doi.org/10.1002/prot.21376.

De Voss, J. J., K. Rutter, B. G. Schroeder, and C. E. Barry, III. 1999. "Iron Acquisition and Metabolism by Mycobacteria." *Journal of Bacteriology* 181 (15): 4443-4451.

Deb, C., C. M. Lee, V. S. Dubey, J. Daniel, B. Abomoelak, T. D. Sirakova, S. Pawar, L. Rogers, and P. E. Kolattukudy. 2009. "A Novel In Vitro Multiple-Stress Dormancy Model for *Mycobacterium tuberculosis* Generates a Lipid-Loaded, Drug-Tolerant, Dormant Pathogen." *PLoS One* 4 (6). https://doi.org/10.1371/journal.pone.0006077.

Deutscher, J., C. Francke, and P. W. Postma. 2006. "How Phosphotransferase System-Related Protein Phosphorylation Regulates Carbohydrate Metabolism in Bacteria." *Microbiology and Molecular Biology Reviews* 70 (4): 939-+. https://doi.org/10.1128/mmbr.00024-06.

Dhar, N., V. Rao, and A. K. Tyagi. 2004. "Immunogenicity of Recombinant BCG Vaccine Strains Overexpressing Components of the Antigen 85 Complex of *Mycobacterium tuberculosis*." *Medical Microbiology and Immunology* 193 (1): 19-25. https://doi.org/10.1007/s00430-002-0170-x.

Dick, T., B. H. Lee, and B. Murugasu-Oei. 1998. "Oxygen Depletion Induced Dormancy in *Mycobacterium smegmatis*." *FEMS Microbiology Letters* 163 (2): 159-164. https://doi.org/S0378109798001669.

Ehrt, S., X. V. Guo, C. M. Hickey, M. Ryou, M. Monteleone, L. W. Riley, and D. Schnappinger. 2005. "Controlling Gene Expression in Mycobacteria with Anhydrotetracycline and Tet Repressor." *Nucleic Acids Research.* 33 (2): e21. https://doi.org/33/2/e21.

Ergan, B., L. Coplu, A. Alp, and M. Artvinli. 2004. "*Mycobacterium smegmatis* Pneumonia." *Respirology* 9 (2): 283-285. https://doi.org/10.1111/j.1440-1843.2004.00570.x.

Ewann, F., M. Jackson, K. Pethe, A. Cooper, N. Mielcarek, D. Ensergueix, B. Gicquel, C. Locht, and P. Supply. 2002. "Transient Requirement of the PrrA-PrrB Two-Component System for Early Intracellular Multiplication of *Mycobacterium tuberculosis*." *Infection and Immunity* 70 (5): 2256-2263.

Ewann, F., C. Locht, and P. Supply. 2004. "Intracellular Autoregulation of the *Mycobacterium tuberculosis* PrrA Response Regulator." *Microbiology (Reading, England)* 150 (Pt 1): 241-246. https://doi.org/10.1099/mic.0.26516-0.

Fabret, C., and J. A. Hoch. 1998. "A Two-Component Signal Transduction System Essential for Growth of *Bacillus subtilis*: Implications for Anti-Infective Therapy." *Journal Bacteriology* 180 (23): 6375-6383.

Fang, X., A. Wallqvist, and J. Reifman. 2012. "Modeling Phenotypic Metabolic Adaptations of *Mycobacterium tuberculosis* H37Rv under Hypoxia." *PLoS Computational Biology* 8 (9). https://doi.org/10.1371/journal.pcbi.1002688.

Ferrari, G., H. Langen, M. Naito, and J. Pieters. 1999. "A Coat Protein on Phagosomes Involved in the Intracellular Survival of Mycobacteria." *Cell* 97 (4): 435-447. https://doi.org/S0092-8674(00)80754-0.

Filippova, E. V., B. Zemaitaitis, T. Aung, A. J. Wolfe, and W. F. Anderson. 2018. "Structural Basis for DNA Recognition by the Two-Component Response Regulator RcsB." *Mbio* 9 (1). https://doi.org/10.1128/mBio.01993-17.

Forrellad, M. A., L. I. Klepp, A. Gioffre, J. S. Y. Garcia, H. R. Morbidoni, M. D. Santangelo, A. A. Cataldi, and F. Bigi. 2013. "Virulence Factors of the *Mycobacterium tuberculosis* Complex." *Virulence* 4 (1): 3-66. https://doi.org/10.4161/viru.22329.

Forst, S., D. Comeau, S. Norioka, and M. Inouye. 1987. "Localization and Membrane Topology of EnvZ, a Protein Involved in Osmoregulation of OmpF and OmpC in *Escherichia coli*." *The Journal of Biological Chemistry* 262 (34): 16433-16438.

Fratti, R. A., J. Chua, I. Vergne, and V. Deretic. 2003. "*Mycobacterium tuberculosis* Glycosylated Phosphatidylinositol Causes Phagosome Maturation Arrest." *Proceedings of the National Academy of Sciences of the United States of America* 100 (9): 5437-5442. https://doi.org/10.1073/pnas.0737613100.

Frieden, T. R., T. Sterling, A. Pablos-Mendez, J. O. Kilburn, G. M. Cauthen, and S. W. Dooley. 1993. "The Emergence of Drug-Resistant Tuberculosis in New York City." *The New England Journal of Medicine* 328 (8): 521-526. https://doi.org/10.1056/NEJM199302253280801.

Fritz, C., S. Maass, A. Kreft, and F. C. Bange. 2002. "Dependence of *Mycobacterium bovis* BCG on Anaerobic Nitrate Reductase for Persistence is Tissue Specific." *Infection and Immunity* 70 (1): 286-291. https://doi.org/10.1128/iai.70.1.286-291.2002.

Galamba, A., K. Soetaert, X. M. Wang, J. De Bruyn, P. Jacobs, and J. Content. 2001. "Disruption of *adhC* Reveals a Large Duplication in the *Mycobacterium smegmatis* mc^2155 Genome." *Microbiology-Sgm* 147: 3281-3294. https://doi.org/10.1099/00221287-147-12-3281.

Gallant, J. L., A. J. Viljoen, P. D. van Helden, and I. J. F. Wiid. 2016. "Glutamate Dehydrogenase Is Required by *Mycobacterium bovis* BCG for Resistance to Cellular Stress." *PLoS One* 11 (1). https://doi.org/10.1371/journal.pone.0147706.

Ganapathy, U., J. Marrero, S. Calhoun, H. Eoh, L. P. S. de Carvalho, K. Rhee, and S. Ehrt. 2015. "Two Enzymes with Redundant Fructose Bisphosphatase Activity Sustain Gluconeogenesis and Virulence in *Mycobacterium tuberculosis*." *Nature Communications* 6. https://doi.org/10.1038/ncomms8912.

Gao, R., and A. M. Stock. 2009. "Biological Insights from Structures of Two-Component Proteins." *Annual Reviews in Microbiology* 63: 133-154. https://doi.org/10.1146/annurev.micro.091208.073214.

Garnier, T., K. Eiglmeier, J. C. Camus, N. Medina, H. Mansoor, M. Pryor, S. Duthoy, *et al*. 2003. "The Complete Genome Sequence of *Mycobacterium bovis*." *Proceedings of the National Academy of Sciences of the United States of America* 100 (13): 7877-7882. https://doi.org/10.1073/pnas.1130426100.

Garton, N. J., H. Christensen, D. E. Minnikin, R. A. Adegbola, and M. R. Barer. 2002. "Intracellular Lipophilic Inclusions of Mycobacteria in vitro and in Sputum." *Microbiology (Reading, England)* 148 (Pt 10): 2951-2958. https://doi.org/10.1099/00221287-148-10-2951.

Gatfield, J., and J. Pieters. 2000. "Essential Role for Cholesterol in Entry of Mycobacteria into Macrophages." *Science (New York, N.Y.)* 288 (5471): 1647-1650. https://doi.org/8572.

Gengenbacher, M., S. P. S. Rao, K. Pethe, and T. Dick. 2010. "Nutrient-Starved, Non-Replicating *Mycobacterium tuberculosis* Requires Respiration, ATP Synthase and Isocitrate Lyase for Maintenance of ATP Homeostasis and Viability." *Microbiology-Sgm* 156: 81-87. https://doi.org/10.1099/mic.0.033084-0.

Georgellis, Dimitris, and Ohsuk Kwon. 2001. "Quinones as the Redox Signal for the Arc Two-Component System of Bacteria." *Science* 292 (5525): 2314-2316.

Gerstmeir, R., A. Cramer, P. Dangel, S. Schaffer, and B. J. Eikmanns. 2004. "RamB, a Novel Transcriptional Regulator of Genes Involved in Acetate Metabolism of *Corynebacterium glutamicum*." *Journal of Bacteriology* 186 (9): 2798-2809. https://doi.org/10.1128/jn.186.9.2798-2809.2004.

Giri, P. K., I. Verma, and G. K. Khuller. 2006. "Enhanced Immunoprotective Potential of *Mycobacterium tuberculosis* Ag85 Complex Protein Based Vaccine Against Airway *Mycobacterium tuberculosis* Challenge Following Intranasal Administration." *FEMS Immunology and Medical Microbiology* 47 (2): 233-241. https://doi.org/10.1111/j.1574-695X.2006.00087.x.

Giuffre, A., V. B. Borisov, D. Mastronicola, P. Sarti, and E. Forte. 2012. "Cytochrome *bd* Oxidase and Nitric Oxide: From Reaction Mechanisms to Bacterial Physiology." *FEBS Letters* 586 (5): 622-629. https://doi.org/10.1016/j.febslet.2011.07.035.

Glover, R. T., J. Kriakov, S. J. Garforth, A. D. Baughn, and W. R. Jacobs, Jr. 2007. "The Two-Gomponent Regulatory System *senX3-regX3* Regulates Phosphate-Dependent Gene Expression in *Mycobacterium smegmatis*." *Journal of Bacteriology* 189 (15): 5495-5503. https://doi.org/10.1128/jb.00190-07.

Gonzalo-Asensio, J., C. Y. Soto, A. Arbues, J. Sancho, M. del Carmen Menendez, M. J. Garcia, B. Gicquel, and C. Martin. 2008. "The *Mycobacterium tuberculosis phoPR* Operon is Positively Autoregulated in the Virulent Strain H37Rv." *Journal of Bacteriology* 190 (21): 7068-7078. https://doi.org/10.1128/JB.00712-08.

Goren, M. B., O. Brokl, and W. B. Schaefer. 1974. "Lipids of Putative Relevance to Virulence in *Mycobacterium tuberculosis*: Phthiocerol Dimycocerosate and the Attenuation Indicator Lipid." *Infection and Immunity* 9 (1): 150-158.

Gouzy, A., G. Larrouy-Maumus, D. Bottai, F. Levillain, A. Dumas, J. B. Wallach, I. Caire-Brandli, *et al*. 2014. "*Mycobacterium tuberculosis* Exploits Asparagine to Assimilate Nitrogen and Resist Acid Stress During Infection." *PLoS Pathogens* 10 (2): e1003928. https://doi.org/10.1371/journal.ppat.1003928.

Gouzy, A., G. Larrouy-Maumus, T. D. Wu, A. Peixoto, F. Levillain, G. Lugo-Villarino, J. L. Guerquin-Kern, L. P. de Carvalho, Y. Poquet, and O. Neyrolles. 2013. "*Mycobacterium tuberculosis* Nitrogen Assimilation and Host Colonization Require Aspartate." *Nature Chemical Biology* 9 (11): 674-676. https://doi.org/10.1038/nchembio.1355.

Graf, S., O. Fedotovskaya, W. C. Kao, C. Hunte, P. Adelroth, M. Bott, C. von Ballmoos, and P. Brzezinski. 2016. "Rapid Electron Transfer within the III-IV Supercomplex in *Corynebacterium glutamicum*." *Scientific Reports* 6. https://doi.org/10.1038/srep34098.

Graham, J. E., and J. E. Clark-Curtiss. 1999. "Identification of *Mycobacterium tuberculosis* RNAs Synthesized in Response to Phagocytosis by Human Macrophages by Selective Capture of Transcribed Sequences (SCOTS)." *Proceedings of the National Academy of Sciences of the United States of America* 96 (20): 11554-11559.

Griffin, J. E., J. D. Gawronski, M. A. Dejesus, T. R. Ioerger, B. J. Akerley, and C. M. Sassetti. 2011. "High-Resolution Phenotypic Profiling Defines Genes Essential for Mycobacterial Growth and Cholesterol Catabolism." *PLoS Pathogens* 7 (9): e1002251. https://doi.org/10.1371/journal.ppat.1002251.

Gumber, S., D. L. Taylor, I. B. Marsh, and R. J. Whittington. 2009. "Growth Pattern and Partial Proteome of *Mycobacterium avium* subsp. paratuberculosis During the Stress Response to Hypoxia and Nutrient Starvation." *Veterinary Microbiology* 133 (4): 344-357. https://doi.org/10.1016/j.vetmic.2008.07.021.

Gutka, H. J., K. Rukseree, P. R. Wheeler, S. G. Franzblau, and F. Movahedzadeh. 2011. "*glpX* Gene of *Mycobacterium tuberculosis*: Heterologous Expression, Purification, and Enzymatic Characterization of the Encoded Fructose 1,6-bisphosphatase II." *Applied Biochemistry and Biotechnology* 164 (8): 1376-1389. https://doi.org/10.1007/s12010-011-9219-x.

Guzman-Verri, C., L. Manterola, A. Sola-Landa, A. Parra, A. Cloeckaert, J. Garin, J. P. Gorvel, I. Moriyon, E. Moreno, and I. Lopez-Goni. 2002. "The Two-component System BvrR/BvrS Essential for *Brucella abortus* Virulence Regulates the Expression of Outer Membrane Proteins with Counterparts in Members of the *Rhizobiaceae*." *Proceedings of the National Acadamy of Sciences of the Unites States of America.* 99 (19): 12375-12380. https://doi.org/10.1073/pnas.192439399.

Haagsma, A. C., N. N. Driessen, M. M. Hahn, H. Lill, and D. Bald. 2010. "ATP Synthase in Slow- and Fast-Growing Mycobacteria is Active in ATP Synthesis and Blocked in ATP Hydrolysis Direction." *FEMS Microbiology Letters* 313 (1): 68-74. https://doi.org/10.1111/j.1574-6968.2010.02123.x.

Haagsma, A. C., I. Podasca, A. Koul, K. Andries, J. Guillemont, H. Lill, and D. Bald. 2011. "Probing the Interaction of the Diarylquinoline TMC207 with Its Target Mycobacterial ATP Synthase." *PLoS One* 6 (8). https://doi.org/10.1371/journal.pone.0023575.

Hall, M. N., and T. J. Silhavy. 1981. "The *ompB* Locus and the Regulation of the Major Outer Membrane Porin Proteins of *Escherichia coli* K12." *Journal of Molecular Biology* 146 (1): 23-43. https://doi.org/0022-2836(81)90364-8.

Hang, S. Y., A. E. Purdy, W. P. Robins, Z. P. Wang, M. Mandal, S. Chang, J. J. Mekalanos, and P. I. Watnick. 2014. "The Acetate Switch of an Intestinal Pathogen Disrupts Host Insulin Signaling and Lipid Metabolism." *Cell Host & Microbe* 16 (5): 592-604. https://doi.org/10.1016/j.chom.2014.10.006.

Hanks, S. K., A. M. Quinn, and T. Hunter. 1988. "The Protein Kinase Family: Conserved Features and Deduced Phylogeny of the Catalytic Domains." *Science* 241 (4861): 42-52. https://doi.org/10.1126/science.3291115.

Hards, K., J. R. Robson, M. Berney, L. Shaw, D. Bald, A. Koul, K. Andries, and G. M. Cook. 2015. "Bactericidal Mode of Action of Bedaquiline." *Journal of Antimicrobial Chemotherapy* 70 (7): 2028-2037. https://doi.org/10.1093/jac/dkv054.

Harland, C. W., D. Rabuka, C. R. Bertozzi, and R. Parthasarathy. 2008. "The *Mycobacterium tuberculosis* Virulence Factor Trehalose Dimycolate Imparts Desiccation Resistance to Model Mycobacterial Membranes." *Biophysical Journal* 94 (12): 4718-4724. https://doi.org/10.1529/biophysj.107.125542.

Harper, C. J., D. Hayward, M. Kidd, I. Wiid, and P. van Helden. 2010. "Glutamate Dehydrogenase and Glutamine Synthetase are Regulated in Response to Nitrogen Availability in *Myocbacterium smegmatis*." *BMC Microbiology* 10: 138-2180-10-138. https://doi.org/10.1186/1471-2180-10-138.

Harth, G., and M. A. Horwitz. 1999. "An Inhibitor of Exported *Mycobacterium tuberculosis* Glutamine Synthetase Selectively Blocks the Growth of Pathogenic Mycobacteria in Axenic Culture and in Human Monocytes: Extracellular Proteins as Potential Novel Drug Targets." *Journal of Experimental Medicine* 189 (9): 1425-1435. https://doi.org/10.1084/jem.189.9.1425.

Hartkoorn, R. C., S. Uplekar, and S. T. Cole. 2014. "Cross-Resistance between Clofazimine and Bedaquiline through Upregulation of MmpL5 in *Mycobacterium tuberculosis*." *Antimicrobial Agents and Chemotherapy* 58 (5): 2979-2981. https://doi.org/10.1128/aac.00037-14.

Haydel, S. E. 2010. "Extensively Drug-Resistant Tuberculosis: A Sign of the Times and an Impetus for Antimicrobial Discovery." *Pharmaceuticals* 3 (7): 2268-2290. https://doi.org/10.3390/ph3072268.

Haydel, S. E., W. H. Benjamin, Jr., N. E. Dunlap, and J. E. Clark-Curtiss. 2002. "Expression, Autoregulation, and DNA Binding Properties of the *Mycobacterium tuberculosis* TrcR Response Regulator." *Journal of Bacteriology* 184 (8): 2192-2203.

Haydel, S. E., and J. E. Clark-Curtiss. 2004. "Global Expression Analysis of Two-Component System Regulator Genes during *Mycobacterium tuberculosis* Growth in Human Macrophages." *FEMS Microbiology Letters.* 236 (2): 341-347. https://doi.org/10.1016/j.femsle.2004.06.010.

Haydel, S. E., V. Malhotra, G. L. Cornelison, and J. E. Clark-Curtiss. 2012. "The *prrAB* Two-Component System is Essential for *Mycobacterium tuberculosis* Viability and is Induced Under Nitrogen-Limiting Conditions." *Journal of Bacteriology* 194 (2): 354-361. https://doi.org/10.1128/JB.06258-11.

He, H. J., R. Hovey, J. Kane, V. Singh, and T. C. Zahrt. 2006. "MprAB is a Stress-Responsive Two-Component System that Directly Regulates Expression of Sigma Factors SigB and SigE in *Mycobacterium tuberculosis*." *Journal of Bacteriology* 188 (6): 2134-2143. https://doi.org/10.1128/jb.188.6.2134-2143.2006.

He, H. J., and T. C. Zahrt. 2005. "Identification and Characterization of a Regulatory Sequence Recognized by *Mycobacterium tuberculosis* Persistence Regulator MprA." *Journal of Bacteriology* 187 (1): 202-212. https://doi.org/10.1128/jb.187.1.202-212.2005

Hernandez, M. A., A. Arabolaza, E. Rodriguez, H. Gramajo, and H. M. Alvarez. 2013. "The *atf2* Gene is Involved in Triacylglycerol Biosynthesis and Accumulation in the Oleaginous *Rhodococcus opacus* PD630." *Applied Microbiology and Biotechnology* 97 (5): 2119-2130. https://doi.org/10.1007/s00253-012-4360-1.

Hernandez, M. A., J. Lara, G. Gago, H. Gramajo, and H. M. Alvarez. 2017. "The Pleiotropic Transcriptional Regulator NOR Contributes to the Modulation of Nitrogen Metabolism, Lipogenesis and Triacylglycerol Accumulation in Oleaginous Rhodococci." *Molecular Microbiology* 103 (2): 366-385. https://doi.org/10.1111/mmi.13564.

Hicks, D. B., D. M. Cohen, and T. A. Krulwich. 1994. "Reconstitution of Energy-Linked Activities of the Solubized F_1F_0 ATP Synthase from *Bacillus subtilis*." *Journal of Bacteriology* 176 (13): 4192-4195.

Himpens, S., C. Locht, and P. Supply. 2000. "Molecular Characterization of the Mycobacterial SenX3-RegX3 Two-Component System: Evidence for Autoregulation." *Microbiology*

(Reading, England) 146 Pt 12: 3091-3098. https://doi.org/10.1099/00221287-146-12-3091.

Hmama, Z., S. Pena-Diaz, S. Joseph, and Y. Av-Gay. 2015. "Immunoevasion and Immunosuppression of the Macrophage by *Mycobacterium tuberculosis*." *Immunological Reviews* 264 (1): 220-232. https://doi.org/10.1111/imr.12268.

Hoch, J. A. 2000. "Two-component and Phosphorelay Signal Transduction." *Current Opinions in Microbiology* 3 (2): 165-170. https://doi.org/S1369-5274(00)00070-9.

Hoffmann, C., A. Leis, M. Niederweis, J. M. Plitzko, and H. Engelhardt. 2008. "Disclosure of the Mycobacterial Outer Membrane: Cryo-Electron Tomography and Vitreous Sections Reveal the Lipid Bilayer Structure." *Proceedings of the National Academy of Sciences of the United States of America* 105 (10): 3963-3967. https://doi.org/10.1073/pnas.0709530105.

Honaker, R. W., R. K. Dhiman, P. Narayanasamy, D. C. Crick, and M. I. Voskuil. 2010. "DosS Responds to a Reduced Electron Transport System To Induce the *Mycobacterium tuberculosis* DosR Regulon." *Journal of Bacteriology* 192 (24): 6447-6455. https://doi.org/10.1128/jb.00978-10.

Hutchings, M. I., H. J. Hong, and M. J. Buttner. 2006. "The Vancomycin Resistance VanRS Two-Component Signal Transduction System of *Streptomyces coelicolor*." *Molecular Microbiology* 59 (3): 923-935. https://doi.org/MMI4953.

Indest, K. J., J. O. Eberly, D. B. Ringelberg, and D. E. Hancock. 2015a. "The Effects of Putative Lipase and Wax Ester Synthase/Acyl-CoA:Diacylglycerol Acyltransferase Gene Knockouts on Triacylglycerol Accumulation in *Gordonia* sp. KTR9." *Journal of Industrial Microbiology & Biotechnology* 42 (2): 219-227. https://doi.org/10.1007/s10295-014-1552-y.

Indrigo, J., R. L. Hunter, and J. K. Actor. 2003. "Cord Factor Trehalose 6,6 '-Dimycolate (TDM) Mediates Trafficking Events During Mycobacterial Infection of Murine Macrophages." *Microbiology-Sgm* 149: 2049-2059. https://doi.org/10.1099/mic.0.26226-0.

Ioanoviciu, A., E. T. Yukl, P. Moenne-Loccoz, and P. R. de Montellano. 2007. "DevS, a Heme-Containing Two-Component Oxygen Sensor of *Mycobacterium tuberculosis*." *Biochemistry* 46 (14): 4250-4260. https://doi.org/10.1021/bi602422p.

Jacob, K., A. Rasmussen, P. Tyler, M. M. Servos, M. Sylla, C. Prado, E. Daniele, J. S. Sharp, and A. E. Purdy. 2017. "Regulation of Acetyl-CoA Synthetase Transcription by the CrbS/R Two-Component System is Conserved in Genetically Diverse Environmental Pathogens." *PLoS One* 12 (5). https://doi.org/10.1371/journal.pone.0177825.

Jaggi, R., W. C. van Heeswijk, H. V. Westerhoff, D. L. Ollis, and S. G. Vasudevan. 1997. "The Two Opposing Activities of Adenylyl Transferase Reside in Distinct Homologous Domains, with Intramolecular Signal Transduction." *The EMBO Journal* 16 (18): 5562-5571. https://doi.org/10.1093/emboj/16.18.5562.

Jenkins, V. A., G. R. Barton, B. D. Robertson, and K. J. Williams. 2013. "Genome Wide Analysis of the Complete GlnR Nitrogen-Response Regulon in *Mycobacterium smegmatis*." *BMC Genomics* 14: 301-2164-14-301. https://doi.org/10.1186/1471-2164-14-30.

Jenkins, V. A., B. D. Robertson, and K. J. Williams. 2012. "Aspartate D48 is Essential for the GlnR-Mediated Transcriptional Response to Nitrogen Limitation in *Mycobacterium*

smegmatis." *FEMS Microbiology Letters* 330 (1): 38-45. https://doi.org/10.1111/j.1574-6968.2012.02530.x.

Jessberger, N., Y. Lu, J. Amon, F. Titgemeyer, S. Sonnewald, S. Reid, and A. Burkovski. 2013. "Nitrogen Starvation-Induced Transcriptome Alterations and Influence of Transcription Regulator Mutants in *Mycobacterium smegmatis*." *BMC Research Notes* 6: 482-0500-6-482. https://doi.org/10.1186/1756-0500-6-482.

Ji, B. H., A. Chauffour, K. Andries, and V. Jarlier. 2006. "Bactericidal Activities of R207910 and Other Newer Antimicrobial Agents against *Mycobacterium leprae* in Mice." *Antimicrobial Agents and Chemotherapy* 50 (4): 1558-1560. https://doi.org/10.1128/aac.50.4.1558-1560.2006.

Jiang, P., A. E. Mayo, and A. J. Ninfa. 2007. "*Escherichia coli* Glutamine Synthetase Adenylyltransferase (ATase, EC 2.7.7.49): Kinetic Characterization of Regulation by PII, PII-UMP, Glutamine, and α-Ketoglutarate." *Biochemistry* 46 (13): 4133-4146. https://doi.org/10.1021/bi0620510.

Jung, J. Y., R. Madan-Lala, M. Georgieva, J. Rengarajan, C. D. Sohaskey, F. C. Bange, and C. M. Robinson. 2013. "The Intracellular Environment of Human Macrophages That Produce Nitric Oxide Promotes Growth of Mycobacteria." *Infection and Immunity* 81 (9): 3198-3209. https://doi.org/10.1128/iai.00611-13.

Kaddor, C., K. Biermann, R. Kalscheuer, and A. Steinbuchel. 2009. "Analysis of Neutral Lipid Biosynthesis in *Streptomyces avermitilis* MA-4680 and Characterization of an Acyltransferase Involved Herein." *Applied Microbiology and Biotechnology* 84 (1): 143-155. https://doi.org/10.1007/s00253-009-2018-4.

Kadner, Robert J. 1995. “Expression of the Uhp Sugar-Phosphate Transport System of *Escherichia coli*.” in *Two-Component Signal Transduction*, edited by James A. Hoch and Thomas J. Silhavy. Washington, D.C.: American Society for Microbiology.

Kalscheuer, R., and A. Steinbuchel. 2003. "A Novel Bifunctional Wax Ester Synthase/Acyl-CoA:Diacylglycerol Acyltransferase Mediates Wax Ester and Triacylglycerol Biosynthesis in *Acinetobacter calcoaceticus* ADP1." *The Journal of Biological Chemistry* 278 (10): 8075-8082. https://doi.org/10.1074/jbc.M210533200.

Kamisuki, S., Q. Mao, L. Abu-Elheiga, Z. Gu, A. Kugimiya, Y. Kwon, T. Shinohara, *et al*. 2009. "A Small Molecule that Blocks Fat Synthesis by Inhibiting the Activation of SREBP." *Chemistry & Biology* 16 (8): 882-892. https://doi.org/10.1016/j.chembiol.2009.07.007.

Kana, B. D., E. A. Weinstein, D. Avarbock, S. S. Dawes, H. Rubin, and V. Mizrahi. 2001. "Characterization of the *cydAB*-Encoded Cytochrome *bd* Oxidase from *Mycobacterium smegmatis*." *Journal of Bacteriology* 183 (24): 7076-7086. https://doi.org/10.1128/JB.183.24.7076-7086.2001.

Karimova, G., J. Bellalou, and A. Ullmann. 1996. "Phosphorylation-Dependent Binding of BvgA to the Upstream Region of the *cyaA* Gene of *Bordetella pertussis*." *Molecular Microbiology.* 20 (3): 489-496.

Kashket, E. R. 1981. "Effects of Aerobiosis and Nitrgen Source on the Proton Motive Force in Growing *Escherichia coli* and *Klebsiella pneumoniae* Cells." *Journal of Bacteriology* 146 (1): 377-384.

Keating, L. A., P. R. Wheeler, H. Mansoor, J. K. Inwald, J. Dale, R. G. Hewinson, and S. V. Gordon. 2005. "The Pyruvate Requirement of Some Members of the *Mycobacterium tuberculosis* Complex is Due to an Inactive Pyruvate Kinase: Implications for in vivo Growth." *Molecular Microbiology* 56 (1): 163-174. https://doi.org/MMI4524.

Keener, J., and S. Kustu. 1988. "Protein Kinase and Phosphoprotein Phosphatase Activities of Nitrogen Regulatory Proteins NTRB and NTRC of Enteric Bacteria: Roles of the Conserved Amino-Terminal Domain of NTRC." *Proceedings of the National Academy of Sciences of the United States of America* 85 (14): 4976-4980.

Kendall, S. L., P. Burgess, R. Balhana, M. Withers, A. ten Bokum, J. S. Lott, C. Gao, I. Uhia-Castro, and N. G. Stoker. 2010. "Cholesterol Utilization in Mycobacteria is Controlled by Two TetR-Type Transcriptional Regulators: *kstR* and *kstR2*." *Microbiology-Sgm* 156: 1362-1371. https://doi.org/10.1099/mic.0.034538-0.

Kendall, S. L., M. Withers, C. N. Soffair, N. J. Moreland, S. Gurcha, B. Sidders, R. Frita *et al*. 2007. "A Highly Conserved Transcriptional Repressor Controls a Large Regulon Involved in Lipid Degradation in *Mycobacterium smegmatis* and *Mycobacterium tuberculosis*." *Molecular Microbiology* 65 (3): 684-699. https://doi.org/10.1111/j.1365-2958.2007.05827.x.

Keren, I., S. Minami, E. Rubin, and K. Lewis. 2011. "Characterization and Transcriptome Analysis of *Mycobacterium tuberculosis* Persisters." *Mbio* 2 (3). https://doi.org/10.1128/mBio.00100-11.

Khan, A., S. Akhtar, J. N. Ahmad, and D. Sarkar. 2008. "Presence of a Functional Nitrate Assimilation Pathway in *Mycobacterium smegmatis*." *Microbial Pathogenesis* 44 (1): 71-77. https://doi.org/S0882-4010(07)00103-9.

Kim, M. J., J. Kim, H. Y. Lee, H. J. Noh, K. H. Lee, and S. J. Park. 2015. "Role of AcsR in Expression of the Acetyl-CoA Synthetase Gene in *Vibrio vulnificus*." *BMC Microbiology* 15. https://doi.org/10.1186/s12866-015-0418-4. <

Kingdon, H. S., B. M. Shapiro, and E. R. Stadtman. 1967. "Regulation of Glutamine Synthetase. 8. Glutamine Synthetase Adenylyltransferase, an Enzyme that Catalyzes Alterations in Regulatory Properties of Glutamine Synthetase." *Proceedings of the National Academy of Sciences of the United States of America* 58 (4): 1703-&. https://doi.org/10.1073/pnas.58.4.1703.

Knipfer, N., A. Seth, and T. E. Shrader. 1997. "Unmarked Gene Integration into the Chromosome of *Mycobacterium smegmatis* via Precise Replacement of the *pyrF* Gene." *Plasmid* 37 (2): 129-140. https://doi.org/S0147-619X(97)91286-5 [.

Kofoid, E. C., and J. S. Parkinson. 1988. "Transmitter and Receiver Modules in Bacterial Signaling Proteins." *Proceedings of the National Academy of Sciences of the United States of America* 85 (14): 4981-4985.

Korshunov, S., K. R. Imlay, and J. A. Imlay. 2016. "The Cytochrome *bd* Oxidase of *Escherichia coli* Prevents Respiratory Inhibition by Endogenous and Exogenous Hydrogen Sulfide." *Molecular Microbiology* 101 (1): 62-77. https://doi.org/10.1111/mmi.13372.

Krauss, J. C., H. Y. Poo, W. Xue, L. Mayobond, R. F. Todd, and H. R. Petty. 1994. "Reconstitution of Antibody-Dependent Phagocytosis in Fibroblasts Expressing FC Gamma Receptor IIIB and the Complement Receptor Type 3." *Journal of Immunology* 153 (4): 1769-1777.

Kumar, A., J. C. Toledo, R. P. Patel, J. R. Lancaster, Jr., and A. J. Steyn. 2007. "*Mycobacterium tuberculosis* DosS is a Redox Sensor and DosT is a Hypoxia Sensor." *Proceedings of the National Academy of Sciences of the United States of America* 104 (28): 11568-11573. https://doi.org/0705054104.

Lam, G. Y., J. Huang, and J. H. Brumell. 2010. "The Many Roles of NOX2 NADPH Oxidase-Derived ROS in Immunity." *Seminars in Immunopathology* 32 (4): 415-430. https://doi.org/10.1007/s00281-010-0221-0.

Larsen, M. H., C. Vilcheze, L. Kremer, G. S. Besra, L. Parsons, M. Salfinger, L. Heifets, *et al*. 2002. "Overexpression of *inhA*, but not *kasA*, Confers Resistance to Isoniazid and Ethionamide in *Mycobacterium smegmatis*, *M. bovis* BCG and *M. tuberculosis*." *Molecular Microbiology* 46 (2): 453-466. https://doi.org/3162.

Lawhon, S. D., R. Maurer, M. Suyemoto, and C. Altier. 2002. "Intestinal Short-Chain Fatty Acids Alter *Salmonella typhimurium* Invasion Gene Expression and Virulence Through BarA/SirA." *Molecular Microbiology* 46 (5): 1451-1464. https://doi.org/10.1046/j.1365-2958.2002.03268.x.

Lee, A. I., A. Delgado, and R. P. Gunsalus. 1999. "Signal-Dependent Phosphorylation of the Membrane-Bound NarX Two-Component Sensor-Transmitter Protein of *Escherichia coli*: Nitrate Elicits a Superior Anion Ligand Response Compared to Nitrite." *Journal of Bacteriology* 181 (17): 5309-5316.

Lee, W., B. C. VanderVen, S. Walker, and D. G. Russell. 2017. "Novel Protein Acetyltransferase, Rv2170, Modulates Carbon and Energy Metabolism in *Mycobacterium tuberculosis*." *Scientific Reports* 7. https://doi.org/10.1038/s41598-017-00067-1.

Leistikow, R. L., R. A. Morton, I. L. Bartek, I. Frimpong, K. Wagner, and M. I. Voskuil. 2010. "The *Mycobacterium tuberculosis* DosR Regulon Assists in Metabolic Homeostasis and Enables Rapid Recovery from Nonrespiring Dormancy." *Journal of Bacteriology* 192 (6): 1662-70. https://doi.org/10.1128/JB.00926-09.

Levin, M. E., and G. F. Hatfull. 1993. "*Mycobacterium smegmatis* RNA Polymerase: DNA Supercoiling, Action of Rifampicin and Mechanism of Rifampicin Resistance." *Molecular Microbiology* 8 (2): 277-285.

Lewis, R. J., J. A. Brannigan, K. Muchova, I. Barak, and A. J. Wilkinson. 1999. "Phosphorylated Aspartate in the Structure of a Response Regulator Protein." *Journal of Molecular Biology* 294 (1): 9-15. https://doi.org/10.1006/jmbi.1999.3261.

Lin, W., V. Mathys, E. L. Ang, V. H. Koh, J. M. Martinez Gomez, M. L. Ang, S. Z. Zainul Rahim, M. P. Tan, K. Pethe, and S. Alonso. 2012. "Urease Activity Represents an Alternative Pathway for *Mycobacterium tuberculosis* Nitrogen Metabolism." *Infection and Immunity* 80 (8): 2771-2779. https://doi.org/10.1128/IAI.06195-11.

Liu, C., D. P. Miller, Y. Wang, M. Merchant, and R. J. Lamont. 2017. "Structure-Function Aspects of the *Porphyromonas gingivalis* Tyrosine Kinase Ptk1." *Molecular Oral Microbiology* 32 (4): 314-323. https://doi.org/10.1111/omi.12173.

Liu, F. L., T. VanToai, L. P. Moy, G. Bock, L. D. Linford, and J. Quackenbush. 2005. "Global Transcription Profiling Reveals Comprehensive Insights into Hypoxic Response in

Arabidopsis." *Plant Physiology* 137 (3): 1115-1129. https://doi.org/10.1104/pp.104.055475.

Livak, K. J., and T. D. Schmittgen. 2001. "Analysis of Relative Gene Expression Data Using Real-Time Quantitative PCR and the $2^{-\Delta\Delta Ct}$ Method." *Methods* 25 (4): 402-8. https://doi.org/10.1006/meth.2001.1262.

Lofthouse, E. K., P. R. Wheeler, D. J. Beste, B. L. Khatri, H. Wu, T. A. Mendum, A. M. Kierzek, and J. McFadden. 2013. "Systems-Based Approaches to Probing Metabolic Variation within the *Mycobacterium tuberculosis* Complex." *PLoS One* 8 (9): e75913. https://doi.org/10.1371/journal.pone.0075913.

Lois, A. F., G. S. Ditta, and D. R. Helinski. 1993. "The Oxygen Sensor FixL of *Rhizobium meliloti* is a Membrane Protein Containing Four Possible Transmembrane Segments." *Journal of Bacteriology* 175 (4): 1103-1109.

Lu, P., M. H. Heineke, A. Koul, K. Andries, G. M. Cook, H. Lill, R. van Spanning, and D. Bald. 2015. "The Cytochrome *bd*-Type Quinol Oxidase is Important for Survival of *Mycobacterium smegmatis* Under Peroxide and Antibiotic-Induced Stress." *Scientific Reports* 5. https://doi.org/10.1038/srep10333.

Lukat, G. S., W. R. McCleary, A. M. Stock, and J. B. Stock. 1992. "Phosphorylation of Bacterial Response Regulator Proteins by Low Molecular Weight Phospho-Donors." *Proceedings of the National Academy of Sciences of the United States of America* 89 (2): 718-722.

Luque-Almagro, V. M., V. J. Lyall, S. J. Ferguson, M. D. Roldan, D. J. Richardson, and A. J. Gates. 2013. "Nitrogen Oxyanion-Dependent Dissociation of a Two-Component Complex that Regulates Bacterial Nitrate Assimilation." *Journal of Biological Chemistry* 288 (41): 29692-29702. https://doi.org/10.1074/jbc.M113.459032.

Maarsingh, J. D., and S. E. Haydel. 2018. "*Mycobacterium smegmatis* PrrAB Two-Component System Influences Triacylglycerol Accumulation During Ammonium Stress." *Microbiology-Sgm* 164 (10): 1276-1288. https://doi.org/10.1099/mic.0.000705.

MacFarlane, S. A., and M. Merrick. 1985. "The Nucleotide Sequence of the Nitrogen Regulation Gene *ntrB* and the *glnA-ntrBC* Intergenic Region of *Klebsiella pneumoniae*." *Nucleic Acids Research* 13 (21): 7591-7606.

MacMicking, J. D., R. J. North, R. LaCourse, J. S. Mudgett, S. K. Shah, and C. F. Nathan. 1997. "Identification of Nitric Oxide Synthase as a Protective Locus Against Tuberculosis." *Proceedings of the National Academy of Sciences of the United States of America* 94 (10): 5243-5248. https://doi.org/10.1073/pnas.94.10.5243.

Majumdar, S. D., A. Vashist, S. Dhingra, R. Gupta, A. Singh, V. K. Challu, V. D. Ramanathan, P. Kumar, and J. S. Tyagi. 2012. "Appropriate DevR (DosR)-Mediated Signaling Determines Transcriptional Response, Hypoxic Viability and Virulence of *Mycobacterium tuberculosis*." *PLoS One* 7 (4): e35847. https://doi.org/10.1371/journal.pone.0035847.

Makino, K., H. Shinagawa, M. Amemura, T. Kawamoto, M. Yamada, and A. Nakata. 1989. "Signal Transduction in the Phosphate Regulon *of Escherichia coli* Involves Phosphotransfer Between PhoR and PhoB Proteins." *Journal of Molecular Biology* 210 (3): 551-559. https://doi.org/0022-2836(89)90131-9.

Malhotra, V., D. Sharma, V. D. Ramanathan, H. Shakila, D. K. Saini, S. Chakravorty, T. K. Das, *et al*. 2004. "Disruption of Response Regulator Gene, *devR*, Leads to Attenuation in

Virulence of *Mycobacterium tuberculosis*." *FEMS Microbiology Letters* 231 (2): 237-245. https://doi.org/10.1016/s0378-1097(04)00002-3.

Malm, S., Y. Tiffert, J. Micklinghoff, S. Schultze, I. Joost, I. Weber, S. Horst, *et al*. 2009. "The Roles of the Nitrate Reductase NarGHJI, the Nitrite Reductase NirBD and the Response Regulator GlnR in Nitrate Assimilation of *Mycobacterium tuberculosis*." *Microbiology (Reading, England)* 155 (Pt 4): 1332-1339. https://doi.org/10.1099/mic.0.023275-0.

Manning, J. M., S. Moore, W. B. Rowe, and A. Meister. 1969. "Identification of L-Methionine *S*-Sulfoximine as the Diastereoisomer of L-Methionine *SR*-Sulfoximine that Inhibits Glutamine Synthetase." *Biochemistry* 8 (6): 2681-2685.

Marrero, J., K. Y. Rhee, D. Schnappinger, K. Pethe, and S. Ehrt. 2010. "Gluconeogenic Carbon Flow of Tricarboxylic Acid Cycle Intermediates is Critical for *Mycobacterium tuberculosis* to Establish and Maintain Infection." *Proceedings of the National Academy of Sciences of the United States of America* 107 (21): 9819-9824. https://doi.org/10.1073/pnas.1000715107.

Marrero, J., C. Trujillo, K. Y. Rhee, and S. Ehrt. 2013. "Glucose Phosphorylation is Required for *Mycobacterium tuberculosis* Persistence in Mice." *PLoS Pathogens* 9 (1): e1003116. https://doi.org/10.1371/journal.ppat.1003116.

Martin, P. K., T. Li, D. Sun, D. P. Biek, and M. B. Schmid. 1999. "Role in Cell Permeability of an Essential Two-Component System in *Staphylococcus aureus*." *Journal of Bacteriology* 181 (12): 3666-3673.

Martinez-Hackert, E., and A. M. Stock. 1997. "The DNA-Binding Domain of OmpR: Crystal Structures of a Winged Helix Transcription Factor." *Structure (London, England : 1993)* 5 (1): 109-124. https://doi.org/S0969-2126(97)00170-6.

Masiewicz, P., A. Brzostek, M. Wolanski, J. Dziadek, and J. Zakrzewska-Czerwinska. 2012. "A Novel Role of the PrpR as a Transcription Factor Involved in the Regulation of Methylcitrate Pathway in *Mycobacterium tuberculosis*." *PLoS One* 7 (8): e43651. https://doi.org/10.1371/journal.pone.0043651.

Masiewicz, P., M. Wolanski, A. Brzostek, J. Dziadek, and J. Zakrzewska-Czerwinska. 2014. "Propionate Represses the *dnaA* Gene via the Methylcitrate Pathway-Regulating Transcription Factor, PrpR, in *Mycobacterium tuberculosis*." *Antonie Van Leeuwenhoek International Journal of General and Molecular Microbiology* 106 (5): 1071-1071. https://doi.org/10.1007/s10482-014-0278-1.

Matsoso, L. G., B. D. Kana, P. K. Crellin, D. J. Lea-Smith, A. Pelosi, D. Powell, S. S. Dawes, H. Rubin, R. L. Coppel, and V. Mizrahi. 2005. "Function of the Cytochrome bc_1-aa_3 Branch of the Respiratory Network in Mycobacteria and Network Adaptation Occurring in Response to its Disruption." *Journal of Bacteriology* 187 (18): 6300-6308. https://doi.org/10.1128/jb.187.18.6300-6308.2005.

Matyash, V., G. Liebisch, T. V. Kurzchalia, A. Shevchenko, and D. Schwudke. 2008. "Lipid Extraction by Methyl-*tert*-Butyl Ether for High-Throughput Lipidomics." *Journal of Lipid Research* 49 (5): 1137-1146. https://doi.org/10.1194/jlr.D700041-JLR200.

Mdluli, K., R. A. Slayden, Y. Q. Zhu, S. Ramaswamy, X. Pan, D. Mead, D. D. Crane, J. M. Musser, and C. E. Barry, III. 1998. "Inhibition of a *Mycobacterium tuberculosis* β-Ketoacyl ACP Synthase by Isoniazid." *Science* 280 (5369): 1607-1610. https://doi.org/10.1126/science.280.5369.1607.

Megehee, J. A., J. P. Hosler, and M. D. Lundrigan. 2006. "Evidence for a Cytochrome *bcc-aa*$_3$ Interaction in the Respiratory Chain of *Mycobacterium smegmatis*." *Microbiology (Reading, England)* 152 (Pt 3): 823-829. https://doi.org/152/3/823.

Mehra, S., T. W. Foreman, P. J. Didier, M. H. Ahsan, T. A. Hudock, R. Kissee, N. A. Golden, U. *et al*. 2015. "The DosR Regulon Modulates Adaptive Immunity and Is Essential for *Mycobacterium tuberculosis* Persistence." *American Journal of Respiratory Critical Care and Medicine* 191 (10): 1185-96. https://doi.org/10.1164/rccm.201408-1502OC.

Meier-Wagner, J., L. Nolden, M. Jakoby, R. Siewe, R. Kramer, and A. Burkovski. 2001. "Multiplicity of Ammonium Uptake Systems in *Corynebacterium glutamicum*: Role of Amt and AmtB." *Microbiology-Uk* 147: 135-143. https://doi.org/10.1099/00221287-147-1-135.

Micklinghoff, J. C., K. J. Breitinger, M. Schmidt, R. Geffers, B. J. Eikmanns, and F. C. Bange. 2009. "Role of the Transcriptional Regulator RamB (Rv0465c) in the Control of the Glyoxylate Cycle in *Mycobacterium tuberculosis*." *Journal of Bacteriology* 191 (23): 7260-7269. https://doi.org/10.1128/JB.01009-09.

Mishra, A. K., S. M. Yabaji, R. K. Dubey, E. Dhamija, and K. K. Srivastava. 2017. "Dual Phosphorylation in Response Regulator Protein PrrA is Crucial for Intracellular Survival of Mycobacteria Consequent Upon Transcriptional Activation." *Biochemical Journal* 474 (24): 4119-4136. https://doi.org/10.1042/BCJ20170596.

Mizuno, T. 1997. "Compilation of All Genes Encoding Two-Component Phosphotransfer Signal Transducers in the Genome of *Escherichia coli*." *DNA research: An International Journal for Rapid Publication of Reports on Genes and Genomes* 4 (2): 161-168.

Mogi, T., Y. Murase, M. Mori, K. Shiomi, S. Omura, M. P. Paranagama, and K. Kita. 2009. "Polymyxin B Identified as an Inhibitor of Alternative NADH Dehydrogenase and Malate: Quinone Oxidoreductase from the Gram-Positive Bacterium *Mycobacterium smegmatis*." *Journal of Biochemistry* 146 (4): 491-499. https://doi.org/10.1093/jb/mvp096.

Morth, J. P., S. Gosmann, E. Nowak, and P. A. Tucker. 2005. "A Novel Two-Component System Found in *Mycobacterium tuberculosis*." *FEBS Letters* 579 (19): 4145-4148. https://doi.org/S0014-5793(05)00784-2.

Munoz-Elias, E. J., and J. D. McKinney. 2005. "*Mycobacterium tuberculosis* Isocitrate Lyases 1 and 2 are Jointly Required for in vivo Growth and Virulence." *Nature Medicine* 11 (6): 638-644. https://doi.org/nm1252.

Munoz-Elias, E. J., A. M. Upton, J. Cherian, and J. D. McKinney. 2006. "Role of the Methylcitrate Cycle in *Mycobacterium tuberculosis* Metabolism, Intracellular Growth, and Virulence." *Molecular Microbiology* 60 (5): 1109-1122. https://doi.org/MMI5155.

Nakano, M., H. Imamura, M. Toei, M. Tamakoshi, M. Yoshida, and K. Yokoyama. 2008. "ATP Hydrolysis and Synthesis of a Rotary Motor V-ATPase from *Thermus thermophilus*." *Journal of Biological Chemistry* 283 (30): 20789-20796. https://doi.org/10.1074/jbc.M801276200..

Nambi, S., K. Gupta, M. Bhattacharyya, P. Ramakrishnan, V. Ravikumar, N. Siddiqui, A. T. Thomas, and S. S. Visweswariah. 2013. "Cyclic AMP-Dependent Protein Lysine Acylation in Mycobacteria Regulates Fatty Acid and Propionate Metabolism." *Journal of Biological Chemistry* 288 (20): 14114-14124. https://doi.org/10.1074/jbc.M113.463992.

Nazarova, E. V., M. O. Shleeva, N. S. Morozova, Y. K. Kudykina, G. N. Vostroknutova, A. O. Ruzhitsky, A. A. Selishcheva, G. M. Sorokoumova, V. I. Shvets, and A. S. Kaprelyants. 2011. "Role of Lipid Components in Formation and Reactivation of *Mycobacterium smegmatis* "Nonculturable" Cells." *Biochemistry-Moscow* 76 (6): 636-644. https://doi.org/10.1134/s0006297911060034.

Nguyen, L., S. Chinnapapagari, and C. J. Thompson. 2005. "FbpA-Dependent Biosynthesis of Trehalose Dimycolate is Required for the Intrinsic Multidrug Resistance, Cell Wall Structure, and Colonial Morphology of *Mycobacterium smegmatis*." *Journal of Bacteriology* 187 (19): 6603-6611. https://doi.org/10.1128/jb.187.19.6603-6611.2005.

Niebisch, A., and M. Bott. 2003. "Purification of a Cytochrome bc_1-aa_3 Supercomplex with Quinol Oxidase Activity from *Corynebacterium glutamicum* - Identification of a Fourth Subunit of Cytochrome aa_3 Oxidase and Mutational Analysis of Diheme Cytochrome c_1." *Journal of Biological Chemistry* 278 (6): 4339-4346. https://doi.org/10.1074/jbc.M210499200.

Niesteruk, A., M. Hutchison, S. Sreeramulu, H. R. A. Jonker, C. Richter, R. Abele, C. Bock, and H. Schwalbe. 2018. "Structural Characterization of the Intrinsically Disordered Domain of *Mycobacterium tuberculosis* Protein Tyrosine Linase A." *FEBS Letters* 592 (7): 1233-1245. https://doi.org/10.1002/1873-3468.13022.

Nixon, B. T., C. W. Ronson, and F. M. Ausubel. 1986. "Two-Component Regulatory Systems Responsive to Environmental Stimuli Share Strongly Conserved Domains with the Nitrogen Assimilation Regulatory Genes *ntrB* and *ntrC*." *Proceedings of the National Academy of Sciences of the United States of America* 83 (20): 7850-7854.

Nowak, E., S. Panjikar, P. Konarev, D. I. Svergun, and P. A. Tucker. 2006a. "The Structural Basis of Signal Transduction for the Response Regulator PrrA from *Mycobacterium tuberculosis*." *Journal of Biological. Chemistry* 281 (14): 9659-9666. https://doi.org/M512004200.

Nowak, E., S. Panjikar, J. P. Morth, R. Jordanova, D. I. Svergun, and P. A. Tucker. 2006b. "Structural and Functional Aspects of the Sensor Histidine Kinase PrrB from *Mycobacterium tuberculosis*." *Structure (London, England : 1993)* 14 (2): 275-285. https://doi.org/S0969-2126(06)00037-2.

Noy, T., O. Vergnolle, T. E. Hartman, K. Y. Rhee, W. R. Jacobs, Jr., M. Berney, and J. S. Blanchard. 2016. "Central Role of Pyruvate Kinase in Carbon Co-Catabolism of *Mycobacterium tuberculosis*." *The Journal of Biological Chemistry* 291 (13): 7060-7069. https://doi.org/10.1074/jbc.M115.707430.

O'Hare, H. M., R. Duran, C. Cervenansky, M. Bellinzoni, A. M. Wehenkel, O. Pritsch, G. Obal, *et al*. 2008. "Regulation of Glutamate Metabolism by Protein Kinases in Mycobacteria." *Molecular Microbiology* 70 (6): 1408-1423. https://doi.org/10.1111/j.1365-2958.2008.06489.x.

O'Toole, R., M. J. Smeulders, M. C. Blokpoel, E. J. Kay, K. Lougheed, and H. D. Williams. 2003. "A Two-Component Regulator of Universal Stress Protein Expression and Adaptation to Oxygen Starvation in *Mycobacterium smegmatis*." *Journal of Bacteriology* 185 (5): 1543-1554.

Olukoshi, E. R., and N. M. Packter. 1994. "Importance of Stored Triacylglycerols in *Streptomyces* – Possible Carbon Source for Antibiotics." *Microbiology-Sgm* 140: 931-943. https://doi.org/10.1099/00221287-140-4-931.

Pabreja, S., T. Garg, G. Rath, and A. K. Goyal. 2016. "Mucosal Vaccination Against Tuberculosis Using Ag85A-Loaded Immunostimulating Complexes." *Artificial Cells Nanomedicine and Biotechnology* 44 (2): 532-539. https://doi.org/10.3109/21691401.2014.966195.

Pace, J., and E. E. McDermott. 1952. "Methionine Sulphoximine and Some Enzyme Systems Involving Glutamine." *Nature* 169 (4297): 415-416.

Pan, J., Z. Zha, P. Zhang, R. Chen, C. Ye, and T. Ye. 2017. "Serine/Threonine Protein Kinase PpkA Contributes to the Adaptation and Virulence in *Pseudomonas aeruginosa*." *Microbial Pathogenesis* 113: 5-10. https://doi.org/S0882-4010(17)30989-0.

Parandhaman, D. K., P. Sharma, D. Bisht, and S. Narayanan. 2014. "Proteome and Phosphoproteome Analysis of the Serine/Threonine Protein Kinase E Mutant of *Mycobacterium tuberculosis*." *Life Sciences* 109 (2): 116-126. https://doi.org/10.1016/j.lfs.2014.06.013.

Parish, T., and N. G. Stoker. 2000. "*glnE* is an Essential Gene in *Mycobacterium tuberculosis*." *Journal of Bacteriology* 182 (20): 5715-5720.

Park, H. D., K. M. Guinn, M. I. Harrell, R. Liao, M. I. Voskuil, M. Tompa, G. K. Schoolnik, and D. R. Sherman. 2003. "Rv3133c/dosR is a Transcription Factor that Mediates the Hypoxic Response of *Mycobacterium tuberculosis*." *Molecular Microbiology* 48 (3): 833-43. https://www.ncbi.nlm.nih.gov/pubmed/12694625.

Parkinson, J. S. 1976. "*cheA*, *cheB*, and *cheC* genes of *Escherichia coli* and Their Role in Chemotaxis." *Journal of Bacteriology* 126 (2): 758-770.

Payton, M., R. Auty, R. Delgoda, M. Everett, and E. Sim. 1999. "Cloning and Characterization of Arylamine N-Acetyltransferase Genes from *Mycobacterium smegmatis* and *Mycobacterium tuberculosis*: Increased Expression Results in Isoniazid Resistance." *Journal of Bacteriology* 181 (4): 1343-1347.

Pernestig, A. K., D. Georgellis, T. Romeo, K. Suzuki, H. Tomenius, S. Normark, and O. Melefors. 2003. "The *Escherichia coli* BarA-UvrY Two-Component System is Needed for Efficient Switching Between Glycolytic and Gluconeogenic Carbon Sources." *Journal of Bacteriology* 185 (3): 843-853. https://doi.org/10.1128/jb.185.3.843-853.2003.

Pethe, K., P. Bifani, J. C. Jang, S. Kang, S. Park, S. Ahn, J. Jiricek, *et al*. 2013. "Discovery of Q203, a Potent Clinical Candidate for the Treatment of Tuberculosis." *Nature Medicine* 19 (9): 1157-1160. https://doi.org/10.1038/nm.3262.

Petit, J. F., A. Adam, J. Wietzerbin-Falszpan, E. Lederer, and J. M. Ghuysen. 1969. "Chemical Structure of the Cell Wall of *Mycobacterium smegmatis*. I. Isolation and Partial Characterization of the Peptidoglycan." *Biochemical and Biophysical Research Communications* 35 (4): 478-485. https://doi.org/0006-291X(69)90371-4.

Petrella, S., E. Cambau, A. Chauffour, K. Andries, V. Jarlier, and W. Sougakoff. 2006. "Genetic Basis for Natural and Acquired Resistance to the Diarylquinoline R207910 in Mycobacteria." *Antimicrobial Agents and Chemotherapy* 50 (8): 2853-2856. https://doi.org/10.1128/aac.00244-06.

Petridis, M., C. Vickers, J. Robson, J. L. McKenzie, M. Bereza, A. Sharrock, H. L. Aung, V. L. Arcus, and G. M. Cook. 2016. "Structure and Function of AmtR in *Mycobacterium smegmatis*: Implications for Post-Transcriptional Regulation of Urea Metabolism through

a Small Antisense RNA." *Journal of Molecular Biology* 428 (21): 4315-4329. https://doi.org/S0022-2836(16)30373-4.

Pflock, M., N. Finsterer, B. Joseph, H. Mollenkopf, T. F. Meyer, and D. Beier. 2006. "Characterization of the ArsRS Regulon of *Helicobacter pylori,* Involved in Acid Adaptation." *Journal of Bacteriology* 188 (10): 3449-3462. https://doi.org/188/10/3449.

Phong, W. Y., W. Lin, S. P. Rao, T. Dick, S. Alonso, and K. Pethe. 2013. "Characterization of Phosphofructokinase Activity in *Mycobacterium tuberculosis* Reveals that a Functional Glycolytic Carbon Flow is Necessary to Limit the Accumulation of Toxic Metabolic Intermediates Under Hypoxia." *PLoS One* 8 (2): e56037. https://doi.org/10.1371/journal.pone.0056037.

Phummarin, N., H. I. Boshoff, P. S. Tsang, J. Dalton, S. Wiles, C. E. Barry, III, and B. R. Copp. 2016. "SAR and Identification of 2-(quinolin-4-yloxy)Acetamides as *Mycobacterium tuberculosis* Cytochrome bc_1 Inhibitors." *MedChemComm* 7 (11): 2122-2127. https://doi.org/10.1039/c6md00236f.

Pierre-Audigier, C., E. Jouanguy, S. Lamhamedi, F. Altare, J. Rauzier, V. Vincent, D. Canioni, *et al*. 1997. "Fatal Disseminated *Mycobacterium smegmatis* Infection in a Child with Inherited Interferon Gamma Receptor Deficiency." *Clinical Infectious Diseases* 24 (5): 982-984.

Puckett, S., C. Trujillo, H. Eoh, J. Marrero, J. Spencer, M. Jackson, D. Schnappinger, K. Rhee, and S. Ehrt. 2014. "Inactivation of Fructose-1,6-Bisphosphate Aldolase Prevents Optimal Co-Catabolism of Glycolytic and Gluconeogenic Carbon Substrates in *Mycobacterium tuberculosis*." *PLoS Pathogens* 10 (5): e1004144. https://doi.org/10.1371/journal.ppat.1004144.

Purdy, G. E., S. Pacheco, J. Turk, and F. F. Hsu. 2013. "Characterization of Mycobacterial Triacylglycerols and Monomeromycolyl Diacylglycerols from *Mycobacterium smegmatis* Biofilm by Electrospray Ionization Multiple-Stage and High-Resolution Mass Spectrometry." *Analytical and Bioanalytical Chemistry* 405 (23): 7415-7426. https://doi.org/10.1007/s00216-013-7179-4.

Rahi, A., S. K. Matta, A. Dhiman, J. Garhyan, M. Gopalani, S. Chandra, and R. Bhatnagar. 2017. "Enolase of *Mycobacterium tuberculosis* is a Surface Exposed Plasminogen Binding Protein." *Biochimica et Biophysica Acta* 1861 (1 Pt A): 3355-3364. https://doi.org/S0304-4165(16)30307-5.

Rajagopalan, M., R. Dziedzic, M. Al Zayer, D. Stankowska, M. C. Ouimet, D. P. Bastedo, G. T. Marczynski, and M. V. Madiraju. 2010. "*Mycobacterium tuberculosis* Origin of Replication and the Promoter for Immunodominant Secreted Antigen 85B are the Targets of MtrA, the Essential Response Regulator." *The Journal of Biological Chemistry* 285 (21): 15816-15827. https://doi.org/10.1074/jbc.M109.040097.

Ramesh, A., S. DebRoy, J. R. Goodson, K. A. Fox, H. Faz, D. A. Garsin, and W. C. Winkler. 2012. "The Mechanism for RNA Recognition by ANTAR Regulators of Gene Expression." *PLoS Genetics* 8 (6). https://doi.org/10.1371/journal.pgen.1002666.

Rao, M., T. L. Streur, F. E. Aldwell, and G. M. Cook. 2001. "Intracellular pH Regulation by *Mycobacterium smegmatis* and *Mycobacterium bovis* BCG." *Microbiology-UK* 147: 1017-1024. https://doi.org/10.1099/00221287-147-4-1017.

Rao, S. P., S. Alonso, L. Rand, T. Dick, and K. Pethe. 2008. "The Protonmotive Force is Required for Maintaining ATP Homeostasis and Viability of Hypoxic, Nonreplicating *Mycobacterium tuberculosis*." *Proceedings of the National Academy of Sciences of the United States of America* 105 (33): 11945-11950. https://doi.org/10.1073/pnas.0711697105.

Reed, M. B., S. Gagneux, K. Deriemer, P. M. Small, and C. E. Barry, III. 2007. "The W-Beijing Lineage of *Mycobacterium tuberculosis* Overproduces Triglycerides and has the DosR Dormancy Regulon Constitutively Upregulated." *Journal of Bacteriology* 189 (7): 2583-2589. https://doi.org/JB.01670-06.

Reyrat, J. M., and D. Kahn. 2001. "*Mycobacterium smegmatis*: an Absurd Model for Tuberculosis?" *Trends in Microbiology* 9 (10): 472-474. https://doi.org/S0966-842X(01)02168-0.

Rhee, K. Y., L. P. S. de Carvalho, R. Bryk, S. Ehrt, J. Marrero, S. W. Park, D. Schnappinger, A. Venugopal, and C. Nathan. 2011. "Central Carbon Metabolism in *Mycobacterium tuberculosis*: an Unexpected frontier." *Trends in Microbiology* 19 (7): 307-314. https://doi.org/10.1016/j.tim.2011.03.008.

Roberts, D. M., R. P. Liao, G. Wisedchaisri, W. G. Hol, and D. R. Sherman. 2004. "Two Sensor Kinases Contribute to the Hypoxic Response of *Mycobacterium tuberculosis*." *The Journal of Biological Chemistry* 279 (22): 23082-23087. https://doi.org/10.1074/jbc.M401230200.

Robinson, V. L., T. Wu, and A. M. Stock. 2003. "Structural Analysis of the Domain Interface in DrrB, a Response Regulator of the OmpR/PhoB Subfamily." *Journal of Bacteriology* 185 (14): 4186-4194.

Rochette, P., D. A. Angers, M. H. Chantigny, M. O. Gasser, J. D. MacDonald, D. E. Pelster, and N. Bertrand. 2013. "NH_3 Volatilization, Soil NH_4^+ Concentration and Soil pH Following Subsurface Banding of Urea at Increasing Rates." *Canadian Journal of Soil Science* 93 (2): 261-268. https://doi.org/10.4141/cjss2012-095.

Rodbell, Martin. 1980. "The Role of Hormone Receptors and GTP-Regulatory Proteins in Membrane Transduction." *Nature* 284 (5751): 17-22. https://doi.org/10.1038/284017a0.

Rohde, K. H., R. B. Abramovitch, and D. G. Russell. 2007. "*Mycobacterium tuberculosis* Invasion of Macrophages: Linking Bacterial Gene Expression to Environmental Cues." *Cell Host & Microbe* 2 (5): 352-364. https://doi.org/10.1016/j.chom.2007.09.006.

Rohde, K. H., D. F. Veiga, S. Caldwell, G. Balazsi, and D. G. Russell. 2012. "Linking the Transcriptional Profiles and the Physiological States of *Mycobacterium tuberculosis* During an Extended Intracellular infection." *PLoS Pathogens* 8 (6): e1002769. https://doi.org/10.1371/journal.ppat.1002769.

Ruecker, N., R. Jansen, C. Trujillo, S. Puckett, P. Jayachandran, G. G. Piroli, N. Frizzell, H. Molina, K. Y. Rhee, and S. Ehrt. 2017. "Fumarase Deficiency Causes Protein and Metabolite Succination and Intoxicates *Mycobacterium tuberculosis*." *Cell Chemical Biology* 24 (3): 306-315. https://doi.org/10.1016/j.chembiol.2017.01.005.

Rustad, Tige R., David M. Roberts, R. Liao, and D. R. Sherman. “Isolation of Mycobacterial RNA.” In *Mycobacteria Protocols*, edited by T. Parish and A. C. Brown. 2nd ed. Vol. 465. Totowa, NJ: Humana Press, 2010.

Rybniker, J., A. Vocat, C. Sala, P. Busso, F. Pojer, A. Benjak, and S. T. Cole. 2015. "Lansoprazole is an Antituberculous Prodrug Targeting Cytochrome bc_1." *Nature Communications* 6. https://doi.org/10.1038/ncomms8659.

Sabnis, N. A., H. H. Yang, and T. Romeo. 1995. "Pleiotropic Regulation of Central Carbohydrate Metabolism in *Escherichia coli* via the Gene *csrA*." *Journal of Biological Chemistry* 270 (49): 29096-29104. https://doi.org/10.1074/jbc.270.49.29096.

Saini, D. K., V. Malhotra, D. Dey, N. Pant, T. K. Das, and J. S. Tyagi. 2004. "DevR-DevS is a bona fide Two-Component System of *Mycobacterium tuberculosis* that is Hypoxia-Responsive in the Absence of the DNA-Binding Domain of DevR." *Microbiology* 150 (Pt 4): 865-875. https://doi.org/10.1099/mic.0.26218-0.

Sanders, D. A., B. L. Gillece-Castro, A. M. Stock, A. L. Burlingame, and D. E. Koshland, Jr. 1989. "Identification of the Site of Phosphorylation of the Chemotaxis Response Regulator Protein, CheY." *The Journal of Biological Chemistry* 264 (36): 21770-21778.

Sarkar, M. K., K. Paul, and D. Blair. 2010. "Chemotaxis Signaling Protein CheY Binds to the Rotor Protein FliN to Control the Direction of Flagellar Rotation in *Escherichia coli*." *Proceedings of the National Academy of Sciences of the United States of America* 107 (20): 9370-9375. https://doi.org/10.1073/pnas.1000935107.

Saviola, B., and W. R. Bishai. 2004. "Method to Integrate Multiple Plasmids into the Mycobacterial Chromosome." *Nucleic Acids Research* 32 (1). https://doi.org/10.1093/nar/gnh005.

Savvi, S., D. F. Warner, B. D. Kana, J. D. McKinney, V. Mizrahi, and S. S. Dawes. 2008. "Functional Characterization of a Vitamin B12-Dependent Methylmalonyl Pathway in *Mycobacterium tuberculosis*: Implications for Propionate Metabolism During Growth on Fatty Acids." *Journal of Bacteriology* 190 (11): 3886-3895. https://doi.org/10.1128/JB.01767-07.

Schlessinger, J. 2000. "Cell Signaling by Receptor Tyrosine Kinases." *Cell* 103 (2): 211-225. https://doi.org/S0092-8674(00)00114-8.

Schnappinger, D., S. Ehrt, M. I. Voskuil, Y. Liu, J. A. Mangan, I. M. Monahan, G. Dolganov, B. Efron, P. D. Butcher, C. Nathan, and G. K. Schoolnik. 2003a. "Transcriptional Adaptation of *Mycobacterium tuberculosis* within Macrophages: Insights into the Phagosomal Environment." *The Journal of Experimental Medicine* 198 (5): 693-704. https://doi.org/10.1084/jem.20030846.

Schnell, R., D. Agren, and G. Schneider. 2008. "1.9 Angstrom Structure of the Signal Receiver Domain of the Putative Response Regulator NarL from *Mycobacterium tuberculosis*." *Acta Crystallographica Section F-Structural Biology and Crystallization Communications* 64: 1096-1100. https://doi.org/10.1107/s1744309108035203.

Schulz, A. A., H. J. Collett, and S. J. Reid. 2001. "Nitrogen and Carbon Regulation of Glutamine Synthetase and Glutamate Synthase in *Corynebacterium glutamicum* ATCC 13032." *FEMS Microbiology Letters* 205 (2): 361-367. https://doi.org/S0378109701005018.

Segala, E., W. Sougakoff, A. Nevejans-Chauffour, V. Jarlier, and S. Petrella. 2012. "New Mutations in the Mycobacterial ATP Synthase: New Insights into the Binding of the Diarylquinoline TMC207 to the ATP Synthase C-Ring Structure." *Antimicrobial Agents and Chemotherapy* 56 (5): 2326-2334. https://doi.org/10.1128/aac.06154-11.

Seiler, P., T. Ulrichs, S. Bandermann, L. Pradl, S. Jorg, V. Krenn, L. Morawietz, S. H. E. Kaufmann, and P. Aichele. 2003. "Cell-Wall Alterations as an Attribute of *Mycobacterium tuberculosis* in Latent Infection." *Journal of Infectious Diseases* 188 (9): 1326-1331. https://doi.org/10.1086/378563

Sherman, D. R., P. J. Sabo, M. J. Hickey, T. M. Arain, G. G. Mahairas, Y. Yuan, C. E. Barry, III, and C. K. Stover. 1995. "Disparate Response to Oxidative Stress in Saprophytic and Pathogenic Mycobacteria." *Proceedings of the National Academy of Sciences of the United States of America* 92 (14): 6625-6629. https://doi.org/10.1073/pnas.92.14.6625.

Sherman, D. R., M. Voskuil, D. Schnappinger, R. Liao, M. I. Harrell, and G. K. Schoolnik. 2001. "Regulation of the *Mycobacterium tuberculosis* Hypoxic Response Gene Encoding α-Crystallin." *Proceedeing of the National Acadamy of Sciences of the United States of America* 98 (13): 7534-7539. https://doi.org/10.1073/pnas.121172498.

Shi, L., C. D. Sohaskey, B. D. Kana, S. Dawes, R. J. North, V. Mizrahi, and M. L. Gennaro. 2005. "Changes in Energy Metabolism of *Mycobacterium tuberculosis* in Mouse Lung and Under in vitro Conditions Affecting Aerobic Respiration." *Proceedings of the National Academy of Sciences of the United States of America* 102 (43): 15629-15634. https://doi.org/0507850102.

Shi, L., C. D. Sohaskey, C. Pheiffer, P. Datta, M. Parks, J. McFadden, R. J. North, and M. L. Gennaro. 2010. "Carbon Flux Rerouting During *Mycobacterium tuberculosis* Growth Arrest." *Molecular Microbiology* 78 (5): 1199-1215. https://doi.org/10.1111/j.1365-2958.2010.07399.x.

Shiloh, M. U., P. Manzanillo, and J. S. Cox. 2008. "*Mycobacterium tuberculosis* Senses Host-Derived Carbon Monoxide During Macrophage Infection." *Cell Host & Microbe* 3 (5): 323-330. https://doi.org/10.1016/j.chom.2008.03.007.

Shrivastava, R., A. K. Ghosh, and A. K. Das. 2009. "Intra- and Intermolecular Domain Interactions Among Novel Two-Component System Proteins Coded by Rv0600c, Rv0601c and Rv0602c of *Mycobacterium tuberculosis*." *Microbiology-Sgm* 155: 772-779. https://doi.org/10.1099/mic.0.019059-0.

Siewe, R. M., B. Weil, A. Burkovski, B. J. Eikmanns, M. Eikmanns, and R. Kramer. 1996. "Functional and Genetic Characterization of the (Methyl)Ammonium Uptake Carrier of *Corynebacterium glutamicum*." *Journal of Biological Chemistry* 271 (10): 5398-5403. https://doi.org/10.1074/jbc.271.10.5398.

Singh, D. K., P. K. Singh, S. Tiwari, S. K. Singh, R. Kumari, D. K. Tripathi, and K. K. Srivastava. 2014. "Phosphorylation of Pyruvate Kinase A by Protein Kinase J Leads to the Altered Growth and Differential Rate of Intracellular Survival of Mycobacteria." *Applied Microbiology and Biotechnology* 98 (24): 10065-10076. https://doi.org/10.1007/s00253-014-5859-4.

Sirakova, T. D., V. S. Dubey, C. Deb, J. Daniel, T. A. Korotkova, B. Abomoelak, and P. E. Kolattukudy. 2006. "Identification of a Diacylglycerol Acyltransferase Gene Involved in Accumulation of Triacylglycerol in *Mycobacterium tuberculosis* Under Stress." *Microbiology* 152 (Pt 9): 2717-2725. https://doi.org/152/9/2717.

Slayden, R. A., and C. E. Barry, III. 2001. "Analysis of the Lipids of *Mycobacterium tuberculosis*." *Methods in Molecular Medicine* 54: 229-245. https://doi.org/10.1385/1-59259-147-7:229.

Small, P. M., and P. I. Fujiwara. 2001. "Medical Progress: Management of Tuberculosis in the United States." *New England Journal of Medicine* 345 (3): 189-200. https://doi.org/10.1056/nejm200107193450307.

Snapper, S. B., R. E. Melton, S. Mustafa, T. Kieser, and W. R. Jacobs, Jr. 1990. "Isolation and Characterization of Efficient Plasmid Transformation Mutants of *Mycobacterium smegmatis*." *Molecular Microbiology* 4 (11): 1911-1919.

Sohaskey, C. D. 2008. "Nitrate Enhances the Survival of *Mycobacterium tuberculosis* During Inhibition of Respiration." *Journal of Bacteriology* 190 (8): 2981-2986. https://doi.org/10.1128/jb.01857-07.

Soncini, F. C., E. G. Vescovi, and E. A. Groisman. 1995. "Transcriptional Autoregulation of the *Salmonella typhimurium phoPQ* Operon." *Journal of Bacteriology* 177 (15): 4364-4371.

Stewart, R. J., C. A. Tsang, R. H. Pratt, S. F. Price, and A. J. Langer. 2018. "Tuberculosis - United States, 2017." *Morbidity and Mortality Weekly Report* 67 (11): 317-323.

Steyn, A. J. C., J. Joseph, and B. R. Bloom. 2003. "Interaction of the Sensor Module of *Mycobacterium tuberculosis* H37Rv KdpD with Members of the Lpr Family." *Molecular Microbiology* 47 (4): 1074-1089. https://doi.org/10.1046/j.1365-2958.2003.03356.x.

Stock, A., T. Chen, D. Welsh, and J. Stock. 1988. "CheA Protein, a Central Regulator of Bacterial Chemotaxis, Belongs to a Family of Proteins that Control Gene Expression in Response to Changing Environmental Conditions." *Proceedings of the National Academy of Sciences of the United States of America* 85 (5): 1403-1407.

Stock, A. M., V. L. Robinson, and P. N. Goudreau. 2000. "Two-Component Signal Transduction." *Annual Reviews in Biochemistry* 69: 183-215. https://doi.org/69/1/183.

Strosser, J., A. Ludke, S. Schaffer, R. Kramer, and A. Burkovski. 2004. "Regulation of GlnK Activity: Modification, Membrane Sequestration and Proteolysis as Regulatory Principles in the Network of Nitrogen Control in *Corynebacterium glutamicum*." *Molecular Microbiology* 54 (1): 132-147. https://doi.org/10.1111/j.1365-2958.2004.04247.x.

Sturgill-Koszycki, S., U. E. Schaible, and D. G. Russell. 1996. "Mycobacterium-Containing Phagosomes are Accessible to Early Endosomes and Reflect a Transitional State in Normal Phagosome Biogenesis." *EMBO Journal* 15 (24): 6960-6968. https://doi.org/10.1002/j.1460-2075.1996.tb01088.x.

Sturgill-Koszycki, S., P. H. Schlesinger, P. Chakraborty, P. L. Haddix, H. L. Collins, A. K. Fok, R. D. Allen, S. L. Gluck, J. Heuser, and D. G. Russell. 1994. "Lack of Acidification in *Mycobacterium* Phagosomes Produced by Exclusion of the Vesicular Proton ATPase." *Science* 263 (5147): 678-681. https://doi.org/10.1126/science.8303277.

Taneja, N. K., and J. S. Tyagi. 2007. "Resazurin Reduction Assays for Screening of Anti-Tubercular Compounds Against Dormant and Actively Growing *Mycobacterium tuberculosis*, *Mycobacterium bovis* BCG and *Mycobacterium smegmatis*." *Journal of Antimicrobial Chemotherapy* 60 (2): 288-293. https://doi.org/10.1093/jac/dkm207.

Tanner, J. J. 2008. "Structural Biology of Proline Catabolism." *Amino Acids* 35 (4): 719-730. https://doi.org/10.1007/s00726-008-0062-5.

The World Health Organization. *Global tuberculosis report 2018.* 2018. Geneva: World Health Organization (Geneva, Switzerland).

Tian, J., R. Bryk, M. Itoh, M. Suematsu, and C. Nathan. 2005a. "Variant Tricarboxylic Acid Cycle in *Mycobacterium tuberculosis*: Identification of α-Ketoglutarate Decarboxylase." *Proceedings of the National Academy of Sciences of the United States of America* 102 (30): 10670-10675. https://doi.org/10.1073/pnas.0501605102.

Tian, J., R. Bryk, S. Shi, H. Erdjument-Bromage, P. Tempst, and C. Nathan. 2005b. "*Mycobacterium tuberculosis* Appears to Lack α-Ketoglutarate Dehydrogenase and Encodes Pyruvate Dehydrogenase in Widely Separated Genes." *Molecular Microbiology* 57 (3): 859-868. https://doi.org/MMI4741.

Timm, J., F. A. Post, L. G. Bekker, G. B. Walther, H. C. Wainwright, R. Manganelli, W. T. Chan *et al*. 2003. "Differential Expression of Iron-, Carbon-, and Oxygen-Responsive Mycobacterial Genes in the Lungs of Chronically Infected Mice and Tuberculosis Patients." *Proceeding of the National Acadamy of Sciences of the United States of America* 100 (24): 14321-6. https://doi.org/10.1073/pnas.2436197100.

Tran, S. L., and G. M. Cook. 2005. "The F_1F_0-ATP Synthase of *Mycobacterium smegmatis* is Essential for Growth." *Journal of Bacteriology* 187 (14): 5023-5028. https://doi.org/10.1128/jb.187.14.5023-5028.2005.

Tripathi, D., H. Chandra, and R. Bhatnagar. 2013. "Poly-L-Glutamate/Glutamine Synthesis in the Cell Wall of *Mycobacterium bovis* is Regulated in Response to Nitrogen Availability." *BMC Microbiology* 13: 226-2180-13-226. https://doi.org/10.1186/1471-2180-13-226.

Trujillo, C., A. Blumenthal, J. Marrero, K. Y. Rhee, D. Schnappinger, and S. Ehrt. 2014. "Triosephosphate Isomerase is Dispensable in vitro Yet Essential for *Mycobacterium tuberculosis* to Establish Infection." *mBio* 5 (2): e00085-14. https://doi.org/10.1128/mBio.00085-14.

Tsai, M. C., S. Chakravarty, G. Zhu, J. Xu, K. Tanaka, C. Koch, J. Tufariello, J. Flynn, and J. Chan. 2006. "Characterization of the Tuberculous Granuloma in Murine and Human Lungs: Cellular Composition and Relative Tissue Oxygen Tension." *Cellular Microbiology* 8 (2): 218-232. https://doi.org/CMI612.

Tsukamura, M. 1976. "Properties of *Mycobacterium smegmatis* Freshly Isolated from Soil." *Japanese Journal of Microbiology* 20 (4): 355-356. https://doi.org/10.1111/j.1348-0421.1976.tb00999.x.

Tuckman, D., R. J. Donnelly, F. X. Zhao, W. R. Jacobs, Jr., and N. D. Connell. 1997. "Interruption of the Phosphoglucose Isomerase Gene Results in Glucose Auxotrophy in *Mycobacterium smegmatis*." *Journal of Bacteriology* 179 (8): 2724-2730.

Tullius, M. V., G. Harth, and M. A. Horwitz. 2003. "Glutamine Synthetase GlnA1 is Essential for Growth of *Mycobacterium tuberculosis* in Human THP-1 Macrophages and Guinea Pigs." *Infection and Immunity* 71 (7): 3927-3936.

Uhl, M. A., and J. F. Miller. 1996. "Integration of Multiple Domains in a Two-Component Sensor Protein: the *Bordetella pertussis* BvgAS Phosphorelay." *The EMBO Journal* 15 (5): 1028-1036.

Ulrichs, T., and S. H. E. Kaufmann. 2006. "New Insights into the Function of Granulomas in Human Tuberculosis." *Journal of Pathology* 208 (2): 261-269. https://doi.org/10.1002/path.1906.

Upton, A. M., and J. D. McKinney. 2007. "Role of the Methylcitrate Cycle in Propionate Metabolism and Detoxification in *Mycobacterium smegmatis*." *Microbiology (Reading, England)* 153 (Pt 12): 3973-3982. https://doi.org/153/12/3973.

Urabe, H., H. Ogawara, and K. Motojima. 2015. "Expression and Characterization of *Streptomyces coelicolor* Serine/Threonine Protein Kinase PkaE." *Bioscience, Biotechnology, and Biochemistry* 79 (5): 855-862. https://doi.org/10.1080/09168451.2014.996204.

van Kessel, J. C., and G. F. Hatfull. 2007. "Recombineering in *Mycobacterium tuberculosis*." *Nature Methods* 4 (2): 147-152. https://doi.org/nmeth996.

Ventura, M., B. Rieck, F. Boldrin, G. Degiacomi, M. Bellinzoni, N. Barilone, F. Alzaidi, P. M. Alzari, R. Manganelli, and H. M. O'Hare. 2013. "GarA is an Essential Regulator of Metabolism in *Mycobacterium tuberculosis*." *Molecular Microbiology* 90 (2): 356-366. https://doi.org/10.1111/mmi.12368.

Viljoen, A. J., C. J. Kirsten, B. Baker, P. D. van Helden, and I. J. Wiid. 2013. "The Role of Glutamine Oxoglutarate Aminotransferase and Glutamate Dehydrogenase in Nitrogen Metabolism in *Mycobacterium bovis* BCG." *PLoS One* 8 (12): e84452. https://doi.org/10.1371/journal.pone.0084452.

Voggu, L., S. Schlag, R. Biswas, R. Rosenstein, C. Rausch, and F. Gotz. 2006. "Microevolution of Cytochrome *bd* Oxidase in Staphylococci and its Implication in Resistance to Respiratory Toxins released by *Pseudomonas*." *Journal of Bacteriology* 188 (23): 8079-8086. https://doi.org/188/23/8079.

Voskuil, M. I., D. Schnappinger, K. C. Visconti, M. I. Harrell, G. M. Dolganov, D. R. Sherman, and G. K. Schoolnik. 2003. "Inhibition of Respiration by Nitric Oxide Induces a *Mycobacterium tuberculosis* Dormancy Program." *Journal of Experimental Medicine* 198 (5): 705-713. https://doi.org/10.1084/jem.20030205.

Voskuil, M. I., K. C. Visconti, and G. K. Schoolnik. 2004. "*Mycobacterium tuberculosis* Gene Expression During Adaptation to Stationary Phase and Low-Oxygen Dormancy." *Tuberculosis* 84 (3-4): 218-227. https://doi.org/10.1016/j.tube.2004.02.003.

Wallace, R. J., Jr., D. R. Nash, M. Tsukamura, Z. M. Blacklock, and V. A. Silcox. 1988. "Human Disease Due to *Mycobacterium smegmatis*." *The Journal of Infectious Diseases* 158 (1): 52-59.

Walter, B., E. Hanssler, J. Kalinowski, and A. Burkovski. 2007. "Nitrogen Metabolism and Nitrogen Control in Corynebacteria: Variations of a Common Theme." *Journal of Molecular Microbiology and Biotechnology* 12 (1-2): 131-138. https://doi.org/000096468.

Walter, B., M. Kuspert, D. Ansorge, R. Kramer, and A. Burkovski. 2008. "Dissection of Ammonium Uptake Systems in *Corynebacterium glutamicum*: Mechanism of Action and Energetics of AmtA and AmtB." *Journal of Bacteriology* 190 (7): 2611-2614. https://doi.org/10.1128/JB.01896-07.

Waltermann, M., H. Luftmann, D. Baumeister, R. Kalscheuer, and A. Steinbuchel. 2000. "*Rhodococcus opacus* Strain PD630 as a New Source of High-Value Single-Cell Oil? Isolation and Characterization of Triacylglycerols and Other Storage Lipids." *Microbiology-UK* 146: 1143-1149.

Walters, S. B., E. Dubnau, I. Kolesnikova, F. Laval, M. Daffe, and I. Smith. 2006. "The *Mycobacterium tuberculosis* PhoPR Two-Component System Regulates Genes Essential for Virulence and Complex Lipid Biosynthesis." *Molecular Microbiology* 60 (2): 312-330. https://doi.org/MMI5102

Wang, L., R. A. Slayden, C. E. Barry, III, and J. Liu. 2000. "Cell Wall Structure of a Mutant of *Mycobacterium smegmatis* Defective in the Biosynthesis of Mycolic Acids." *Journal of Biological Chemistry* 275 (10): 7224-7229. https://doi.org/10.1074/jbc.275.10.7224

Warner, D. F., G. Etienne, X. M. Wang, L. G. Matsoso, S. S. Dawes, K. Soetaert, N. G. Stoker, J. Content, and V. Mizrahi. 2006. "A Derivative of *Mycobacterium smegmatis* mc^2155 that Lacks the Duplicated Chromosomal Region." *Tuberculosis* 86 (6): 438-444. https://doi.org/10.1016/j.tube.2005.10.001.

Wayne, L. G., and L. G. Hayes. 1996. "An in vitro Model for Sequential Study of Shiftdown of *Mycobacterium tuberculosis* Through Two Stages of Nonreplicating Persistence." *Infection and Immunity* 64 (6): 2062-2069.

Wayne, L. G., and K. Y. Lin. 1982. "Glyoxylate Metabolism and Adaptation of *Mycobacterium tuberculosis* to Survival Under Anaerobic Conditions." *Infection and Immunity* 37 (3): 1042-1049.

Wayne, L. G., and C. D. Sohaskey. 2001. "Nonreplicating Persistence of *Mycobacterium tuberculosis*." *Annual Review of Microbiology* 55: 139-163. https://doi.org/10.1146/annurev.micro.55.1.139.

Wayne, L. G., and H. A. Sramek. 1994. "Metronidazole is Bactericidal to Dormant Cells of *Mycobacterium tuberculosis*." *Antimicrobial Agents and Chemotherapy* 38 (9): 2054-2058. https://doi.org/10.1128/aac.38.9.2054.

Welch, M., K. Oosawa, S. Aizawa, and M. Eisenbach. 1993. "Phosphorylation-Dependent Binding of a Signal Molecule to the Flagellar Switch of Bacteria." *Proceedings of the National Academy of Sciences of the United States of America* 90 (19): 8787-8791.

Werninghaus, K., A. Babiak, O. Gross, C. Holscher, H. Dietrich, E. M. Agger, J. Mages, *et al*. 2009. "Adjuvanticity of a Synthetic Cord Factor Analogue for Subunit *Mycobacterium tuberculosis* Vaccination Requires FcRγ-Syk-Card9-Dependent Innate Immune Activation." *Journal of Experimental Medicine* 206 (1): 89-97. https://doi.org/10.1084/jem.20081445.

White, M. J., J. P. Savaryn, D. J. Bretl, H. He, R. M. Penoske, S. S. Terhune, and T. C. Zahrt. 2011. "The HtrA-Like Serine Protease PepD Interacts with and Modulates the *Mycobacterium tuberculosis* 35-kDa Antigen Outer Envelope Protein." *PLoS One* 6 (3): e18175. https://doi.org/10.1371/journal.pone.0018175.

Williams, K. J., M. H. Bennett, G. R. Barton, V. A. Jenkins, and B. D. Robertson. 2013. "Adenylylation of Mycobacterial Glnk (PII) Protein is Induced by Nitrogen Limitation." *Tuberculosis (Edinburgh, Scotland)* 93 (2): 198-206. https://doi.org/10.1016/j.tube.2012.12.003.

Williams, K. J., W. A. Bryant, V. A. Jenkins, G. R. Barton, A. A. Witney, J. W. Pinney, and B. D. Robertson. 2013. "Deciphering the Response of *Mycobacterium smegmatis* to Nitrogen Stress Using Bipartite Active Modules." *BMC Genomics* 14: 436-2164-14-436. https://doi.org/10.1186/1471-2164-14-436.

Williams, K. J., V. A. Jenkins, G. R. Barton, W. A. Bryant, N. Krishnan, and B. D. Robertson. 2015. "Deciphering the Metabolic Response of *Mycobacterium tuberculosis* to Nitrogen Stress." *Molecular Microbiology* 97 (6): 1142-1157. https://doi.org/10.1111/mmi.13091.

Worley, M. V., and S. J. Estrada. 2014. "Bedaquiline: A Novel Antitubercular Agent for the Treatment of Multidrug-Resistant Tuberculosis." *Pharmacotherapy* 34 (11): 1187-1197. https://doi.org/10.1002/phar.1482.

Wu, M. L., M. Gengenbacher, and T. Dick. 2016. "Mild Nutrient Starvation Triggers the Development of a Small-Cell Survival Morphotype in Mycobacteria." *Frontiers in Microbiology* 7: 947. https://doi.org/10.3389/fmicb.2016.00947.

Zahrt, T. C., and V. Deretic. 2000. "An Essential Two-Component Signal Transduction System in *Mycobacterium tuberculosis*." *Journal of Bacteriology* 182 (13): 3832-3838.

Zahrt, T. C., and Deretic, V. 2001. "Mycobacterium Tuberculosis Signal Transduction System Required for Persistent Infections." *Proceedings of the National Academy of Sciences of the United States of America* 98 (22): 12706-12711. https://doi.org/10.1073/pnas.221272198.

Zapf, J., M. Madhusudan, C. E. Grimshaw, J. A. Hoch, K. I. Varughese, and J. M. Whiteley. 1998. "A Source of Response Regulator Autophosphatase Activity: The Critical Role of a Residue Adjacent to the Spo0F Autophosphorylation Active Site." *Biochemistry* 37 (21): 7725-7732. https://doi.org/10.1021/bi9729615.

Zhang, Y., B. Heym, B. Allen, D. Young, and S. Cole. 1992. "The Catalase-Peroxidase Gene and Isoniazid Resistance of *Mycobacterium tuberculosis*." *Nature* 358 (6387): 591-593. https://doi.org/10.1038/358591a0.

Zhong, W., L. Cui, B. C. Goh, Q. Cai, P. Ho, Y. H. Chionh, M. Yuan, *et al*. 2017. "Allosteric Pyruvate Kinase-Based "Logic Gate" Synergistically Senses Energy and Sugar Levels in *Mycobacterium tuberculosis*." *Nature Communications* 8 (1): 1986-017-02086-y. https://doi.org/10.1038/s41467-017-02086-y.

Zimhony, O., J. S. Cox, J. T. Welch, C. Vilcheze, and W. R. Jacobs, Jr. 2000. "Pyrazinamide Inhibits the Eukaryotic-Like Fatty Acid Synthetase I (FASI) of *Mycobacterium tuberculosis*." *Nature Medicine* 6 (9): 1043-1047. https://doi.org/10.1038/79558.